



Scientific Activities

Institute for Cosmic Ray Research, The University of Tokyo

Report to the Review Committee

29 October 2012

CONTENTS

OVERVIEW	1
NEUTRINO AND ASTROPARTICLE DIVISION	8
Super-Kamiokande	
T2K Experiment	
XMASS Experiment	
Hyper-Kamiokande (R & D)	
HIGH ENERGY COSMIC RAY DIVISION	50
TA: Telescope Array	
CANGAROO	
Tibet AS γ Project	
High Energy Astrophysics Group	
Ashra	
CTA (R & D)	
ASTROPHYSICS AND GRAVITY DIVISION	109
Gravitational Wave Group	
Observational Cosmology Group	
Primary Cosmic Ray Group	
Theory Group	
FACILITIES	165
Kamioka Observatory	
Akeno Observatory	
Norikura Observatory	
Research Center for Cosmic Neutrinos	
Low-Level Radioisotope Measurement Facility	
Gravitational Wave Project Office	
APPENDIX	189
A.1: Organization	
A.2: ICRR Staffs (2012)	
A.3: Budget (FY2007–2011)	
B.1: Agreements of International Academic Cooperation	
B.2: International Meetings	
B.3: Inter-University Collaborative Researches	
B.4: Educational Activities	
B.5: Public Relations	
C: Report from the Future Planning Committee (2007)	

OVERVIEW

The Institute for Cosmic Ray Research (ICRR) has its origin at a lodge for research, called Asahi Hut, built on Mt. Norikura based on Asahi Academic Grant. In 1953, it was established as the Cosmic Ray Observatory of the University of Tokyo. This Observatory was Japan's first research facility for nationwide joint use. In 1976, the Cosmic Ray Observatory was reorganized into the Institute for Cosmic Ray Research (ICRR) of the University of Tokyo. Since the era of Cosmic Ray Observatory, ICRR has been functioning as "Inter University Research Institution", where researchers in Japan in the field of cosmic rays carry out diverse researches using various facilities in ICRR.

In 2004, the Japanese National Universities, including the University of Tokyo, became independent administrative agencies (National University Corporations). The concept was to strengthen the Universities by mutual competition. At that time, the concept of "independent administrative agencies" and "Inter University Research Institution" did not go along well.

This problem was recognized by the Ministry of Education, Culture, Sports, Science and Technology in Japan. A new system, called "Joint Usage / Research Center", was established. ICRR was selected as one of these Centers in 2010. Since then, ICRR's research style as "Inter University Research Institution" has been officially re-recognized by the Japanese government.

The external review panel of ICRR has been organized approximately every six years since 1994, the last one having been held on 19-20 October, 2006. This report provides the material prepared for the External Review Panel to be held on 16-18 January 2013 to examine the research activity of the ICRR. The prime purposes of the present Review are:

- (1) to give oversight to the institute's scientific activities between 2006 and 2012, whether they meet the international scientific standard and have given sufficient impacts on the community,
- (2) to assess the scientific merits of individual research activities and make recommendations about future support,
- (3) to assess technical competence of the proponents and feasibility of the R&D experiments or projects,
- (4) to assess the Institute's policy and its role in the scientific community.

At present, ICRR consists of 23 faculties, 1 project associate professor¹, 14 research associates, 14 project research associates², 17 post-doctoral fellows and 8 supporting technical staffs, and consists of three divisions — Neutrino and Astroparticle Division, High-Energy Cosmic Ray Division, and Astrophysics & Gravity Division. They are further subdivided into twelve research groups. Most of the activities receive participations by other university members that partially offset small numbers of staffs of the ICRR. The faculties are counted as members of the Faculty of Science of the Graduate School and are engaged in the teaching of graduate students of this university, jointly with those who belong to Department of Physics and Department of Astronomy in the Hongo campus.

ICRR runs 8 facilities (observatories and a center; 3 overseas) to perform its research projects. The overseas facilities are operated jointly in collaboration with academic institutions of respective countries under memoranda of understanding. The Institute also supports, directly or indirectly, some of cosmic-ray related research activities of research scientists in this country. More information as to the structure of ICRR is given in Appendix A.1.

Divisions

Neutrino and Astroparticle Division

This division is focused on particle and astroparticle physics with primary interests in the physics of neutrinos, proton decay, and dark matter using underground experimental detectors at Kamioka Observatory. The primary detector is the Super-Kamiokande (SK), which is a 50,000 ton water Cherenkov detector studying neutrino physics and proton decay. The Tokai-to-Kamioka (T2K) long-baseline neutrino experiment is also a focus project of this division. A liquid xenon detector (XMASS) has been constructed and aims for a direct detection of dark matter interactions. Further, research and development activities towards a future megaton-sized water Cherenkov detector, Hyper-Kamiokande, are ongoing.

High Energy Cosmic Ray Division

This division is devoted to the study of very high energy cosmic rays and cosmic gamma rays, consisting of

*1 fixed-term associate professor

*2 fixed-term research associates

three major research activities, TA, Cherenkov γ , and Tibet AS γ , with one theoretical group and an individual research activity.

Telescope Array (TA) experiment explores extreme phenomena in the universe by measuring energy spectrum, particle composition, and arrival direction distribution of cosmic rays with energies of $10^{18} - 10^{20}$ eV or higher. In May 2008 this experiment started full operation of the largest detector in the northern hemisphere (Utah, USA).

For Cherenkov γ , CANGAROO telescopes were operated near Woomera, Australia to observe TeV gamma rays from astrophysical objects in the southern hemisphere, and completed their mission in 2011. CTA is an international project to construct the next generation large scale imaging atmospheric Cherenkov telescope array.

Tibet AS γ Collaboration is operating a ground air shower array of scintillation counters at high altitude (4300m) in Yangbajing, Tibet, China realizing high statistics studies of cosmic rays with energies $10^{12} - 10^{17}$ eV sensitive for both charged cosmic rays and gamma rays.

A theoretical group, High Energy Astrophysics group, aims at making theoretical and observational studies of violent astrophysical phenomena in which nonthermal cosmic ray particles are begin accelerated.

In addition there is another research activity, Ashra (=All-Sky Survey High Resolution Air-Shower detector). On Mauna Loa (Hawaii, USA), Ashra operates an unconventional optical collector complex with a very wide field of view which is to image air showers caused by neutrinos of energies of $10^{15} - 10^{18}$ eV or higher from violent astrophysical sources like gamma ray bursts.

Astrophysics and Gravity Division

This division consists of the Gravitational Wave Group, the Observational Cosmology Group, the Primary Cosmic Ray group, and the Theory Group.

The Gravitational Wave group aims at direct detection of gravitational waves with the large scale cryogenic gravitational wave telescope named as KAGRA. The KAGRA detector is being built at Kamioka in these three years and its design is based on the previous results and experiences by both TAMA and CLIO.

The Observational Cosmology Group is conducting an optical sky survey with prime interests in cosmology and extragalactic astrophysics. The group participated in the SDSS survey under international collaboration. At present, the group is contributing to the Subaru Hyper Suprime-Cam (HSC) narrow band (NB) project whose observations will start in 2013.

The Primary Cosmic Ray group aims to make observational studies on solar dynamo, solar modulation or galactic cosmic rays, and their impacts on terrestrial environment.

The Theory group is making theoretical studies on phenomenology-oriented particle physics, astro/cosmoparticle physics and cosmology.

Facilities

ICRR's facilities include six Observatories, one Center, one Facility, and one Office. Six of them are domestic and the others are overseas. These facilities are all open to researchers, and the use will be admitted after a proper review process.

Domestic

- **Kamioka Observatory.** This observatory is located 1000 m underground (2700 m.w.e.) in the Kamiokande Mine, Gifu prefecture. The SK water Cherenkov detector is located in this observatory. The observatory is also used by the XMASS experiment. The observatory offers a well-developed and maintained, low vibration and low radioactivity environment. Therefore, it is used by a number of research groups both inside and outside ICRR, including the CANDLES double beta decay experiment led by Osaka University, the NewAGE dark matter experiment led by Kobe University, a cryogenic test experiment for gravitational wave detection (CLIO: Cryogenic Laser Interferometer Gravitational-Wave Observatory) run by ICRR, as well as seismic and geophysical experiments performed by the Earthquake Research Institute of the University of Tokyo and others.
- **Akeno Observatory.** The AGASA array was deployed at this observatory, but now the observatory is used for small scale cosmic ray experiments and as a test and detector assembly facility. The AGASA array was dismantled in 2007.
- **Norikura Observatory (at 2770m altitude).** This observatory, located close to the summit of Mt. Norikura, was historically a very important station of ICRR. This is now used for long-term monitors of cosmic ray muons and solar neutrons, mainly by teams from Nagoya University and from Shinshu University. It is occasionally used for various types of research (not necessarily cosmic ray proper) that require the high altitude environment, as it now offers a unique high altitude facility in Japan.

- **Low-Level Radioisotope Measurement Facility.** This is located underground in the Kashiwa building, and is used for measurements of the concentration of natural radioisotope by interested researchers in the country.
- **Research Center for Cosmic Neutrinos.** This was established in 1999 primarily to promote research of neutrino physics. This center has been organizing neutrino meetings and neutrino public lectures. It also acts as a body for accepting ICRR's inter university programmes related to Low-Level Radioisotope Measurement Facility, and is in charge of the computer system of the institute.
- **Gravitational Wave Project Office.** This is an internal branch in the research division of Astrophysics and Gravity for conducting the construction of the large scale cryogenic gravitational wave telescope, KAGRA, which has been funded in 2010.

Overseas

ICRR holds three overseas facilities, two of which play central roles to carry out its research projects, jointly with various academic institutions in respective countries:

- The Tibet AS γ Observatory, Yangbajing, Tibet, China
- Observatory for Highest Energy Cosmic Rays, Utah, U. S. A.
- Chacaltaya Observatory of Cosmic Physics, Mt. Chacaltaya, Bolivia

ICRR had held another oversea facility for the CANGAROO project, International Astrophysical Observatory near Woomera, Australia, which was closed in 2011.

Historical Remarks and Funding Sources

Brief histories are described for each group, including the financial view point. In general there are two channels for funding: the use of Grant-in-Aids from the Japan Society for the Promotion of Science (JSPS) by individual scientists, and the fund from the government revenue directly to the Institute through the University finance. The former applies to short term projects, say for 5 years with no guarantees beyond, and the latter to long-term projects that usually costs more than that defrayed by the former. The square parentheses indicate

present institute's personnel of each group. The current status and scientific goals of the projects are summarized in the table.

- **Super-Kamiokande**

The detector was constructed from 1991 to 1996, and data acquisition began in April 1996. Construction and operation costs are covered by funds provided by the government. Super-Kamiokande discovered atmospheric neutrino oscillations in 1998 and solar neutrino oscillations in 2001. The K2K (KEK to Kamioka) long-baseline accelerator experiment, operated from 1999 to 2004, confirmed the existence of atmospheric neutrino oscillations. Since full reconstruction work performed in 2005 and 2006, the detector has been running stably and high precision oscillation studies have been performed. The readout electronics and on-line data acquisition system were updated in 2008 to ensure stable operations over the longterm. [8 faculties + 7 research associates + 3 project research associates + 1 post-doctoral fellow]

- **T2K**

The Tokai-to-Kamioka (T2K) long-baseline accelerator neutrino experiment started in 2009. The SK detector functions as the far detector of the T2K experiment and ICRR is responsible for operating the far detector. Host institutes of the T2K experiment are KEK and ICRR. Based on data taken up until March 2011, the T2K collaboration announced an indication of electron neutrino appearance, and therefore non-zero θ_{13} , with a statistical significance of 2.5σ in June 2011. After the recovery of the J-PARC accelerator site from damage sustained in the earthquake, the T2K experiment resumed operations in March 2012. With data taken up until June 2012, the significance of the non-zero θ_{13} measurement has improved to 3.2σ . [7 faculties + 7 research associates + 3 project research associates]

- **XMASS**

XMASS project and its R&D study was initiated in 2000. Based on the study, the first prototype of the XMASS detector (100 kg fiducial mass) for dark matter search was designed and the construction started in 2007. The construction completed at the end of 2010 and subsequent commissioning run continued by June 2012. With the commissioning data, low-mass WIMPs, annual modulation of event rate, and axions were studied. In Aug. 2012,

detector refurbishment to reduce the surface background started. A next stage detector, XMASS1.5, started to be designed. The project is mainly supported by Grant-in-Aids of the Ministry of Education, Culture, Sports, Science and Technology. [4 faculties + 1 project associate professor + 3 research associates + 3 project research associates + 1 post-doctoral fellow]

- Hyper-Kamiokande R&D

The Hyper-Kamiokande (Hyper-K) detector is proposed as a next generation underground water Cherenkov detector. The detector is approximately 20 times larger in volume than Super-Kamiokande and has discovery potential of leptonic CP violation and proton decays. The recent evidence of $\nu_\mu \rightarrow \nu_e$ oscillation by the T2K boosts the expectation of discovery of CP violation by Hyper-K and accelerates Hyper-K R&D activities. New photosensor R&D and physics potential studies were initiated by two Grant-in-Aids for Scientific Research (B) in the past. [8 faculties + 7 research associates + 3 project research associates + 1 post-doctoral fellow]

- TA

The TA project received a fund by Grant-in-Aid for Scientific Research in Priority Areas (2003 - 2008) for its construction and commissioning. A continued fund for 5 years of operation (2009-2013) was granted as Grant-in-Aid for the Specially Promoted Research. The TA consists of a ground array of scintillation counters and fluorescence telescopes. The hybrid observation of cosmic ray air showers with TA started in May 2008, and has been maintained by the contributions of Japan, USA, Korea, Russia and Belgium. The TA collaboration confirmed GZK suppression with 3.9σ significance. Mass composition of cosmic rays above $10^{18.2}$ eV is consistent with proton. [2 faculties + 2 research associates + 2 project research associates + 3 project researchers + 2 technical specialists + 2 skilled assistants]

- CANGAROO

The second phase of this project, CANGAROO-II, was founded by a Grant-in-Aid for Priority Area Research from 1995 to 1998. With the CANGAROO-II 7 m telescope, TeV gamma-ray signals were first detected from some celestial objects such as the Galactic Center. The project was extended to the third phase (CANGAROO-III) by

a significant sum of money through a Grant-in-Aid for "COE (Centre of Excellence)" Research from 1999 to 2003, and then by a Grant-in-Aid for Scientific Research (A) for 2005–2008. The CANGAROO-III stereoscopic observation began in 2002 with the first two 10 m telescopes, one of which was the CANGAROO-II telescope upgraded to 10 m diameter. The full four telescope observation began in 2004, and ended in 2011. [2 faculties + 1 research associate]

- Tibet AS γ

The Tibet air shower array was constructed with gradual upgrades from 1988 to 2003, by the funds from Grants-in-Aid and from the government. It observed the Sun's shadow in the cosmic-ray flux in 1993, the all-particle energy spectrum around the knee energy region in 1996 and the TeV gamma-ray emission from the Crab nebula in 1999. Then, the TeV-100TeV cosmic-ray anisotropy was observed with high precision in 2006, where new anisotropy around the Cygnus region was discovered with some extended source candidates. The proton and helium energy spectra around the knee energy region was also measured with small systematic uncertainties in 2006. As a hybrid experiment, new air shower core detectors and large underground muon detectors are being constructed. [1 faculty + 1 research associate + 2 researchers + 1 technical staff]

- High Energy Astrophysics

This group was created recently in December 2009 with one faculty member. From April 2013 a new position in the rank of the research associate will be made available for this group by the administration of the University of Tokyo. The selection procedure for this position is now under way. The group has recently presented new insights into acceleration processes in turbulence, and environmental effects by gamma rays from magnetars. [1 faculty + 1 research associate to be assigned + 2 postdoctoral fellows]

- Ashra

Ashra was funded by the Coordination Fund for Promoting Science and Technology and Grant-in-Aid for Scientific Research since 2003. In 2004, University of Hawaii (UH) joined as a local host institute. After the state of Hawaii permitted the site use, the construction of light collectors in shelters on Mauna Loa was carried out in

2007. Since 2008, optical transient observation has started. Commissioning of astronomical tau neutrino search was performed. In 2011, the 10-year extension of the site use permit was granted. Since 2012, efficient physics observations for tau neutrinos, nucleons and optical transients have continued. [1 faculty + 1 research associate + 1 post-doctoral fellow + 1 technical staff]

- CTA R&D

CTA R&D program is financed by a Grant-in-Aid for Specially Promoted Research (2012-2016). The first CTA Large Size Telescope (LST) with a 23m dish will be constructed with this grant in the cooperation with Germany, Spain and France. CTA is the next generation ground-based gamma ray observatory and provides an order of magnitude higher sensitivity and wider energy coverage than currently working telescopes, H.E.S.S., MAGIC and VERITAS. CTA-Japan is planning to make a major contribution to the construction of CTA LSTs. [2 faculties + 1 research associate + 1 post-doctoral fellow]

- Gravitational Wave

TAMA 300 detector had been built to detect gravitational wave (GW) from nearby our Galaxy and operated at the highest sensitivity with the first stable operation in 2000. In order to realize practical detection of GW events by more sensitive detector, the Large-scale Cryogenic Gravitational wave Telescope (LCGT, nick-named as KAGRA in 2012) was planned for GW events within 200 Mpc and its funding was requested. The first demonstration of cryogenic thermal noise sensitivity by CLIO as of KAGRA prototype in 2010 lead the partial funding under a new category of government revenue funding, "Leading-edge Research Infrastructure Program", from 2010 to 2012 and the site excavation underground at Kamioka has been started in May, 2012. This project is supported by both KEK and NAOJ. [4 faculties + 1 research associate + 3 project research associates + 2 post-doctoral fellows + 5 technical staff(2 tenured + 3 project-oriented)]

- Observational Cosmology

Japanese SDSS key members moved to ICRR in 1996 with a Grant-in-Aid for Specially Promoted Area, and completed SDSS-I and II programs by 2008 with additional supports from JSPS and RES-CUE at the Physics Department. After the com-

pletion of SDSS, the ICRR group has started new observational cosmology programs mainly with Subaru Hyper Suprime-Cam (HSC) narrowbands (NBs) since July 2010 on the arrival of a new faculty member who wins a Grant-in-Aid for Scientific Research (A) for 2011-2014. Accordingly, the appointment of new research associate was made in April 2012. The commissioning of HSC is undertaken, and the HSC-NB survey is planned to start from 2013 for 5 years. [1 associate professor + 1 research associate + 2 project researchers]

- Primary cosmic ray

This group had been temporarily closed, but restarted with a new member in October 2008. Since then, prehistorical variability of incident galactic cosmic rays is studied using Accelerator Mass Spectrometry. It received a fund of Grants-in-Aid for Scientific Research (A) for 2010-2012. It confirmed the importance of heliospheric environment on terrestrial climate in 2010. [1 project research associate]

- Theory

Theory group has a long history, but there was a reset of the group in April 2001 owing to the retirement of the first group leader. A new group was established in 2002 with two faculty members, and one of the member served as the Director of the Institute for three years (2001-2004). Although one faculty member moved in June 2010, the group had a new faculty and recovered its full activity in February 2011. The group is currently studying theories beyond the standard model of particle physics and applying them to the early universe to understand the origin of matter and its fluctuations. [2 faculties + 3 post-doctoral fellow]

Summary of 2006-2012 Activities

Important events related to the ICRR's activity in 2006-2012 since the previous external review in 2006 are summarized below.

- Super-Kamiokande was rebuilt with the original photo-sensor coverage, and started the new phase of experiment, Super-Kamiokande-III, in 2006.
- The committee for the planning of the future ICRR research projects was formed in 2007. The report from this committee was released in 2008 (see appendix).

- The Telescope Array (TA) experiment for the highest energy cosmic ray studies started the observation in 2008.
- Super-Kamiokande-IV with the new electronics started in 2008.
- High energy astrophysics group, which studies various high-energy phenomena in the Universe theoretically, was formed at the end of 2009.
- The T2K (Tokai-to-Kamioka) long baseline experiment started data taking in 2010.
- The Institute for Cosmic Ray Research was selected as one of “Joint Usage / Research Center” in 2010.
- The construction of the Large scale Cryogenic Gravitational wave Telescope (its present name is KAGRA) was approved in 2010.
- The XMASS dark matter experiment started data taking in 2010.
- The Gravitational Wave Project Office was established on April 1, 2011.
- Due to the Earthquake in the Tohoku area, the central computer system of ICRR was partially shut-down for about half a year in order to minimize the usage of electricity.
- A part of the ICRR members (those of the Research Center for Cosmic Neutrinos and a part of the gravitational wave group) moved to the Kashiwa Research Complex 2 building in 2011.
- The T2K experiment published the indication for $\nu_{\mu} \rightarrow \nu_e$ oscillation in 2011.
- The CANGAROO experiment (Cherenkov TeV gamma ray telescope) finished the operation in 2011.
- The emulsion development system finished the operation in 2011.
- The first spring school on Universe and Elementary Particle was held in order to encourage graduate course studies in ICRR.
- The TA experiment published the sharp spectrum change in the highest energy cosmic rays, which is consistent with the expected GZK cut-off in 2012. This experiment also published the results on the isotropy of the highest energy cosmic ray flux.
- The committee for the planning of the future ICRR research projects was formed in 2012.

Details of above activities related to the research are described in the following sections.

Project status and main scientific goals

Neutrino and Astroparticle Division

Project	Status	Main Scientific Goals
Super-Kamiokande	running	Study of neutrino oscillations, proton decay, and astrophysical phenomena such as supernova burst
T2K	running	Precise measurement of neutrino oscillation parameters using SK with accelerator neutrino beam
XMASS	detector refurbishment	Direct search for dark matter with a liquid xenon detector
Hyper-Kamiokande	planned / R&D	Study of neutrino CP violation, proton decays and supernova neutrinos with a megaton water Cherenkov detector

High Energy Cosmic Ray Division

Project	Status	Main Scientific Goals
Telescope Array	running	Study of extremely-high energy cosmic rays; their origin, propagation and interaction
CANGAROO	completed	Study of non-thermal phenomena of very-high-energy gamma-ray sources in the southern hemisphere
Tibet AS γ	running	Study of origin, acceleration mechanism and modulation of high-energy cosmic rays
Ashra	running	Search for astronomical high-energy neutrino sources
CTA	planned / R&D	VHE Gamma Ray Astronomy, study of cosmic-ray origin, particle acceleration and indirect search for dark matter

Astrophysics and Gravity Division

Project name	Status	Main Scientific Goals
CLIO	commissioning	Prototype test of a cryogenic laser interferometer for gravitational wave detection and study its performance
KAGRA	under construction	Through detection of gravitational wave, study physics of gravitational waves and open gravitational wave astronomy
SDSS-II	completed	Mapping the local universe for cosmic structure formation, and measuring the cosmic expansion rate with supernovae
Subaru-HSC-NB	under development	Uncovering physical processes and history of cosmic reionization and early galaxy formation

NEUTRINO AND ASTROPARTICLE DIVISION

SUPER-KAMIOKANDE

Introduction

Super-Kamiokande(SK) is a 50kton water Cherenkov detector studying the physics of neutrinos, proton decay, and astrophysical phenomena such as supernova. Data taking started in April 1996 and atmospheric neutrino oscillations were discovered in 1998. Solar neutrino oscillations were discovered by a comparison of SK solar neutrino data with SNO charged current data in 2001. The first data phase of Super-K, SK-I, ran from April 1996 to July 2001. Due to an accident in 2001 about 60% of the PMTs in the detector were destroyed and the detector was reconstructed in 2002 using the remaining PMTs. Since the accident, the PMTs have been encased in acrylic and FRP (fiber-reinforced plastic) shells which prevent shock-wave production even if a single PMT implodes. With this setup the second data phase, SK-II, ran from December 2002 to October 2005. The missing PMTs were reproduced and full reconstruction of the detector was performed from October 2005 to July 2006.

This review covers the data taking period after the full reconstruction. As described below, high precision neutrino oscillation data were taken using both atmospheric and solar neutrinos during this period, and significant progress in the study of proton decay, supernova physics, and other physics targets has been achieved. The third data phase, SK-III, lasted from July 2006 to August 2008. To ensure stable operation over the long term and to improve the sensitivity of the detector, the electronics system was fully upgraded in September 2008.¹ Since this upgrade the fourth data phase, SK-IV, has been running.

Summary from 2006 to 2012

First of all, here summarized the noticeable achievements during the period of this review, i.e. after January 2006.

^{*1} Since the upgrade of the electronics and online systems was performed during the period of this review, details of the SK-IV electronics and the online system are described later (after the descriptions of the physics results).

- Due to the large statistics of atmospheric neutrino sample at SK and the small systematic error on the up/down ratio, we achieved most accurate measurement of θ_{23} mixing angle as $0.39 < \sin^2 \theta_{23} < 0.63$ at 90% CL. With the sophisticated event selection, the evidence of ν_τ appearance was observed with 3.8σ significance confirming that the atmospheric neutrino oscillations are predominantly through the $\nu_\mu \rightarrow \nu_\tau$ channel.
- High accuracy solar neutrino measurements were resumed after the Super-K full reconstruction. Because of improvements in the water circulation system, backgrounds to the analysis were reduced and the energy threshold was lowered to 4.0MeV. As a result the Super-K solar neutrino measurement provided better determination of θ_{12} mixing angle and the Δm_{21}^2 mass squared difference. Also, a direct measurement of the effect of matter on neutrino oscillations is in progress and a finite day/night asymmetry has already been observed at the 2.3σ level.
- The nucleon decay lifetime reached more than 10^{34} years for the $p \rightarrow e^+ \pi^0$ and $p \rightarrow \mu^+ \pi^0$ decay modes. These limits were original goal when the Super-K proposal was written. Searches for other decay modes were also performed.
- SK has been searching for galactic supernovae with the efforts to minimize the dead time. A flux upper limit of supernova relic neutrinos(SRN) was obtained using all data from SK-I to III that has reached within a factor of model predictions. In order to detect the SRN signal, tagging neutrons is necessary. For this purpose, a small-scale gadolinium loaded water Cherenkov detector has been constructed.
- New electronics using the state-of-the-art technology were installed in 2008. At the same time, the online data acquisition system was also replaced using high speed digital data transfer technology. This new online sys-

phase	SK-I	SK-II	SK-III	SK-IV
start	Apr. 1996	Sep. 2002	Jul. 2006	Sep. 2008
end	Jul. 2001	Oct. 2005	Aug. 2008	continuing
ID PMTs (photo coverage)	11,146 (40%)	5,182 (19%)	11,129 (40%)	11,129 (40%)
OD PMTs	1,885	1,885	1,885	1,885
electronics	ATM	ATM	ATM	QBEE
trigger	hardware	hardware	hardware	software

Table 1. Data taking phases of Super-Kamiokande.

tem reads all detector channels unconditionally and an event trigger is applied afterwards. This method enabled us to collect all hit information without any data loss, which is essential for rare data such as T2K beam events and supernova burst events.

Atmospheric Neutrinos

Neutrino oscillation was discovered in the study of atmospheric neutrinos in SK in 1998 [5]. Two flavor $\nu_\mu \rightarrow \nu_\tau$ oscillation hypothesis successfully describe the SK atmospheric neutrino data with maximum mixing angle ($\theta_{23}=\pi/4$). Recently the mixing angle between the first and third generations (θ_{13}) has been measured by the accelerator (T2K ², MINOS ³) and reactor neutrino experiments (Double CHOOZ ⁴, Daya-bay ⁵, RENO ⁶). $\nu_\mu \rightarrow \nu_e$ oscillation channel due to the finite value of θ_{13} will provide us the opportunity to probe the unknown properties such as CP violation and mass hierarchy in lepton sector, which may be a hint for solving the origin of the matter.

The work of the SK group during 2006 and 2012 were mainly devoted to the quest for the above ν_e oscillation. We have analyzed the atmospheric neutrino data accumulated of SK-I+II+III+IV (1489+799+518+1097 days for full-contained (FC) / partially-contained (PC) and 1646+828+636+1097 days for upward-going muons). We studied oscillation effects in all types of data that are categorized into FC events, PC events, and upward-going muons. FC events are characterized by the primary vertex position that

is located inside the 22.5 kton fiducial volume of the detector and all the visible secondary particles stopped in the inner detector. PC events have the primary vertex position in the fiducial volume but at least one charged particle escaping from the inner detector. In most cases, the escaping particle is a muon. Upward-going muons originate from high energy muon-neutrino interactions in the rock surrounding the detector. Only the muon traveling through the detector upward is identified.

FC sample are divided into sub-GeV and multi-GeV according to the visible energy, and also separated into electron-like and muon-like events by particle identification algorithm. Though it is difficult to distinguish neutrino and antineutrino interactions on an event-by-event basis in the water Cherenkov detector, the statistical separation between ν_e and $\bar{\nu}_e$ in multi-GeV sample are carried out by using the difference of their kinematics properties at interactions in order to improve the sensitivity of the mass hierarchy determination.

Figure 1 compares the zenith angle and lepton momentum distributions of the atmospheric neutrino data with Monte Carlo (MC) expectations with and without neutrino oscillations for FC, PC and upward-going muon events. This demonstrates that the presence of neutrino oscillation, and the atmospheric neutrino data is consistent with $\nu_\mu \rightarrow \nu_\tau$ in a wide energy range from sub-GeV to several 10 TeV energy range. Figure 2 shows the allowed regions of neutrino oscillation parameters obtained by two flavor $\nu_\mu \rightarrow \nu_\tau$ oscillation and three flavor oscillation. Though the allowed region by three flavor oscillation is slightly extended compared to those by two flavor oscillation due to additional uncertainties of other oscillation parameters, they are consistent with the results from accelerator experiments.

*² K. Abe *et al.* (T2K), Phys. Rev. Lett. 107, 041801 (2011)

*³ P. Adamson *et al.* (MINOS), Phys. Rev. Lett. 107, 181802 (2011)

*⁴ Y. Abe *et al.* (Double Chooz), Phys. Rev. Lett. 108, 131801 (2012)

*⁵ F. P. An *et al.* (Daya Bay), Phys. Rev. Lett. 108, 171803 (2012)

*⁶ J. K. Ahn *et al.* (RENO), Phys. Rev. Lett. 108, 191802 (2012)

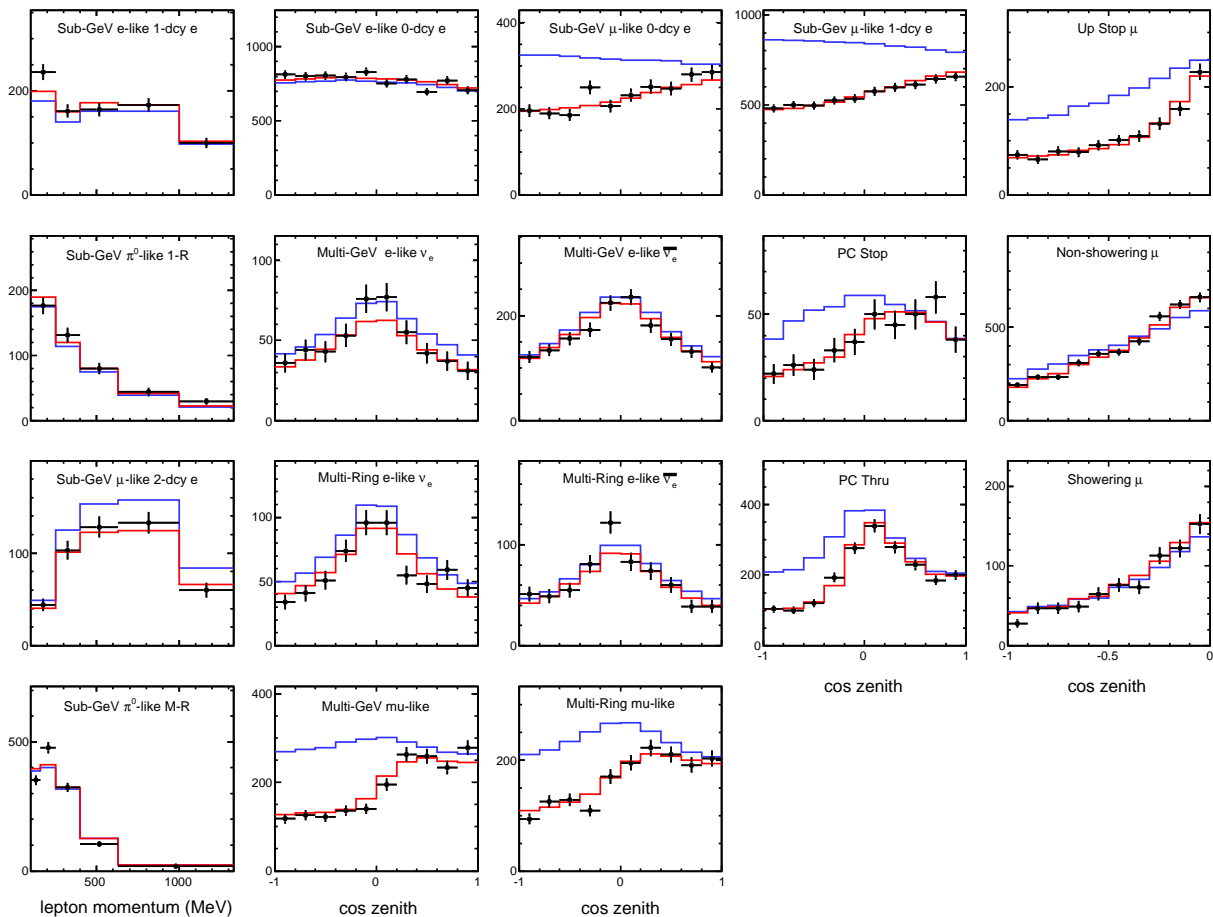


Fig. 1. The zenith angle and lepton momentum distributions for atmospheric neutrino events observed in Super-Kamiokande-I+II+III+IV. In zenith angle distributions, $\cos\Theta = 1(-1)$ corresponds to vertically down-going (up-going) direction. Points with error bars are data with statistical error. The blue histograms show the MC predictions without neutrino oscillation and the red histograms show the MC predictions for $\nu_\mu \rightarrow \nu_\tau$ 2-flavor oscillation with $\sin^2\theta=0.99$ and $\Delta m^2=2.3\times 10^{-3}\text{eV}^2$.

Full parameter oscillation analysis

We aimed at probing the unknown oscillation parameters, such as leptonic CP violation and mass hierarchy, by measuring $\nu_\mu \rightarrow \nu_e$ oscillation other than $\nu_\mu \rightarrow \nu_\tau$ oscillation in the atmospheric neutrino data. Several effects as listed below will be expected based on the standard three flavor oscillation framework:

- A resonant enhancement by the matter effect is expected in $\nu_\mu \leftrightarrow \nu_e$ oscillation driven by θ_{13} in the 5 to 10 GeV energy range. This effect will be observable as an excess of electron-like events in the upward-going direction, and to some degree in the oscillations of multi-GeV muon-like events.
- The above ν_e enhancement is selective for either ν_e or $\bar{\nu}_e$ depending on mass hierarchy.
- The effects of the solar oscillation parameters

and non-maximal mixing are observable as a ν_e oscillation effect on the event rate of the Sub-GeV electron-like samples.

- If the CP violating term δ_{CP} is also considered, there are additional sub-dominant oscillation effects predicted across many of the SK atmospheric neutrino samples.

We have performed an extended oscillation analysis including all the mixing parameters and the CP violating term, δ_{CP} . In the oscillation analysis, the matter effect in the Earth is considered, and both the normal and inverted mass hierarchies are tested. In order to consider the θ_{13} constraint according to the recent precise measurements by the reactor experiments, θ_{13} is fixed to be $\sin^2\theta_{13}=0.025$.

Table 2 shows the oscillation parameters at the global best fit point and their allowed ranges for each hierarchy assumption.

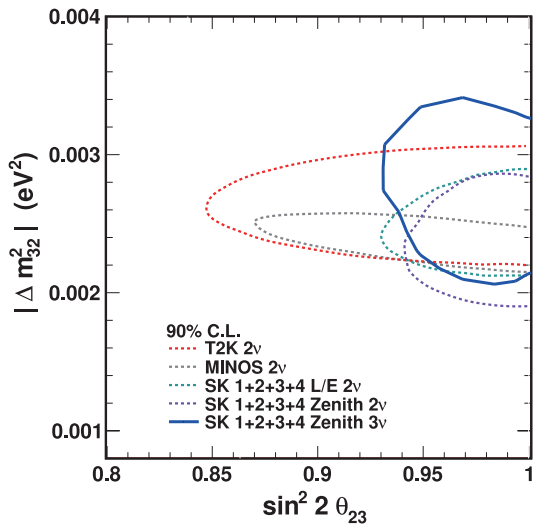


Fig. 2. Allowed oscillation parameter regions of 90% confidence levels obtained by oscillation analyses based on the Super-Kamiokande-I+II+III+IV data. The regions allowed by SK L/E analysis, $\nu_\mu \rightarrow \nu_\tau$ two flavor oscillation analysis, and full parameter three flavor oscillation analysis are shown along with T2K, MINOS results.

	Normal		Inverted	
	best fit	90% C.L.	best fit	90% C.L.
$\Delta m_{32}^2 (\times 10^{-3} \text{eV}^2)$	2.66	2.06 - 3.04	2.66	2.14 - 3.04
$\sin^2 \theta_{23}$	0.425	0.391 - 0.619	0.575	0.393 - 0.630
δ_{CP}	300°	all allowed	260°	all allowed

Table 2. Oscillation parameters at best fit and of 90% C.L. allowed region obtained by three flavor oscillation analysis for normal and inverted hierarchy assumptions, respectively. The oscillation fits are performed with the constraint of $\sin^2 \theta_{13}=0.025$.

Figure 3 shows $\Delta\chi^2$ as a function of $\sin^2 \theta_{23}$ and δ_{CP} parameters with normal and inverted hierarchy assumptions, respectively. Still CP violation parameter and octant of $\sin^2 \theta_{23}$ cannot be constraint more than 90% C.L., however some indications on those parameters can be seen. $\sin^2 \theta_{23}$ at best fit point is slightly deviated from the maximal mixing ($\theta_{23}=\pi/4$). The second octant of $\sin^2 \theta_{23}$ is favored in inverted hierarchy while the first octant becomes preferred by introducing θ_{13} constraint in normal hierarchy. The large region of δ_{CP} is preferred for both hierarchy assumptions.

Figure 4 shows the comparison of fitted χ^2 value as a function of δ_{CP} between normal and inverted hierarchy assumptions. The global minimum χ^2 value is slightly smaller for inverted hierarchy by 1.2.

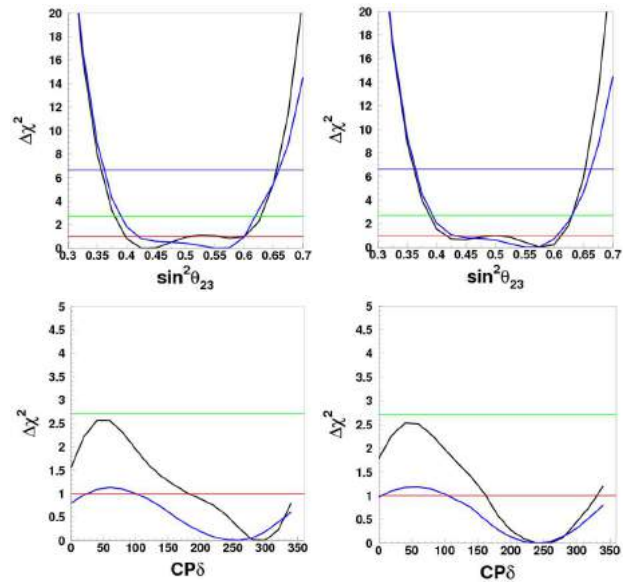


Fig. 3. Upper figures show distributions of $\Delta\chi^2$ versus $\sin^2 \theta_{23}$, and lower figures show $\Delta\chi^2$ versus δ_{CP} , for normal (left) and inverted (right) hierarchy assumption. $\Delta\chi^2$ means the difference from the minimum χ^2 among the oscillation fits in each hierarchy assumption. Black and blue curves show the distributions with and without reactor θ_{13} constraint, respectively. The region below red (green) line is allowed by 68% (90%) confidence level.

CPT violation test

It becomes possible to search for CPT violation effects in the neutrino system via differences in the oscillation probabilities of neutrinos and antineutrinos. By inspiring oscillation result by MINOS⁷, we also performed a CPT violation test of the atmospheric neutrino data using separated two-neutrino disappearance model, which allows neutrino and antineutrino to oscillate with different parameter sets of $(\Delta m^2, \theta)$ and $(\Delta \bar{m}^2, \bar{\theta})$, respectively. According to the fitting result, the allowed region for antineutrino mixing parameters is shown in Figure 5. The atmospheric mixing parameters for antineutrino oscillations are consistent with those for neutrinos and therefore no evidence for CPT violation is found.

Search for ν_τ interactions

Tau events, which are produced via ν_τ charge current (CC) interactions oscillated from ν_μ , are expected to be observed in SK. It would bring the direct evidence of $\nu_\mu \rightarrow \nu_\tau$ oscillation, however, the detection of ν_τ CC events in SK is challenging; the interaction rate of ν_τ charged current events is low

*7 P. Adamson *et al.* (MINOS), Phys. Rev. Lett. 107, 021801 (2011)

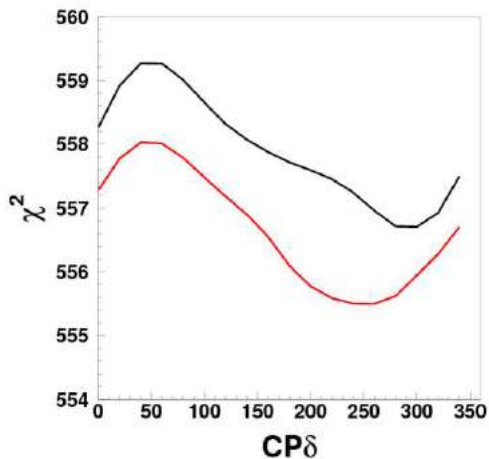


Fig. 4. χ^2 distributions as a function of CP violating term, δ_{CP} for normal (black) and inverted (red) hierarchy assumption. In each δ_{CP} point, other oscillation parameters are marginalized with fixed θ_{13} .

since the neutrino energy threshold is 3.5 GeV and the atmospheric neutrino flux above this energy is relatively low. Also tau events are difficult to be identified individually because they tend to produce multiple particles. Tau analysis is performed employing neural network technique to discriminate tau events of hadronic decay from backgrounds of atmospheric ν_e and ν_μ events [62]. Figure 6 shows the zenith angle distribution of tau-selected events. Tau events are expected to appear in the upward-going events because they originate $\nu_\mu \rightarrow \nu_\tau$ oscillation. The zenith angle shape of data is fitted with the MC expectation including tau signal and background with their normalizations free. According to the fitting result, the signal excess is estimated to 180.1 ± 4.3 (stat) $^{+17.8}_{-15.2}$ (syst) events compared to an expectation of 120.2 $^{+34.2}_{-34.8}$ (syst) and the detection significance correspond to 3.8σ level.

Search for WIMP annihilation in the Sun

From recent observations, Weakly Interacting Massive Particles (WIMPs) are considered a favorite candidate for cold dark matter. From the viewpoint of minimum supersymmetric extensions of the Standard Model, the most well-motivated candidate for WIMPs in the universe is the lightest supersymmetric neutral particle (LSP). One method of searching for a WIMP dark matter signal is an indirect search where decay or annihilation products from WIMPs are observed as originating from the center of a gravitational potential well such as a celestial body. WIMP annihilation products in the

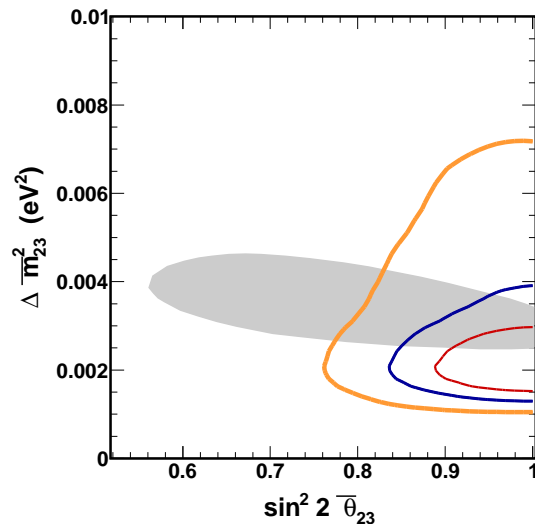


Fig. 5. Allowed regions for the antineutrino mixing parameters for SK-I+II+III data set. The 68%, 90%, and 99% allowed region appear in red thin, blue medium, and orange thick lines, respectively. The shaded region shows the 90% C.L. allowed region for antineutrino disappearance in an antineutrino beam from MINOS.

form of muon-neutrinos are an excellent instrument for indirect searches since they can pass through the matter of the Sun, and interact in the Earth. Here we investigate upward-going muons (upmu) which are generated from high energy neutrinos come from the WIMP annihilations using Super-Kamiokande [57]. We search in the direction of the Sun, and an excess of neutrino flux above the atmospheric neutrino background is sought in the upmu events. Although volume array detectors such as IceCube have larger acceptances for higher mass WIMPs, SK is better equipped for the search of lower mass WIMPs (<100 GeV) due to its lower energy threshold for neutrino signals. The calculated upper limit is shown in Fig. 7 with the results from direct detection experiments.

Other studies

A number of new analyses conducted in the last 5 years includes non-standard oscillation (NSI) [56], matter-dependent oscillation [46], search for Q-balls [43], search for astrophysical neutrino point source [52, 41], diffuse neutrino flux in ultra-high energy [40], GRB 080319B [51], and analysis using new technique of proton identification [50].

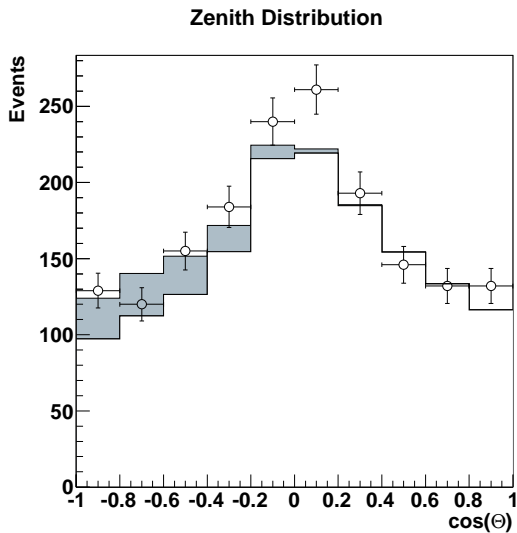


Fig. 6. Zenith angle distribution of tau-selected events by neural network method for SK-I+II+III dataset. Zenith angle $\cos(\theta)=-1$ (1) indicates upward-going (downward-going) direction. The data (dot with error bar) and the best-fit MC including tau signal (shaded region) and background from atmospheric neutrinos (ν_e and ν_μ) are shown.

Future prospect

We plan to continue studies of sub-leading neutrino oscillation by improving the analysis method in neutrino and anti-neutrino separation and reducing systematic errors on the hadronic events in multi-GeV energies. The mass hierarchy determination by the atmospheric neutrinos is important for the future project of water Cherenkov detector, such as Hyper-Kamiokande. Also neutrino and antineutrino separation could be improved in sub-GeV energies by studying 2.2 MeV gammas which emitted by the capture of the recoil neutron in water.

Solar Neutrinos

SK detects solar neutrinos through neutrino-electron elastic scattering, $\nu + e \rightarrow \nu + e$, where the energy, direction, and time of the recoil electron are measured. Due to its large (22.5 kiloton) fiducial mass SK makes precise measurements of ^8B solar neutrinos, including precision information on their energy spectrum and its time variation. To achieve these measurements, precise calibrations using both an electron LINAC [6] and ^{16}N radioisotopes generated by a deuterium-tritium neutron generator[13] are employed to determine the Super-K energy scale, energy and angular resolution, and the vertex position resolution with high

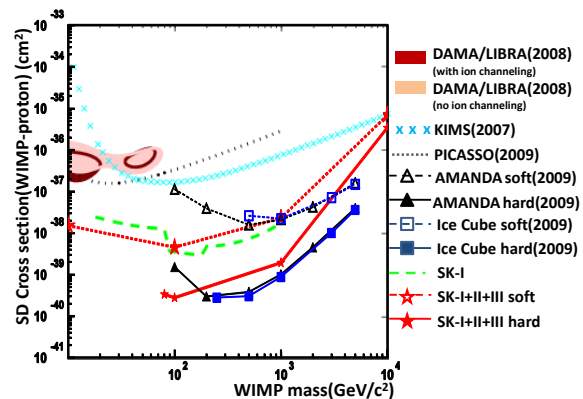


Fig. 7. Limit on the WIMP-proton spin-dependent cross section as a function of WIMP mass. Limits from direct detection experiments: DAMA/LIBRA allowed region (dark red and light red filled, for with and without ion channeling, respectively), KIMS (light blue crosses), and PICASSO (grey dotted line) are shown. Also we show here the results of indirect detection (neutrino telescopes): AMANDA (black line with triangles), IceCube (blue line with squares), and this analysis (red line with stars). Two annihilation scenarios, soft channel ($b\bar{b}$) and hard channel (W^+W^-), are considered. Also the previous limit from Super-K (green dashed line) is shown.

precision.

By the year 2006, a solar neutrino oscillation scenario had been established by the solar neutrino experiments (SK, SNO, and radio chemical experiments) and the KamLAND reactor experiment. The next step then for solar neutrino measurements is the precise determination of the oscillation parameters and the role of matter therein. For that purpose, SK has been collecting high statistics solar neutrino data to attempt measurements of a day-night flux difference and a distortion of the energy spectrum.

Since SK-III started, many efforts have been made to reduce backgrounds and to increase the precision of the detector calibrations, both of which are crucial for solar neutrino measurements. The most serious background comes from the beta decay of ^{214}Bi , which is produced in the decays of radon in the air and detector materials (PMT glass and FRP(fiber reinforced plastic) cases) as well as from radium in the water. In order to reduce the ^{214}Bi background, the SK water system was upgraded. First, a new reverse osmosis unit was added to further reduce the radium content of the water. Second, a new heat exchanger was added to supply water without inducing convection in the tank, which transports radon near the PMTs into the fiducial volume. Third, new membrane degasifier units

were added to increase the efficiency of radon removal from the supply water. Additionally, the water flow in the detector was precisely investigated and optimized to reduce the the background contamination in the fiducial volume as much as possible. During the SK-IV period we have introduced a precise temperature control system for the inlet water to further reduce convection in the water. As a result of these improvements, the background rate in the lower energy region (below 6 MeV) in SK-IV has been reduced by a factor of more than three compared to the SK-I period. Further, it has allowed a lower analysis energy threshold: down to 3.5 MeV from 4.5 MeV of kinetic energy.

In the analysis of SK-III and SK-IV data the event reconstruction tools and the detector simulation were improved. The timing offset of each PMT was updated using precise calibration of the readout electronics and the systematic shift of the reconstructed vertex position from its true position has been reduced. Further, the position dependence of the water transparency within the tank has been implemented in the detector simulation. Additionally, the reflectivity of the sheeting that optically separates the inner detector from the outer detector, was carefully measured and updated. Because of these improvements, the systematic error on the flux measurement has been improved as described in detail below.

Up until the end of March 2012, 1069.3 days of SK-IV solar neutrino data for analysis was taken. One of the most important improvements has been the reduction of the energy threshold, which now triggers at 100% efficiency at 4.0 MeV electron kinetic energy. A clear solar neutrino signal in the 3.5-4.0 MeV energy region can also be seen at more than 7σ as shown in Fig.8. This success was achieved as a result of the background reduction efforts described above. The systematic uncertainty on the total flux in the energy region between 4.0 and 19.5 MeV during SK-IV becomes $\pm 1.7\%$, which is nearly half that of the SK-I period, $^{+3.5}_{-3.2}\%$ [38]. This reduction comes from improvements in the uncertainty of the fiducial volume size ($\pm 1.3\%$ in SK-I, $\pm 0.17\%$ in SK-IV), better understanding of the absolute energy scale ($\pm 0.64\%$ in SK-I, $\pm 0.54\%$ in SK-IV), and careful studies of the data reduction. During SK-IV the measured ^8B flux is $2.34 \pm 0.03(\text{stat.}) \pm 0.04(\text{sys.}) \times 10^6 \text{cm}^{-2}\text{s}^{-1}$, which is consistent with previous measurements

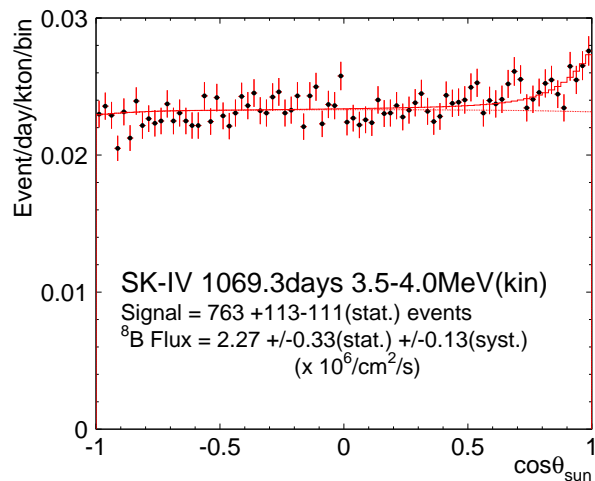


Fig. 8. Solar angle distributions of 1069.3 days SK-IV data sample with energy between 3.5-4.0 MeV.

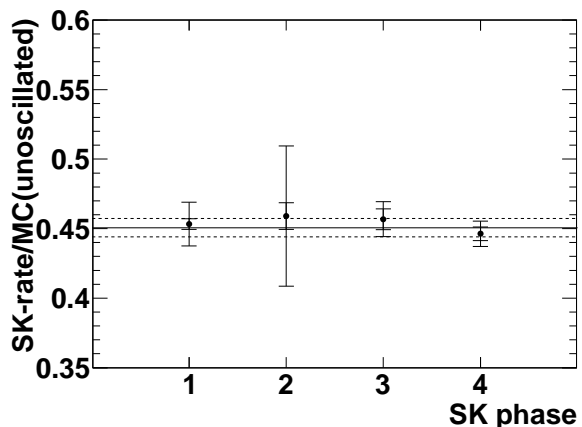


Fig. 9. Solar neutrino flux measurements from SK-I to SK-IV with statistic and systematic errors and normalized to the unoscillated MC prediction using a ^8B flux of $5.25 \times 10^6 / \text{cm}^2/\text{sec}$. The dashed lines show the averaged over all phases.

from SK-I, II, and III and is shown in Fig.9.

The measured energy spectrum from SK-III and SK-IV is shown in Fig.10(top and middle), respectively. The vertical axis shows the ratio of the observed energy spectrum to the expectation from the unoscillated MC simulation assuming a ^8B flux of $5.25 \times 10^6 / \text{cm}^2/\text{sec}$. Fig.10(bottom) shows SK-I to SK-IV combined energy spectrum with expectations from the solar global and solar+KamLAND as well as flat reduction of the neutrino spectrum. The combined energy spectrum is consistent with the flat prediction, but the level of favoring flat over the upturn is $1.1 \sim 1.9\sigma$ level.

Concerning differences in the day and night fluxes the expected flux asymmetry, defined as

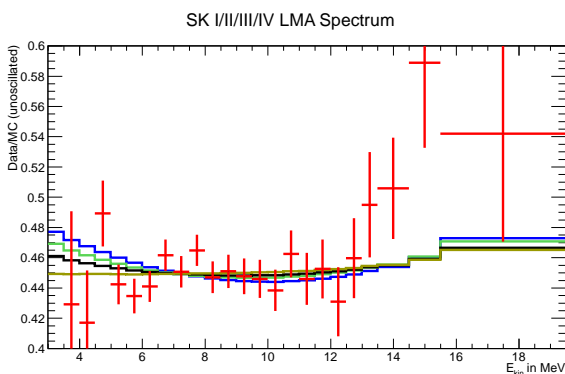
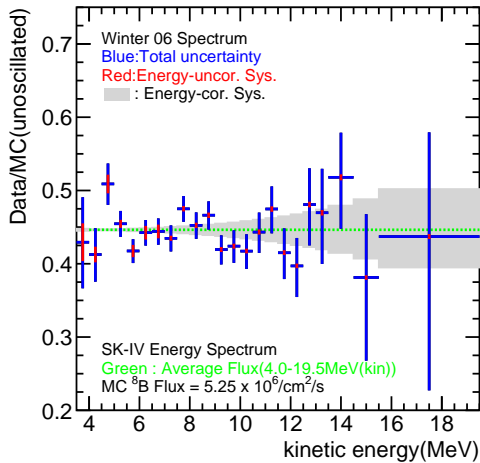
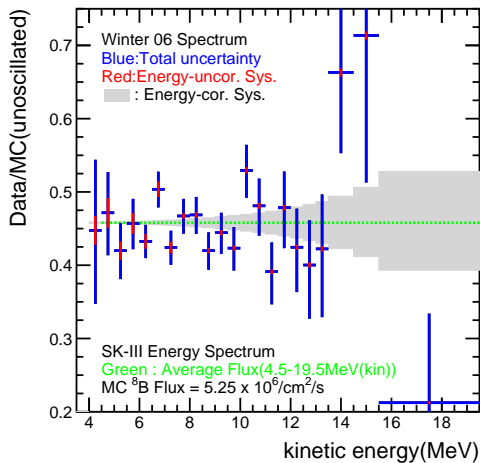


Fig. 10. SK-III(top) and SK-IV(middle) solar neutrino energy spectrum. Each point shows the ratio of the data to the expected flux using an unoscillated ^8B solar neutrino spectrum. The bottom shows the spectrum combined SK-I to SK-IV with predictions for (1) $\sin^2\theta_{12} = 0.304$ and $\Delta m_{21}^2 = 7.4 \times 10^{-5} \text{eV}^2$ (blue), (2) $\sin^2\theta_{12} = 0.314$ and $\Delta m_{21}^2 = 4.8 \times 10^{-5} \text{eV}^2$ (light blue), (3) flat probability (black), and (4) flat probability and $d\sigma/dE$ shape for pure $\nu_e + e$ scattering (blond)

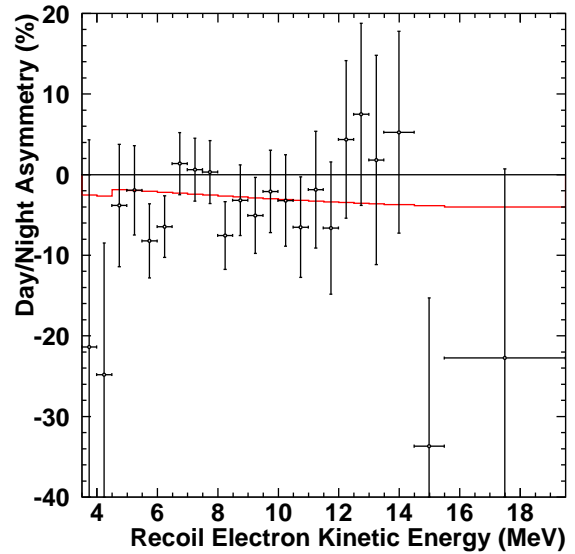


Fig. 11. The day-night asymmetry as a function of energy in the combined SK-I,II,III and IV data. The red line shows the predicted amplitude assuming neutrino oscillations with $\sin^2\theta_{12} = 0.314$ and $\Delta m_{21}^2 = 4.8 \times 10^{-5} \text{eV}^2$.

$A_{DN} = (\text{day} - \text{night}) / \frac{1}{2}(\text{day} + \text{night})$, is about 2% based on current understanding of neutrino oscillation parameters. Although this is not a large effect, long term observations by SK enable discussion of a finite value of the day-night asymmetry. The A_{DN} value using the combined SK-I to SK-IV data is $-2.8 \pm 1.1 \pm 0.5\%$, which is a 2.3σ difference from zero. Fig.11 shows the A_{DN} distribution as a function of energy. The day-night asymmetry is obtained by fitting the observed time variation during the night with its expected variation, meaning that A_{DN} depends on the assumed value of Δm^2 . Fig.12 shows A_{DN} as a function of Δm^2 together with the expectation. The observed A_{DN} is consistent with the expectation using the best fit Δm^2 from both KamLAND and the global solar analysis.

A global solar neutrino oscillation analysis has been performed including all SK data (SK-I[38],SK-II[47], SK-III[55], and SK-IV) as well as the most recent results from SNO⁸, the radiochemical experiments^{9, 10} and the latest ^7Be flux measurement from Borexino¹¹. This analysis was then compared and combined with the reactor neutrino results from KamLAND¹². The green contours in

^{*8} B. Aharmim et al., arXiv:1109.0763 [nucl-ex]

^{*9} Bruce T. Cleveland et al., Astrophys. J. 496 (1998) 505

^{*10} J. N. Abdurashitov et al., Phys. Rev. C80 (2009) 015807

^{*11} G. Bellini et al., Phys. Rev. Lett. 107 (2011) 141302

^{*12} A. Gando et al., Phys. Rev. D83 (2011) 052002

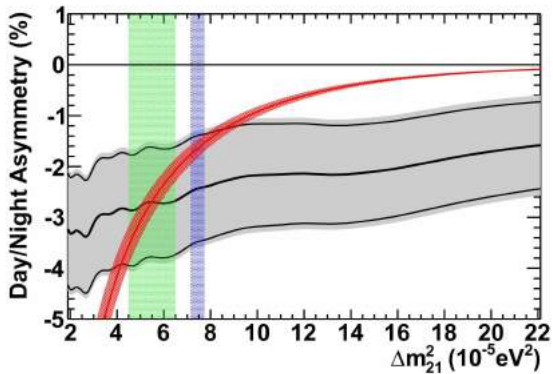


Fig. 12. The day-night asymmetry as a function of Δm^2 . A thick black line shows the result of the SK fit and the surrounding gray band indicates statistical and systematic uncertainty (thin black lines for statistical error only). The red curve shows the expectation assuming $\sin^2(\theta_{12}) = 0.314$. The light blue and light green vertical bands show the allowed range of Δm^2 from the KamLAND reactor and solar global, respectively.

Fig.13 show the allowed region of the neutrino oscillation parameters $\sin^2\theta_{12}$ and $\sin^2\theta_{13}$ in $1-\sigma$ steps from 1 to 5 σ . The obtained range of $\sin^2\theta_{13}$ from the solar global analysis is $0.014^{+0.027}_{-0.021}$, while the value of the KamLAND reactor analysis is $0.031^{+0.038}_{-0.036}$. The dependence of neutrino oscillations on θ_{12} and θ_{13} are different for solar neutrinos and reactor neutrinos because of the existence of matter effects in the higher energy part of the solar neutrino spectrum. For this reason their combination could give more sensitivity to θ_{13} . In the combined fit $\sin^2\theta_{13}$ was found to be $0.030^{+0.017}_{-0.015}$, which is a roughly 2 σ hint that θ_{13} is different from zero. This hint has been discussed prior to 2010¹³[55]. After 2011, the T2K, Double Chooz, Daya Bay, and Reno experiments presented indications and later evidence for a finite θ_{13} . The combination of their measurements yields $\sin^2\theta_{13} = 0.025^{+0.003}_{-0.004}$ and the result of the combined analysis of the global solar and KamLAND reactor data is consistent with this value. Figure 14 shows the allowed region of neutrino oscillation parameters in the Δm^2_{21} and $\sin^2\theta_{12}$ plane assuming $\sin^2\theta_{13}$ is fixed at 0.025. The obtained parameters from the global solar analysis are $\Delta m^2_{21} = (4.86^{+1.44}_{-0.52}) \times 10^{-5} \text{eV}^2$ and $\sin^2\theta_{12} = 0.310^{+0.014}_{-0.015}$. Comparing these values with those from KamLAND, ($\Delta m^2_{21} = (7.49^{+0.20}_{-0.19}) \times 10^{-5} \text{eV}^2$ and $\sin^2\theta_{12} = 0.309^{+0.039}_{-0.029}$),

*¹³ G. L. Fogli, E. Lisi, A. Marrone, A. Palazzo, and A. M. Rotunno, Phys. Rev. Lett. 101(2008) 141801

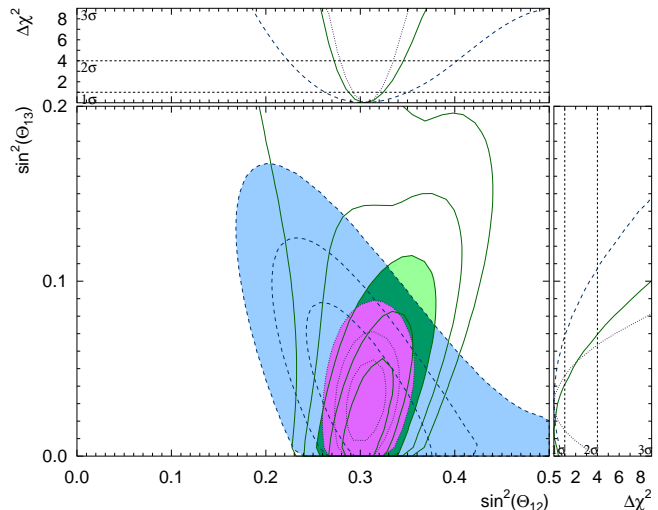


Fig. 13. Allowed regions of the neutrino oscillation parameters $\sin^2\theta_{12}$ and $\sin^2\theta_{13}$ from the global solar neutrino analysis (green) and the KamLAND reactor neutrino data (light blue). The purple region shows the contour from the combined global solar and KamLAND reactor analyses. Curves are drawn for each $1-\sigma$ step between 1 and 5 σ for the global solar analysis, and $1-3\sigma$ for the KamLAND and solar+KamLAND regions. Contours at 3 σ are filled with their colors.

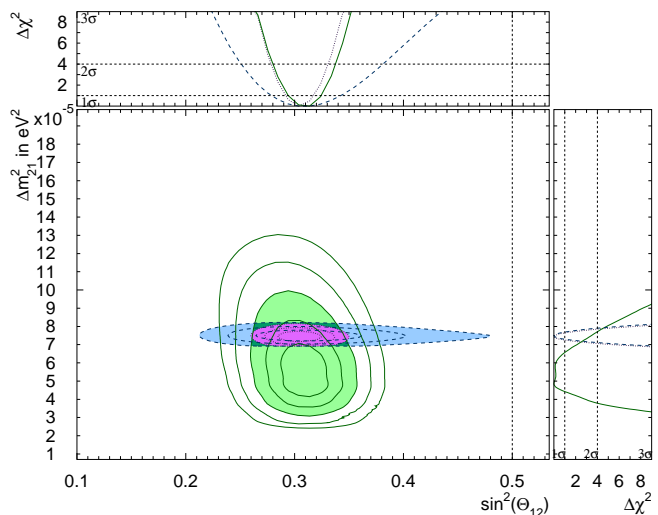


Fig. 14. Allowed regions of neutrino oscillation parameters in the Δm^2_{21} and $\sin^2\theta_{12}$ plane with $\sin^2\theta_{13}$ fixed at 0.025 from the global solar neutrino analysis (green) and the KamLAND reactor neutrino data (light blue). The purple area shows the combined contour of the global solar and the KamLAND reactor analyses. The curves are drawn for each $1-\sigma$ step from 1-5 σ for the global solar, and from 1-3 σ for the KamLAND and solar+KamLAND results. Contours at 3 σ are filled with their colors.

	Δm_{21}^2 (10^{-5}eV^2)	$\sin^2 \theta_{12}$
Super-K with ${}^8\text{B}$ flux from SNO NC	$4.69^{+1.80}_{-0.83}$	$0.339^{+0.028}_{-0.024}$
Solar global	$4.86^{+1.44}_{-0.52}$	$0.310^{+0.014}_{-0.015}$
KamLAND reactor	$7.49^{+0.20}_{-0.19}$	$0.309^{+0.039}_{-0.029}$
Solar + KamLAND	$7.44^{+0.20}_{-0.19}$	0.304 ± 0.013

Table 3. Neutrino oscillation parameters of Δm_{21}^2 and $\sin^2 \theta_{12}$ obtained by Super-K, solar global analysis, KamLAND reactor, and solar+KamLAND. $\sin^2 \theta_{13}$ is fixed at 0.025.

there is a 1.8σ level tension in the Δm_{21}^2 results, which is evident in the figure. Combining the global solar data with KamLAND, the oscillation parameters become $\Delta m_{21}^2 = (7.44^{+0.20}_{-0.19}) \times 10^{-5} \text{eV}^2$ and $\sin^2 \theta_{12} = 0.304 \pm 0.013$. Obtained values of those oscillation parameters are summarized in Table 3.

Summary and future prospects

High accuracy solar neutrino measurements were resumed after SK-III. Because of improvements in the water circulation system, the background in the low energy region was reduced by a factor of more than three and the energy threshold for the oscillation analysis was lowered to 4.0 MeV. And solar neutrino signals are observed even at 3.5–4.0 MeV energy bin in SK-IV. The measured energy spectrum from SK-III and SK-IV are consistent with flat, but the level of favoring flat spectrum over the predicted upturn from the oscillation is $1.1 \sim 1.9 \sigma$ level. The day/night asymmetry value using the combined SK-I to SK-IV data is $-2.8 \pm 1.1 \pm 0.5\%$, which is a 2.3σ difference from zero.

The combined analysis of the global solar and the KamLAND reactor gave 2σ level hint of the finite θ_{13} . Although mixing angle of global solar and KamLAND reactor are consistent with the finite θ_{13} , there is about 1.8σ -level tension in Δm_{21}^2 between them.

The energy spectrum and day/night asymmetry are quite important for understanding the matter effect of the neutrino oscillation. The solar neutrino measurement at SK will continue, and those measurements will be discussed with meaningful statistical significance with further increase of the SK-IV

data.

Nucleon Decay Searches

Nucleon decay search gives us a unique window to test Grand Unified Theories (GUTs) of elementary particles. Super-Kamiokande (SK) is the world's largest detector to search for nucleon decays and it has accumulated data of 91.7 kt-yr (SK-I), 49.2 kt-yr (SK-II), 31.9 kt-yr (SK-III), and 46.5 kt-yr (SK-IV until March 2011), resulting in 220kt-yrs of data in total. Various nucleon decay modes have been searched for in SK, but no significant signal has been seen so far, as is shown in Table 4. The lifetime limits reached more than 10^{33} years in important decay modes, especially, the limits for $p \rightarrow e^+ \pi^0$ and $p \rightarrow \mu^+ \pi^0$ have exceeded the original goals written in the SK proposal. The new electronics introduced from SK-IV made improvement in selection efficiency of $p \rightarrow \mu^+ \pi^0$ and $p \rightarrow \bar{\nu} K^+$ by increasing tagging efficiency of Michel electron from muon. We describe the detail of these important modes.

The proton decay into one positron and one neutral pion ($p \rightarrow e^+ \pi^0$) is the one that occurs in a large number of theoretical models. This decay mode is mediated by super-heavy gauge bosons. Discovery of a signal would give us information about the mass of the gauge bosons, M_X , because the proton lifetime is predicted to be proportional to M_X^4 . To discriminate the signal from atmospheric neutrino background, we reconstruct the total visible energy and total momentum corresponding to the parent proton mass and the proton's Fermi momentum in oxygen, respectively. Although the photo coverage area in SK-II is about half that of other period (19 % for SK-II and 40 % for the others), we achieved almost same efficiency and background rate as those of the other period. This fact has impact on designs of future water Cherenkov detectors such as Hyper-Kamiokande. Because there are no candidate events in the combined SK-I + SK-II + SK-III + SK-IV data (220kt-yrs), we obtained a lower limit on the partial lifetime of the proton: $\tau/B_{p \rightarrow e^+ \pi^0} > 1.3 \times 10^{34}$ years at a 90% confidence level.

$p \rightarrow \mu^+ \pi^0$ mode was also analyzed by using 220kt-yrs data. In SK-IV period, we updated the electronics and it can record every hit in the detector without dead time. As a result, the detec-

mode	expo- sure ($kt \cdot yr$)	ϵB_m (%)	obser- ved event	B.G.	τ/B limit ($10^{33} yrs$)
$p \rightarrow e^+ \pi^0$	220	44-45	0	0.5	13
$p \rightarrow \mu^+ \pi^0$	220	35-44	0	0.6	11
$p \rightarrow \bar{\nu} K^+$	220				4.0
– μ^+ spec.		36-44	–	–	
– prompt γ		6-8	0	0.4	
– $\pi^+ \pi^0$		5-8	0	1.2	

Table 4. Summary of nucleon decay search results in Super-Kamiokande.

tion efficiency of Michael electron is improved and the selection efficiency of ($p \rightarrow \mu^+ \pi^0$) mode is increased to 44 % (SK-I:36 %), which is almost same level as $p \rightarrow e^+ \pi^0$. The obtained proton lifetime limit for $p \rightarrow \mu^+ \pi^0$ mode is also exceed 10^{34} years, $\tau/B_{p \rightarrow \mu^+ \pi^0} > 1.1 \times 10^{34}$ years at a 90% confidence level. We carried out systematic search for the other modes in which a nucleon decay into a lepton and a meson by SK-I and SK-II data [60]. There were no signal excess and they are consistent with expected background.

$p \rightarrow \bar{\nu} K^+$ is also important because it is a dominant mode in SUSY-GUTs. In this mode, most of K^+ stops in water and decays into two particles, $\nu \mu^+$ or $\pi^+ \pi^0$, which have monochromatic momentum and are back-to-back each other. Thus we looked for single muon ring events with 236 MeV/c. Another important feature is that the remaining nuclei may emit de-excited gamma rays after the proton decay and this γ should be emitted before $K^+ \rightarrow \nu \mu^+$ (lifetime: 12 nsec). Thus we looked for the prompt gamma rays in the single muon ring sample.

For $K^+ \rightarrow \pi^+ \pi^0$, the momentum of charged pion is just above the Cherenkov threshold and it doesn't make clear Cherenkov ring. We searched for monochromatic π^0 s which have PMT activities in the backward.

Those three searches were carried out for $p \rightarrow \bar{\nu} K^+$ mode by using 220kt-yrs data. Because the tagging efficiency of Michael electron has been improved in SK-IV, the efficiencies of the prompt γ method and $\pi^+ \pi^0$ method were increased by 13 % and 20 %, respectively. In addition, the prompt γ search method was improved and, as a result, the backgrounds were considerably suppressed. In SK-I paper [34], the expected background of the prompt γ method was 0.7 events for 1489 days run and it

has been reduced to 0.2 events.

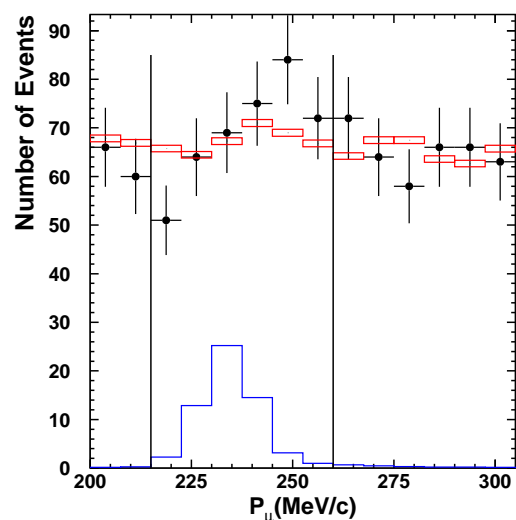


Fig. 15. The comparison of muon momentum distribution for single-ring μ -like events between data and fitted BG Monte Carlo (MC). The filled circles show data with statistical errors and the solid line shows $p \rightarrow \bar{\nu} K^+$ MC. The squares shows the best fitted atmospheric neutrino MC with free normalization. Events between 215 and 260 MeV/c shown by two vertical lines are selected as signal candidates.

Figure 15 shows the comparison of the muon momentum distribution for single-ring μ -like events between data and fitted background from Monte Carlo (MC) simulation. We observed no excess of events above background in the signal region. In other searches, there was also no significant signal excess. Therefore we concluded that there is no evidence of $p \rightarrow \bar{\nu} K^+$ and calculated partial lifetime limits, taking into account systematic uncertainties. The obtained limits are 4.0×10^{33} years at 90% confidence level.

Super-Kamiokande also looked for the other various nucleon decay modes and Figure 16 shows

summary of the lower limit of the nucleon lifetime. We have obtained the world's strongest nucleon lifetime limits for most of the modes.

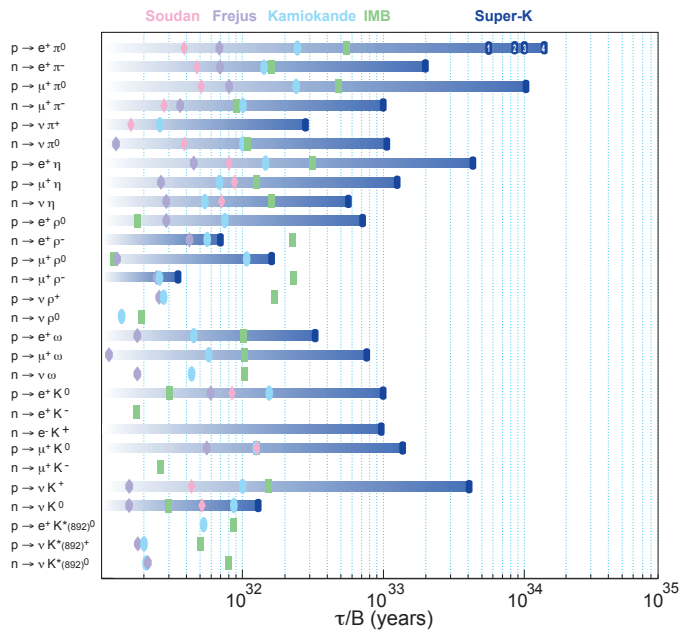


Fig. 16. Summary of nucleon decay search results in Super-Kamiokande.

Future prospect

As seen in this section, the new electronics installed in SK-IV contributes to improve efficiencies of several nucleon decay modes. In this meaning, we can keep increasing better data than SK-I to III. In addition, because the number of background events expected in the analyzed exposure are still small (< 1) in many decay modes, partial lifetime sensitivities will be almost proportional to exposure time even in the future.

Figure 17 shows comparison between the nucleon lifetime limit from SK data and some theoretical predictions. The minimal SU(5) of SUSY and non-SUSY GUTs are already excluded. The proton lifetime limits derived from Super-Kamiokande data have reached to the predicted ranges by several models, thus it is expected that we can observe the nucleon decay signal in near future.

Supernova Neutrinos

Kamiokande and IMB observed the neutrino burst from supernova 1987a. This observation con-

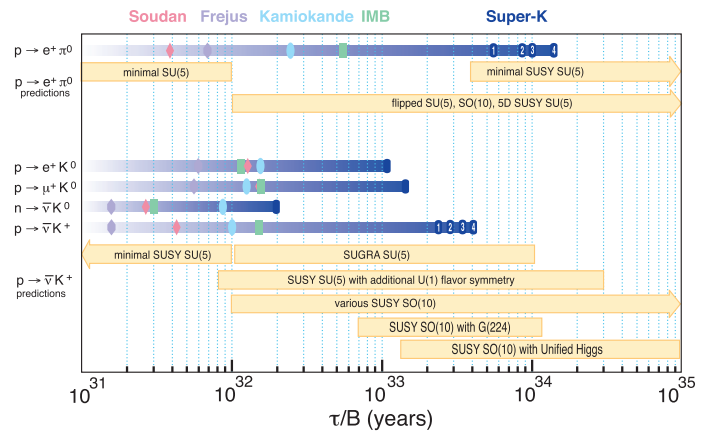


Fig. 17. Comparison of the lifetime limit between SK results and theoretical predictions in major decay mode.

firmed that the energy released by neutrinos is about several $\times 10^{53}$ ergs. However, the observed number of events were only 11 by Kamiokande and 8 by IMB, respectively. Super-Kamiokande would be able to detect several thousand neutrino events if a supernova happened near the center of our galaxy. Such an observation would enable us to investigate in detail the mechanism of the supernova explosion.

We have no galactic supernovae in these years, but they have been and are searched for almost real time at SK with the effort to minimizing dead time. The online data acquisition system running in the mine sends data to the offline computer system in the surface building of Kamioka observatory. As soon as a block of data (usually a block corresponds to several minutes) is transferred to the offline system, a program called SNWATCH installed in 1996 searches for time clustered events. It has been upgraded and the current criteria are (1) more than or equal to 7 events within 0.5sec, (2) more than or equal to 8 events within 2sec, and (3) more than or equal to 13 events within 10sec. When at least one of these criteria is met, SNWATCH reconstructs vertex position and energy of the events together with neighboring cosmic ray muons. In most cases, these clusters are due to spallation products whose vertex positions are aligned with their parent cosmic ray muon. If SNWATCH finds an event cluster whose vertex spread is larger than a given criterion, an alarm signal is sent to experts by an e-mail. Then, the experts check whether it is a real supernova signal or not by looking at various plots which are uploaded to a secured site accessible from the Internet (including i-mode keitai).

Such alarms happen almost once per month. They are usually due to the accidental coincidence of two cosmic ray induced clusters. If the cluster is found to be a real supernova, an announcement containing information of the time, number of events and reconstructed supernova direction is given to the world. We have a supernova drill at least once per year. The SNWATCH is operating for all the SK phases continuously. The dead time is being reduced by improving the online program, and currently is less than 1% for the normal data taking mode. The replacement of the electronics system at SK phase IV has also improved the data collection efficiency for nearby supernovae. Further efforts to increase the efficiency will be made by introducing huge amount of memory with an upgraded data acquisition system. So far, no real supernova neutrino burst signal has been observed at SK.

We also search for neutrinos from old supernovae, which are called Supernova Relic Neutrinos (SRNs). The SRN signal is the diffuse supernova neutrino background from all the supernovae in the past. This signal has never been detected, but it is expected to be detectable in 16-30 MeV energy region, which is the gap between the energy ranges of solar neutrinos and atmospheric neutrinos. We have applied carefully tuned data selection to enhance the SRN candidates, improving the efficiency of our search by over 20% compared to the 2003 SK-I study[20], which provided the world's best limit on SRN flux. Our improved data selection also allows us to now search the 15.5-17.5 MeV positron kinetic energy region, which was previously unusable due to spallation background. Our updated search utilizes SK-II and SK-III data as well as SK-I, considers two new background channels, and performs a sophisticated maximum likelihood search in multiple regions of the Cherenkov angle distribution to extract the most accurate flux limit possible(Fig.18). Multiple systematic errors are considered. A flux limit of between 2.8 and 3.1 $\bar{\nu}_e cm^{-2}s^{-1}$ (positron energy > 15.5 MeV) is our new result, with the exact value depending on the shape of the neutrino spectrum assumed. This new result will replace the 2003 study to be the most accurate measure of the SRN signal ever performed, and it is published at [59]. Furthermore, a new method of presenting the SRN flux limit is also ready which is of great use to theorists and does not depend on any particular model (Fig.19).

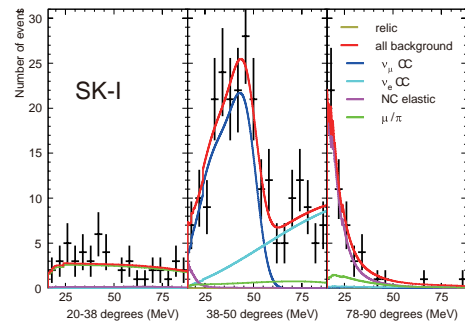


Fig. 18. Energy distributions of SK-I data for the supernova relic analysis with the best fit of various background contributions. The left, middle and right figures are for different “Cherenkov angle” parameter ranges, and the middle is for the signal search and the others are for estimating background.

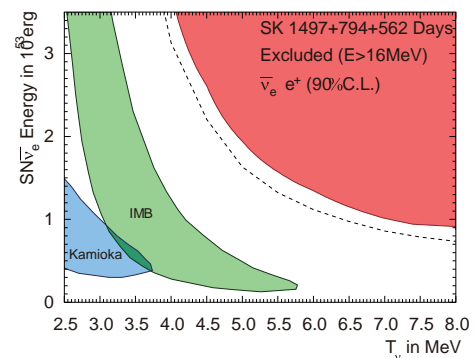


Fig. 19. Results plotted as an exclusion contour in SN neutrino luminosity vs. neutrino temperature parameter space. The green and blue contours show IMB and Kamiokande allowed areas for 1987a data, respectively. The red shows our new 90% c.l. result. The dashed line shows the individual 90% c.l. results of each temperature considered separately, which is not a true 2-D exclusion contour.

SK-IV electronics

Figure 20 shows a picture of the new front-end electronics, QBEE (QTC-Based Electronics with Ethernet). The QBEE has 24 input channels. Essential components on the QBEE for the analog signal processing and digitization are the QTC (Charge-to-Time Converter) ASIC [53] and the multi-hit TDC(Time-to-Digital Converter). The QTC detects PMT signals by individual built-in discriminators and drives output timing signals whose width represents the integrated charge of the PMT signal. Timing information on both edges of a QTC output signal is digitized by the AMT(ATLAS Muon TDC)-3 multi-hit TDCs. An FPGA then reads and processes the data stored in the TDC internal buffer continuously by a unit of $17\mu sec$. The QBEE realizes high-



Fig. 20. New front-end electronics, QBEE. PMT signals are fed through the backplane (left side). The Ethernet cable for the data readout and the board control is connected at the front panel (right side) as well as the UTP cable for the 60MHz system clock input.

speed signal processing by combining the pipelined components like the QTC, TDC and FPGA. The QBEE has an on-board calibration pulser which is used for monitoring and correcting the charge measurement by the QTCs under possible ambient temperature changes.

The high-speed QTC was developed as a custom ASIC in CMOS 0.35 μ m technology. Figure 21 shows a picture of the internal circuit of the QTC chip. The QTC has three input channels per chip. Each channel has three gain ranges: Small, Medium, and Large. The gain ratio of three ranges, which can be adjusted by external resistor networks, is set to $1:\frac{1}{7}:\frac{1}{49}$. The overall charge dynamic range of the QTC is 0.2-2500pC, which is about 5 times wider than that of the previous front-end electronics used in SK. The width of the charge integration gate in the QTC is set to 400nsec. The charge integration circuits are triggered by the input PMT signal itself (self-triggering scheme). To reduce charge leakage, the PMT signal to be integrated is delayed by a second-order voltage-controlled voltage source (VCVS) low-pass filter (LPF) in the QTC. Soon after the end of the charge gate, the discharging timer operates for ~ 350 nsec. Input signals within ~ 250 nsec after the discharge gate are ignored. In total, processing time for one input signal is ~ 1000 nsec.

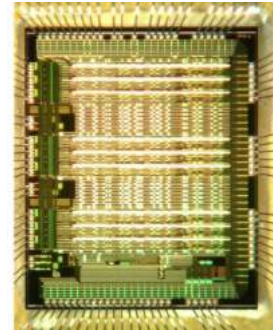


Fig. 21. The internal circuit of the QTC ASIC.

The charge and timing resolutions of the QBEE for the single p.e. level signals are 10% and 0.3nsec, respectively, both better than the intrinsic resolutions of the 20-inch PMTs in SK. The QBEE achieves good charge linearity over a wide dynamic range. The charge nonlinearity (i.e. deviation from a linear fitted function) is within $\pm 1\%$ and satisfies our requirements. The discriminators in the QTC can be operated with a -0.3 mV threshold, equivalent to 1/10p.e.s, without suffering from intrinsic electrical noise or channel crosstalk.

A total of 553 QBEEs are used in SK, 472 for the inner detector PMTs, 80 for the outer detector PMTs, 1 for a special use to record the flash timings of light sources for various detector calibrations. All the QBEEs operate synchronized by a common 60MHz master clock, which is generated by the MCLK module.

We adopted an Ethernet technology for data readout from the QBEE. The network interface sub-board attached to the QBEE has an FPGA network firmware called SiTCP and gives a 100BASE-TX data transfer. The Ethernet enables a parallel readout from the QBEEs. The measured data throughput of a QBEE achieves 11.75MB/sec, which is almost the theoretical limit of the 100BASE-TX and fast enough to realize the “record every hit” data acquisition. In addition, implementing the digital readout on the ethernet daughterboard suppresses readout noise compared to backplane readout, and allows us to achieve a low single photo electron threshold.

The data processed by the QBEEs are collected by 20 Front-end PCs via Ethernet cables and network switches. The hit data are then sorted in time order and sent to the Merger PCs. A software-trigger program is running on the Merger PC to ex-

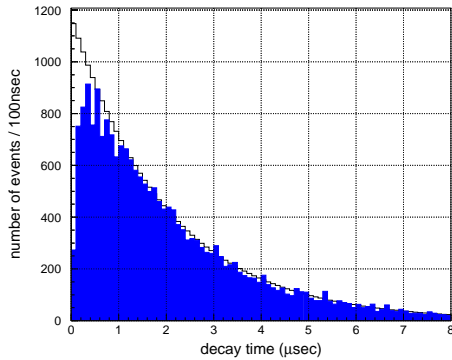


Fig. 22. Decay time of the $\mu \rightarrow e$ decay events. The curve shows the number of electrons by muon decays which is estimated by the muon lifetime and the total number of stopping muon events. The hatched histogram shows the detected $\mu \rightarrow e$ decay events.

tract an event from all the hit data of all the PMTs. A basic condition of the software-trigger is based on the number of hit PMTs in a certain time window. The special conditions triggered by an external signal input are also prepared for detector calibrations. The software-triggered event data are collected by the Organizer PC and recorded on a disk. A large amount of the data taken by the “record every hit” scheme are successfully processed by the parallel distributed processing in the online system.

The SK-IV detector performance/sensitivity is much improved for various observations. For example, the result of a test using a high-rate flashing light pulser shows that the SK-IV can take the data from a supernova neutrino burst up to a rate of 6 million events/10sec with no data loss. This limit is about 100 times as large as that of the previous SK phases and is about 1000 times as large as an expected event rate in case of a supernova at the galactic center. The detection of $\mu \rightarrow e$ decays is very important to classify interactions in neutrino oscillation analyses or nucleon decay searches. Figure 22 shows the decay time distribution of the $\mu \rightarrow e$ decay events. The detection efficiency after $1\mu\text{sec}$ from the parent muon event timing reaches almost 100%. The “record every hit + software-trigger” system will also enable us to detect a delayed signal by the 2.2MeV γ -ray after the neutron capture, which was not feasible with the previous electronics system, because the signal by a 2.2MeV γ -ray is too faint for a hardware trigger.

R&D activity for the Gadolinium Project

As mentioned above, although at SK a few SRN events a year are expected, SRNs have not been detected yet because the large backgrounds constrain our search. The main goal of our research is to reduce these backgrounds and be able to detect SRNs. The observation of SRNs in general or neutrinos from distant supernovae in particular, would provide information about the universe, for example the core collapse rate, and about the neutrino itself too, for example its lifetime. Since most of the neutrinos that can be detected by SK undergo inverse beta decay ($\bar{\nu}_e + p \rightarrow e^+ + n$), electron anti-neutrinos are the most copiously detected neutrinos. Presently, the SK detector can only detect the positrons efficiently, but if we could detect the neutrons then we could greatly reduce the backgrounds that constrain our SRN search. This could be attained by the coincidence detection of positron and neutron (in space, vertices within tens of cm and in time, with the neutron capture delayed about $20\mu\text{sec}$). By adding 0.2% of gadolinium (Gd) sulfate into the water tank we could achieve this goal. Gadolinium has a thermal neutron capture cross section of 49,000 barns (about 5 orders of magnitude larger than that of protons) and emits a gamma cascade of 8 MeV that can be easily detected by SK.

We want to demonstrate that by mixing Gd into the SK water, SK will become the world’s largest electron anti-neutrino detector, able to tag inverse beta decays, while still retaining all of its previous capabilities in other analyses like solar and atmospheric neutrinos. The EGADS (Evaluating Gadolinium’s Action on Detector Systems) project was funded in 2009 and since then a new 2500 m^3 hall near the SK detector has been excavated and a 200 m^3 size stainless steel tank with its ancillary equipment has been constructed in 2010 (Fig.23). The idea is to mimic the conditions of SK inside the 200 m^3 tank. It has been equipped with a novel selective water filtration system that will filter out water impurities while keeping Gd in the water, a Gd pre-mixing and pre-treatment 15 m^3 plastic tank, and a device to measure the water attenuation length (UDEAL). In the first half of 2011, the water circulation system equipped with the selective filtration technology was tested with pure water, and it was demonstrated that this new hybrid system is able to



Fig. 23. In the new cavern the Gd pre-mixing and pre-treatment 15 m³ tank (front left), the selective filtration system (front right) and the 200 m³ tank (rear of the hall) have been installed.

purify water as well as the highly-refined SK water circulation system. As the next step, since then the water circulation system has been running with 0.2% Gd sulfate solution in the 15 m³ plastic tank, allowing the first studies of gadolinium filtration and transparency to begin. By September 2011, the EGADS selective filtration system had achieved a gadolinium retention rate of 99.97% per pass, while simultaneously cleaning unwanted impurities from the water: this was the first large-scale demonstration of a brand-new technology - such selective filtration has never been accomplished anywhere before.

In addition to testing the selective filtration concept and hardware, this second phase of running allowed measurement of the water transparency of the Gd-loaded water without emanation from the materials in the detector. So far, about 80% transparency compared with the SK ultrapure water has been achieved as shown in Fig.24. This is a remarkable accomplishment: in the past, water of this clarity has always required the complete removal of all impurities, including dissolved ions, gases, polymers, biologicals, and non-ionic particulates. We have now demonstrated stable transparency approaching that of such ultrapure water, but in a large batch of solution containing the full loading of gadolinium sulfate needed for efficient neutron tagging in Super-K. Over the first half of 2012 the light loss per unit dissolved gadolinium was more than cut in half, and further improvements are expected in the coming year through continual refining of the EGADS selective filtration system.



Fig. 24. Time variation of the estimated light yield during the Gd-loaded water circulation run. 0.2% Gd₂(SO₄)₃-loaded water was circulated through the selective filtration system. The vertical axis shows Cherenkov light yield at a distance of 20 meters estimated from the measured water transparency at each wavelength.

Now that EGADS has a successful selective filtration system, able to achieve and maintain high transparency of Gd-loaded water while simultaneously incurring insignificant gadolinium losses, it is time to move on to the next steps in conclusively demonstrating that gadolinium loading of Super-Kamiokande will work. To this end, we will soon begin circulating Gd-loaded water through the 200 m³ tank. This will allow us to evaluate the effect of the presence of a large surface area of stainless steel in contact with the Gd-loaded water. Once good transparency is verified under those conditions, the 200 m³ tank will be drained and we will mount 240 50-cm photomultipliers within it; this work will most likely take place during the autumn of 2012. The PMTs will be powered up and connected to a fully functional data acquisition system. After a brief data-taking run with ultrapure water to establish the performance baseline of the phototubes and detector, gadolinium will be re-introduced to the 200 m³ tank around the beginning of 2013.

From that point on, we will have what is essentially a working scale model of an advanced-technology, gadolinium-enriched Super-Kamiokande. This new detector can then be calibrated with both lasers and neutron sources, and its performance and stability over time will be carefully studied. This is the ultimate R&D phase of the EGADS project, and its results will be the primary inputs to the coming decision regarding whether or not to add gadolinium to Super-Kamiokande.

Super-Kamiokande Collaboration

Spokesperson : Yoichiro Suzuki (Kamioka Observatory, ICRR, The University of Tokyo)

Institute	Country	(*)
ICRR, Univ. of Tokyo	Japan	28
Boston Univ.	USA	4
California State Univ.	USA	3
Chonnam Univ.	Korea	4
Duke Univ.	USA	7
Gifu Univ.	Japan	1
KEK	Japan	11
Kobe Univ.	Japan	2
Kyoto Univ.	Japan	11
Miyagi Kyoiku Univ.	Japan	1
Osaka Univ.	Japan	1
Seoul National Univ.	Korea	1
Shizuoka Univ. of Welfare	Japan	1
Stony Brook Univ.	USA	5
SungKyunKwan Univ.	Korea	1
Tokai Univ.	Japan	1
TRIUMF.	Canada	2
Tsinghua University	China	5
Univ. of Washington	USA	3
Univ. of Autonoma Madrid	Spain	1
Univ. of British Columbia	Canada	3
Univ. of California, Irvine	USA	7
Univ. of Hawaii	USA	3
Univ. of Regina	Canada	1
Univ. of Tokyo	Japan	2
Univ. of Toront	Canada	2
Warsaw Univ.	Poland	1
Total		112

(*) Number of collaborators.

Members

Staff

Kamioka Observatory

Yoichiro Suzuki, Professor
 Masayuki Nakahata, Professor
 Shigetaka Moriyama, Assoc. Professor
 Masato Shiozawa, Assoc. Professor
 Yoshinari Hayato, Assoc. Professor
 Yasuhiro Kishimoto, Assoc. Professor (from Dec.2010)
 Yasuo Takeuchi, Assoc. Professor (till Apr.2010)
 Makoto Miura, Research Associate
 Yusuke Koshio, Research Associate
 June Kameda, Research Associate
 Atsushi Takeda, Research Associate

Kou Abe, Research Associate
 Hiroyuki Sekiya, Research Associate
 Yoshihisa Obayashi, Research Associate (till Dec.2011)
 Roger Wendell, Research Associate (from May 2012)
 Shoei Nakayama, Project Research Associate (from Apr.2007)
 Tomonobu Tomura, Project Research Associate (from Mar.2011)
 Satoru Yamada, Project Research Associate (Oct.2006 - Nov.2010)
Research Center for Cosmic Neutrinos
 Takaaki Kajita, Professor
 Kimihiro Okumura, Assoc. Professor
 Kenji Kaneyuki, Assoc. Professor (till May 2010, deceased)
 Yasuhiro Nishimura, Project Research Associate (from Apr.2012)

Postdoctoral Fellows

Kamioka Observatory

Lluis Magro Marti (from Apr.2011)
 Yasuhiro Nishimura (Apr.2011 - Mar.2012)
 Hideki Watanabe (Apr.2006 - Mar.2009)
Research Center for Cosmic Neutrinos
 Hiroshi Kaji (Apr.2009 - Mar.2012)
 Andrew Brian Laing (Jan.2011 - Mar.2012)
 Nao Tanimoto (Feb. 2008 - Mar.2010)
 Yuuki Shimizu (Apr. 2008 - Mar.2010)
 Shoei Nakayama (till Mar.2007)
 Itaru Higuchi (till Mar.2008)

Graduate students

Six students were awarded doctor degrees and five students earned master degrees during 2006–2012, supervised by ICRR staff members.

List of Publications

Before Year 2006

- [1] “Measurement of a small atmospheric ν_{μ}/ν_e ratio”, Super-Kamiokande Collaboration (Y. Fukuda et al.), Phys. Lett. B **433**, 9 (1998), **Cited 842 times.**
- [2] “Study of the atmospheric neutrino flux in the multi-GeV energy range”, Super-Kamiokande

- Collaboration (Y. Fukuda et al.), Phys. Lett. B **436**, 33 (1998), **Cited 779 times.**
- [3] “Measurements of the solar neutrino flux from Super-Kamiokande’s first 300 days”, Super-Kamiokande Collaboration (Y. Fukuda et al.), Phys. Rev. Lett. **81**, 1158 (1998) [Erratum-ibid. **81**, 4279 (1998)], **Cited 667 times.**
- [4] “Search for proton decay via $p \rightarrow e^+\pi^0$ in a large water Cherenkov detector”, Super-Kamiokande Collaboration (M. Shiozawa et al.), Phys. Rev. Lett. **132**, 3319 (1998). **Cited 132 times.**
- [5] “Evidence for oscillation of atmospheric neutrinos”, Super-Kamiokande Collaboration (Y. Fukuda et al.), Phys. Rev. Lett. **81**, 1562 (1998), **Cited 3707 times.**
- [6] “Calibration of Super-Kamiokande using an electron linac”, Super-Kamiokande Collaboration (M. Nakahata et al.), Nucl. Instrum. Meth. A **421**, 113 (1999). **Cited 122 times.**
- [7] “Constraints on neutrino oscillation parameters from the measurement of day-night solar neutrino fluxes at Super-Kamiokande”, Super-Kamiokande Collaboration (Y. Fukuda et al.), Phys. Rev. Lett. **82**, 1810 (1999), **Cited 468 times.**
- [8] “Measurement of the solar neutrino energy spectrum using neutrino electron scattering”, Super-Kamiokande Collaboration (Y. Fukuda et al.), Phys. Rev. Lett. **82**, 2430 (1999), **Cited 451 times.**
- [9] “Measurement of the flux and zenith-angle distribution of upward through-going muons by Super-Kamiokande”, Super-Kamiokande Collaboration (Y. Fukuda et al.), Phys. Rev. Lett. **82**, 2644 (1999), **Cited 722 times.**
- [10] “Observation of the east-west anisotropy of the atmospheric neutrino flux”, Super-Kamiokande Collaboration (Y. Futagami et al.), Phys. Rev. Lett. **82**, 5194 (1999). **Cited 97 times.**
- [11] “Search for proton decay through $p \rightarrow \bar{\nu}K^+$ in a large water Cherenkov detector”, Super-Kamiokande Collaboration (Y. Hayato et al.), Phys. Rev. Lett. **83**, 1529 (1999). **Cited 119 times.**
- [12] “Neutrino-induced upward stopping muons in Super-Kamiokande”, Super-Kamiokande Collaboration (Y. Fukuda et al.), Phys. Lett. B **467**, 185 (1999), **Cited 272 times.**
- [13] “N-16 as a calibration source for Super-Kamiokande”, Super-Kamiokande Collaboration (E. Blaufuss et al.), Nucl. Instrum. Meth. A **458**, 638 (2001). **Cited 24 times.**
- [14] “Tau neutrinos favored over sterile neutrinos in atmospheric muon-neutrino oscillations”, Super-Kamiokande Collaboration (S. Fukuda et al.), Phys. Rev. Lett. **85**, 3999 (2000), **Cited 811 times.**
- [15] “Detection of accelerator produced neutrinos at a distance of 250-km”, K2K Collaboration (S.H. Ahn et al.), Phys. Lett. B **511**, 178 (2001), **Cited 296 times.**
- [16] “Solar B-8 and hep neutrino measurements from 1258 days of Super-Kamiokande data”, Super-Kamiokande Collaboration (S. Fukuda et al.), Phys. Rev. Lett. **86**, 5651 (2001), **Cited 1051 times.**
- [17] “Constraints on neutrino oscillations using 1258 days of Super-kamiokande solar neutrino data”, Super-Kamiokande Collaboration (S. Fukuda et al.), Phys. Rev. Lett. **86**, 5656 (2001), **Cited 691 times.**
- [18] “Search for neutrinos from gamma-ray bursts using Super-Kamiokande”, Super-Kamiokande Collaboration (S. Fukuda et al.), Astrophys. J. **578**, 317 (2002), **Cited 20 times.**
- [19] “Determination of solar neutrino oscillation parameters using 1496 days of Super-Kamiokande I data”, Super-Kamiokande Collaboration (S. Fukuda et al.), Phys. Lett. B **539**, 179 (2002), **Cited 789 times.**
- [20] “Search for supernova relic neutrinos at Super-Kamiokande”, Super-Kamiokande Collaboration (M. Malek et al.), Phys. Rev. Lett. **90**, 061101 (2003), **Cited 142 times.**
- [21] “Indications of neutrino oscillation in a 250 km long baseline experiment”, K2K Collaboration (M.H. Ahn et al.), Phys. Rev. Lett. **90**, 041801 (2003), **Cited 928 times.**

- [22] “Search for anti- $\nu(e)$ from the sun at Super-Kamiokande I”, Super-Kamiokande Collaboration (Y. Gando et al.), Phys. Rev. Lett. **90**, 171302 (2003), **Cited 46 times**.
- [23] “The Super-Kamiokande detector”, Super-Kamiokande collaboration (Y. Fukuda et al.), Nucl. Instrum. Meth. A **501**, 418 (2003),
- [24] “Development of super-high sensitivity radon detector for the Super-Kamiokande detector”, C. Mitsuda, T. Kajita, K. Miyano, S. Moriyama, M. Nakahata, Y. Takeuchi, S. Tasaka, Nucl. Instrum. Meth. A **497**, 414 (2003),
- [25] “A search for periodic modulations of the solar neutrino flux in Super-Kamiokande I”, Super-Kamiokande Collaboration (J. Yoo et al.), Phys. Rev. D **68**, 092002 (2003), **Cited 51 times**.
- [26] “Precise measurement of the solar neutrino day / night and seasonal variation in Super-Kamiokande-1”, Super-Kamiokande Collaboration (M.B. Smy et al.), Phys. Rev. D **69**, 011104 (2004), **Cited 209 times**.
- [27] “Limits on the neutrino magnetic moment using 1496 days of Super-Kamiokande-I solar neutrino data”, Super-Kamiokande Collaboration (D.W. Liu et al.), Phys. Rev. Lett. **93**, 021802 (2004), **Cited 47 times**.
- [28] “Search for electron neutrino appearance in a 250 km long baseline experiment”, K2K Collaboration (M.H. Ahn et al.), Phys. Rev. Lett. **93**, 051801 (2004), **Cited 69 times**
- [29] “Search for dark matter wimps using upward through-going muons in Super-Kamiokande”, Super-Kamiokande Collaboration (S. Desai et al.), Phys. Rev. D **70** 083523 (2004) [Erratum-ibid. D **70** 109901 (2004)], **Cited 259 times**
- [30] “Evidence for an oscillatory signature in atmospheric neutrino oscillation”, Super-Kamiokande Collaboration (Y. Ashie et al.), Phys. Rev. Lett. **93**: 101801, 2004, **Cited 619 times**.
- [31] “Measurement of single π^0 production in neutral current neutrino interactions with water by a 1.3-GeV wide band muon neutrino beam”, K2K Collaboration (S. Nakayama et al.), Phys. Lett. B **61**, 255 (2005). **Cited 67 times**.
- [32] “Evidence for muon neutrino oscillation in an accelerator-based experiment”, K2K Collaboration (E. Aliu et al.), Phys. Rev. Lett. **94** 081802 (2005), **Cited 422 times**.
- [33] “A measurement of atmospheric neutrino oscillation parameters by Super-Kamiokande I”, Super-Kamiokande Collaboration (Y. Ashie et al.) et al., Phys. Rev. D **71**: 112005, 2005, **Cited 702 times**.
- [34] “Search for nucleon decay via modes favored by supersymmetric grand unification models in Super-Kamiokande-I”, Super-Kamiokande Collaboration (K. Kobayashi et al.), Phys. Rev. D **72**, 052007 (2005), **Cited 69 times**.
- [35] “An improved search for $\nu_\mu \rightarrow \nu_e$ oscillation in a long-baseline accelerator experiment”, K2K Collaboration (S. Yamamoto et al.), Phys. Rev. Lett. **96**, 181801 (2006), **Cited 54 times**.

After Year 2006

- [36] “Measurement of Neutrino Oscillation by the K2K Experiment”, K2K Collaboration (M. H. Ahn et al.), Phys. Rev. D **74** 072003 (2006), **Cited 466 times**
- [37] “Observation of the Anisotropy of 10 TeV Primary Cosmic Ray Nuclei Flux with the Super-Kamiokande-I Detector”, The Super-Kamiokande Collaboration (G. Guillian et al.), Phys. Rev. D **75**, 062003 (2007), **Cited 45 times**.
- [38] “Solar neutrino measurements in Super-Kamiokande-I”, The Super-Kamiokande Collaboration (J. Hosaka et al.), Phys. Rev. D **73**, 112001 (2006), **Cited 257 times**.
- [39] “Three flavor neutrino oscillation analysis of atmospheric neutrinos in Super-Kamiokande”, The Super-Kamiokande Collaboration (J. Hosaka et al.), Phys. Rev. D **74**, 032002 (2006), **Cited 164 times**.
- [40] “Search for Diffuse Astrophysical Neutrino Flux Using Ultra-High Energy Upward-Going

- Muons in Super-Kamiokande I”, The Super-Kamiokande Collaboration (M. E. C. Swanson et al.), *Astrophys.J.* **652** 206 (2006), **Cited 15 times.**
- [41] “High energy neutrino astronomy using upward-going muons in Super-Kamiokande-I”, The Super-Kamiokande Collaboration (K. Abe et al.), *Astrophys.J.* **652**, 198 (2006), **Cited 25 times.**
- [42] “A Measurement of Atmospheric Neutrino Flux Consistent with Tau Neutrino Appearance”, The Super-Kamiokande Collaboration (K. Abe et al.), *Phys. Rev. Lett.* **97**, 171801 (2006), **Cited 110 times.**
- [43] “Search for Neutral Q-balls in Super-Kamiokande II”, The Super-Kamiokande Collaboration (T. Takenaga et al.), *Phys. Lett. B* **647**, 18 (2007), **Cited 23 times.**
- [44] “Search for Supernova Neutrino Bursts at Super-Kamiokande”, The Super-Kamiokande Collaboration (M. Ikeda et al.), *Astrophys J.* **669**, (2007) 519, **Cited 36 times.**
- [45] “Study of TeV Neutrinos with Upward Showering Muons in Super-Kamiokande”, The Super-Kamiokande Collaboration (S. Desai et al.), *Astropart. Phys.* **29**, 42 (2008), **Cited 44 times.**
- [46] “Search for Matter-Dependent Atmospheric Neutrino Oscillations in Super-Kamiokande”, The Super-Kamiokande Collaboration (K. Abe et al.), *Phys. Rev. D* **77**, 052001 (2008), **Cited 12 times.**
- [47] “Solar neutrino measurements in Super-Kamiokande-II”, The Super-Kamiokande Collaboration (J. P. Cravens), *Phys. Rev. D* **78**, 032002 (2008), **Cited 108 times.**
- [48] “First Study of Neutron Tagging with a Water Cherenkov Detector”, The Super-Kamiokande Collaboration (H. Watanabe et al.), *Astropart. Phys.* **31**, 320 (2009), **Cited 20 times.**
- [49] “Search for Proton Decay via $p \rightarrow e^+\pi^0$ and $p \rightarrow \mu^+\pi^0$ in a Large Water Cherenkov Detector”, The Super-Kamiokande Collaboration (H. Nishino et al.), *Phys. Rev. Lett.* **102**, 141801 (2009), **Cited 52 times.**
- [50] “Kinematic reconstruction of atmospheric neutrino events in a large water Cherenkov detector with proton identification”, The Super-Kamiokande Collaboration (M. Fechner et al.), *Phys. Rev. D* **79**, 112010 (2009), **Cited 4 times.**
- [51] “Search for Neutrinos from GRB 080319B at Super-Kamiokande”, The Super-Kamiokande Collaboration (E. Thrane et al.), *Astrophys. J.* **697**, 730 (2009), **Cited 2 times.**
- [52] “Search for Astrophysical Neutrino Point Sources at Super-Kamiokande”, The Super-Kamiokande Collaboration (E. Thrane et al.), *Astrophys. J.* **704**, 503 (2009), **Cited 16 times.**
- [53] “High-speed charge-to-time converter ASIC for the Super-Kamiokande detector”, H. Nishino et al., *Nucl. Instrum. Meth. A* **610**, 710 (2009) **Cited 4 times.**
- [54] “Atmospheric neutrino oscillation analysis with sub-leading effects in Super-Kamiokande I, II and III”, The Super-Kamiokande Collaboration (R. Wendell et al.), *Phys. Rev. D* **81**, 092004 (2010), **Cited 82 times.**
- [55] “Solar neutrino results in Super-Kamiokande-III”, The Super-Kamiokande Collaboration (K. Abe et al.), *Phys. Rev. D* **83**, 052010 (2011), **Cited 50 times.**
- [56] “Study of Non-Standard Neutrino Interactions with Atmospheric Neutrino Data in Super-Kamiokande I and II”, The Super-Kamiokande Collaboration (G. Mitsuka et al.), *Phys. Rev. D* **84**, 113008 (2011) **Cited 3 times.**
- [57] “An Indirect Search for WIMPs in the Sun using 3109.6 days of upward-going muons in Super-Kamiokande”, The Super-Kamiokande Collaboration (T. Tanaka et al.), *Astrophys. J.* **742**, 78 (2011), **Cited 20 times.**
- [58] “Search for Differences in Oscillation Parameters for Atmospheric Neutrinos and Antineutrinos at Super-Kamiokande”, The Super-Kamiokande Collaboration (K. Abe et al.), *Phys. Rev. Lett.* **107**, 241801 (2011), **Cited 6 times.**

- [59] “Supernova Relic Neutrino Search at Super-Kamiokande”, Super-Kamiokande Collaboration (K. Bays et al.), Phys. Rev. D. **85**, 052007 (2012).
- [60] “Search for Nucleon Decay into Charged Anti-lepton plus Meson in Super-Kamiokande I and II”, The Super-Kamiokande Collaboration (H. Nishino et al.), Phys. Rev. D. **85**, 112001 (2012), **Cited 3 times**.
- [61] “Search for GUT monopoles at Super-Kamiokande”, The Super-Kamiokande Collaboration (K. Ueno et al.), Astropart. Phys. **36**, 121 (2012).
- [62] “A Measurement of the Appearance of Atmospheric Tau Neutrinos by Super-Kamiokande”, The Super-Kamiokande Collaboration (K. Abe et al.), submitted to Phys. Rev. Lett., arXiv:1206.0328 .

T2K EXPERIMENT

Introduction

The T2K (Tokai-to-Kamioka) is a long baseline neutrino oscillation experiment aims at the discovery of the unknown oscillation parameter θ_{13} and the precise measurements of another oscillation parameters θ_{23} and Δm_{32}^2 . When this experiment was started, θ_{13} had not been measured and only zero consistent upper limit was set by CHOOZ¹ and MINOS² experiments. Therefore, the first challenge of this experiment was to discover and measure the non-zero θ_{13} using the appearance of ν_e from ν_μ beam from the accelerator. Also, the intense neutrino beam makes it possible to reduce the error of the other two oscillation parameters, θ_{23} and Δm_{32}^2 by another order of magnitude using the disappearance of ν_μ .

T2K uses a conventional neutrino beam produced at J-PARC and directed 2.5° off-axis to Super-Kamiokande at a distance 295km. With this configuration, so-called off-axis beam configuration, it is possible to produce the narrow-band ν_μ beam³. The peak energy of μ_ν at Super-Kamiokande comes at the first oscillation maximum, $E_\nu \simeq 0.6\text{GeV}$. If θ_{13} has non-zero value, ν_μ oscillates into ν_e while traveling and it is expected to be identified as ν_e appearance in the SK detector. Most of the ν_μ from the J-PARC accelerator oscillates into ν_τ before arriving at SK and thus, the number of ν_μ charged current events is expected to be largely suppressed and also, the ν_μ energy spectrum distortion is expected to be observed.

The J-PARC is a new accelerator complex in Tokai village, Ibaraki, Japan. The neutrino beam line in J-PARC was built for T2K and its construction was completed in 2009 and the commissioning was started just after the completion. Then, the physics data taking was started in January 2010.

The T2K neutrino beam is monitored by two kind of detectors, the muon monitors and the neutrino detectors. The muon monitors (MUMON) are located just downstream of the hadron absorber at the end of the decay tunnel. Because the directional

distributions and intensity of the muons, which penetrate the hadron absorber, have good correlation with the neutrinos and it is useful and important to monitor the stability of the distributions of muons spill by spill basis. The neutrino detector complex in J-PARC site is located 280m downstream from the target. There are two sets of neutrino detectors. The first set is the on-axis Interactive Neutrino GRID (INGRID). INGRID is designed to monitor the neutrino beam direction and intensity daily basis by means of neutrino interactions in iron. It consists of 14 identical detectors arranged as a cross of two identical groups along the horizontal and vertical axes and two additional separate modules are located at the off-axis directions outside of the main cross. Each of the detector consists of a sandwich structure of nine iron plates and 11 tracking scintillator planes surrounded by veto scintillator planes. The other set is the off-axis detectors. The off-axis detector complex is prepared to measure intensities and energy spectra of each neutrino flavor. These detectors are also used to understand the interaction of neutrinos with various target material. This detector complex consists of three large volume time projection chambers (TPCs) interleaved with two fine grained tracking detectors (FGDs), a π^0 optimized detector and surrounding electromagnetic calorimeters. These detectors are embedded in the refurbished UA1 magnet, whose magnetic field is set to 0.2T. Also, there are scintillators instrumented in the magnet yokes as a side muon range detector.

The SK detector is used as the far detector of T2K. The absolute beam extraction timing information, measured by GPS in Tokai, are sent to Kamioka spill by spill within a few hundreds of milliseconds and the SK DAQ system uses this information to keep all the PMT hit information from the detector including the dark noise hits for $\pm 500\mu$ sec. These stored event data are processed offline to search for the T2K neutrino event candidates. With this scheme, there is no energy threshold or the other possible biases in collecting the data and also, it is possible to test various kinds of methods to search for the neutrino candidate events.

The expected neutrino energy spectra for each

*¹ Chooz Collaboration, M. Apollonio et al., Eur. Phys. J. C **27**, 331 (2003)

*² MINOS Collaboration, P. Adamson et al., Phys. Rev. D **82**, 051102 (2010)

*³ E889 Collaboration, D. Beavis, A. Carroll, I Chiang et al., Physics Design Report BNL No. 52459 (1995).

neutrino flavor are computed with the custom made simulation program, which uses experimental results of hadron productions as an input. Among of the experiments, the results from NA61⁴ are extensively used for the simulation. The expected neutrino energy spectrum is shown in Fig. 1. The neu-

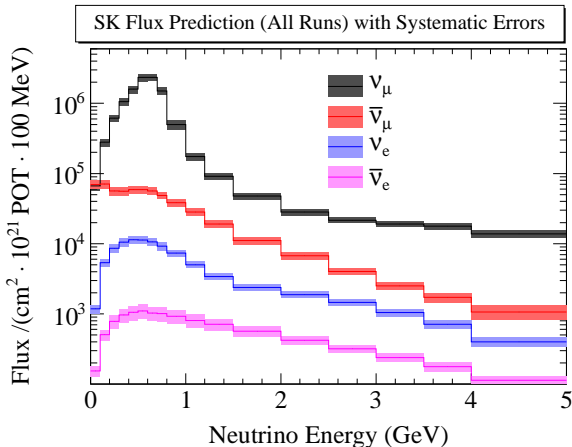


Fig. 1. SK flux prediction with systematic (including MC stat.) error bars. Broken down by neutrino flavor. Prediction is for the POT average of runs normalized to $1e^{21}$ POT.

trino interaction is simulated by the same program library, NEUT⁵, which has been used in the SK and the K2K experiments. Another neutrino interaction simulation package GENIE⁶ is also used for cross-check and for the estimation of the uncertainties.

Current status of T2K

The physics data taking was started in January 2010 and stopped in June 2010 for the summer shutdown. From November 2010, the beam resumed and took data until March 2011. Until March 2011, we have accumulated 1.43×10^{20} protons on target (POT). After the earthquake, it took about 9 months to recover the facility. The accelerator resumed its operation in December 2011 and the commissioning of the neutrino beamline was performed. Then, the data taking started in early 2012 and continuously taking data until June 9th. The total number of protons on target is 3.01×10^{20} until June 9, 2012.

The neutrino beam profile and its intensity during the data taking period are monitored by IN-GRID. The results are consistent with the expectation and confirmed to be stable. Especially, the

beam profile center is stable within ± 1 mrad. Also, the direction of the muon has been monitored by MUMON and it is also stable.

The data from the off-axis neutrino detectors in Tokai are extensively used to constrain the energy spectra and interaction rates of neutrinos in SK. In the first analyses, released in June 2011, we used the results from the inclusive ν_μ charged current (CC) measurements to constrain the absolute interaction rate differences between the data and Monte-Carlo expectation. For the neutrino oscillation analyses in 2012, we separate the sample into charged current quasi-elastic (CCQE) like and non-CCQE like samples. Also, simultaneous fits of parameters, not only related to the flux uncertainties but also neutrino interactions and succeeded in reducing the systematic uncertainties. After the fitting, the data samples in the near detectors are well reproduced by the simulation.

Search for the ν_e appearance

We have performed ν_e appearance analysis[2] using entire data sample.

If ν_μ oscillates into ν_e , appeared ν_e can be identified through events produced by CC interactions in SK. Because of the expected energy spectrum of oscillated ν_e peaks around 0.6 GeV, dominant interaction is CC quasi-elastic scattering. These signal events are identified as single ring e-like events in SK. The major background are intrinsic ν_e in the beam and neutral current (NC) interactions with a misidentified π^0 . In order to reduce the contamination from the π^0 , new algorithm was developed to identify weak ring from low energy gamma ray coming from asymmetric decay of π^0 .

There are 88 fully contained in fiducial volume (FCFV) events by March 2011 and we used this sample for our first neutrino oscillation analyses. We select single-ring e-like events without delayed electrons. In order to reject the electrons generated from μ , electron equivalent energy is required to be larger than 100 MeV. Then, π^0 detection algorithm is applied but the reconstructed π^0 mass of each event is always smaller than the pre-defined criteria, $105 \text{ MeV}/c^2$. Finally, the reconstructed neutrino energy is calculated assuming the quasi-elastic interaction neglecting Fermi motion. The candidate events are required to have reconstructed neutrino energy smaller than 1250 MeV. This selection rejects the events from intrinsic beam ν_e . The se-

*⁴ NA61/SHINE Collaboration, Abgrall et al., Phys. Rev. C **84**, 034604 (2011)

*⁵ Y. Hayato, Acta Phys. Polon. B**40**, 2477 (2009)

*⁶ C. Andreopoulos et al., Nucl. Instrum. Methods Phys. Res., Sect. A **614**, 87 (2010)

Table 1. Contributions from various sources and the total relative uncertainty for $\sin^2 2\theta_{13}=0$ and 0.1, and $\delta_{CP} = 0$.

Source	$\sin^2 2\theta_{13} = 0$	$\sin^2 2\theta_{13} = 0.1$
(1) neutrino flux	$\pm 8.5\%$	$\pm 8.5\%$
(2) near detector	$+5.6\%$ -5.2%	$+5.6\%$ -5.2%
(3) near det. statistics	$\pm 2.7\%$	$\pm 2.7\%$
(4) cross section	$\pm 14.0\%$	$\pm 10.5\%$
(5) far detector	$\pm 14.7\%$	$\pm 9.4\%$
Total $\delta N_{SK}^{exp}/N_{SK}^{exp}$	$+22.8\%$ -22.7%	$+17.6\%$ -17.5%

lection efficiency of the oscillated ν_e signal is estimated to be 66% while rejection for $\nu_\mu + \bar{\nu}_\mu$ CC, intrinsic ν_e CC and NC are $>99\%$, 77% and 99%, respectively. After applying all these cuts, 6 events remain. The expected number of events from the background is estimated to be 1.5 ± 0.3 (syst.). Among of 1.5 events, 0.8 events are from intrinsic ν_e , 0.6 events are from neutral current interactions and 0.03 events are coming from ν_μ and $\bar{\nu}_\mu$ charged current events. Contributions from various sources and total relative uncertainty are summarized in Table 1.

In the first ν_e oscillation appearance analysis, we used the number of ν_e candidate events to extract the oscillation parameters. The allowed region of the oscillation parameters are obtained by comparing the number of ν_e candidate events with predictions, varying $\sin^2 2\theta_{13}$ for each δ_{CP} value. In this analysis, we fixed the other oscillation parameters as follows: $\Delta m_{12}^2 = 7.6 \times 10^{-5} \text{ eV}^2$, $\Delta m_{32}^2 = +2.4 \times 10^{-3} \text{ eV}^2$, $\sin^2 2\theta_{12} = 0.8704$, $\sin^2 2\theta_{32} = 1.0$, an average Earth density $\rho=3.2 \text{ g/cm}^3$. The probability to observe six or more candidates is 7×10^{-3} for a three flavor neutrino oscillation scenario with $\sin^2 2\theta_{13} = 0$. In conclusion, our data indicates ν_e appearance from a ν_μ beam. Also, the allowed regions of $\sin^2 2\theta_{13}$ and δ_{CP} for both normal and inverted mass hierarchy was obtained as shown in Fig. 2. This was the first experimental indication of the non-zero θ_{13} .

After the release of our results of non-zero θ_{13} , several other experiments started releasing the new results. In 2012, the Daya-Bay experiment announced their results of θ_{13} measurements. The Daya-Bay experiment uses $\bar{\nu}_e$ from reactors and study the disappearance of $\bar{\nu}_e$. Their obtained value of θ_{13} value is $\sin^2 2\theta_{13} = 0.089 \pm 0.010(\text{stat}) \pm 0.005(\text{syst})$ ⁷ and this value is consistent with our

^{*7} Daya Bay Collaboration, D. Dwyer et al., Talk presented at the XXV International Conference on Neutrino Physics and Astrophysics (NEU-

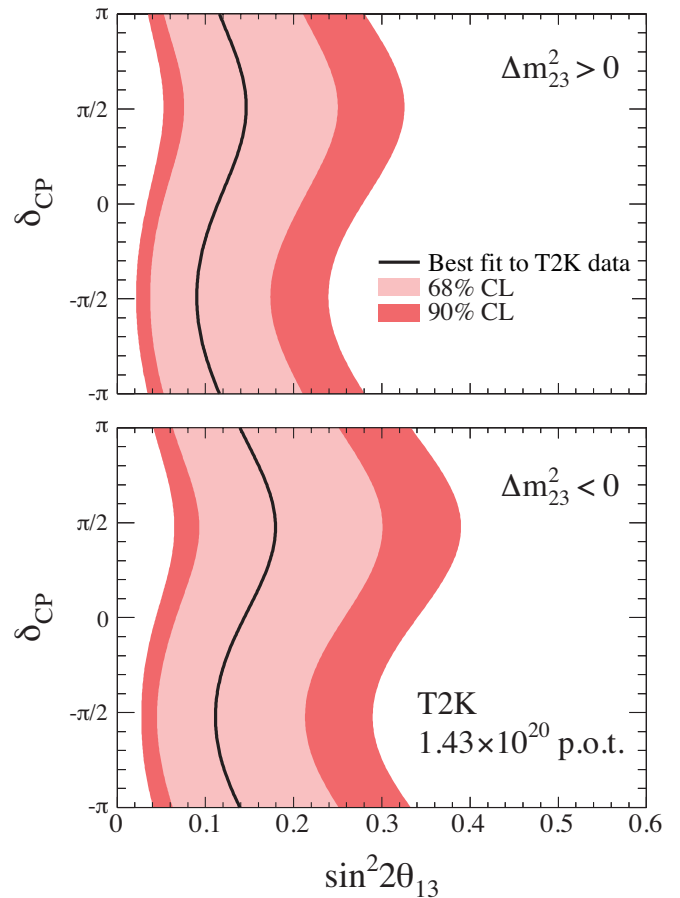


Fig. 2. The 60% and 90% C.L. regions for $\sin^2 2\theta_{13}$ for each value of δ_{CP} , consistent with the observed number of events in the three flavor oscillation case for normal (top) and inverted (bottom) mass hierarchy. These plots are from the first ν_e appearance analysis of the T2K experiment published in 2011[2]. The best fit values are shown in solid lines. The other oscillation parameters are fixed as explained in the text.

result.

We also performed the analyses with the increased statistics in 2012. (By June 9, 2012, we observed 174 FCFV events. Among of them, 11 events are identified as ν_e candidate.)

This time, we use not only the number of candidate ν_e events but the other observables. There are two additional analyses, the first one uses the direction and energy of electron in the ν_e candidate events and the other analysis uses the reconstructed energy of ν_e . The reconstructed energy of ν_e candidate events are shown in Fig. 3. All

the three analyses provides consistent results with each other and also, the previous analysis released in 2011. Owing to the increase of the statistics, non-zero θ_{13} is excluded at 3.2σ level and the 90 % C.L. allowed region is $0.033 < \sin^2 2\theta_{13} < 0.188$ ($0.041 < \sin^2 2\theta_{13} < 0.228$) for the normal (inverted) hierarchy case as shown in Fig. 4.

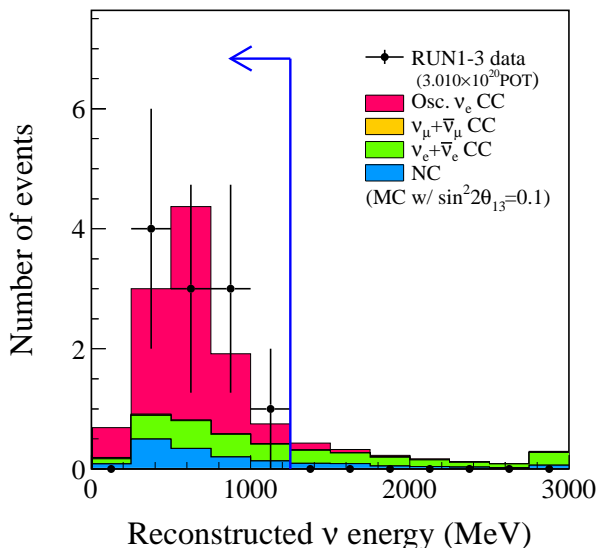


Fig. 3. Reconstructed neutrino energy spectrum of the events which pass all ν_e appearance signal selection criteria with the exception of the final energy cut. The vertical line shows the applied cut at 1250 MeV. The data are shown using points with error bars (statistical error only) and the MC predictions are in shaded histograms, corresponding to ν_e CC signal and various background sources for $\sin^2 2\theta_{13} = 0.1$.

The dominant systematic uncertainties are coming from the uncertainty of the neutrino interactions. Among of them, effective axial vector coupling constant, the normalization parameter and nuclear model dependence of the charged current quasi-elastic (CCQE) scattering are the largest and each of them is almost comparable size (~ 5 to 8%) with the beam flux uncertainty ($\sim 8\%$). Therefore, further studies of the neutrino interactions, especially, CCQE, in the near neutrino detectors become one of the most important thing to achieve higher precision of the measurements.

Disappearance of ν_μ

We have performed the ν_μ disappearance analysis [3] using the run 1 and 2 data sample. ν_μ to ν_τ oscillation not only reduces the number of charged current ν_μ events in SK but also distorts the energy spectrum. The oscillation parameter determi-

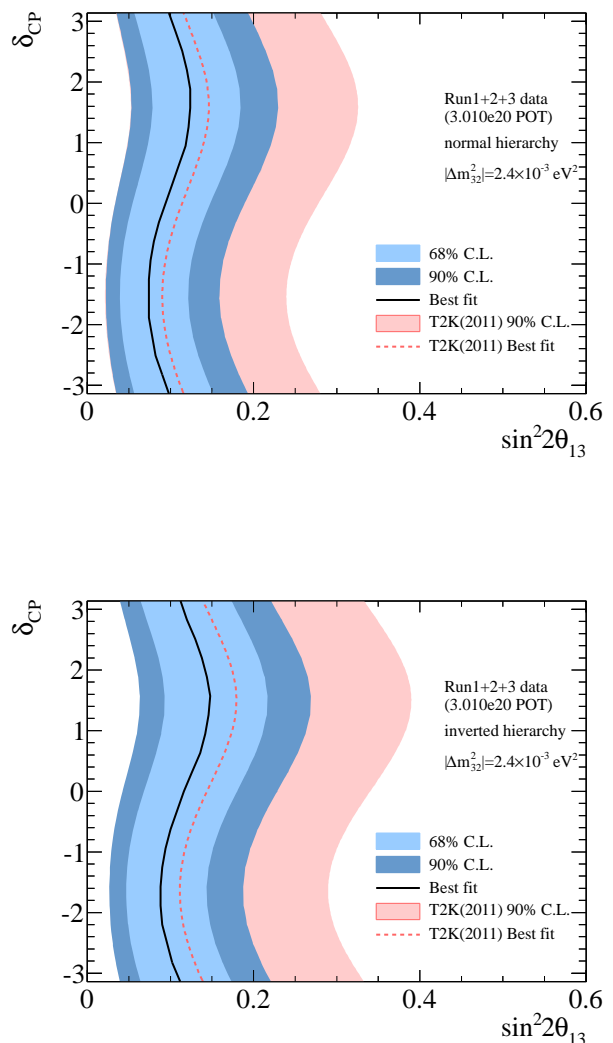


Fig. 4. The 60% and 90% C.L. regions for $\sin^2 2\theta_{13}$ for each value of δ_{CP} , consistent with the observed number of events in the three flavor oscillation case for normal (top) and inverted (bottom) mass hierarchy. The best fit values are shown in solid lines. The other oscillation parameters are fixed as explained in the text.

nation is performed using the observed number of events and the reconstructed energy spectrum of ν_μ in SK. As described, dominant interactions of neutrinos from the T2K beam near the oscillation peak is CCQE and thus, we used ν_μ single ring events to study ν_μ disappearance. The selection criteria of events used for the ν_μ to ν_τ oscillation analysis are as follows: events should be FCFV, there is one ring and identified as μ -like, reconstructed momentum of muon should be larger than 200 MeV/c and there is no more than 1 delayed electron associated with

Table 2. Systematic uncertainties on the predicted number of SK selected events without oscillations and for oscillations with $\sin^2(2\theta_{23}) = 1.0$ and $|\Delta m_{32}^2| = 2.4 \times 10^{-3} \text{ eV}^2$.

Source	$\delta N_{SK}^{exp}/N_{SK}^{exp}$ (%, no osc)	$\delta N_{SK}^{exp}/N_{SK}^{exp}$ (%, with osc)
SK CCQE efficiency	± 3.4	± 3.4
SK CC non-QE efficiency	± 3.3	± 6.5
SK NC efficiency	± 2.0	± 7.2
ND280 efficiency	+5.5 -5.3	+5.5 -5.3
ND280 event rate	± 2.6	± 2.6
Flux normalization (SK/ND280)	± 7.3	± 4.8
CCQE cross section	± 4.1	± 2.5
CC1 π /CCQE cross section	+2.2 -1.9	+0.4 -0.5
Other CC/CCQE cross section	+5.3 -4.7	+4.1 -3.6
NC/CCQE cross section	± 0.8	± 0.9
Final-state interactions	± 3.2	± 5.9
Total	+13.3 -13.0	+15.0 -14.8

the event. The efficiency and purity of ν_μ CCQE events are estimated to be 72% and 61%, respectively. The observed number of events is 31 while the expected number of events without oscillation is $103.6^{+13.8}_{-13.4}$. The systematic uncertainties on the expected numbers of events are summarized in Table .

We have performed two independent analyses to obtain the allowed region of oscillation parameters θ_{23} and Δm_{32}^2 . The first analysis uses the method by Feldman and Cousins⁸. For this case, statistical variations are taken into account by Poisson fluctuations of toy MC data sets and systematic uncertainties are incorporated using the method of Cousins and Highland⁹. The second analysis uses the maximum likelihood method. The likelihood function is defined as the product of number of events, neutrino energy spectrum shape and systematic term. The first term is the Poisson probability for the observed number of events and the second term is the un-binned likelihood for the reconstructed neutrino energy spectrum and the last term is a multidimensional Gaussian probability for the systematic error parameters. Results from these two analyses are consistent with each other. The best fit values of θ_{23} and Δm_{32}^2 from the first analysis are 0.98 and $2.65 \times 10^{-3} \text{ eV}^2$, respectively. The values from the second analysis are 0.99 and $2.63 \times 10^{-3} \text{ eV}^2$, respectively. The reconstructed energy spectrum with and without oscillation together with the data points are shown in Fig. 5. The obtained allowed regions of oscillation parameters are shown in the Fig. 6.

*⁸ G. J. Feldman and R. D. Cousins, Phys. Rev. D **57**, 3873 (1998)

*⁹ R. Cousins and V. Highland, Nucl. Instrum. Meth. A **320**, 331 (1992)

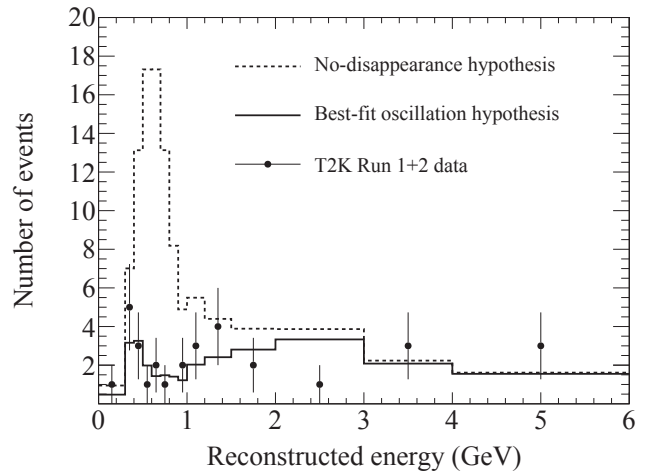


Fig. 5. Reconstructed neutrino energy spectrum of the events which pass all ν_μ disappearance signal selection criteria. The dashed line shows the expectation without oscillation and the solid line shows the expectation assuming the best fit oscillation parameters.

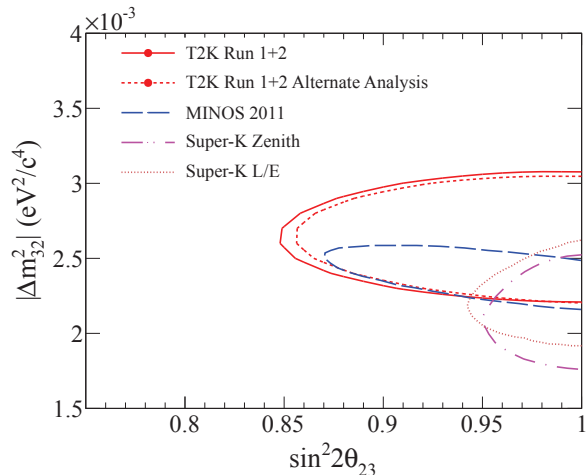


Fig. 6. The 90% confidence regions for $\sin^2 2\theta_{23}$ and $|\Delta m_{32}^2|$. Results from the two analyses are compared with those from MINOS and SK

Summary of T2K Experiment

Here summarized are the noticeable achievements and future prospects of the T2K experiment.

- The beam power has reached $\sim 200 \text{ kW}$ and more improvements are planned to reach the design value of 750 kW and more. J-PARC was quickly recovered in 9 months after the big earthquake on March 11, 2011.
- The T2K successfully accumulated J-PARC neutrino beam data at the near detectors and the far detector Super-K. Total amount of data

corresponds to 3.01×10^{20} protons on target taken from January 2010 until June 2012.

- By the data taken until 2012, the T2K reported first evidence of $\nu_\mu \rightarrow \nu_e$ appearance phenomena driven by nonzero θ_{13} [4] confirming the T2K's 2011 results of the indication of electron neutrino appearance [2]. The future goal of the T2K would be to measure the appearance probability with $\sim 5\%$ accuracy to constrain the neutrino parameters such as octant of θ_{23} , Dirac CP phase, neutrino mass hierarchy which are involved in the appearance probability.
- The evidence of $\nu_\mu \rightarrow \nu_e$ appearance would be a critical milestone in the overall neutrino physics program. The existence of $\nu_\mu \rightarrow \nu_e$ channels enables us to experimentally test CP violation in the lepton sector – by comparing oscillations of neutrinos and anti-neutrinos – which is the leading candidate for the origin of the excess of matter over anti-matter in the universe. For discovery of the leptonic CP violation, upgrade of both the neutrino beam facility and the far detector are necessary. The Hyper-Kamiokande, which is currently being developed and has 20 times larger detector volume than Super-K, is designed to be the next generation far detector for the study of CP violation.
- The first ν_μ disappearance analysis and measurements of θ_{23} and Δm_{32}^2 by the off-axis beam technique was reported [3]. We expect to achieve world best measurements of these oscillation parameters in future by accumulating more beam data.

T2K Collaboration

Spokesperson : Takashi Kobayashi (High Energy Accelerator Research Organization (KEK)).

Host institutes of the T2K experiment are KEK and ICRR. A member of the Executive Committee of the experiment is from ICRR, Yoichiro Suzuki (till 2011) and Masato Shiozawa (since 2011).

Institute	Country	(*)
ICRR, Univ. of Tokyo	Japan	23
KEK, High Energy Accelerator Research Organization	Japan	22
Kobe Univ.	Japan	5
Kyoto Univ.	Japan	16
Miyagi Univ. of Education	Japan	1
Osaka City Univ.	Japan	7
Univ. of Tokyo	Japan	4
TRIUMF	Canada	12
Univ. of Alberta	Canada	1
Univ. of British Columbia	Canada	9
Univ. of Regina	Canada	6
Univ. of Toronto	Canada	2
Univ. of Victoria	Canada	5
Univ. of Winnipeg	Canada	1
Yokoe Univ.	Canada	1
CEA/DAPNIA Saclay	France	5
IPN Lyon (IN2P3)	France	3
LLR Ecole polytechnique	France	4
LPNHE-Paris	France	7
RWTH Sezione de Bari	Germany	5
INFN sezione di Bari	Italy	4
INFN sezione di Roma	Italy	2
Napoli Univ. and INFN	Italy	2
Padova Univ. and INFN	Italy	3
Chonnan National Univ.	Korea	3
Dongshin Univ.	Korea	1
Seoul National Univ.	Korea	2
IFJ,PAN,Cracow	Poland	3
NCBJ, Warsaw	Poland	8
Technical Univ., Warsaw	Poland	5
Univ. of Silesia, Warsaw	Poland	5
Warsaw Univ.	Poland	3
Wroclaw Univ.	Poland	3
INR	Russia	7
IFAE, Barcelona	Spain	5

Institute	Country	(*)
IFIC, Valencia	Spain	7
Bern	Switzerland	7
ETHZ	Switzerland	7
Univ. of Geneva	Switzerland	9
Imperial College London	UK	12
Lancaster Univ.	UK	7
Oxford Univ.	UK	6
Queen Marry, Univ. of London	UK	10
STFC/RAL/Daresbury Laboratory	UK	9
Univ. of Liverpool	UK	10
Univ. of Sheffield	UK	4
Univ. of Warwick	UK	8
Boston Univ.	USA	5
Colorado State Univ.	USA	13
Duke Univ.	USA	5
Louisiana State Univ.	USA	7
Stoby Brook Univ.	USA	9
Univ. of California, Irvine	USA	5
Univ. of Colorado	USA	5
Univ. of Pittsburgh	USA	5
Univ. of Rochester	USA	4
Univ. of Washington	USA	4
Total		353

(*) Number of collaborators.

Members

Staff

Kamioka Observatory

Yoichiro Suzuki, Professor
 Masayuki Nakahata, Professor
 Shigetaka Moriyama, Assoc. Professor
 Masato Shiozawa, Assoc. Professor
 Yoshinari Hayato, Assoc. Professor
 Yasuo Takeuchi, Assoc. Professor (till Apr.2010)
 Makoto Miura, Research Associate
 Yusuke Koshio, Research Associate
 June Kameda, Research Associate
 Atsushi Takeda, Research Associate
 Kou Abe, Research Associate
 Hiroyuki Sekiya, Research Associate
 Yoshihisa Obayashi, Research Associate (till Dec.2011)
 Roger Wendell, Research Associate (from May 2012)
 Shoei Nakayama, Project Research Associate (from Apr.2007)

Tomonobu Tomura, Project Research Associate (from Mar.2011)
 Satoru Yamada, Project Research Associate (Oct.2006 - Nov.2010)
Research Center for Cosmic Neutrinos
 Takaaki Kajita, Professor
 Kimihiro Okumura, Assoc. Professor
 Kenji Kaneyuki, Assoc. Professor (till May 2010, deceased)
 Yasuhiro Nishimura, Project Research Associate (from Apr.2012)

Postdoctoral Fellows

Kamioka Observatory

Yasuhiro Nishimura (Apr.2011 - Mar.2012)
Research Center for Cosmic Neutrinos
 Hiroshi Kaji (Apr.2009 - Mar.2012)
 Andrew Brian Laing (Jan.2011 - Mar.2012)
 Nao Tanimoto (Feb. 2008 - Mar.2010)
 Yuuki Shimizu (Apr. 2008 - Mar.2010)

Graduate students

One student were awarded doctor degrees and three students earned master degrees during 2006–2012, supervised by ICRR staff members.

List of Publications

- [1] “The T2K Experiment”, T2K Collaboration (K. Abe et al.), Nucl. Instrum. Meth. A659 (2011) 106-135, **Cited 35 times.**
- [2] “Indication of Electron Neutrino Appearance from an Accelerator-produced Off-axis Muon Neutrino Beam”, T2K Collaboration (K. Abe et al.), Phys. Rev. Lett. **107**, 041801 (2011), **Cited 318 times.**
- [3] “First Muon-Neutrino Disappearance Study with an Off-Axis Beam”, T2K Collaboration (K. Abe et al.), Phys. Rev. D. **85**, 031103(R) (2012), **Cited 7 times.**
- [4] “NEW Results from T2K”, T. Nakaya, talk presented at the XXV International Conference on Neutrino Physics and Astrophysics (NEUTRINO 2012).

XMASS EXPERIMENT

XMASS is a multi-purpose experiment using liquid xenon which aims at the detection of cold dark matter, search for neutrinoless double beta decay, and detection of low energy solar neutrinos. The name XMASS stands for these three aims: Xenon detector for weakly interacting MASSive particles, Xenon neutrino MASS detector for double beta decay, and Xenon MASSive detector for Solar neutrino.

Astronomical observations suggest that there is dark matter (non-luminous particles with mass) in the universe. One of the most likely candidates for dark matter is a weakly interacting massive particle (WIMP), for example the lightest supersymmetric particle. A recoil of a xenon nucleus from an interaction with dark matter will produce scintillation light in liquid xenon.

The Super-Kamiokande experiment shows that neutrinos have mass. However, we do not yet know the absolute mass of neutrinos and whether the neutrinos are Majorana type or Dirac type. Xenon nuclei with mass number 136 is one of the double beta decay nuclei which is best suited for this research.

The energy spectrum of the solar neutrino is measured by Super-Kamiokande, SNO, and Borexino but that of low energy solar neutrinos (pp neutrinos, etc.) is not measured yet. With 10-ton liquid xenon, it will be able to detect pp neutrinos and ^7Be neutrinos by $\nu+e$ scattering with a rate of 10 events/day and 5 events/day, respectively.

For all these purposes, background caused by gamma rays which comes outside liquid xenon is needed to be suppressed. The key idea to reduce background is that gamma rays can be absorbed by liquid xenon itself (self-shielding)[1]. A sphere of liquid xenon absorbs low energy gamma rays from the outside within 10-20 cm thickness and realizes a low background at the central volume. WIMPs and neutrinos, however, interact throughout the detector. Therefore, if the vertices of the events can be reconstructed, WIMPs and neutrinos can be observed in a low background environment by extracting only events which observed deep inside the detector. The event reconstruction can be accomplished by observing photons with the many photo multipliers mounted outside the fiducial vol-

ume (FV). Liquid xenon has the following advantages to realize this idea:

- With the high atomic number of xenon ($Z = 54$) and the high density of liquid xenon ($\sim 3\text{ g/cm}^3$), external gamma-rays can be absorbed in a short distance from the detector wall (self-shielding).
- A large light yield of 42,000 photons/MeV, which is as good as NaI(Tl) scintillator, enables good event reconstruction as well as detection of small energy signals like dark matter recoil.
- 175 nm scintillation light of liquid xenon can be read out by typical photomultiplier tubes (PMTs) of bi-alkaline photocathode with a quartz window.
- Purification is easier than other materials (e.g. distillation is possible).
- Isotope separation is possible. It is possible to enrich ^{136}Xe for double beta decay or deplete ^{136}Xe for solar neutrino measurements.

We have been studying liquid xenon detector since the year 2000. A 3 kg FV liquid xenon detector has been developed for R&D study and test data have been taken [2].

Based on the study, we designed and started to construct the first prototype of the XMASS detector (100 kg FV) for dark matter search from 2007. Its projected sensitivity for 100 GeV WIMPs is $2 \times 10^{-45}\text{ cm}^2$. As is shown in the following section in detail, commissioning data is now being taken. The data consist of calibration data, test runs for understanding the detector performance, and normal runs for dark matter search. At present,

- A low mass dark matter have been searched for in whole the detector volume with the lowest energy threshold of 0.3 keV by taking the maximum advantage of the highest light yield among other similar experiments. We have obtained comparable results to previous experiments.
- A search for the super-WIMPs dark matter and axion-like particles from the sun have been conducted.

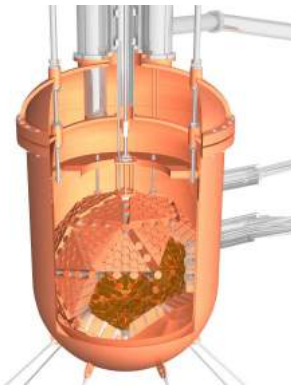


Fig. 1. Liquid xenon detector with 100 kg fiducial volume was constructed for dark matter search. The central part of liquid xenon is surrounded by 642 hexagonal PMTs arranged spherically. Most part of the detector consists of oxygen-free copper to minimize radioactive background.

- A detailed modeling of detector response and an optimization of the FV cut have been made. This is underway and crucial to search for dark matter with 100 GeV.

We have found unexpected background on the inner surface. The background was found to come from beta rays and X rays from ^{238}U series contained in aluminum seal used for PMTs, and from surface ^{210}Pb contamination (radon daughters). Because of those unexpected backgrounds, we need rather sophisticated reconstruction programs to perform a fiducialization analysis which is now underway.

We also try to refurbish the detector to reduce the effect of backgrounds from aluminum. We make a kind of mask over the aluminum since we are not able to replace PMTs. We can at least confirm how the background can be handled and could get better understanding on remaining backgrounds. The best fiducial volume analysis can be obtained then.

Required sensitivity has now moved from the range where 100 kg detector can explore to 1 ton detector can do. A single phase detector has an advantage of its scalability. Therefore we need to construct a 1 ton scale detector as soon as possible. All the necessary developments should be done in parallel to other efforts.

Construction of a 100 kg fiducial volume detector

The construction of the 100 kg FV detector was approved in 2007. The detailed detector design and manufacturing PMTs were started at that time.



Fig. 2. PMT holders and backside of PMTs

Figure 1 shows a schematic drawing of 100 kg FV liquid-xenon detector. The liquid xenon at the central part is 80 cm in diameter and viewed by 642 2-inch hexagonal PMTs which were developed for low background purposes. The PMTs have high quantum efficiencies (typical 30%) for 175 nm scintillation light of liquid xenon. The PMTs as well as copper holders are immersed in liquid xenon so that photoelectron yield is maximized. Surrounding two layers of copper vessels are important for thermal insulation.

Figure 2 is a photograph of the PMT holder and backside of the PMTs. They are all made of oxygen-free copper in order to minimize the radioactive background. The copper was electrorefined just before delivery to the mine. This was intended to minimize production of radioactivity, such as ^{60}Co , by cosmic ray muons on the ground surface. The detector structure was assembled under a clean environment with radon free air. During the assembling work, dust level was less than 1000 particles/ft³ and radon concentration was about 200 mBq/m³ which is 1/100 of that in atmosphere. Many white cables in the photograph are coaxial cables for PMT signals and high voltage cables. All the material were examined so that we can have gamma ray and radon emission as small as possible.

As shown in the figure 3, the detector is placed in a cylindrical pure-water tank with two layers of copper vessels for thermal insulation. The water



Fig. 3. Detector with copper vessel and an inner view of the water shield

tank is 10 m in diameter and 10.5 m in height to reduce gamma rays, neutron and radon backgrounds. The water tank is equipped with 72 20-inch inward facing PMTs to tag incoming cosmic ray muons. This is the first case to adopt a pure-water tank as an active and passive shield for dark matter experiments.

All the construction was done by the fall of the year 2010. Before filling the detector with liquid xenon, we purified xenon gas using a distillation system which was developed for reducing Krypton contamination. As it is described in the latter section, the system produced xenon gas with a contamination of Krypton less than 2.3 parts per trillion (ppt) which is the world best purity achieved for the dark matter experiments.

Finally, xenon gas was introduced into the detector by liquefying with refrigerators. Since contamination such as water molecules in liquid xenon absorb scintillation lights, we collected and vaporized liquid xenon, and introduced through purifiers. Photoelectron yield from a calibration source at the center of the detector increased 16% because of this purification.

Commissioning data with a 100 kg fiducial-volume detector

Commissioning data were taken from December 2010. Figure 4 shows a calibration data taken with a radioactive source, ^{57}Co , at the center of the detector. The two peaks observed correspond to 122-keV full absorption peak of ^{57}Co and 60-keV fluorescence X-ray peak from tungsten wire inside. The dashed line is showing simulated data which gives a reasonable agreement with real data. Similar calibration data in various points along an

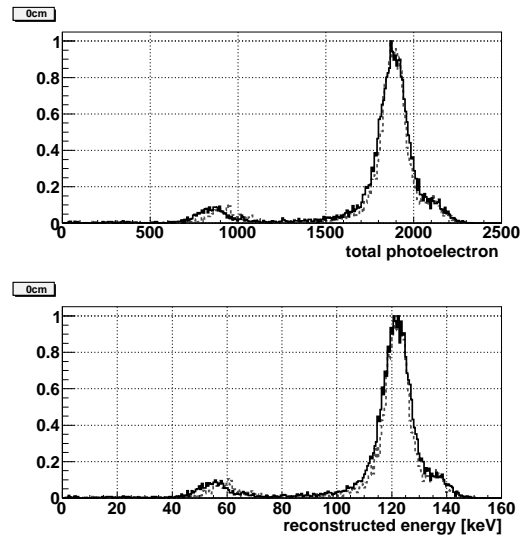


Fig. 4. Calibration data with ^{57}Co source at the center of the detector. The top figure shows a distribution for observed total photo electron and the bottom figure shows the reconstructed energy. The solid histograms and dotted histograms depict real data and Monte Carlo simulation, respectively.

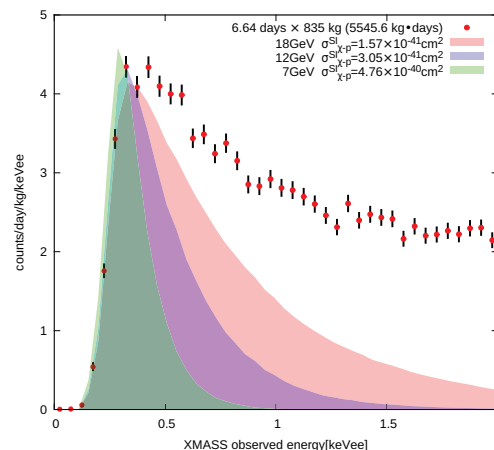


Fig. 5. Observed energy spectrum and predictions for various mass of dark matter.

axis of the sphere were taken. From this data, the photoelectron yield was found to be higher than expected (14.7 photoelectrons for one keV deposit by 122 keV gamma rays) which is the best light yield among existing detectors for dark matter search. This is a great advantage for a dark matter search, especially for light WIMPs.

A search for light WIMPs has been carried out by taking advantage of the high light yield. Since the energy threshold is low (0.3 keV electron-equivalent, keVee), the detector is sensitive to low mass WIMPs. We used whole the detector volume since FV cut based on the event reconstruction cannot be used due to a limited number of photoelec-

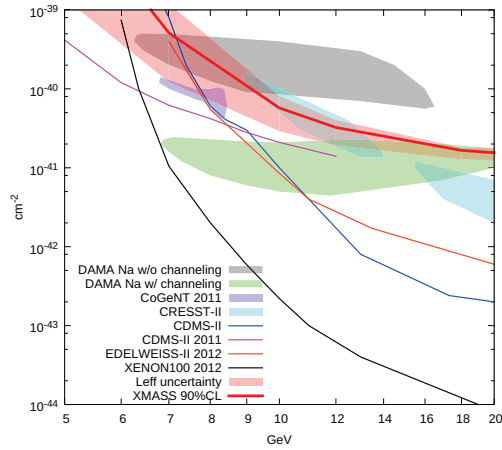


Fig. 6. Preliminary result of constraints on low mass WIMPs (red thick line) with uncertainties of scintillation efficiency (red dark region). Allowed region for DAMA (gray area) and CoGeNT (blue area) are also shown.

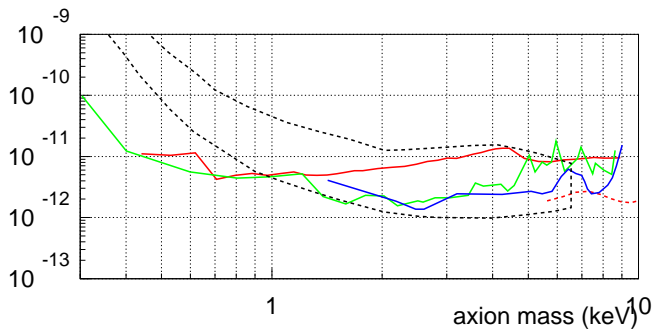


Fig. 7. Limit on the axion-electron coupling constant assuming the dark matter consists of axions. The red line shows the constraint with our data set. The black-dotted area shows the parameter space which is argued to cause annual modulation in DAMA experiment. The solid green and blue lines are showing constraints by CoGeNT and CDMS experiments. The red dashed line shows a result of sensitivity study with a model of background.

trons at the lowest energy range. Figure 5 shows the energy spectrum after rejection of noisy events and Cherenkov events mainly caused by potassium in photo cathodes. In the same figure, expectations of dark matter signals are shown. Since the signals cannot exceed the observed energy spectrum, limits on the cross section for the light WIMPs have been derived. Figure 6 shows the limit on the cross section. Though we have uncertainty originated from the scintillation efficiency for nuclear recoil (red band), some part of allowed region by the DAMA experiment was excluded.

Some studies have been done to search axion-like particle. One study is for the candidate of

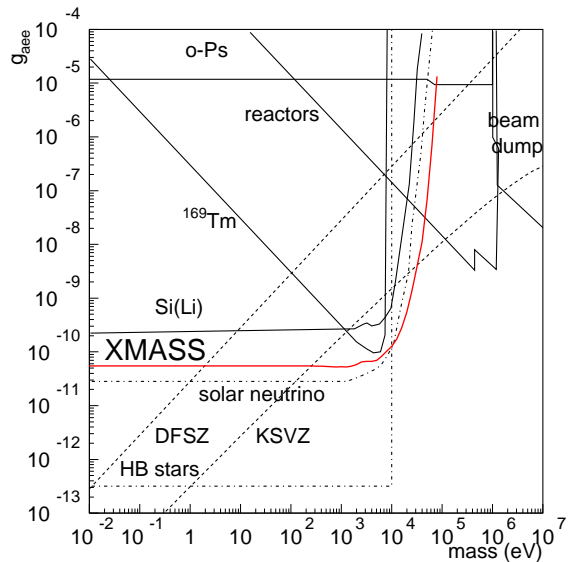


Fig. 8. Result of the search for solar axions produced by bremsstrahlung and Compton effect in the sun. The red line shows the limit with our data set and other lines are from other experiments, astrophysical arguments, and theoretical predictions. Our result is factor four to five improvement from the latest experimental result.

dark matter which might cause the annual modulation observed by DAMA group. If the dark matter consists of such particles, their signal would be detected through axio-electric effect. The data set for the light WIMPs search was used to find the mono-energetic signals which correspond to rest mass of the non-relativistic dark matter. Since there is no prominent peak in the observed data, limits on the axion-electron coupling are given as shown in Fig. 7¹.

Another study is for the solar axions. Axions produced by bremsstrahlung and Compton process in the sun could be observed by axio-electric effect. By taking into account the effect of the mass of axions on the production in the sun and the detection in the laboratory, comparison between expected signals and the observed spectrum was performed. Since no indication of signals in the observed energy spectrum was found, the corresponding limit of axion-electron coupling is also derived (Fig. 8). The limit is factor four to five improvement from a latest experimental result².

We found unexpected background on the inner surface and studied the origin of background. As a conclusion, one of the most significant source

^{*1} CoGeNT: C. E. Aalseth *et al.* PRL 106, 131301 (2011), CDMS: Z. Ahmed *et al.* PRL 103, 141802 (2009)

^{*2} A. V. Derbin *et al.* arXiv:1206.4142 and references therein

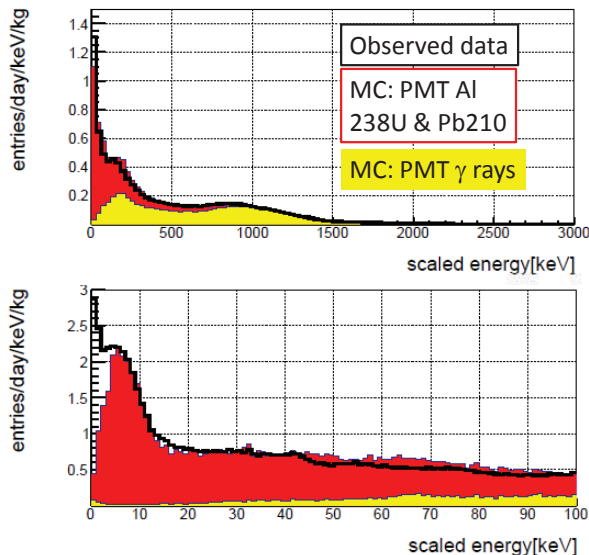


Fig. 9. Observed energy spectrum and Monte Carlo (MC) prediction of background. The horizontal axis is the observed number of photo electrons divided by the photo electron yield, i.e., $14.7(\text{p.e./keV})$. The black thick line shows the observed spectrum. The yellow and red histograms are simulated background caused by PMT gamma rays, and radioactive contamination in aluminum seal between PMT window and its body, respectively. See details in text.

is found to be aluminum sealing material between PMT window and its body. We found significant amount of ^{238}U and ^{210}Pb in the material by a measurement with a germanium detector. Another one is the radon daughters attached on the inner surface of detector. Figure 9 shows the agreement between observed energy spectrum and expected background originated from aluminum and radon daughters. The good agreement above 5 keV implies a good understanding of current background components above our dark matter analysis threshold. In future detectors, those must be reduced as much as possible. As for the aluminum seal, aluminum with smaller amount of ^{238}U must be used for future PMTs. We already found they are commercially available. As for the surface contamination, a careful treatment of inner surface material (etching to remove contamination, minimum exposure to radon, etc.) must be done. To confirm that the surface contamination will not a problem in future detectors, we plan to place metal covers on top of aluminum seal of the 100 kg detector since it is difficult to replace all the PMTs. With the current level of understanding of background, we have a good prospect to have significant reduction of back-

ground after the improvement. This study additionally enables us to perform following studies: (1) reduction and further understanding of background, (2) a standard WIMP search ($\sim 100\text{ GeV}$), (3) a low-mass WIMP search, a search for annual modulation, and a search for axion-like particles.

Other origins of background, such as radon gas in liquid xenon, is also important but found to be small at this stage. To evaluate ^{222}Rn contamination as well as its daughter nuclei, we measured it through ^{214}Bi - ^{214}Po consecutive decay and found to be $8.2 \pm 0.5\text{ mBq}$ inside the detector. With a similar method, ^{220}Rn was measured to be less than $280\text{ }\mu\text{Bq}$ (90% C.L.). By taking into account an upper limit for ^{85}Kr contamination, an evaluated background originating from radioactive contamination in liquid xenon is factor three higher than our target. However, this is acceptable at this moment and we are planning to reduce ^{222}Rn using charcoal filters as described in the following section.

The expected sensitivity of the 100 kg detector for 100 GeV WIMPs is $2 \times 10^{-45}\text{ cm}^2$ with an assumption of analysis threshold at 5 keVee, and 1 year lifetime, and background level at the threshold is $10^{-4}/\text{keVee/kg/day}$. To achieve this goal, an optimization of fiducial volume cut is necessary and underway. An improvement of background by hardware improvement surely helps the sensitivity in near future.

XMASS 1.5

The advantage of the single phase detector is scalability. It enables us to build a 1 ton, 10 ton, even a 100 ton detector without such difficulties as high electric field and long electron drift length required by double phase detectors. The latest experimental result tells us the region where the 100 kg FV detector can explore is more or less excluded. Therefore a detector such as 1 ton or 10 ton must be operated as soon as possible. After settling down the current problem of the background, the next stage detector, XMASS1.5 with 1 ton FV must be designed and constructed. Its design should be common and scalable to a 10 ton detector so that we can make the full 10 ton detector with minimum modifications. The detector is expected to have a sensitivity around 10^{-46} cm^2 for the WIMPs with a mass of 100 GeV.

The basic design of the detector is same as the one for the 100 kg FV detector but with an im-

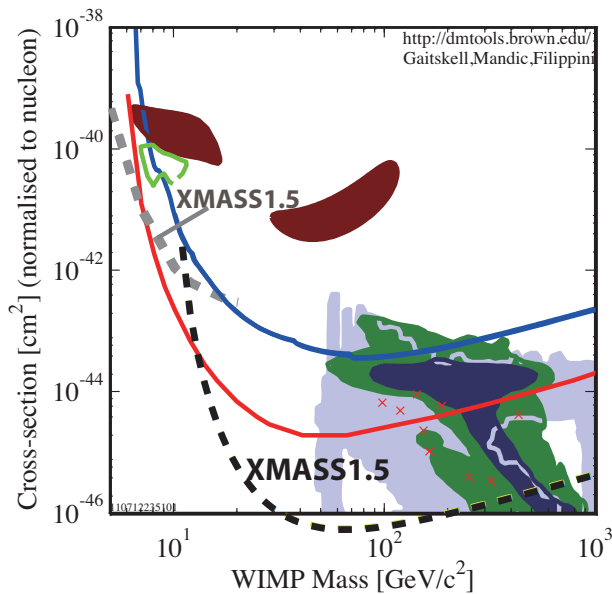


Fig. 10. Expected sensitivity of the XMASS 1.5 detector. The lower dashed line shows a sensitivity with 2 keV electron-equivalent threshold and 1 year livetime. The two solid lines show the experimental limits by CDMS and XENON100. Three areas around 10^{-41} to 10^{-40} cm^2 are for positive results by DAMA and CoGeNT group. The dashed line below 10 GeV shows expected sensitivity for low mass WIMPs using whole volume. The hatched areas and crosses at the right bottom correspond to theoretical predictions. The plot was partly made by a web site <http://dmtools.brown.edu/>.

provement of the discrimination between the surface background and the inner events. For that purpose, we are developing a new type of PMTs. They have convex-shape photocathodes which has advantage to detect direct light from the inner surface of the detector. The new PMT design is expected to enforce the discrimination between events around the wall and inner volume, and minimizes leakage events from undesirable surface background after the FV cut. A detailed design is underway based on the knowledge of the current detector.

Figure 10 shows the expected sensitivity with the XMASS1.5 detector³. We are planning to design the detail of the detector in 2013, and be able to start construction in 2014 if the project is approved.

Other important studies

As discussed in the previous section, radiations from PMTs must be reduced by the FV cut and an improvement of surface treatments. On the other hand, radioactivities inside liquid xenon must be

reduced by other methods. For that purpose, two studies for physical removal of radioactivities and one study for reduction based on scintillation waveforms were done. A study for different detector design for double beta decay search was also performed.

Development of a Distillation System to Remove Krypton

Since xenon is produced from air, contamination of ^{85}Kr is a problem for low background experiment. Commercial xenon usually contains a few ppm of Kr but next-generation dark matter detectors require less than a few ppt of Kr. To overcome this problem, a distillation system to remove Krypton was developed and proved to meet the requirement [3]. A special technique was developed to measure a few ppt level of Krypton.

Based on the development, a larger scale (higher processing speed) distillation system was constructed and applied to 1 ton of xenon for the 100 kg FV detector. The Kr contamination in the product was found to be less than 2.3 ppt which is satisfactory for the current dark matter search.

Radon Removal from Gaseous Xenon

Another serious background would be ^{222}Rn . So far, any methods of reducing radon in xenon has not been established. One candidate is activated charcoal which contains a large amount of pores inside. We tested some of them and found a certain kind of charcoal column under low temperature caused slower flow speed for contaminated radon than that for xenon [4]. Since radon decays with 3.8 days half life, we can expect radon reduction by its decay during the flow. Based on the data, we designed, constructed and tested a charcoal system which reduces radon with a factor 1/14. Its would be applied to the 100 kg detector.

Study on Pulse Shape Discrimination

It is known that the liquid xenon scintillator gives different pulse shapes of scintillation light for different types of radiations. We have studied the performance of discrimination based on the pulse shapes in a dedicated test setup [5]. This study was unique since the photoelectron yield was quite higher (20.9 photoelectrons/keV) than the previous studies. If we can discriminate nuclear recoil signals from common background caused by gamma

*³ DAMA: R. Bernabei *et al.* EPJ C56 (2008) 333, CoGeNT: C. E. Aalseth *et al.* PRL 106, 131301 (2011), XENON100: arXiv:1207.5988, CDMS: Z. Ahmed *et al.* Science 327 (2010) 1619

rays and electrons, we could reduce background effectively.

As a result of study, we confirmed a reduction of background caused by electrons and gammas with a factor $7.7 \pm 1.1(\text{stat.}) \pm_{0.6}^{1.2}(\text{sys.}) \times 10^{-2}$ at energies between 4.8 and 7.2keV while keeping efficiency of 50% for nuclear recoils. This provides another method of background reduction.

Scintillation Yield of Liquid Xenon at Room Temperature

A study on a double beta decay search requires lower background than that we can achieve the current detector configurations. This is mainly because the PMTs are arranged to be close to the liquid xenon. If it is possible to use liquid xenon at room temperature, it would enable various new possibilities for detectors and make detector construction easier. For that purpose, a study on the intensity of scintillation light emission at room temperature was performed. We used a small chamber which can be used at room temperature (1 °C) as well as low temperature (−100°C). The scintillation light yield at 1 °C was measured to be $0.64 \pm 0.02(\text{stat.}) \pm 0.06(\text{sys.})$ of that at −100°C [6]. This result shows that liquid xenon gives high light yield even at room temperature.

Summary

We have done following things in last six years:

- The first prototype of the XMASS detector, 100 kg FV detector was designed and constructed successfully.
- Purification of liquid xenon has been done and high light yield was obtained.
- Commissioning runs for detailed understanding of the detector were performed.
- A detector calibration has been done. Good agreement with Monte Carlo simulation was observed.
- Searches for light WIMPs, super-WIMPs and solar axions have been performed.
- Competitive results from searches for light WIMPs, super WIMPs and solar axions have been obtained.
- Unexpected background were found.

- A FV analysis will be further developed and optimized.
- Further reduction of backgrounds are underway by modifying the hardware configuration.
- XMASS with 1 ton fiducial mass is now under consideration.

We have good achievement on those topics and further improvement can be expected after development of the FV cut and hardware improvement in future. We have significant progress in the last six years and good prospects in next few years.

XMASS Collaboration

Spokesperson : Yoichiro Suzuki (Kamioka Observatory, ICRR, The University of Tokyo)

Institute	Country	(*)
ICRR, Univ. of Tokyo	Japan	20
IPMU, Univ. of Tokyo	Japan	2
Kobe Univ.	Japan	5
Tokai Univ.	Japan	3
Gifu Univ.	Japan	1
Yokohama National Univ.	Japan	3
Miyagi Kyoiku Univ.	Japan	1
Nagoya Univ.	Japan	5
Sejong Univ.	Korea	2
Korea Research Institute of Standards and Science (KRISS)	Korea	5
Total		47

(*) Number of collaborators.

Members

Staff

Yoichiro Suzuki, Professor
 Masayuki Nakahata, Professor
 Shigetaka Moriyama, Assoc. Professor
 Yasuhiro Kishimoto, Assoc. Professor (from Dec.2010)
 Yasuo Takeuchi, Assoc. Professor (till Apr.2010)
 Atsushi Takeda, Research Associate
 Kou Abe, Research Associate
 Hiroyuki Sekiya, Research Associate
 Masaki Yamashita, Project Assoc. Professor
 Hiroshi Ogawa, Project Research Associate (from Oct. 2007)
 Kazuyoshi Kobayashi, Project Research Associate (from Oct. 2007)

Katsuki Hiraide, Project Research Associate (from Feb.2010)

Postdoctorial Fellows

Byeongsu Yang (from July 2011)
Katsuki Hiraide (Apr.2009 - Jan.2010)
Hiroshi Ogawa (Oct.2004 - Sep.2007)

Graduate students

Two students were awarded doctor degrees and five students earned master degrees during 2006–2012, supervised by ICRR staff members.

List of Publications

- [1] Y. Suzuki et al., “Low energy solar neutrino detection by using liquid xenon”, Aug. 2000, hep-ph/0008296.
- [2] A. Minamino et al. (The XMASS collaboration), “Self-shielding effect of a single phase liquid xenon detector for direct dark matter search”, *Astropart. Phys.* 35 (2012) 609.
- [3] K. Abe et al. (The XMASS collaboration), “Distillation of liquid xenon to remove krypton”, *Astropart. Phys.* 31 (2009) 290.
- [4] K. Abe et al. (The XMASS collaboration), “Radon Removal from Gaseous Xenon with Activated Charcoal”, *Nucl. Instr. and Meth A* 661 (2012) 50.
- [5] K. Ueshima et al. (The XMASS collaboration), “Scintillation-only Based Pulse Shape Discrimination for Nuclear and Electron Recoils in Liquid Xenon”, *Nucl. Instr. and Meth. A* 659 (2011) 161.
- [6] K. Ueshima et al. (The XMASS collaboration), “Scintillation yield of liquid xenon at room temperature”, *Nucl. Instr. and Meth. A* 594 (2008) 148.

HYPER-KAMIOKANDE (R & D)

The quest for nonzero θ_{13} was advanced by the T2K experiment announcing in June 2011 that an indication of ν_e appearance in ν_μ beam has been observed and zero θ_{13} is disfavored at 2.5σ significance¹. With more accumulated data, T2K presented an evidence for $\nu_\mu \rightarrow \nu_e$ oscillations in 2012². Furthermore the Daya Bay Reactor Neutrino Experiment announced in March 2012 that it has observed $\bar{\nu}_e$ disappearance³ and the latest measured θ_{13} value is $\sin^2 2\theta_{13} = 0.089 \pm 0.010(\text{stat}) \pm 0.005(\text{syst})$ ⁴ which is consistent with the ν_e appearance observed in T2K. These events would be a critical milestone in the overall neutrino physics program. The existence of $\nu_\mu \rightarrow \nu_e$ oscillation phenomena enables us to experimentally explore CP δ parameter because the magnitude of CP violation in $\nu_l \rightarrow \nu_{l'}$ and $\bar{\nu}_l \rightarrow \bar{\nu}_{l'}$ oscillations is proportional to the size of both $\sin 2\theta_{13}$ and $\sin \delta$ values. The value of the CP phase is a question of general interest because (1) the δ is now the last unknown oscillation parameter in the MNS matrix, and (2) a leptonic CP asymmetry is a leading candidate for understanding of the origin of the existing matter-dominated (over antimatter) universe.

The Hyper-Kamiokande (Hyper-K) is the third generation underground water Cherenkov detector in Kamioka that holds 1 million ton water target being about 20 times larger than the Super-Kamiokande (Super-K)⁵ [1]. It serve as a far detector in a long baseline neutrino oscillation experiment with intense neutrino beam produced by the upgraded J-PARC for unprecedented precision measurement of neutrino oscillation probabilities. By the long baseline experiment along with high statistical atmospheric neutrino study, Hyper-K will explore the full picture of neutrino masses and mixings by discovery of CP δ , determination of the neutrino mass hierarchy, and the octant of θ_{23} . The

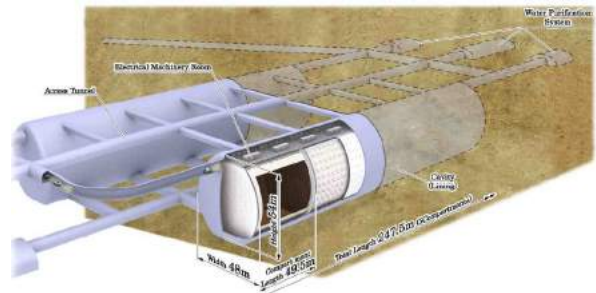


Fig. 1. Schematic view of the Hyper-Kamiokande. The detector consists of two cylindrical tanks holding 500 kton ultra-pure water (1 Mton in total). The each tank is divided by segmentation walls every 50m.

detector is also capable of searching for baryon-number-violated nucleon decays with the sensitivity beyond the world largest detector Super-K by more than one order of magnitude. Particle and astroparticle physics studies by using extraterrestrial neutrinos from Sun, Supernova, Galaxy, and so on are also within the scope of the detectors. In addition, its capability to detect a large number of atmospheric neutrinos enables us to perform the neutrino oscillation radiography for the Earth's core.

Extensive development works by the Hyper-Kamiokande working group have been performed on geological surveys in the candidate sites, design of cavern and tank, water purification and circulation system design, new photon sensor and DAQ system, detector calibration system, analysis software, and physics sensitivities. The group discussed the R&D works in international conferences [2, 3, 4, 5, 6] and released a letter of intent [7] in which the detector's baseline design and physics potential of Hyper-K are described. The highlight of the R&D works is shown in following sections.

Baseline design of the Hyper-K

The baseline design of Hyper-K is based on the well-proven technologies employed and advanced at Kamiokande and Super-K. The schematic view of the Hyper-K detector is illustrated in Fig. 1. The outer dimensions of two lying tanks is $48\text{ (W)} \times 54\text{ (H)}\text{ m}^2$ egg-shaped cross section with horizontal length of 250 m. The total (fiducial) mass of the detector is 0.99 (0.56) million tons, which is about

*1 K. Abe *et al.* [T2K Collaboration], Phys. Rev. Lett. **107**, 041801 (2011) [arXiv:1106.2822 [hep-ex]].

*2 T. Nakaya, Talk presented at the XXV International Conference on Neutrino Physics and Astrophysics (NEUTRINO 2012).

*3 F. P. An *et al.* [DAYA-BAY Collaboration], Phys. Rev. Lett. **108**, 171803 (2012) [arXiv:1203.1669 [hep-ex]].

*4 Dan Dwyer, Talk presented at the XXV International Conference on Neutrino Physics and Astrophysics (NEUTRINO 2012).

*5 M. Koshiba, Phys. Rept. **220**, 229 (1992).

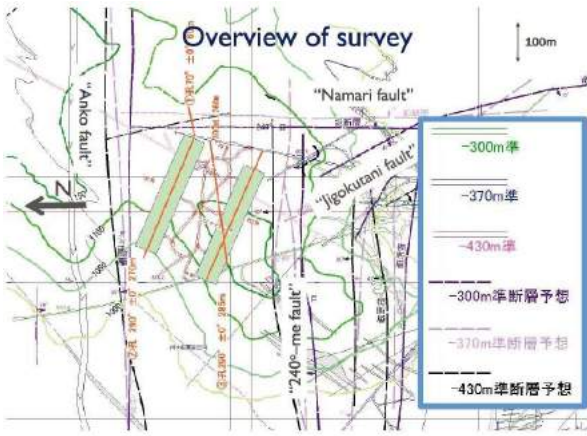


Fig. 2. Schematic view of the geological survey in the candidate site. We conducted bore-hole coring survey illustrated by red lines. Two green boxes are proposed location of the two cavern.

20 (25) times larger than that of Super-K. 99,000 20-inch PMTs will be instrumented, corresponding to the PMT density of 20% photo-cathode coverage (one half of that of Super-K). A proposed location for Hyper-K is about 8 km south of Super-K and 295 km away from J-PARC, and under the peak of Nijuugo-yama providing 1,750 meters water equivalent (or 648 m of rock) overburden. In terms of the J-PARC neutrino beam, the off-axis angles with the Hyper-K is same as the one with the Super-K. Site studies and design of the detector were conducted – geological survey for rock/fault distributions illustrated in Fig. 2, rock property measurements, FEM analysis and optimization for the twin cavities were performed.

By taking into account the estimated construction periods and production rate of photo-sensors, Hyper-K is expected to start operation in 2023.

Development Work for Photo-sensors and Others

The 20-inch PMTs which have been used in the Super-K satisfy necessary requirement of Hyper-K. However, lower-cost higher-sensitivity photo-sensors are preferred because one of main cost drivers is the PMT. A hybrid photomultiplier (HPD) using a photocathode and an avalanche photo-diode with ~ 10 kV high voltage is being developed [8, 9]. Proof-test will be conducted in 2012 by long term operation of several prototypical HPDs installed in a 100 ton scale water Cherenkov detector. Photo-sensors using other techniques are also being considered.

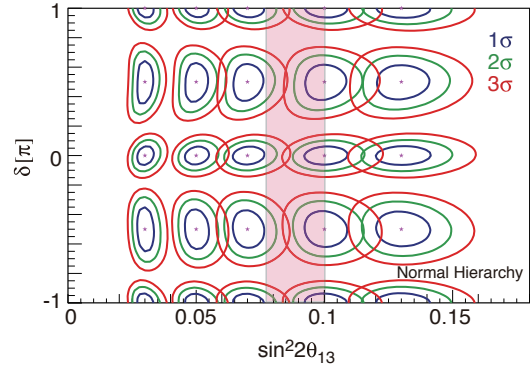


Fig. 3. Expected sensitivity for $\sin^2 2\theta_{13}$ and CP phase δ assuming the 2.25 Mton-years of ν and 5.25 Mton-years of $\bar{\nu}$ runs. The pink band represents the measurement by Daya Bay reactor experiment

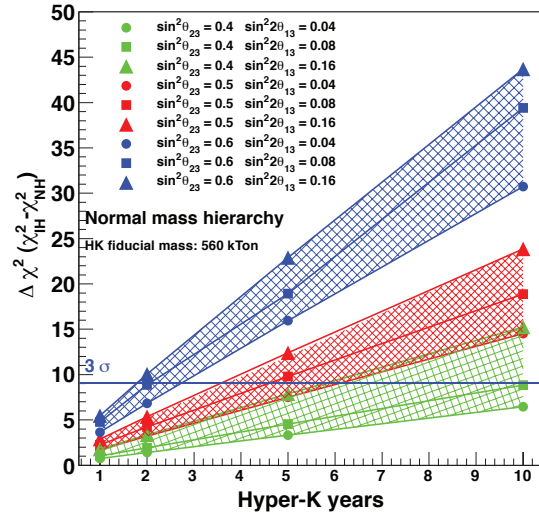


Fig. 4. Expected discrimination power for neutrino mass hierarchy as a function of observation years. Blue horizontal line shows $\Delta\chi^2$ of nine which corresponds to hierarchy determination with 3σ significance. Typical observation years to reach the 3σ level is 5 years.

In parallel, many development works are going on or starting mainly to enhance the physics potential of the detector and optimize its construction cost. DAQ electronics and computer system design was made based upon the Super-K. R&D of the front-end electronics under water is being started. The design of water purification system is going on with companies in Japan and US. The water flow control in the big tank is under investigation. Moreover, sophisticated detector calibration system and dedicated software development are also under discussions.

Physics Potential

Hyper-K provides rich neutrino physics programs. In particular, it has unprecedented potential for precision measurements of neutrino oscillation parameters and discovery reach for CP violation in the lepton sector. Figure 3 shows expected sensitivity for $\sin^2 2\theta_{13}$ and CP phase δ . With 2.25 Mton-years of ν and 5.25 Mton-years of $\bar{\nu}$ runs, it is expected that the CP phase δ can be determined to better than 18 degrees for all values of δ and that CP violation can be established with a statistical significance of 3σ for 74% of the δ parameter space. Thanks to the large $\sin^2 2\theta_{13}(= 0.1)$, the mass hierarchy can be determined with more than 3σ statistical significance for 46% of the δ parameter space with this program alone.

The high statistics data sample of atmospheric neutrinos obtained by Hyper-K will also allow us to extract information on the mass hierarchy and the octant of θ_{23} . With a full 10 year period of data taking, the significance for the mass hierarchy determination is expected to reach 3σ or greater as is shown in Fig. 4. If $\sin^2 2\theta_{23}$ is less than 0.99, it is possible to identify the octant of θ_{23} , *i.e.* discriminate $\sin^2 \theta_{23} < 0.5$ from > 0.5 .

Hyper-K extends the sensitivity to nucleon decays far beyond that of Super-K. The sensitivity to the partial lifetime of protons for the decay mode $p \rightarrow e^+ \pi^0$, the mode considered to be most model independent, is expected to be 1.3×10^{35} years. It is the only realistic detector option known today able to reach this sensitivity. The sensitivity for the decay mode $p \rightarrow \bar{\nu} K^+$, the mode favored by super symmetry (SUSY) models, reaches 2.5×10^{34} years, and therefore Hyper-K would discover proton decay if some of the SUSY models are correct.

Furthermore, the detector has the following physics potential:

- Detailed study of supernova explosion mechanism using high statistics ν events (170,000 \sim 260,000 events are expected for a supernova at 10 kpc) and of neutrino properties themselves.
- Observation of supernova relic neutrinos and study of heavy element synthesis in the universe.
- Measurement of energy spectrum distortion and day/night flux difference of ^8B solar neutrinos expected from the Large Mixing Angle (LMA) solution.

- Search for neutrinos from various astrophysical objects, *e.g.* WIMP origin neutrinos from Sun, Earth, and Galaxy, or neutrinos from solar flares, gamma ray bursts, and so on.
- Radiography for the Earth's core by observing the MSW effect in a large number of atmospheric neutrino events.

Summary

The evidence for $\nu_\mu \rightarrow \nu_e$ appearance opened the future of neutrino physics program. The Hyper-K working group proposed the next generation water Cherenkov detector based on well-proven technology which has rich physics topics and unprecedented sensitivities for them including discovery potential for leptonic CP violation and nucleon decays.

Here summarized are milestones already achieved and to be achieved in order to realize the project.

- Baseline design of the Hyper-K detector was made and described in the letter of intent [7]. The document also describes Hyper-K's rich physics potentials which cover wide physics topics, *i.e.* neutrino oscillation physics, nucleon decay searches, astrophysical studies using various astrophysical objects like Sun, Supernova etc.. The total (fiducial) mass of the detector is 0.99 (0.56) million metric tons, which is about 20 (25) times larger than that of Super-K. With 7.5 MW \times years of J-PARC/Hyper-K data, it is expected that CP violation can be established with a statistical significance of 3σ for 74% of the δ parameter space. The sensitivities to the partial lifetime of protons for the decay modes of $p \rightarrow e^+ \pi^0$ and $p \rightarrow \bar{\nu} K^+$ are expected to exceed 10^{35} years and 10^{34} years, respectively.
- The working group is being expanded to an international organization to accelerate the project. Regular international meetings are planned and extensive development works will be made in the international framework. In parallel, we need to form an organization that treats management tasks of the project such as securing budget for feasibility studies and constructions, scheduling, costing, and treating various organization issues and legal issues.

- We need appropriate path to request budget for such big project. We also need mechanism for the budget to allow some contingency.

Hyper-Kamiokande Working Group

Project leader : Masato Shiozawa
(Kamioka Observatory, ICRR, The University of Tokyo)

Members at ICRR

Staff

Kamioka Observatory

Yoichiro Suzuki, Professor
Masayuki Nakahata, Professor
Shigetaka Moriyama, Assoc. Professor
Masato Shiozawa, Assoc. Professor
Yoshinari Hayato, Assoc. Professor
Yasuhiro Kishimoto, Assoc. Professor (from Dec.2010)
Yasuo Takeuchi, Assoc. Professor (till Apr.2010)
Makoto Miura, Research Associate
Yusuke Koshio, Research Associate
June Kameda, Research Associate
Atsushi Takeda, Research Associate
Kou Abe, Research Associate
Hiroyuki Sekiya, Research Associate
Yoshihisa Obayashi, Research Associate (till Dec.2011)
Roger Wendell, Research Associate (from May 2012)
Shoei Nakayama, Project Research Associate (from Apr.2007)
Tomonobu Tomura, Project Research Associate (from Mar.2011)

Research Center for Cosmic Neutrinos

Takaaki Kajita, Professor
Kimihiro Okumura, Assoc. Professor
Kenji Kaneyuki, Assoc. Professor (till May 2010, deceased)
Yasuhiro Nishimura, Project Research Associate (from Apr.2012)

Postdoctoral Fellows

Kamioka Observatory

Lluís Magro Martí (from Apr.2011)
Yasuhiro Nishimura (Apr.2011 - Mar.2012)

Research Center for Cosmic Neutrinos
Shoei Nakayama (till Mar.2007)

List of Publications

- [1] K. Nakamura and M. Shiozawa, in The Proceedings of New Initiatives on Lepton Flavor Violation and Neutrino Oscillation with High Intense Muon and Neutrino Sources, ed. Y. Kuno et al. (World Scientific, Singapore, 2002), p. 232
- [2] M. Shiozawa, “Large Underground Water Cherenkov Detectors,” talk given in the XXIV International Conference on Neutrino Physics and Astrophysics (NEUTRINO 2010);
- [3] M. Yokoyama, “LBNE with Hyper-Kamiokande and JPARC,” M. Shiozawa, “Hyper-Kamiokande design,” H. Sekiya, “Review of photo-sensor R&D for future water Cherenkov detectors,” talks given in the International Workshop on Next generation Nucleon Decay and Neutrino Detectors (NNN10).
- [4] M. Yokoyama, “Hyper-Kamiokande detector design and physics potential,” talk given in the International Workshop on Fundamental Physics at the Intensity Frontier;
- [5] J. Yamatomi, “Hyperkamiokande excavation study,” M. Shiozawa, “Design and physics potential of Hyper-Kamiokande,” Y. Hayato, “Review of photo-sensor R&D for future water Cherenkov detectors,” talks given in the International Workshop on Next generation Nucleon Decay and Neutrino Detectors (NNN11).
- [6] M. Yokoyama, “Future (underground) Water Cherenkov Detectors,” talk given in the XXV International Conference on Neutrino Physics and Astrophysics (NEUTRINO 2012);
- [7] K. Abe *et al.*, “Letter of Intent: The Hyper-Kamiokande Experiment — Detector Design and Physics Potential —,” arXiv:1109.3262 [hep-ex].
- [8] Y. Kawai, H. Nakayama, A. Kusaka, H. Kakuno, T. Abe, M. Iwasaki, H. Aihara and M. Tanaka *et al.*, “Large-aperture hybrid

photo-detector,” Nucl. Instrum. Meth. A **579**, 42 (2007).

- [9] T. Abe, H. Aihara, M. Iwasaki, H. Fujimori, K. Kasimura, S. Mineo, T. Uchida and M. Tanaka *et al.*, “R&D status of a large-aperture hybrid avalanche photo-detector,” Nucl. Instrum. Meth. A **623**, 279 (2010).

HIGH ENERGY COSMIC RAY DIVISION

TA: TELESCOPE ARRAY

Introduction

The Telescope Array (TA) is the largest Ultra-High Energy Cosmic Ray (UHECR) observatory in the northern hemisphere. The aim of the TA experiment is to explore the origin, propagation and interaction of extremely-high energy (EHE) cosmic rays by measuring energy, arrival direction and mass composition. The TA consists of a surface array of 507 plastic scintillator detectors (SD) and three stations of fluorescence detectors (FD). It is located in the desert of Utah in USA (lat. 39.3°N , long. 112.9°W , alt. ~ 1400 m). All three FD stations started the observation in November 2007. Major construction of the SD array was completed in February 2007, and started the full operation in March 2008. The TA is operated by the international collaboration of researchers from US, Russia, Korea, Belgium and Japan.

Summary from 2006 to 2012

First we summarize the recent achievements with the TA:

- The cosmic-ray energy spectrum was measured with the TA SD. Here we scaled SD energy to FD energy. The ankle structure and the suppression at the highest energies (GZK suppression^{1 2}) are clearly visible. The significance of GZK suppression is 3.9σ . The TA SD spectrum is consistent with the HiRes spectrum and the other TA spectra with the MD monocular FD data and hybrid data.
- The measurement of the depth of shower maximum (X_{max}) in extensive air shower development above $10^{18.2}$ eV is consistent with proton composition.
- We checked the correlation of the TA data above 57 EeV with the positions of nearby Active Galactic Nuclei (AGN) using the same search parameters as the Pierre Auger Observatory (PAO) in 2007. Out of 25 observed events, 11 have been found to correlate with

the AGNs while 5.9 are expected from random coincidence, of which the chance probability is 2%.

- There is no clustering of the arrival directions of the TA data at small scales, neither at the angular scale of 2.5° above 40 EeV as reported by the AGASA (Akeno Giant Air Shower Array) experiment, nor at any angular scale from 0 to 40 degrees above 10 EeV, 40 EeV and 57 EeV. There is a hint of grouping of events at angular scales between 20 and 30° at the highest energies. However, the statistical significance of this feature is not sufficient.
- The distribution of arrival directions of UHECRs above 10 EeV is consistent with the hypothesis of the Large-Scale Structure (LSS) of the Universe with the realistic Galactic Magnetic Field (GMF) and proton composition although it is also consistent with isotropic model with the current statistics.

TA detector

Figure 1 is the TA layout. The SDs were deployed on a grid with 1.2 km spacing, and the SD array covers ~ 700 km². The green squares show the locations of three FD sites.

Each SD has two layers of 1.2 cm thick scintillator. The light is gathered by wavelength shifting fibers in the grooves of a scintillator layer and brought out to a PMT for each layer. We use 12-bit FADCs with 50 MHz sampling. Solar power system supplies power for the PMTs and electronics. The SDs are divided into three sub-arrays which communicate via wireless LAN each with an SD host electronics at a communication tower in their sub-array. Figure 2 shows an SD in the field. The boundary trigger was installed to save the SD data divided into multiple sub-arrays. We installed hybrid trigger system, by which filtered FD trigger signals trigger SD data taking. In addition to shower trigger data, we collect a variety of monitor information for SD calibration and maintenance. The fraction of running time is greater than 96%. The performance of the SD is described in [9].

*¹ K. Greisen, *Phys. Rev. Lett.* **16** (1966) 748-750.

*² G.T. Zatsepin and V.A. Kuz'min, *JETP Lett.* **4** (1966) 78-80 [Pis'ma Zh. Eksp. Teor. Fiz. **4** (1966) 114].

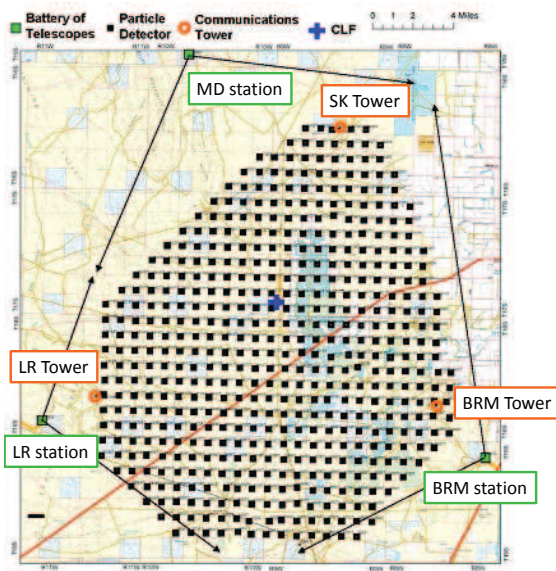


Fig. 1. The TA layout. The black squares represent the surface detectors. Three communication towers marked BRM, LR, and SK Towers are located near the edge of the SD array. Three FD stations marked BRM, LR, and MD stations overlook the SD array.



Fig. 2. A surface detector in the field.

The Middle Drum (MD) FD site is located to the north of the TA site, and is instrumented with 14 refurbished telescopes from the HiRes-I site. The cameras each contain 256 hexagonal Photonics PMTs in a 16×16 array. Each PMT views $\sim 1^\circ$ of sky. The telescopes view from $3\text{--}31^\circ$ above horizon and 114° in azimuth.

The Black Rock Mesa (BRM) and Long Ridge (LR) FD sites are located to the southeast and southwest of the TA site, respectively. They are each instrumented with 12 new telescopes [10]. The cameras use a Hamamatsu PMT with the 1° field of view. The PMTs are calibrated with a laser [11]. The relative calibration is described in [6]. The sites



Fig. 3. The BRM FD station.

view $3\text{--}33^\circ$ above horizon and 108° in azimuth. The trigger system is described in [1, 5]. The BRM and LR FD sites have duty cycles of 12 and 10%, respectively.

A monostatic LIDAR (Light Detection And Ranging) system, in which the laser and receiver are collocated, is located in the BRM site to measure atmospheric transparency [8]. The BRM site has an IR camera to monitor clouds. Figure 3 shows the BRM FD station.

A laser facility (CLF) sits at the center of the three FD sites. This allows one to measure the atmospheric transmission parameters [12] as well as to directly compare the reconstruction of the three FD sites.

No absolute energy calibration source existed on the sites of previous UHECR experiments. At KEK in Japan, we built an electron linear accelerator (ELS, Electron Light Source) for an end-to-end energy calibration of the FD [4]. The maximum beam energy is 40 MeV and the charge of one pulse is $10^9 e^-$. The ELS was installed 100 m forward from the BRM FD in March 2009. With the FD, we observed pseudo air shower induced by an electron beam that was shot in the air from ELS in September, 2010 as shown in Fig. 4.

Results

Energy Spectrum

The HiRes³ and PAO⁴ published the results of energy spectrum. The HiRes observed the GZK cutoff and the PAO confirmed it. We present energy spectra using three different methods: the MD monocular FD, hybrid, and SD analyses.

*³ R.U. Abbasi *et al.*, *Phys. Rev. Lett.* **100** (2008) 101101.

*⁴ J. Abraham *et al.*, *Phys. Rev. Lett.* **101** (2008) 061101.

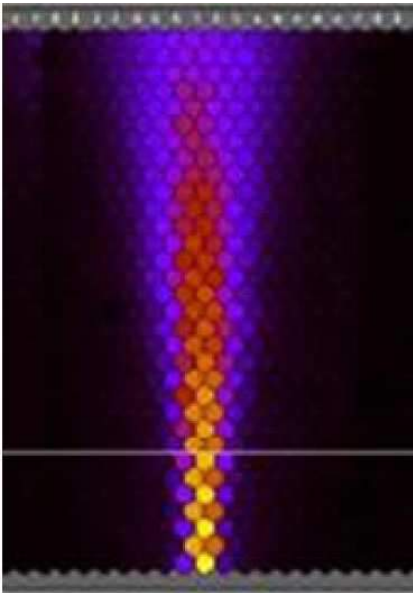


Fig. 4. The observed image of atmospheric fluorescence light from pseudo air shower induced by ELS.

The analysis of the MD monocular FD data provides a direct comparison between the TA and HiRes energy spectra. The MD spectrum uses the data collected between December 16, 2007 and December 16, 2010 [13]. The spectrum is measured using the reconstruction technique developed by the HiRes-I. The MD monocular energy spectrum is shown in Fig. 5. The spectrum is in good agreement with the other TA results.

The hybrid events detected both by FD and SD are useful to compare the reconstructed results from FD and SD. We can improve the reconstruction of FD events by adding information of SD. Here we use timing of one SD. The 1978 hybrid events were selected from May 27, 2008 through September 7, 2010. The total systematic uncertainty is 21% in energy measurement. Figure 5 shows the preliminary hybrid energy spectrum, which is consistent with the other TA results.

We measured the energy spectrum by using the SD data from May 11, 2008 through April 25, 2011. The exposure is $\sim 2640 \text{ km}^2 \text{ sr yr}$. The Monte Carlo (MC) data were generated by CORSIKA air shower simulation with QGSJET-II proton model. GEANT4 simulation is used for the detector simulation. The correlation of S_{800} and zenith angle with primary energy from MC study is used for the first estimation of the CR energy. Here S_{800} is the

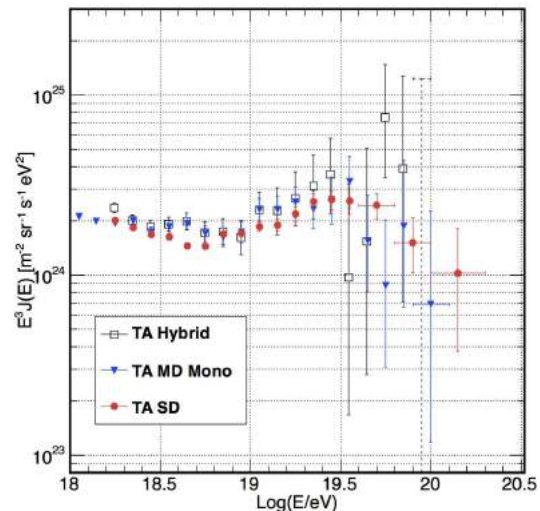


Fig. 5. The TA energy spectra measured by hybrid analysis (black open squares), MD monocular FD analysis (blue filled triangles), and SD analysis (red filled circles).

charge density at a distance of 800 m from shower core.

We compare the FD and SD energies using hybrid events. The SD energy is 27% larger than that of FD. The SD energy is rescaled by 27%. The plot of the energies is shown in Fig. 6.

We obtain 10997 reconstructed events with zenith angles below 45° . The energy spectrum is shown together with other experiments in Fig. 7 [15]. The SD spectrum is consistent with HiRes spectra. Using a power-law fit, we found the two breaks at $(4.9 \pm 0.3) \times 10^{18} \text{ eV}$ and at $(4.8 \pm 0.1) \times 10^{19} \text{ eV}$, which correspond to the ankle and the GZK suppression, respectively. We observed 28 events above the break at $4.8 \times 10^{19} \text{ eV}$ while a linear extrapolation of the power law below the break predicts 54.9 events above the break. This result provides evidence for the flux suppression with the significance of 3.9σ . The difference of the TA and Auger fluxes corresponds to the difference of the TA and Auger energy scales of approximately 20%, which is consistent with systematic energy uncertainties.

Mass Composition

The dependence of X_{max} on the primary energy is used to determine the mass composition. The Auger data suggests a change to a heavier composition⁵ for $E > 10^{18.5} \text{ eV}$ while the HiRes data is

⁵J. Abraham *et al.*, *Phys. Rev. Lett.* **104** (2010) 09110.

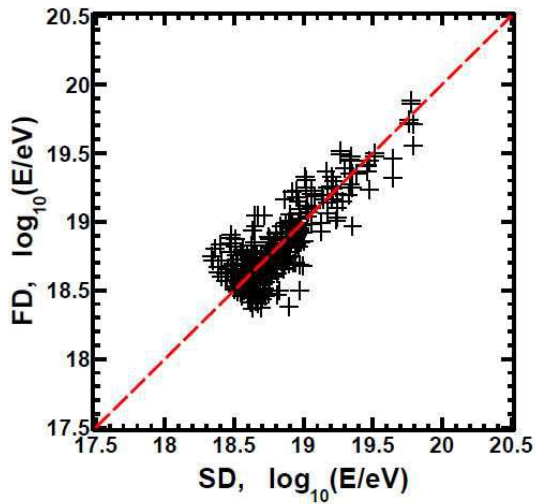


Fig. 6. The SD and FD energy comparison after applying 27% normalization to the SD. The dashed line corresponds to $E_{SD} = E_{FD}$.

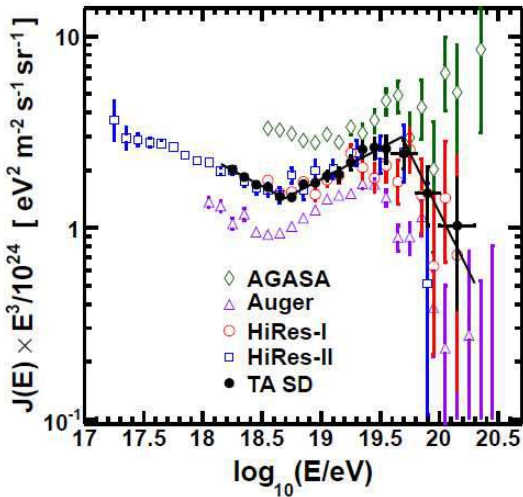


Fig. 7. The TA SD spectrum together with the spectra from other experiments: the TA SD (black filled circles), AGASA (green open diamonds), PAO (purple open triangles), HiRes-1 (red open circles), and HiRes-2 (blue open squares). Solid line shows the broken power line fit to the TA SD data.

consistent with constant elongation rate which stays with proton⁶.

The events simultaneously observed at two new FD stations (stereo events) from November 2007 through September 2010 are used. The distribution of reconstructed X_{max} for the TA data with QGSJET-01 MC data is shown in Fig. 8 and is in good agreement with the proton distribution.

The evolution of the average X_{max} with energy was shown with the MC data in the energy range

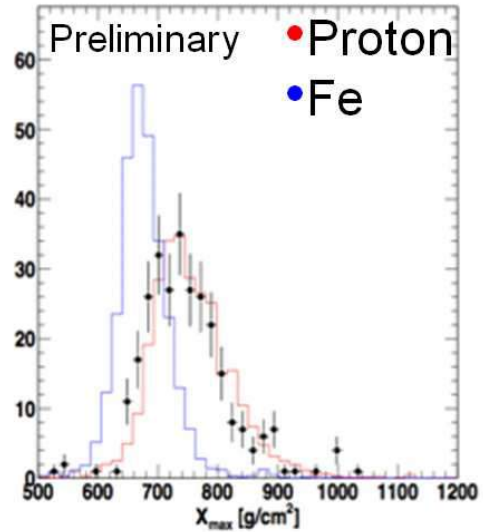


Fig. 8. The preliminary reconstructed X_{max} distribution for the data (points) with QGSJET-01 MC data above $10^{18.0}$ eV. The red and blue histograms are the proton and iron predictions, respectively.

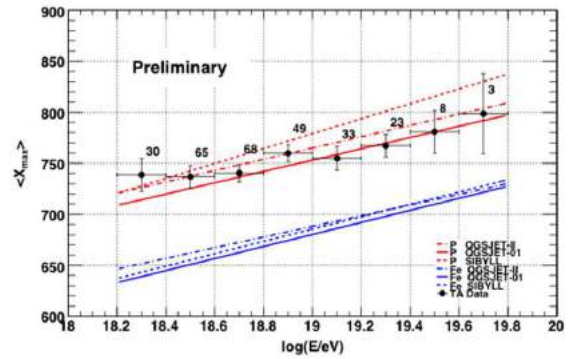


Fig. 9. The preliminary TA average reconstructed X_{max} (black points) as a function of energy. The upper set of red lines are predictions for pure protons with the interaction models of QGSJET-01 (solid line), QGSJET-II (dot-dash line) and SIBYLL (dashed line). The lower set of blue lines are under the assumption of iron.

from $10^{18.2}$ to $10^{19.8}$ eV in Fig. 9. The observed TA data are in good agreement with the QGSJET-01 pure proton prediction. The details of the mass composition study are described in [59].

Arrival Directions of UHECRs

We report the analysis of UHECRs for correlations with AGNs, autocorrelations and correlations with the LSS [14]. The SD data set from May 11, 2008 through September 15, 2011 contains 988 events above 10 EeV, 57 events above 40 EeV, and 25 events above 57 EeV.

The PAO reported correlations between the ar-

*⁶ R.U. Abbasi *et al.*, *Phys. Rev. Lett.* **104** (2010) 161101

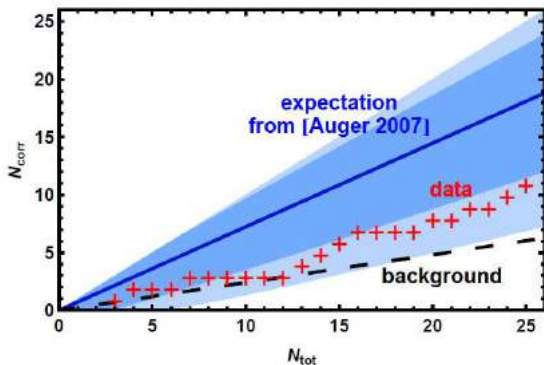


Fig. 10. The TA result of the correlations with AGN. The horizontal axis is the number of observed events and the vertical axis is the number of correlated events with AGN. The red crosses are the TA data. The black dashed line is the prediction from isotropic distribution. The expectation from the original PAO claim is represented by the blue line together with the 1- and 2- σ bands.

rival directions of UHECRs with $E > 57$ EeV and positions of nearby AGN from Véron 2006 catalog with $0 < z \leq 0.018$ in 2007⁷. The probability that the correlations for angular separations less than 3.1° occurred by chance is 1.7×10^{-3} . The number of correlating events was 9 out of 13, which corresponds to about 69% of events. The PAO has updated the analysis and found that the number of correlating events was 21 out of 55, which corresponds to about 38% of events⁸. The HiRes reported that no correlations had been found⁹. There are 11 correlating events (44%) out of 25 total events while the expected number of random coincidences for this total number of events is 5.9. As is seen in Fig. 10, the TA result is compatible both with isotropic distribution and the AGN hypothesis. By using binomial distribution with the probability of a single event to correlate $p_{iso} = 0.24$, such an excess has probability of $\sim 2\%$ to occur by chance with isotropic distribution.

The small-scale clusters of UHECR arrival directions were observed by the AGASA at the angular scale of 2.5° above 40 EeV^{10 11}. On the other hand, the result by the HiRes is consistent with an isotropic distribution¹². Figure 11 shows the distribution of separation angles for any two cosmic

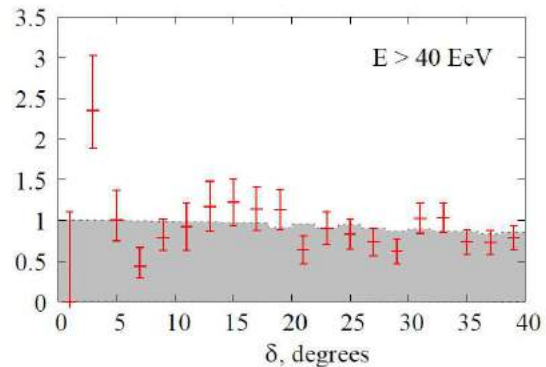


Fig. 11. The distribution of separation angles for any two cosmic rays above 40 EeV normalized by solid angle. The points are the observed data and the shaded region represents the average number of pairs expected for the uniform distribution. The expectation in the first bin is set to be one as the overall normalization.

rays above 40 EeV for the TA data set. We find 0 pair separated by less than 2.5° while 1.5 are expected for the isotropic model. There is no excess of small-scale clusters in the TA data, and no significant excess is found for angles from 0 to 40° and three energy thresholds of 10 EeV, 40 EeV, and 57 EeV. There is a hint of grouping of events at angular scales between 20 and 30° at the highest energies. However, the statistical significance of this feature is not sufficient.

Next we check the compatibility of the TA event sets with the isotropic distribution at large angular scales. The flux sampling test gives the values of statistical probability (p-values) 0.5, 0.9 and 0.6 for the three energy thresholds (10 EeV, 40 EeV, 57 EeV), respectively. The data are compatible with an isotropic distribution.

At large angular scales, the anisotropy in the PAO data was claimed¹³, and that in the HiRes data was not confirmed¹⁴. We use the galaxies at distances from 5 to 250 Mpc and with Ks magnitudes less than 12.5 in the 2MASS Galaxy Redshift Catalog (XSCz)¹⁵. This catalog provides the most accurate information about three-dimensional galaxy distribution. We assume that UHECRs are protons and the effects of the Galactic and extragalactic magnetic fields on each arrival direction are approximated by a Gaussian probability density function with an angular resolution called a smearing angle θ , which is treated as a free parameter.

*⁷ J. Abraham *et al.*, *Science* **318** (2007) 939; J. Abraham *et al.*, *Astropart. Phys.* **29** (2008) 188-204.

*⁸ P. Abreu *et al.*, *Astroparticle Phys.* **34** (2010) 315-326.

*⁹ R.U. Abbasi *et al.*, *Astroparticle Phys.* **30** (2008) 175-179.

*¹⁰ N. Hayashida *et al.*, *Phys. Rev. Lett.* **77** (1996) 1000-1003.

*¹¹ M. Takeda *et al.*, *J. Phys. Soc. Jpn (Suppl.)* **B 70** (2001) 15-21.

*¹² R.U. Abbasi *et al.*, *Ap. J. Lett.*, **610** (2004) 73-76.

*¹³ T. Kashti and E. Waxman, *JCAP* **05** (2008) 006.

*¹⁴ R.U. Abbasi *et al.*, *Ap. J. Lett.* **71B** (2010) 64-68.

*¹⁵ T. Jarrett, arXiv:astro-ph/0405069.

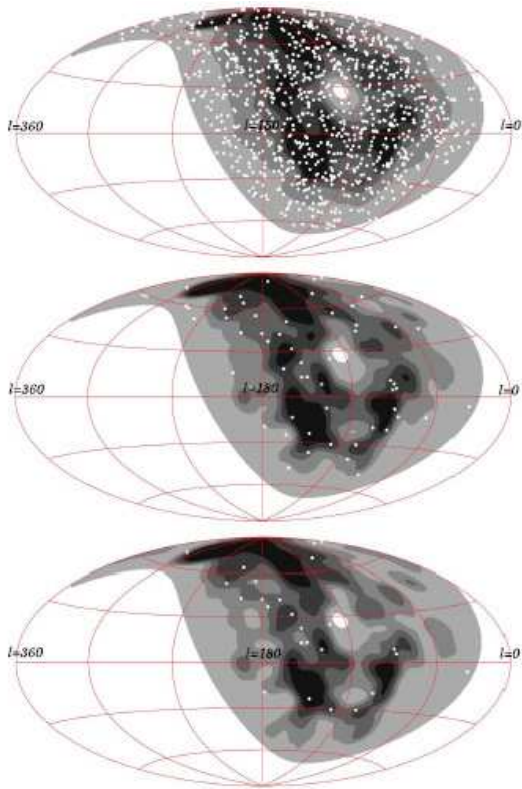


Fig. 12. The sky map of expected flux from LSS model together with the TA events (white dots) at energy thresholds of 10 EeV, 40 EeV, and 57 EeV (from top to bottom) in Galactic coordinates. The smearing angle is 6° . Darker gray region indicates larger flux and each band contains 1/5 of the total flux.

The sky maps of the expected flux at the smearing angle of 6° are shown in Fig. 12 together with the TA events. Figure 13 shows the p-values as a function of the smearing angle. The data both above 40 EeV and 57 EeV are compatible with LSS model even without regular GMF. For $E > 10$ EeV, the data set is compatible with LSS hypothesis that includes the regular GMF with strong and thick halo component. Here we adopt the recent GMF model with the magnitude of $4 \mu\text{G}$ and the thickness of 1.5 kpc for the halo¹⁶.

Future plans

We describe the TA Low-energy Extension (TALE), the possible processes to solve the discrepancies between the TA and Auger results such as energy spectrum and mass composition, and the plan of the next-generation huge aperture experiment including JEM-EUSO.

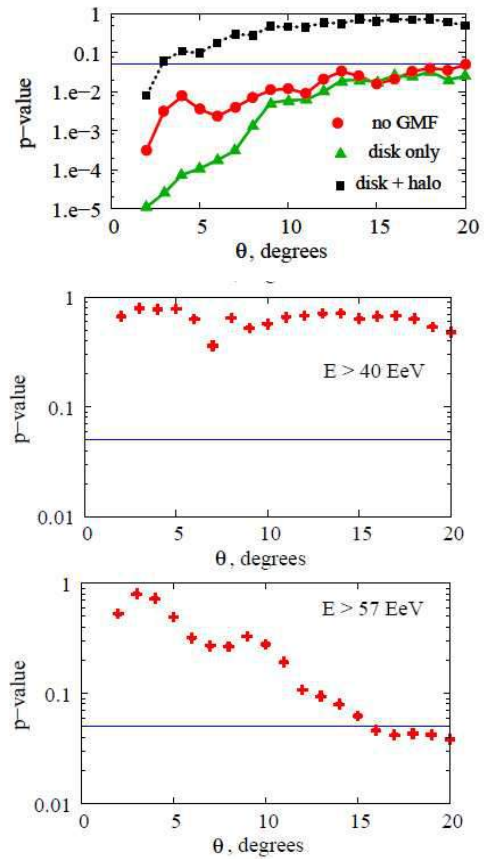


Fig. 13. The results of the statistical test for the compatibility between the data and the LSS hypothesis. The p-values are shown as a function of the smearing angle θ . The horizontal blue line shows a confidence level of 95%. The three panels correspond to energy thresholds of 10 EeV, 40 EeV, and 57 EeV from top to bottom. Red circles represent that with no regular GMF, in the upper panel with $E > 10$ EeV, black squares represent the result of the TA events with the LSS hypothesis with disk and halo components, and green triangles represent that with disk component only.

The TALE will give us the detailed studies of energy spectrum and composition from $10^{16.5}$ eV to the highest energies. The second knee has been observed at about 4×10^{17} eV in the cosmic-ray spectrum by previous experiments. The energy scales of these detectors differed by about a factor of two, so the energy at which this spectral break occurs is quite uncertain. There is a possibility that the transition from galactic cosmic rays to extragalactic cosmic rays occurs around this energy region. Then it is expected to observe the transition of heavier to lighter composition. The laboratory equivalent proton energy is 10^{17} eV in the center of mass energy of 14 TeV at the LHC. The cosmic-ray data to be observed by the TALE and the air shower MC simulation to be tuned by the result of the LHC forward (LHCf) experiment could be compared at

¹⁶ M. Pshirkov, P. Tinyakov, P. Kronberg, K. Newton-McGee, *Ap. J.* **738** (2011) 192.

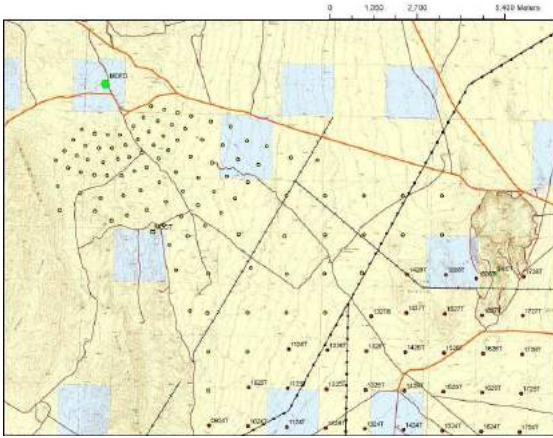


Fig. 14. The layout of TALE together with TA.

about 10^{17} eV.

We will add new telescopes viewing higher elevation (31° - 59°) and an infill array which the new telescopes overlook. Figure 14 shows the layout of the TALE.

The mirror building of the TALE FD was constructed right next to the MD FD building last spring. The US group is responsible for the TALE FD. The 10 telescopes from the HiRes-II are coming. The FDs will be completed in the spring of 2013. In parallel, three large mirrors are being considered to increase the number of events at lower energies. The Korean group is responsible for large mirrors.

The TALE SD array consists of scintillation counters identical to the TA SD. The infill array will consist of 103 counters, of which 76 will form the infill array (40 for 400-m spacing and 36 for 600-m spacing), and 27 will be used at the 1200 m spacing to extend the TA SD out to the infill array. The Japanese group is responsible for the infill array. The 35 spare TA SDs will be installed in the fall of 2012. We plan to add the remaining SDs if we obtain a grant in the fiscal year 2013.

The International Symposium on Future Directions in UHECR Physics (UHECR2012) was held in CERN in February 2012¹⁷. We discussed the highlights and future UHECR experiments. Towards the symposium, we formed five working groups: energy spectrum, composition, anisotropy, multi-messenger, and modeling and description of air showers, which discussed the issues in advance and reported the summaries at the symposium. The

*¹⁷ <http://indico.cern.ch/conferenceDisplay.py?confId=152124>

energy scale difference of approximately 20% between the TA and PAO was partially understood by the energy spectrum working group, for example. After the symposium, the TA and Auger spokespersons discussed a few times and confirmed the following items to solve the discrepancies between the TA and PAO results:

- Continuation of the activities of the working groups,
- Next-generation ground array experiments will be discussed worldwide as the working group including JEM-EUSO,
- Exchange optical calibrations between the TA and PAO to understand more for the energy scale difference between the TA and PAO,
- Joint analysis such as the whole sky anisotropy analysis.

The exchange of analysis programs/data and the exchange of partial detectors between the TA and PAO would be considered.

The ground array 60 times of the TA consisting of 10,000 SDs with 2 km spacing was proposed as a next-generation air-shower ground array experiment [60] in the UHECR2010 symposium. There were talks about a multi-component UHECR observatory consisting of water tanks and electromagnetic detectors such as GHz radio detectors¹⁸, and a large ground array of fluorescence detectors with low cost¹⁹. The merit of the huge ground array experiment is its guaranteed ability of the conventional technique and/or possible ability of new method or new technique to be well calibrated with the existing observatories. We have already started the R&D experiments in the TA site with the group outside the TA. The R&D of the radio echo detection from air showers is being performed in the TA site [61]. An R&D of GHz radio detection in the TA site started in 2012 together with the Auger members from the Karlsruhe Institute of Technology (KIT) and University of Chicago.

The JEM-EUSO is the first space project to investigate EHE cosmic rays by a super-wide view (60°) telescope on the International Space Station

*¹⁸ A. Letessier-Selvon, Proc. of UHECR2012 Symposium, CERN, Geneva, Switzerland, 2012.

*¹⁹ P. Privitera, Proc. of UHECR2012 Symposium, CERN, Geneva, Switzerland, 2012.

(ISS). The advantage is its rather uniform and huge aperture ($1.5 \times 10^6 \text{ km}^2 \text{ sr}$) in the whole sky. The prototype will be tested in the TA site from December, 2012. The TA members in ICRR plans to join JEM-EUSO for optical calibration.

Summary

The TA group confirmed GZK suppression with a significance of 3.9σ and the ankle. The X_{max} measurement above $10^{18.2} \text{ eV}$ is consistent with proton composition. The analyses of arrival directions of UHECRs for the correlations with AGNs, correlations with LSS proton model and autocorrelations show some hints of anisotropy while they are consistent with isotropic model with the current statistics.

We are constructing the TALE mainly to investigate the transition from galactic and extragalactic cosmic rays. Based on the UHECR2012 symposium and continuation of the working groups, we would solve the discrepancies between TA and Auger by the joint studies. The TA results are consistent with proton GZK model, which leads to UHECR astronomy with the next huge ground array and JEM-EUSO.

Telescope Array (TA) Collaboration

The spokespersons of TA are:

Before December 2011

Masaki Fukushima, ICRR, Univ. of Tokyo
Pierre Sokolsky, Dept. of Physics, Univ. of Utah

After December 2011

Hiroyuki Sagawa, ICRR, Univ. of Tokyo
Gordon Thomson, Dept. of Physics, Univ. of Utah

Institute	Country	(*)
Univ. of Utah	USA	31
Univ. of Yamanashi	Japan	11
Tokyo Institute of Technology	Japan	15
Hanyang Univ.	Korea	5
Tokyo Univ. of Science	Japan	3
Kinki Univ.	Japan	2
Yonsei Univ.	Korea	4
KEK	Japan	5
Osaka City Univ.	Japan	13

Institute	Country	(*)
ICRR, Univ. of Tokyo	Japan	17
Kanagawa Univ.	Japan	3
Saitama Univ.	Japan	4
Rutgers Univ.	USA	1+(2)
Tokyo City Univ.	Japan	1
Institute for Nuclear Research of the Russian Academy of Sciences	Russia	5+(1)
Waseda Univ.	Japan	2
Chiba Univ.	Japan	2
Chungnam National Univ.	Korea	3
Ewha Womans Univ.	Korea	4
IPMU, Univ. of Tokyo	Japan	1+(1)
Kyoto Univ.	Japan	1
Kochi Univ.	Japan	1
Ritsumeikan Univ.	Japan	1
Univ. Libre de Bruxelles	Belgium	2
Earthquake Research Institute, Univ. of Tokyo	Japan	1
Hiroshima City Univ.	Japan	1
National Institute of Radiological Science	Japan	1
Ehime Univ.	Japan	1
Total		141

(*) Number of participants as of June 2012.

Members

Staffs

Masaki Fukushima, Professor, April 1999 to the present
Hiroyuki Sagawa, Assoc. Professor, February 2004 to the present
Naoaki Hayashida, Research Associate, to March 2008
Masahiro Takeda, Research Associate, to the present
Toshiyuki Nonaka, Research Associate, March 2011 to the present

Postdoctoral Fellows

Nobuyuki Sakurai, - April 2010
Hisao Tokuno, April 2004 - September 2009
Shigeharu Udo, April 2004 - March 2008
Shunsuke Ozawa, April 2004 - March 2008
Toshiyuki Nonaka, April 2006 - February 2011
Tatsunobu Shibata, April 2005 to the present
Yuichiro Tameda, April 2010 to the present

Daisuke Ikeda, April 2010 to the present
 Kazumasa Kawata, April 2012 to the present
 Eiji Kido, April 2012 to the present

Graduate Students

Three students were awarded doctor degrees and six students earned master degrees during 2006–2012, supervised by ICRR staff members.

List of Publications

Papers in Refereed Journals

- [1] Y. Tameda *et al.*, “Trigger system for the TA fluorescence detector”, Proc. of nano PHYS’07, *Physica E* **40** (2007) 430-433.
- [2] S. Ogio *et al.*, “The Telescope Array Experiment”, *Nucl. Phys. B* (Proc. Suppl.) **175-176** (2008) 221-226.
- [3] H. Tokuno *et al.*, “The Telescope Array Experiment: Status and Prospects”, Proc. of the 10th Int. Conf. on Topics in Astroparticle and Underground Physics (TAUP2007), *J. Phys. Conf. Ser.* **120** (2008) 062027.
- [4] T. Shibata *et al.*, “End-to-end absolute energy calibration of atmospheric fluorescence telescopes by an electron linear accelerator”, *Nucl. Instrum. Methods A* **597** (2008) 61-66.
- [5] Y. Tameda *et al.*, “Trigger electronics of the new Fluorescence Detectors of the Telescope Array Experiment”, *Nucl. Instrum. Methods A* **609** (2009) 227-234.
- [6] H. Tokuno *et al.*, “On site calibration for new fluorescence detectors of the telescope array experiment”, *Nucl. Instrum. Methods A* **601** (2009) 364-371.
- [7] H. Kawai *et al.*, “Measurement of Ultra-high Energy Cosmic Rays by Telescope Array (TA)”, *J. Phys. Soc. Jpn. (Suppl.) A* **78** (2009) 108-113.
- [8] T. Tomida *et al.*, “The atmospheric transparency measured with a LIDAR system at the Telescope Array experiment”, *Nucl. Instrum. Methods A* **654** (2011) 653-660.
- [9] T. Abu-Zayyad *et al.*, “The surface detector array of the Telescope Array experiment”, *Nucl. Instrum. Methods A* **689** (2012) 87-97.
- [10] H. Tokuno *et al.*, “New air fluorescence detectors employed in the telescope Array experiment”, *Nucl. Instrum. Methods A* **676** (2012) 54-65.
- [11] S. Kawana *et al.*, “Calibration of photomultiplier tubes for the fluorescence detector of telescope array experiment using a Rayleigh scattered laser beam”, *Nucl. Instrum. Methods A* **681** (2012) 68-77.
- [12] T. Tomida *et al.*, “Development of atmospheric transparency measurement system”, *International Journal of Nanomanufacturing*, 2012, 047031.
- [13] T. Abu-Zayyad *et al.*, “The Energy Spectrum of Telescope Array’s Middle Drum Detector and the Direct Comparison to the High Resolution Fly’s Eye Experiment”, arXiv:1202.5141 [astro-ph.IM], accepted to *Astroparticle Phys.*
- [14] T. Abu-Zayyad *et al.*, “Search for anisotropy of ultra-high energy cosmic rays with the Telescope Array experiment”, arXiv:1205.5984 [astro-ph.HE], accepted for *Ap. J.*
- [15] T. Abu-Zayyad *et al.*, “The Cosmic Ray Energy Spectrum Observed with the Surface Detector of the Telescope Array Experiment”, arXiv:1205.5067 [astro-ph.HE], submitted for publication.

Papers in Conference Proceedings

- [16] H. Sagawa for TA Collaboration, “Status of TA”, Aspen Workshop on Cosmic Ray Physics (ASPEN2007), 2007/4/15-2007/4/19, Colorado, USA.
- [17] H. Sagawa, “Observation of ultra high energy cosmic rays with the surface detector array of the TA experiment”, 30th Int. Cosmic Ray Conference: 2007/7/3-2007/7/11, Merida, Mexico.
- [18] Y. Tsunesada, “Telescope Array Aperture: Mono, Stereo and Hybrid”, 30th Int. Cosmic Ray Conference: 2007/7/3-2007/7/11, Merida, Mexico.
- [19] S. Ogio, “TA-FD status and first observation”, 30th Int. Cosmic Ray Conference: 2007/7/3-2007/7/11, Merida, Mexico.

- [20] M. Fukushima, "Status and Prospect of Telescope Array (TA) Experiment", 30th Int. Cosmic Ray Conference: 2007/7/3-2007/7/11, Merida, Mexico.
- [21] T. Nonaka, "Calibration of TA Surface Detectors", 30th Int. Cosmic Ray Conference: 2007/7/3-2007/7/11, Merida, Mexico.
- [22] H. Sagawa for TA Collaboration, "Status of Telescope Array Experiment", TeVPA 2008, TeV Particle Astrophysics: 2008/9/24-2008/9/28, IHEP, Beijing, China.
- [23] H. Sagawa for TA Collaboration, "Results from the TA surface detectors", XXI Rencontres de Blois 2009: 2009/6/21-2009/6/26, Blois, France.
- [24] M. Fukushima, "Measurement of High Energy Cosmic Ray above 10^{16} eV", The 31st Int. Cosmic Ray Conference: 2009/7/7-2009/7/15, Lodz, Poland.
- [25] H. Sagawa, "Measurement of Ultra-high Energy Cosmic Rays by Telescope Array (TA)", 31st ICRC: 2009/7/7-2009/7/15, Lodz, Poland.
- [26] T. Nonaka, "Wide area radio network for the Telescope Array experiment", 31st Int. Cosmic Ray Conference: 2009/7/7-2009/7/15, Lodz, Poland.
- [27] Y. Tameda, "Mass Composition Study of Ultra-high Energy Cosmic Ray with the Telescope Array Fluorescence Detector Stereo Events", 31st ICRC: 2009/7/7-2009/7/15, Lodz, Poland.
- [28] N. Sakurai, "Distribution of arrival directions obtained from the first year data of Telescope Array", 31st ICRC: 2009/7/7-2009/7/15, Lodz, Poland.
- [29] D. Ikeda, "Hybrid Measurement of the Telescope Array Experiment", 31st ICRC: 2009/7/7-2009/7/15, Lodz, Poland.
- [30] M. Fukushima, "Measurement of the spectrum of ultra-high energy cosmic rays by the Telescope Array surface array", 31st ICRC: 2009/7/7-2009/7/15, Lodz, Poland.
- [31] T. Shibata, "An Electron Linear Accelerator for end-to-end absolute energy calibration of atmospheric fluorescence telescopes of the Telescope Array experiment", 31st ICRC: 2009/7/7-2009/7/15, Lodz, Poland.
- [32] H. Tokuno, "Performance of the Fluorescence Detector of the Telescope Array experiment", 31st ICRC: 2009/7/7-2009/7/15, Lodz, Poland.
- [33] T. Nonaka, "Performance of TA Surface Array", 31st ICRC: 2009/7/7-2009/7/15, Lodz, Poland.
- [34] H. Sagawa for TA Collaboration, "Results from the Telescope Array experiment (measurement of Ultra-high Energy Cosmic Rays)", IWARA09, 4th International Workshop on Astronomy and Relativistic Astrophysics: 2009/10/4-2009/10/8, Sao Paulo, Brazil.
- [35] H. Tokuno for TA Collaboration, "The Status of the Telescope Array Experiment", CALOR 2010, XIV International Conference on Calorimetry in High Energy Physics: 2010/5/10-2010/5/14, Beijing, China.
- [36] M. Fukushima for TA Collaboration, "Measurement of UHECRs by the Telescope Array (TA) Experiment", ISVHECRI 2010, XVI International Symposium on Very High Energy Cosmic Ray Interactions: 2010/6/28-2010/7/2, Fermilab, USA.
- [37] M. Tameda for TA Collaboration, "Result from the Telescope Array Experiment", TeVPA 2010, TeV Particle Astrophysics: 2010/7/19-2010/7/23, Paris, France.
- [38] D. Ikeda for TA Collaboration, "Results from the Telescope Array Experiment", ECRS 2010, 22nd European Cosmic Ray Symposium: 2010/8/3-2010/8/6, Turk, Finland.
- [39] T. Shibata, "A small linear accelerator for absolute energy calibration of fluorescence detector of Telescope Array project", 7th Air Fluorescence Workshop (AFWS): 2010/9/22-2010/9/24, Coimbra, Portugal.
- [40] T. Tomida, "Atmospheric Monitoring in the Telescope Array Experiment", 7th AFWS: 2010/9/22-2010/9/24, Coimbra, Portugal.

- [41] Y. Tsunesada for TA Collaboration, “Results from the Telescope Array Experiment”, 7th AFWS: 2010/9/22-2010/9/24, Coimbra, Portugal.
- [42] D. Ikeda, “Observation and Reconstruction of Extensive Air Showers with the Fluorescence Detectors of the Telescope Array Experiment”, 7th AFWS: 2010/9/22-2010/9/24, Coimbra, Portugal.
- [43] S. Ogio for TA Collaboration, “Future Plans of Telescope Array”, UHECR 2010, International Symposium on the Recent Progress of UHECR Observation: 2010/12/10-2010/12/12, Nagoya, Japan.
- [44] Y. Tameda for TA Collaboration, “Measurement of UHECR composition by TA”, UHECR 2010: 2010/12/10-2010/12/12, Nagoya, Japan.
- [45] D. Ikeda for TA Collaboration, “Energy measurement and spectrum by the Telescope Array”, UHECR 2010: 2010/12/10-2010/12/12, Nagoya, Japan.
- [46] T. Shibata, “Absolute energy calibration of FD by an electron linear accelerator for Telescope Array”, UHECR 2010: 2010/12/10-2010/12/12, Nagoya, Japan.
- [47] H. Sagawa for TA Collaboration, “Recent Results from the Telescope Array Experiment”, UHECR 2010: 2010/12/10-2010/12/12, Nagoya, Japan.
- [48] T. Nonaka for TA Collaboration, “Observation of UHECRs at Telescope Array Experiment”, Rencontre de Moriond EW2011: 2011/3/13-2011/3/20, La Thuile, France.
- [49] H. Sagawa for TA Collaboration, “The Telescope Array and its prospects”, Multi-Messenger Astronomy of Cosmic Rays: 2011/04/11-2011/04/14, Beijing, China.
- [50] Y. Tsunesada, “Highlights from Telescope Array”, Proc. of the 32nd International Cosmic Ray Conf., Beijing, 2011, arXiv:1111.2507.
- [51] H. Sagawa for TA Collaboration, “Results from the Telescope Array Experiment”, TeVPA 2011, TeV Particle Astrophysics: 2011/8/1-2011/8/5, Stockholm, Sweden.
- [52] D. Ikeda, “Recent Results from Telescope Array”, 12th International Conference on Topics in Astro-particle and Underground Physics (TAUP 2011): 2011/9/5 - 2011/9/9, Munich, Germany.
- [53] Y. Tameda, “Measurement of UHECR Mass Composition by TA FD Stereo”, 8th AFWS 2011: 2011/9/12 - 2011/9/14, Karlsruhe, Germany.
- [54] T. Tomida, “Atmospheric Monitoring for Air Fluorescence Observations in the TA experiment”, 8th Air Fluorescence Workshop (AFWS2011): 2011/9/12-2011/9/14, Karlsruhe, Germany.
- [55] M. Fukushima, “CRAYS: a photometric calibration of TA FD-camera”, 8th Air Fluorescence Workshop (AFWS2011): 2011/9/12-2011/9/14, Karlsruhe, Germany.
- [56] T. Fujii, “Shower Reconstruction with the Telescope Array Fluorescence Detector”, 8th AFWS 2011: 2011/9/12 - 2011/9/14, Karlsruhe, Germany.
- [57] D. Ikeda for TA Collaboration, “Recent Results from Telescope Array”, 8th AFWS 2011: 2011/9/12 - 2011/9/14, Karlsruhe, Germany.
- [58] Y. Tsunesada et al., “WG Review of UHE spectrum data”, Proc. of UHECR2012 Symposium, CERN, Geneva, Switzerland, 2012.
- [59] Y. Tameda et al., “HiRes and TA Composition Measurements”, Proc. of UHECR2012 Symposium, CERN, Geneva, Switzerland, 2012.
- [60] S. Ogio, “Future Plans of the Telescope Array Experiment”, Proc. of UHECR2012 Symposium, CERN, Geneva, Switzerland, 2012.
- [61] J. Belz et al., “TARA: Forward-Scattered Radar Detection of UHECR at the Telescope Array”, Proc. of UHECR2012 Symposium, CERN, Geneva, Switzerland, 2012.
- [62] M. Fukushima, “Experimental summary and future prospects”, UHECR2012 symposium, CERN, Geneva, Switzerland, 2012.
- [63] N. Sakurai, “Telescope Array Experiment”, CA2012: International Workshop on Particles and Radiation from Cosmic Accelerators, 2012/2/20-2/22, Chiba, Japan.

CANGAROO

Introduction

Gamma-ray astronomy plays a crucial role in the exploration of non-thermal, high-energy phenomena in the Universe in their most extreme and violent forms. Charged cosmic rays are deflected by Galactic and intergalactic magnetic fields, while gamma rays come straight from their production site and are the best probes of many hot topics of modern astrophysics, such as the origin of cosmic rays, particle acceleration and radiation processes under extreme astrophysical conditions.

CANGAROO is an acronym for the Collaboration of Australia and Nippon (Japan) for a Gamma Ray Observatory in the Outback, and is a joint project of Japanese and Australian institutions to search for very-high-energy (VHE) gamma rays from celestial objects using imaging atmospheric Cherenkov telescopes (IACTs)¹.

After the operation of the 3.8 m IACT (CANGAROO-I) for 7 years since 1992, which was the first of this kind in the southern hemisphere, we constructed a new telescope of 7 m diameter (CANGAROO-II) in 1999 next to the 3.8 m telescope near Woomera, South Australia (136°47'E, 31°06'E, 160 m a.s.l.). Then, the construction of an array of four 10 m telescopes (CANGAROO-III) was approved and as the first step the 7 m telescope was upgraded to 10 m diameter in 2000, which eventually became the first telescope of the CANGAROO-III array. While continuing observations with the upgraded CANGAROO-II, we have constructed additional three 10 m telescopes located at the corners of a diamond of 100 m side with improved mirrors, cameras, and electronics in the following years. After tuning, we have started stereoscopic observations of Cherenkov light with the four telescope system in March 2004.

Here we summarize results from CANGAROO-III published since the last ICRR external review in 2006, and some other results related to CANGAROO obtained during this period. Since the CANGAROO-III telescopes, which, due to financial considerations, were not sheltered from the harsh desert environment, have seriously deteriorated

over time from their original performance, we have stopped observations in 2011 and the telescopes have been demolished in 2012.

The CANGAROO-III Telescope System

After years of observations with the 3.8 m telescope, which is retrospectively called CANGAROO-I², a new budget to construct a whole new telescope was approved in 1995. This telescope, CANGAROO-II³, was equipped with a reflector⁴ consisting of sixty spherical mirrors of 80 cm in diameter, which is approximately 7 m aperture, with a focal length of 8 m. The base material of the mirrors is CFRP (carbon-fiber reinforced plastic), which was newly developed for use in Cherenkov telescopes, and makes the reflector light-weighted and reduces gravitational deformation of the parabola shape. The attitude of each mirror is remotely adjusted by stepping motors. The 7 m telescope began operation in March 1999. In 1999 we obtained a new budget to construct an array of four 10 m telescopes, which is called CANGAROO-III⁵. As the first step of CANGAROO-III, the 7 m telescope was expanded to 10 m by addition of 54 mirrors in March 2000, which is called 'T1' after installation of other telescopes. In 2002–2004, we have installed the other three 10 m telescopes ('T2', 'T3', and 'T4') at the corners of a diamond of 100 m sides (Figure 1). By detecting Cherenkov light pools at multiple telescopes, air-shower development can be reconstructed and we can determine arrival directions and energies of incident gamma rays more precisely. The major parameters of the CANGAROO-III telescopes are summarized in Table 1. We use basically the same telescope structures, but the last three telescopes are equipped with better spherical mirror facets⁶, wider field-of-view cameras, and faster electronics. The details of the

*² T. Hara et al., Nucl. Instr. Meth. **A332**, 300–309 (1993).

*³ T. Tanimori et al., in Proc. 26th ICRC (Utah), **5**, 203–206 (1999).

*⁴ A. Kawachi et al., Astropart. Phys. **14**, 261–269 (2001).

*⁵ H. Kubo et al., New Astronomy Reviews **48**, 323–329 (2004).

*⁶ The base material of them has changed to GFRP (glass-fiber reinforced plastic) in order to improve surface accuracy.

*¹ J. R. Patterson & T. Kifune, Australian and New Zealand Physicist, **29**, 58–62 (1992).



Fig. 1. The CANGAROO-III telescope system consisting of four 10 m imaging atmospheric Cherenkov telescopes located near Woomera, South Australia. They are called 'T2', 'T4', 'T3', and 'T1' from the left and are set at the corners of a diamond of 100 m sides.

Table 1. Basic specifications of the CANGAROO-III telescopes.

	T1	T2, T3, T4
Mount		Alt-azimuth
Focal length		8 m
Number of mirrors		114 (57 m ² in total)
Reflector type		Parabola
Number of PMTs	552 (1/2")	427 (3/4")
Camera pixel size	0°115	0°168
Readout	TDC (CAMAC) & ADC	TDC (VME) & ADC
Point image size	0°20 (FWHM)	0°14–0°21 (FWHM)
Completion	2000.3	2002.3 (T2), 2002.11 (T3), 2003.7 (T4)

system are described elsewhere⁷

Results from CANGAROO-III

The analysis method used in CANGAROO-III is based on the Cherenkov image parametrization introduced by Hillas⁸, and the stereoscopic reconstruction technique demonstrated by the HEGRA group⁹. In order to improve the signal-to-noise ratio, the Fisher discriminant¹⁰ was used to obtain the following results. The positive detections of the gamma-ray signals were double-checked by independent analyses within the group.

Pulsar Wind Nebula in MSH 15–52

The radio supernova remnant (SNR) MSH 15–52 (G 320.4–1.2) contains the gamma-ray pulsar PSR B1509–58, which has the third

highest spin-down energy loss in the Galaxy, and has been a prime target of TeV gamma-ray observatories. The marginal detection of TeV gamma rays from this source was first reported by CANGAROO-I¹¹. The statistically significant signal was later detected by the H.E.S.S. group in 2004¹², and the morphology coincides with the pulsar wind nebula (PWN) as observed at X-ray energies.

CANGAROO-III has observed this PWN from April to June in 2006. We detected gamma rays above 810 GeV at the 7σ level during a total effective exposure of 48.4 hr [5]. We obtained a differential gamma-ray flux¹³ at 2.35 TeV of $(7.9 \pm 1.5_{\text{stat}} \pm 1.7_{\text{sys}}) \times 10^{-13} \text{ cm}^{-2} \text{ s}^{-1} \text{ TeV}^{-1}$ with a photon index of $2.21 \pm 0.39_{\text{stat}} \pm 0.40_{\text{sys}}$, which is compatible with that of the H.E.S.S. observation in 2004. The morphology shows extended emission compared to our point spread function (PSF) (Figure 2). We

*⁷ R. Enomoto et al., in Proc. 28th ICRC (Tsukuba) 2807–2810 (2003), K. Nishijima et al., in Proc. 29th ICRC (Pune), 5, 327–330 (2005), and references therein.

*⁸ A. M. Hillas., in Proc. 19th ICRC (La Jolla) 3, 445–448 (1985).

*⁹ A. Daum et al., *Astropart. Phys.* **8**, 1–11 (1997).

*¹⁰ R. Enomoto et al., *ApJ* **638**, 397–408 (2006).

*¹¹ T. Sako et al., *ApJ* **537**, 422–428 (2000).

*¹² F. Aharonian et al., *A&A* **435**, L17–L20 (2005).

*¹³ Gamma-ray flux per unit energy.

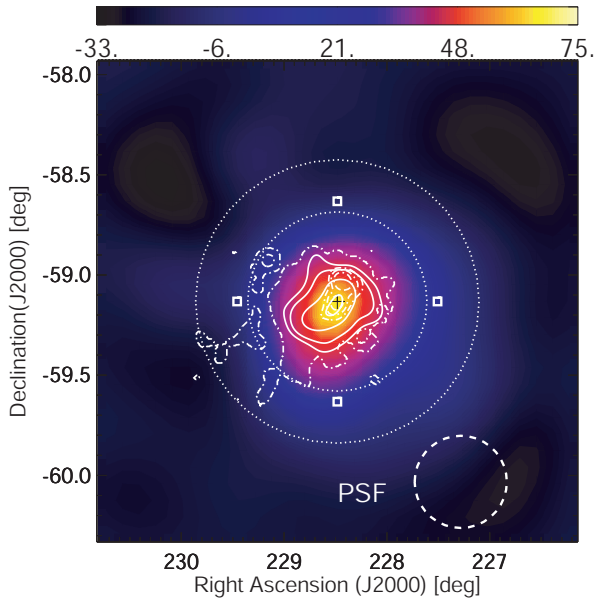


Fig. 2. Morphology of gamma-ray-like events observed from MSH 15–52, smoothed with a Gaussian of $\sigma = 0.23$. Our PSF is also shown by a dashed circle (68% containment radius). The squares and the cross represent tracking positions and the pulsar position, respectively. Solid contours show VHE gamma-ray emission as seen by H.E.S.S. and dotted contours by *ROSAT* 0.6–2.1 keV. The region between thin dotted circles are used for the background study.

considered the plausible origin of the high energy emission based on a multiwavelength spectral analysis and energetics arguments. From the point of view of the energetics, if we do not take into account the expansion loss, a typical supernova could provide sufficient energy for electrons to reproduce the spectral energy distribution (SED), but the proton case is less likely. The morphology of the TeV gamma-ray emission, however, does not support the supernova explosion as the global energy source. Electrons can also be accelerated enough to reproduce the SED when $\geq 4\%$ (the initial spin-down timescale $\tau_0 = 30$ yr is assumed) of the rotational energy of the pulsar is supplied to the kinetic energy.

Blazar PKS 2155–304

The high-frequency-peaked BL Lacertae (HBL) object PKS 2155–304 is one of the most violent blazars in the southern hemisphere. The TeV gamma-ray signal from PKS 2155–304 was first detected by the Durham group in 1997¹⁴, and H.E.S.S. confirmed this object to be a TeV gamma-ray source with observations in 2002–2003¹⁵. We

have observed PKS 2155–304 between 2006 July 28 (MJD 53944) and August 2, triggered by the H.E.S.S. report that the source was in a high state of TeV gamma-ray emission. A signal was detected at the 4.8σ level in an effective live time of 25.1 hr during the outburst period [4]. The flux of VHE gamma rays from the CANGAROO-III observations shows the variability on the time scale of less than a few hours (Figure 3). The averaged integral flux above 660 GeV is $(1.6 \pm 0.3_{\text{stat}} \pm 0.5_{\text{sys}}) \times 10^{-11} \text{ cm}^{-2} \text{ s}^{-1}$ which corresponds to $\sim 45\%$ of the flux observed from the Crab Nebula. Follow-up observations between August 17 (MJD 53964) and 25 indicate the source activity had decreased.

For objects such as PKS 2155–304, which show rapid and complex time variability, continuous monitoring is very important for modeling the emission mechanisms. The difference in longitude between the H.E.S.S. and CANGAROO-III sites is $\sim 120^\circ$, corresponding to an 8 hr time difference. Thus the H.E.S.S. and CANGAROO-III data complement one another. Northern hemisphere blazars, such as Mrk 421, Mrk 501, and 1ES 1959+650, have been observed at TeV energies continuously with more than two geographically distant telescope systems, providing greatly improved time coverage, but PKS 2155–304 is the first object in the southern sky for which such studies have been made.

Unidentified H.E.S.S. Source HESS J1804–216

A Galactic plane survey was performed in 2004 by the H.E.S.S. IACTs with a flux sensitivity of 0.02 Crab for gamma rays above 200 GeV¹⁶. Fourteen new gamma-ray sources were detected at significance levels above 4σ , and 11 of the sources either have no counterpart or possible counterparts with significant positional offsets¹⁷, because of which they are called unidentified H.E.S.S. (or TeV) sources. HESS J1804–216 is one of the brightest, and its spectrum is softest in this survey; the flux is about 0.25 Crab above 200 GeV with a photon index of 2.72 ± 0.06 . In addition, with a size of $\sim 22'$, it is one of the most extended TeV gamma-ray sources.

¹⁴ P. M. Chadwick et al., *ApJ* **513**, 161–167, (1999).

¹⁵ F. Aharonian et al., *A&A* **430**, 865–875 (2005).

¹⁶ F. Aharonian et al, *Science* **307**, 1938–1942 (2005), F. Aharonian et al., *ApJ* **636**, 777–797 (2006).

¹⁷ The numbers of sources have changed since the first report in 2005–2006 as the survey region has been expanded (more sources have been found) and some sources have been identified by follow-up observations in other wavelengths.

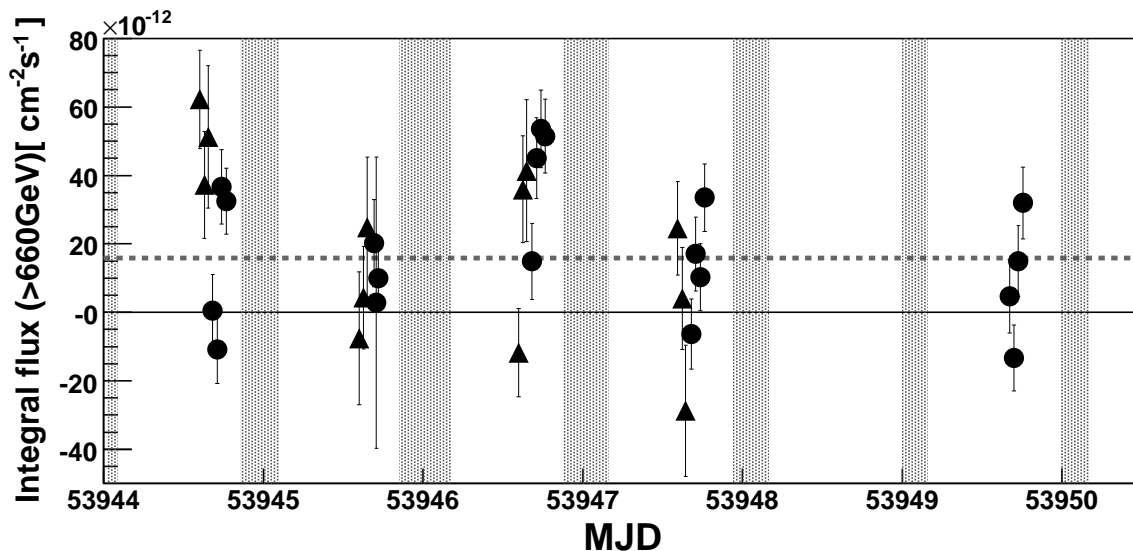


Fig. 3. Light curve of PKS 2155–304 using all the data at zenith angle less than 30° between 2006 July 28 and August 2, expressed by the integral flux above 660 GeV. Closed triangles and closed circles indicate the results from 2-fold (T2 and T4) and 3-fold (T2, T3, and T4) datasets, respectively. Dashed line indicates an average integral flux during this observation period. The bin width is 40 minutes. The shaded areas indicate the H.E.S.S. observation periods.

We observed HESS J1804–216 with the CANGAROO-III IACTs from May to July in 2006. We detected VHE gamma rays above 600 GeV at the 10σ level in an effective exposure of 76 hr. We obtained a differential flux of $(5.0 \pm 1.5_{\text{stat}} \pm 1.6_{\text{sys}}) \times 10^{-12} (E/1 \text{ TeV})^{-\alpha} \text{ cm}^{-2} \text{ s}^{-1} \text{ TeV}^{-1}$ with a photon index α of $2.69 \pm 0.30_{\text{stat}} \pm 0.34_{\text{sys}}$, which is consistent with that of the H.E.S.S. observation in 2004. We also confirmed the extended morphology of the source. By combining our result with multiwavelength observations, we discussed the possible counterparts of HESS J1804–216 and the radiation mechanism based on leptonic and hadronic processes for a SNR and a PWN. For the SNR scenario, the most plausible counterpart is the SNR G 8.7–0.1, and both hadronic and leptonic processes can produce the observed TeV gamma-ray spectrum. For the PWN scenario, we confirmed that the leptonic model with a time-dependent rate of electron injection while considering the braking effect for the spin-down luminosity and the cooling effect due to synchrotron and inverse Compton (IC) energy losses could explain both the high TeV gamma-ray flux and the low X-ray flux (Figure 4). However, a quite high value for the total energy that the pulsar has lost is required for PSR B1800–21 in this model.

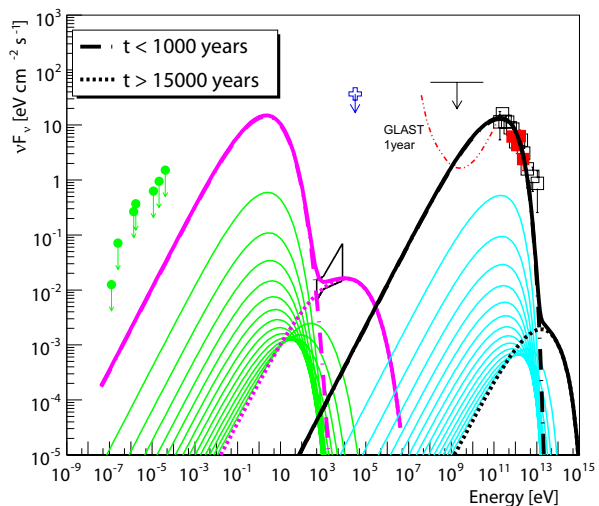


Fig. 4. Spectral energy distribution for HESS J1804–216 and the leptonic model curves for the pulsar wind nebula of PSR B1800–21 with a time-dependent rate of electron-injection with an age $\tau = 16$ kyr, an initial spin-down timescale $\tau_0 = 700$ yr, a braking index of the pulsar $n_{\text{br}} \sim 1.6$, a spectral index of injected electrons $\Gamma_e = 1.5$, and a magnetic field $B = 8 \mu\text{G}$. The right-hand curves show the inverse Compton component, and the left-hand curves show the synchrotron emissions. The dot-dashed curves show the spectra produced by old electrons ($t < 1000$ yr), and the dotted curves show the spectra produced by young electrons ($t > 15000$ yr). The thin solid curves represent their medium per 1000 yr ($1000 < t < 15000$ yr), and the thick solid curves show their total. The CANGAROO-III and H.E.S.S. flux points are shown by the red filled squares and the black open squares, respectively.

Unidentified H.E.S.S. Source HESS J1614–518

HESS J1614–518 is another unidentified TeV source discovered in the H.E.S.S. Galactic plane survey. This source also has a relatively high flux level among the unidentified H.E.S.S. sources (25 % of the Crab flux above 200 GeV), and is possibly associated with the young open star cluster Pismis 22.

CANGAROO-III has observed HESS J1614–518 from May to August 2008 and diffuse gamma-ray emission was detected above 760 GeV at the 8.9σ level during an effective exposure of 54 hr (Figure 5) [13]. The spectrum is represented with a power-law: $(8.2 \pm 2.2_{\text{stat}} \pm 2.5_{\text{sys}}) \times 10^{-12} \times (E/1 \text{ TeV})^{-\gamma} \text{ cm}^{-2} \text{ s}^{-1} \text{ TeV}^{-1}$ with a photon index γ of $2.4 \pm 0.3_{\text{stat}} \pm 0.2_{\text{sys}}$, which is compatible with that of the H.E.S.S. observations. By combining our result with multiwavelength data, we discussed the possible counterparts for HESS J1614–518 and consider radiation mechanisms based on hadronic and leptonic processes for a SNR, stellar winds from massive stars, and a PWN. Although a leptonic origin from a PWN driven by an unknown pulsar remains possible (the nearby known pulsars are not responsible since the spin-down powers are insufficient to produce the observed TeV gamma-ray luminosity), hadronic-origin emission from an unknown SNR is preferred.

High Energy Pulsar PSR B1706–44 and Its Vicinity

A detection of a gamma-ray signal at the 8σ level from PSR B1706–44, which was one of the EGRET-detected pulsars, was reported using the data acquired by CANGAROO-I¹⁸. H.E.S.S., however, claimed no detection from that direction¹⁹. We observed this source for 27 hr (ON) and 29 hr (OFF) with CANGAROO-III in May 2004. Preliminary analyses using the T2 and T3 telescope pair did not show any peaks in the θ^2 distribution²⁰. The upper limit from this result is lower than the flux reported by CANGAROO-I.

CANGAROO-III has performed further observations of PSR B1706–44 over 50 hr from April to June 2007. The observations have given an indication of extended emission of TeV gamma rays around PSR B1706–44 as shown in Figure 6. The strength of the sig-

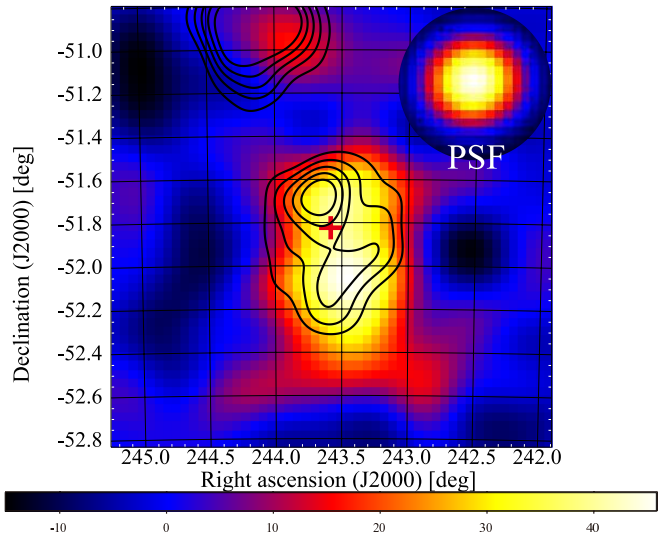


Fig. 5. Morphology of gamma-ray-like events observed from HESS J1614–518. The number of excess events per $0.2^\circ \times 0.2^\circ$ cell is smoothed and plotted in the equatorial coordinate. The black solid contours show the VHE gamma-ray emission seen by H.E.S.S. The red cross shows the center position of HESS J1614–518.

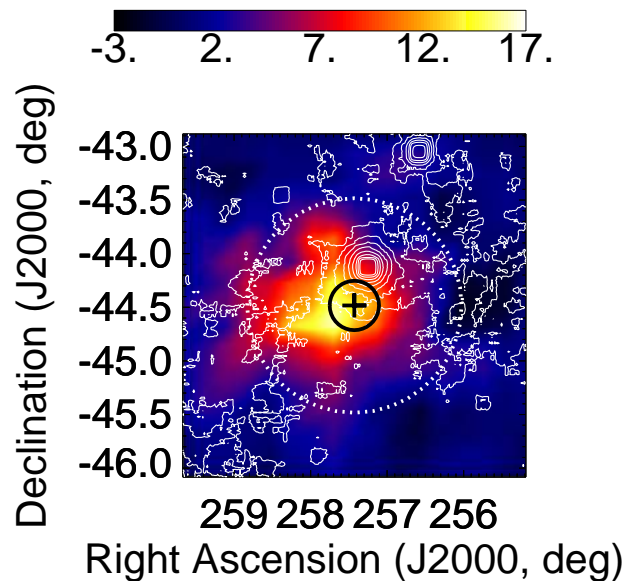


Fig. 6. Skymap of excess events of the 2004 data observed from the vicinity of the high energy pulsar PSR B1706–44. The number of excess events per $0.2^\circ \times 0.2^\circ$ cell is smoothed with adjacent cells and plotted in equatorial coordinates. The black cross at the center of the map indicates the position of PSR B1706–44, the radius of the black circle represents the point spread function (PSF) of $\delta\theta_0 = 0.24^\circ$, and the circle of white dotted line shows the region within 1° radius from the pulsar. The inserted white contours are the hard X-ray map obtained from the ROSAT satellite.

^{*18} T. Kifune et al., *ApJ* **438**, L91–L94 (1995).

^{*19} F. A. Aharonian et al., *A&A* **432**, L9–L12 (2005).

^{*20} T. Tanimori et al., in *Proc. 29th ICRC (Pune)*, **4**, 215–218 (2005).

nal depends on how we estimate angular size of the extended emission. The total flux at 1 TeV is $(4.7 \pm 0.7) \times 10^{-11} (E/1 \text{ TeV})^{-3.1 \pm 0.7} \text{ cm}^{-2} \text{ s}^{-1} \text{ TeV}^{-1}$, when integrated for incident angles within a circle of 1° radius. This corresponds to $(4.9 \pm 0.7) \times 10^{-8} (E/1 \text{ TeV})^{-3.1 \pm 0.7} \text{ cm}^{-2} \text{ s}^{-1} \text{ TeV}^{-1} \text{ sr}^{-1}$ in unit of “per solid angle”. After integration of the gamma-ray energy, E , it is $2.2 \times 10^{-11} \text{ cm}^{-2} \text{ s}^{-1}$ for $E > 1 \text{ TeV}$, which is as large as the Crab flux of $1.8 \times 10^{-11} \text{ cm}^{-2} \text{ s}^{-1}$. A best fit to the radial profile gives two components of diffuse emission, i.e., 0.3° wide plus flat ones. The flux of the 0.3° source is sub-Crab level. The intensity within the area corresponding to the PSF, $\theta < 0.24^\circ$ from PSR B1706–44, is $(3.0 \pm 0.6) \times 10^{-12} \text{ cm}^{-2} \text{ s}^{-1}$ for gamma-ray energy $E > 1 \text{ TeV}$. The flux corresponds to 17% of the Crab flux at 1 TeV, setting constraint on the emission from a compact source, which may underlie below the extended emission. The relative excess of this region compared with that of $0.4^\circ < \theta < 0.6^\circ$ is $6 \pm 4\%$ Crab. These are the results from ON/OFF subtraction method. On the other hand, a statistically significant result could not be obtained from method of the wobble and ring background analysis. The 2σ upper limit on the emission within 0.24° radius from PSR B1706–44 is $1.8 \times 10^{-12} \text{ cm}^{-2} \text{ s}^{-1}$ at 1 TeV, which corresponds to 10% of the Crab flux at 1 TeV.

After reporting this result, H.E.S.S. also has updated their result of the PSR B1706–44 region. They have detected an extended (intrinsic Gaussian width $\sigma = 0.29^\circ$) TeV gamma-ray signal at the 7σ level, of which the integral flux between 1 and 10 TeV is equivalent to 17% Crab, but the position is offset by about 0.3° from the pulsar to the northwest, coinciding with the SNR candidate G 343.1–2.3²¹. No significant point-like emission was detected at the position of the pulsar itself.

Starburst Galaxy NGC 253 (Erratum)

We reported the observation of diffuse gamma-ray emission from the starburst galaxy NGC 253 based on CANGAROO-II data taken in 2000 and 2001, indicating a gamma-ray signal at the 11σ level²². H.E.S.S., however, claimed no detection

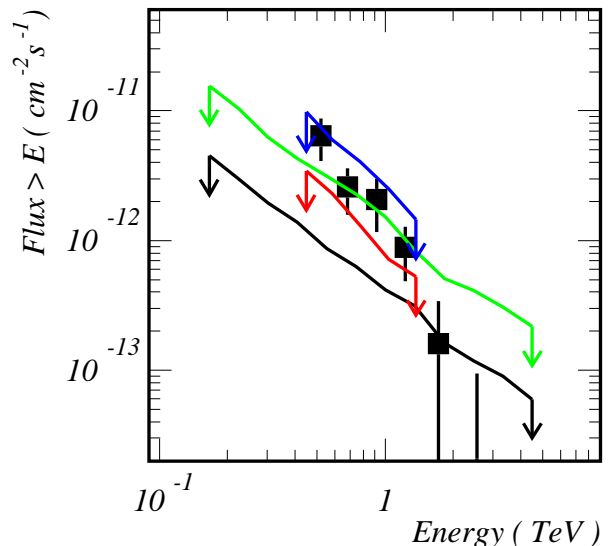


Fig. 7. Integral gamma-ray fluxes from NGC 253. The points with the error bars are the fluxes reported by CANGAROO-II. The black and green curves are the 99% confidence level upper limits obtained by H.E.S.S. for point and diffuse (0.5°) source assumptions, respectively. The red and blue curves are the 2σ upper limits obtained by CANGAROO-III for the same assumptions.

from that direction²³. Their upper limit is slightly below our detection level and also some serious discussion can be found in their report on the possibility on minimum gamma-ray emission from the center of this starburst galaxy. In order to resolve this discrepancy, we analyzed new data observed from NGC 253 using the CANGAROO-III telescopes and also assessed the results reported by CANGAROO-II.

Observations were made with three telescopes of CANGAROO-III in October 2004. We analyzed three-fold coincidence data by using the Fisher discriminant to discriminate gamma-ray events from background events. No significant gamma-ray signal has been detected by CANGAROO-III [3]. The upper limit to the gamma-ray flux was 5.8% Crab at 0.58 TeV for point-source assumption (Figure 7). In addition, the statistical significance of the gamma-ray-like excess obtained by CANGAROO-II was lowered to less than 4σ after assessing treatment of malfunction of photomultiplier tubes.

After the above erratum to the CANGAROO-II result was published, H.E.S.S. reported the detection of VHE gamma rays from NGC 253 with a much larger data sample (119 hr) obtained in 2005,

^{*21} A. Abramowski et al., *A&A* **528**, A143 (2011).

^{*22} C. Ito et al., *A&A* **396**, L1–L4 (2002), C. Ito et al., *A&A* **402**, 443–455 (2003).

^{*23} F. Aharonian et al., *A&A* **442**, 177–183 (2005).

2007, and 2008²⁴. The flux above 220 GeV corresponds to 0.3 % of the Crab flux and the emission is consistent with the PSF of H.E.S.S.

Supernova Remnant 1987A

Optical images of SN 1987A show a triple ring structure. The inner (dust) ring has recently increased in brightness and in the number of hot spots suggesting that the supernova shock wave has collided with the dense pre-existing circumstellar medium, a scenario supported by radio and X-ray observations. Such a shocked environment is widely expected to result in the acceleration of charged particles, and the accompanying emission of VHE gamma rays. We reported the results of CANGAROO-III observations made in 2004 and 2006 which yield upper limits to the TeV gamma-ray flux, which are compared with a theoretical prediction. In addition, we set upper limits to the TeV fluxes for four high energy objects which are located within the same field of view of the observation: the super bubble 30 Dor C, the Crab-like pulsar PSR B0540–69, the X-ray binary LMC X-1, and the SNR N 157B.

Kepler's Supernova Remnant

Kepler's SNR is 400 years old and both younger (Cas A) and older (RX J0852.0–4622, RX J1713.7–3946, etc.) SNRs are known to be TeV gamma-ray sources. Therefore, one might expect a similar level of TeV gamma-ray emission also from Kepler's SNR, if the SNR age is a dominant factor in cosmic-ray acceleration.

CANGAROO-III observed Kepler's SNR in April 2005 for an effective observation time of 874 min. No statistically significant gamma-ray signal has been detected from the SNR and we have estimated 2σ flux upper limits corresponding to the 10–30 % Crab level, which were compared with model predictions obtained by Berezhko et al. (2006)²⁵ considering a reasonably wide range of possibilities for the distance of the SNR (3.4–7.0 kpc), the supernova explosion energy ($(0.5 - 2.0) \times 10^{51}$ erg), and the ambient matter density ($0.4-6.0 \text{ cm}^{-3}$). Limitations on the allowed parameter range in the model were discussed in comparison with the flux upper limits.

²⁴ F. Acero et al., *Science* **326**, 1080–1082 (2009).

²⁵ E. G. Berezhko, L. T. Ksenofontov, & H. J. Völk, *A&A* **452**, 217–221 (2006).

Clusters of Galaxies Abell 3667 and Abell 4038

Clusters of galaxies are candidate sites for the origin of ultra high energy (UHE) cosmic rays because accretion and merger shocks in clusters may accelerate particles to high energies. A prediction was presented for gamma-ray emission from a cluster of galaxies at a detectable level with the current generation of IACTs. The gamma-ray emission is produced via IC upscattering of cosmic microwave background (CMB) photons by electron-positron pairs generated by collisions of UHE cosmic rays in the cluster.

We observed two southern clusters of galaxies, Abell 3667 and Abell 4038, searching for VHE gamma-ray emission with the CANGAROO-III telescope system in 2006 [12]. The ON-source observation times are 29.7 hr and 23.6 hr for Abell 3667 and Abell 4038, respectively. The analysis showed no statistically significant excess around these clusters, yielding upper limits on the gamma-ray emission. From a comparison of the upper limit for the north-west radio relic region of Abell 3667 with a model prediction, we derived a lower limit for the magnetic field of the region of $\sim 0.1 \mu\text{G}$. This shows the potential of gamma-ray observations in studies of the cluster environment. We also discussed the flux upper limit from cluster center regions with a model of gamma-ray emission from neutral pions produced in hadronic collisions of cosmic-ray protons with the intra-cluster medium. The derived upper limits of the cosmic-ray energy densities within this framework are $\sim 20 \text{ eV cm}^{-3}$ for Abell 3667 and $\sim 40 \text{ eV cm}^{-3}$ for Abell 4038, which are an order of magnitude higher than that of our Galaxy.

Blazars H 2356–309, PKS 2155–304, PKS 0537–441, and 3C 279

We have observed four selected blazars, H 2356–309, PKS 2155–304, PKS 0537–441, and 3C 279, with the CANGAROO-III IACTs from 2005 to 2009. No statistically significant excess of events above 510–720 GeV from the direction of any of these objects was found, and we derived flux upper limits for VHE gamma-ray emissions [14]. In addition, we analyzed GeV gamma-ray data between 0.2 and 300 GeV taken with Fermi Large Area Telescope (LAT) from August 2008 to May 2011.

To derive some important physical parameters

of these blazars, we consider a simple leptonic jet model to explain the multiwavelength SEDs including GeV and TeV spectra, even though non-simultaneous. The observed SED of H 2356-309 (HBL) could be explained by a simple synchrotron-self-Compton (SSC) model with a single power-law electron spectrum, and to keep a consistency with GeV spectrum, we need to assume a large beaming factor $\delta = 59$ and weak magnetic field strength of 0.012 G. Radiation from PKS 2155–304, a nearby HBL, was well modeled by the SSC scenario, and obtained parameters are consistent with earlier works. PKS 0537–441, a luminous LBL, was studied and we found SSC + EC (external Compton) model could explain the observed multiwavelength spectrum where the EC component is dominant in the gamma-ray photons. The SED of one of the distant flat spectrum radio quasar (FSRQ), 3C 279, were also well explained by the SSC + EC model.

Additionally, from our parameter fit results as the HBL to the FSRQ of blazar sub-classes, it is seen that the beaming factor becomes smaller, and in contrast the strength of the magnetic field becomes stronger and the size of blob becomes larger. Although we could not take into account of the uncertainties such as simultaneity of the data and the differences of models, these latter two tendencies are in agreement with the proposed blazar sequence.

CANGAROO-II Result

Binary System SS 433/Supernova Remnant W 50

SS 433 is a close proximity binary system consisting of a compact star and a normal star. It is located at the center of the SNR W 50. Jets of material are directed outwards from the vicinity of the compact star symmetrically to the east and west. Non-thermal hard X-ray emission is detected from lobes lying on both sides. Shock accelerated electrons are expected to generate sub-TeV gamma rays through the IC process in the lobes.

CANGAROO-II observed the western X-ray lobe region in August and September 2001, and in July and September 2002. The total observation times are 85.2 hr for ON source and 80.8 hr for OFF source. In the ON-source observations, the telescopes tracked the position from which the hardest power-law X-ray spectrum was obtained by ASCA. No significant excess of sub-TeV gamma rays has been found from 3 regions of the western

X-ray lobe of the SS 433/W 50 system. The 99% confidence level (CL) upper limits to the fluxes of gamma rays at energies greater than 850 GeV have been derived as 1.5, 1.3, and 0.79 in unit of 10^{-12} photons $\text{cm}^{-2} \text{s}^{-1}$ for the 3 regions. The synchrotron/IC model has been applied to the multiwavelength spectra together with radio and X-ray data. Lower limits to the magnetic field strengths have been estimated to be $4.3 \mu\text{G}$ for the brightest X-ray emission region and $6.3 \mu\text{G}$ for the far end from SS 433 in the western X-ray lobe.

Reanalysis of CANGAROO-I Data

Old CANGAROO-I data have been reanalyzed for PSR B1706–44, SN 1006, and the Vela pulsar region [9] in response to the results reported for these sources by the H.E.S.S. Collaboration. Although detections of TeV gamma-ray emission from these sources were claimed by CANGAROO more than 10 years ago, upper limits to the TeV gamma-ray signals from PSR B1706–44 and SN 1006 derived by H.E.S.S. are about an order of magnitude lower. The H.E.S.S. group detected strong diffuse TeV gamma-ray emission from Vela but with a morphology differing from the CANGAROO result²⁶.

In the reanalysis, in which gamma-ray selection criteria have been determined exclusively using gamma-ray simulations and OFF-source data as background samples, no significant TeV gamma-ray signals have been detected from compact regions around PSR B1706–44 or within the northeast rim of SN 1006. The upper limits to the integral gamma-ray fluxes at the 95% CL have been estimated for the 1993 data of PSR B1706–44 to be $F(> 3.2 \pm 1.6 \text{ TeV}) < 8.03 \times 10^{-13}$ photons $\text{cm}^{-2} \text{s}^{-1}$, for the 1996 and 1997 data of SN 1006 to be $F(> 3.0 \pm 1.5 \text{ TeV}) < 1.20 \times 10^{-12}$ photons $\text{cm}^{-2} \text{s}^{-1}$ and $F(> 1.8 \pm 0.9 \text{ TeV}) < 1.96 \times 10^{-12}$ photons $\text{cm}^{-2} \text{s}^{-1}$, respectively. These results are plotted in Figure 8 and Figure 9 together with the other previous results.

The reanalysis did result in a TeV gamma-ray signal from the Vela pulsar region at the 4.5σ level using 1993, 1994, and 1995 data. The excess was located at the same position, $0^\circ 13$ to the

^{*26} T. Yoshikoshi et al., ApJ **487**, L65–L68 (1997).

^{*27} J. Kushida et al., in Proc. 28th ICRC (Tsukuba), **4**, 2493–2496, (2003).

^{*28} T. Tanimori et al., ApJ **497**, L25–L28, (1998).

^{*29} T. Tanimori et al., in Proc. 27th ICRC (Hamburg), **6**, 2465–2468, (2001).

^{*30} S. Hara et al., in Proc. 27th ICRC (Hamburg), **6**, 2455–2458, (2001).

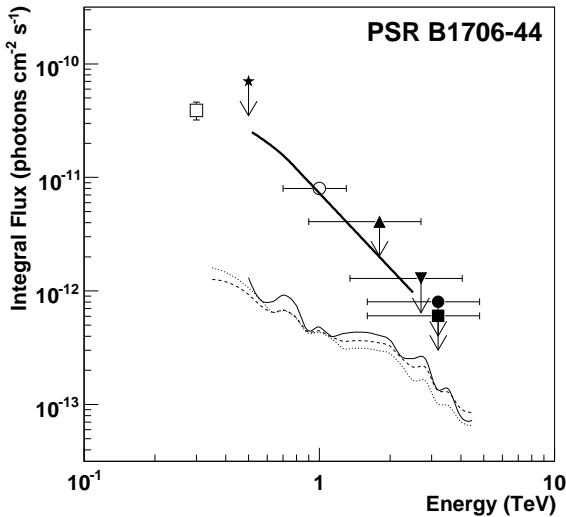


Fig. 8. Integral gamma-ray fluxes from PSR B1706–44 obtained using the CANGAROO-I data. The 95% confidence level (CL) upper limits to the integral flux from PSR B1706–44 obtained from the 1993, 1993 + 1994, 1997, and 1998 data are indicated by the filled circle, filled square, filled triangle, and filled upside-down triangle, respectively. The open circle indicates the integral flux estimated by Kifune et al. (1995)¹⁸ using the 1993 data. The horizontal bars represent the systematic errors of the threshold energies. The 99% CL upper limit curves obtained by H.E.S.S. are indicated by the thin solid, dashed, and dotted lines. The thick solid line is the integral spectrum converted from the preliminary CANGAROO-II result (Kushida et al. 2003²⁷). The open square and filled star indicate the results from the Durham group and BIGRAT, respectively.

southeast of the Vela pulsar, as that reported in the original analysis. We have investigated the effect of the acceptance distribution in the field of view of the 3.8 m telescope, which rapidly decreases toward the edge of the field of the camera, on the detected gamma-ray morphology. The expected excess distribution for the 3.8 m telescope has been obtained by reweighting the distribution of HESS J0835–455 measured by H.E.S.S. with the acceptance of the 3.8 m telescope. The result is morphologically comparable to the CANGAROO excess distribution, although the profile of the acceptance-reweighted H.E.S.S. distribution is more diffuse than that of CANGAROO. The integral gamma-ray flux from HESS J0835–455 has been estimated for the same region as defined by H.E.S.S. from the 1993–1995 data of CANGAROO to be $F(> 4.0 \pm 1.6 \text{ TeV}) = (3.28 \pm 0.92) \times 10^{-12} \text{ photons cm}^{-2} \text{ s}^{-1}$, which is statistically consistent with the integral flux obtained by H.E.S.S.

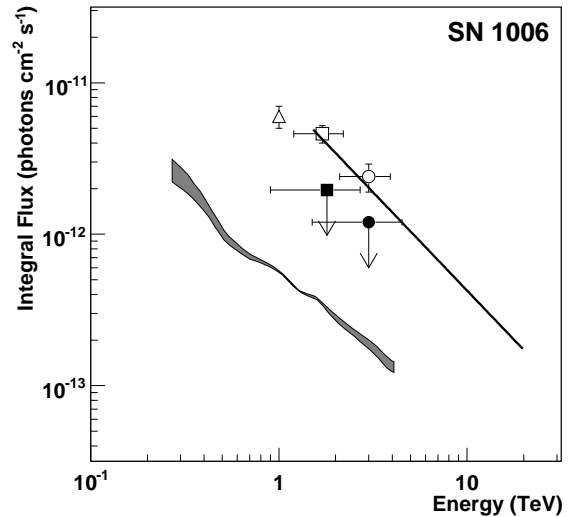


Fig. 9. Integral gamma-ray fluxes from the NE rim of SN 1006 obtained using the CANGAROO-I data. The 95% confidence level (CL) upper limits to the integral fluxes are indicated by the filled circle (1996 data with the selection criteria optimized for the 0.3° offset) and the filled square (1997 data). The open circle and open square are the integral fluxes estimated by Tanimori et al. (1998)²⁸ using the 1996 and 1997 data, respectively. The thick solid line is the integral spectrum converted from the CANGAROO-I differential spectrum (Tanimori et al. 2001²⁹). The horizontal bars represent the systematic errors of the threshold energies. The 99.9% CL upper limits obtained by H.E.S.S. are indicated by the gray band for a range of assumed photon indices (2 to 3). The open triangle indicates the preliminary CANGAROO-II result (Hara et al. 2001³⁰).

as shown in Figure 10.

Summary

CANGAROO has played a pioneering role in VHE gamma-ray astrophysics in the southern hemisphere since 1992 and carried out stereoscopic observations of sub-TeV gamma rays with four CANGAROO-III telescopes since March 2004. The number of VHE sources has grown to more than hundred and several of them were discovered by CANGAROO over its 20 year history. However, some results claimed by CANGAROO were not confirmed by H.E.S.S., which has been exploring the southern sky at TeV energies sky with an amazingly high sensitivity. We have made efforts since 2004 to resolve the contradictions both by re-analyzing old data and by observing the claimed sources by CANGAROO-III. We think that most of them have been resolved at an understandable level.

Since 2004, CANGAROO-III has tried to play a complementary role with H.E.S.S. in the south-

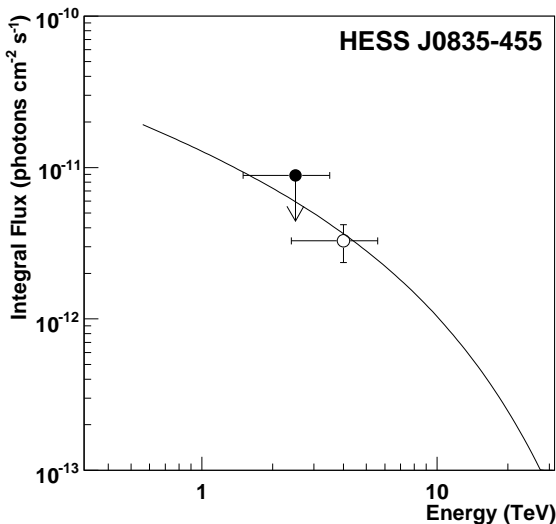


Fig. 10. Integral gamma-ray fluxes from the Vela pulsar region (0.8° radius centered on HESS J0853–455) obtained from the CANGAROO-I data. The open circle represents the integral flux from the 1993 to 1995 data and the filled circle represents the 95% confidence level upper limit to the flux from the 1997 data. The horizontal bars represent the systematic errors of the threshold energies. The solid line is the integral spectrum converted from the differential spectrum of HESS J0853–455 measured by H.E.S.S. assuming a power law with an exponential cutoff.

ern hemisphere by confirming observational results and/or continuously monitoring flaring sources in a different longitude. A good example is the TeV flare of PKS 2155–304 in 2006 in which our observations were triggered by H.E.S.S. We have also confirmed with improved angular resolution of the stereoscopic imaging atmospheric Cherenkov technique that some Galactic TeV sources such as MSH 15–52 and PSR B1706–44 have extended features. However, we decided to stop observations of CANGAROO-III in 2011 since the optical performance of the exposed telescope mirrors had seriously deteriorated and it was not possible to obtain support for a further upgrade of the system. Our activity in this field has moved onto R & D studies for future ground-based gamma-ray observatory projects such as the Cherenkov Telescope Array (CTA).

CANGAROO Team

Spokespersons:

R. W. Clay (Univ. of Adelaide),
T. Tanimori (Kyoto Univ.),
M. Mori (ICRR, until 2009),

R. Enomoto (ICRR, 2009 to 2011),
T. Yoshikoshi (ICRR, 2011 to the present)

Institute	Country	(*)
ICRR, Univ. of Tokyo	Japan	4
Univ. of Adelaide	Australia	4
ATNF, CSIRO	Australia	1
Ibaraki Univ.	Japan	3
Kitasato Univ.	Japan	1
Konan Univ.	Japan	2
Kyoto Univ.	Japan	2
MSO, ANU	Australia	1
NAOJ	Japan	1
STE Lab., Nagoya Univ.	Japan	1
Tokai Univ.	Japan	9
Yamanashi Gakuin Univ.	Japan	2
Yamagata Univ.	Japan	2
Waseda Univ.	Japan	1
Ritsumeikan Univ.	Japan	1
KEK	Japan	1
Total		36

(*) Number of participants as of March 2012.

Members

Staffs

Masaki Mori, Professor, October 2003 to March 2009

Ryoji Enomoto, Assoc. Professor, September 1999 to the present

Takanori Yoshikoshi, Assoc. Professor, May 2004 to the present

Michiko Ohishi, Research Associate, October 2005 to the present

Graduate Students

Six students (including students from other universities) were awarded doctor degrees, and twenty-one students earned master degrees during 2006–2012, supervised by ICRR staff members.

List of Publications

Papers in refereed journals

- [1] “CANGAROO-III Search for Gamma Rays from Centaurus A and the ω Centauri Region”
Kabuki, S. et al., *Astrophys. J.* **668**, 968–973 (2007) [Times cited³¹: 19].

³¹ Number of citations based on the *Web of Science* database as of September 19, 2012.

- [2] “CANGAROO-III Search for Gamma Rays from SN 1987A and the Surrounding Field”
Enomoto, R. et al., *Astrophys. J.* **671**, 1939–1943 (2007) [Times cited: 3].
- [3] “Erratum: Detection of diffuse TeV gamma-ray emission from the nearby starburst galaxy NGC 253”
Itoh, C. et al., *Astron. Astrophys.* **462**, 67–71 (2007).
- [4] “CANGAROO-III Observations of the 2006 Outburst of PKS 2155–304”
Sakamoto, Y. et al., *Astrophys. J.* **676**, 113–121 (2008) [Times cited: 13].
- [5] “Observation of an extended VHE gamma-ray emission from MSH 15–52 with CANGAROO-III”
Nakamori, T. et al., *Astrophys. J.* **677**, 297–305 (2008) [Times cited: 7].
- [6] “CANGAROO-III Search for Gamma Rays from Kepler’s Supernova Remnant”
Enomoto, R. et al., *Astrophys. J.* **683**, 383–388 (2008) [Times cited: 2].
- [7] “Observation of Very High Energy Gamma Rays from HESS J1804–216 with CANGAROO-III Telescopes”
Higashi, Y. et al., *Astrophys. J.* **683**, 957–966 (2008) [Times cited: 6].
- [8] “Very high energy gamma-ray observations of the Galactic Plane with the CANGAROO-III telescopes”
Ohishi, M. et al., *Astropart. Phys.* **30**, 47–53 (2008) [Times cited: 2].
- [9] “Reanalysis of Data Taken by the CANGAROO 3.8 Meter Imaging Atmospheric Cherenkov Telescope: PSR B1706–44, SN 1006, and Vela”
Yoshikoshi, T. et al., *Astrophys. J.* **702**, 631–648 (2009) [Times cited: 2].
- [10] “Search for VHE Gamma Rays from SS 433/W 50 with the CANGAROO-II Telescope”
Hayashi, Sei. et al., *Astropart. Phys.* **32**, 112–119 (2009) [Times cited: 2].
- [11] “CANGAROO-III Observation of TeV Gamma Rays from the Vicinity of PSR B1706–44”
Enomoto, R. et al., *Astrophys. J.* **703**, 1725–1733 (2009) [Times cited: 2].
- [12] “CANGAROO-III Search for TeV Gamma Rays from Two Clusters of Galaxies”
Kiuchi, R. et al., *Astrophys. J.* **704**, 240–246 (2009) [Times cited: 6].
- [13] “CANGAROO-III Observation of TeV Gamma Rays from the Unidentified Gamma-Ray Source HESS J1614–518”
Mizukami, T. et al., *Astrophys. J.* **740**, 78 (2011).
- [14] “Searches for Very High Energy Gamma Rays from Blazars with CANGAROO-III Telescope in 2005–2009”
Mizumura, Y. et al., *Astropart. Phys.* **35**, 563–572 (2012).
- Papers in conference proceedings
- [15] “CANGAROO”
M. Mori et al., Third Workshop on Science with the New Generation of High Energy Gamma-Ray Experiments, Cividale del Friuli, Italy, May 30–June 1 (2005), published as “Science with the New Generation of High Energy Gamma-Ray Experiments” (eds. A. De Angelis and O. Mansutti, World Scientific, Singapore, 2006), pp.21–28.
- [16] “Recent Results from CANGAROO”
M. Mori et al., International Workshop on Energy Budget in the High Energy Universe, February 22–24, 2006, Kashiwa campus of the University of Tokyo, Chiba, Japan published as “Energy Budget in the High Energy Universe” (eds. Katsuhiko Sato and Junji Hisano, World Scientific, Singapore, 2007), pp.152–161.
- [17] “Optical Measurements for CANGAROO-III”
R. Kiuchi et al., *ibid.*, pp.345–348.
- [18] “Consideration of Cassegrain Imaging Atmospheric Cherenkov Telescopes”
Y. Yukawa et al., *ibid.*, pp.349–352.

- [19] “Recent Results from CANGAROO”
M. Mori et al., Forth Workshop on Science with the New Generation of High Energy Gamma-Ray Experiments, Isola d’Elba, Italy, June 20–22 (2006), published in “Science with the New Generation of High Energy Gamma-Ray Experiments, The Variable Gamma-Ray Sources: Their Identification and Counterparts” (eds. M. M. Massai, N. Omodai and G. Spandre, World Scientific, Singapore, 2007), pp.45–52.
- [20] “Recent results from CANGAROO”
M. Mori et al., International Workshop on “Cosmic-Rays and High Energy Universe”, Aoyama Gakuin Univ., Shibuya, Tokyo, Japan, March 5–6 (2007) (published in “Cosmic-Rays and High Energy Universe”, eds. T. Shibata and N. Sakaki, Universal Academy Press, Tokyo, 2007), pp.93–100.
- [21] “Observation of HESS J1303–631 with the CANGAROO-III Telescopes”
J. Kushida et al., 30th International Cosmic Ray Conference, Mérida, México (July 2–11, 2007), published in Proceedings (Universidad Nacional Autónoma de México, Mexico City, Mexico, 2008), Vol.2, pp.597–600.
- [22] “Observations of extended VHE gamma-ray emission from MSH 15–52 with CANGAROO-III”
T. Nakamori et al., *ibid.*, Vol.2, pp.629–632.
- [23] “Observation of VHE gamma rays from HESS J1804–216 with CANGAROO-III Telescopes”
Y. Higashi et al., *ibid.*, Vol.2, pp.645–648.
- [24] “Time variation of the flux of TeV gamma-rays from PKS 2155–304”
K. Nishijima et al., *ibid.*, Vol.3, pp.897–900.
- [25] “Detection of 2006 TeV-outburst of PKS 2155–304 with the CANGAROO-III telescope”
Y. Sakamoto et al., *ibid.*, Vol.3, pp.905–908.
- [26] “Observation of clusters of galaxies with the CANGAROO-III telescope system”
R. Kiuchi et al., *ibid.*, Vol.3, pp.1005–1008.
- [27] “Status of CANGAROO-III”
M. Mori et al., *ibid.*, Vol.3, pp.1309–1312.
- [28] “Recent Results from CANGAROO-III”
Y. Yukawa et al., International Conference on Topics in Astroparticle and Underground Physics (TAUP) 2007, Sendai, Japan (September 11–15, 2007), published as Journal of Physics: Conference Series 120 (2008), 062018.
- [29] “Status of CANGAROO-III”
R. Enomoto et al., 4th International Meeting on High Energy Gamma-Ray Astronomy, Heidelberg, Germany (July 7–11, 2008), published as AIP Conference Proceedings, Vol.1085, pp.661–663.
- [30] “The implications from CANGAROO-III observations of TeV blazar PKS 2155–304”
K. Nishijima et al., *ibid.*, pp.486–489.
- [31] “CANGAROO-III observation of gamma rays from the Galactic Center”
T. Mizukami et al., *ibid.*, pp.364–367.
- [32] “CANGAROO-III Search for TeV Gamma-rays from Two Clusters of Galaxies”
R. Kiuchi et al., 3rd International MAXI Workshop, Wako, Saitama, Japan (June 10–12, 2008), published as JAXA-SP-08-014E (2009).
- [33] “TeV Gamma-Ray Observations of Some Extragalactic Objects with CANGAROO-III”
K. Nishijima et al., 31st International Cosmic Ray Conference, Łódź, Poland (July 7–15, 2009), published in Proceedings (University of Łódź, Łódź, Poland), 0565.
- [34] “Search for TeV Gamma-Rays around the Merger Cluster Abell 3376 with CANGAROO-III”
T. Matoba et al., *ibid.*, 0735.
- [35] “Observations of the Unidentified VHE Gamma-Ray Source HESS J1614–518 with CANGAROO-III”
T. Mizukami et al., *ibid.*, 0973.

TIBET AS γ PROJECT

Introduction

The Tibet air shower experiment has been successfully operated at Yangbajing (90°31' E, 30°06' N; 4300 m above sea level) in Tibet, China since 1990. It has continuously made a wide field-of-view (approximately 2 steradian) observation of cosmic rays and gamma rays in the northern sky.

Summary from 2006 to 2012

Summarized here are the noticeable achievements during the period of this review, i.e., between 2006 and 2012.

- The 2-dimensional anisotropy (0.1 % level) at sidereal time frame is obtained with high-precision in the multi-TeV energy range. The “Tail-in” (hump) and “Loss-cone” (dip) structures are impressive, where we propose a model to well reproduce the observed anisotropy. We find that the observed anisotropy tends to be faint over 300 TeV region. This implies that cosmic rays corotate with our galaxy. Furthermore, we discovered a very interesting large-scale excess in the Cygnus region. A closer view of the Cygnus region shows that the large-scale excess contains a few spatially separated excesses with a smaller scale. The cosmic-ray anisotropy at solar time frame due to terrestrial orbital motion of the Earth (i.e. Compton Getting anisotropy of the order of ~ 0.01 %) is also measured to be consistent with the expected, which assures that our measurement of the anisotropy at sidereal time frame is reliable.
- The primary proton, helium, all-particle energy spectra around the knee region, being inaccessible by any direct observations, are obtained. The absolute flux values of them are estimated within 30% systematic errors. The (all-particle - (proton+He))/all-particle flux ratio indicates that the knee is composed of nuclei heavier than helium. This is the first conclusive (i.e., inclusion of systematic errors) evidence that the chemical composition of cosmic rays in the knee energy region is heavy-nucleus dominant, while the proton-dominant chemical composition was widely believed.
- A clear solar-cycle variation of the Sun’s shadow in 10 TeV cosmic rays are observed by the Tibet air shower array covering a full solar cycle from 1996 to 2009. Numerical simulations of the Sun’s shadow are developed, employing the Potential Field Source Surface (PFSS) model and the Current Sheet Source Surface (CSSS) model for the coronal magnetic field, to interpret the physical implications of the observed solar cycle variation. It is found that the intensity deficit in the simulated Sun’s shadow is very sensitive to the coronal magnetic field structure, and the observed variation of the Sun’s shadow is better reproduced by the CSSS model than the PFSS model. This is the first successful attempt to evaluate the coronal magnetic field models by means of the Sun’s shadow observed in 10 TeV cosmic rays.
- We find a statistical correlation (7 sources) between the Fermi bright source list and TeV excess observation in the northern sky. All the 7 sources are associated with pulsars, and 6 of them are coincident with sources detected by the Milagro experiment at the representative energy of 35 TeV. The result would imply that the excesses are possible candidates for TeV pulsar wind nebulae.
- As an upgrade, new air shower core detectors (YAC) are being constructed for the next-step measurement of the chemical composition in the knee energy region, while a part of the large muon detectors (MD) aiming at higher-sensitivity (by a factor of ~ 10) gamma-ray observation in 10-1000 TeV region are being constructed under the Tibet air shower array. The MD also plays an important role to measure the chemical composition of cosmic rays in the knee energy region.

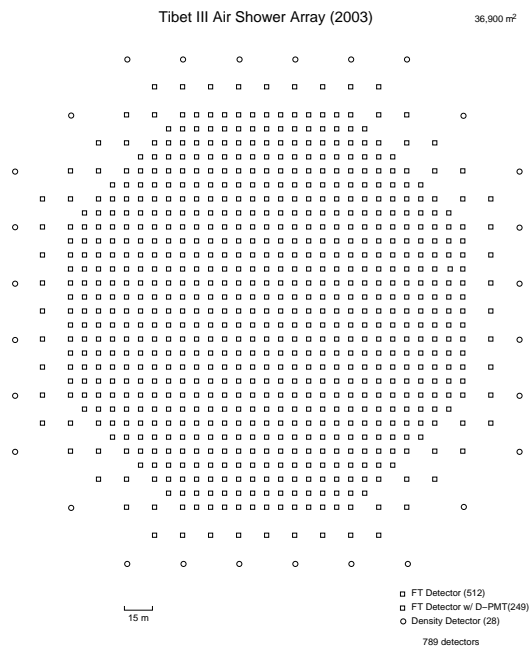


Fig. 1. Schematic view of Tibet III.

Experiment

The Tibet I array was constructed in 1990 and it was gradually upgraded to the Tibet II by 1994 which consisted of 185 fast-timing (FT) scintillation counters placed on a 15 m square grid covering 36,900 m², and 36 density (D) counters around the FT-counter array. Each counter has a plastic scintillator plate of 0.5 m² in area and 3 cm in thickness. All the FT counters are equipped with a fast-timing 2-inch-in-diameter photomultiplier tube (FT-PMT), and 52 out of 185 FT counters are also equipped with a wide dynamic range 1.5-inch-in-diameter PMT (D-PMT) by which we measure up to 500 particles which saturates FT-PMT output, and all the D-counters have a D-PMT. A 0.5 cm thick lead plate is put on the top of each counter in order to increase the counter sensitivity by converting gamma rays into electron-positron pairs in an electromagnetic shower. The mode energy of the triggered events in Tibet II is 10 TeV.

In 1996, we added 77 FT counters with a 7.5 m lattice interval to a 5,200 m² area inside the northern part of the Tibet II array. We called this high-density array Tibet HD. The mode energy of the triggered events in Tibet HD is a few TeV.

In the late fall of 1999, the array was further upgraded by adding 235 FT-counters so as to enlarge the high-density area from 5,200 m² to 22,050 m², and we call this array and further upgraded one Tibet III. In 2002, all of the 36,900 m² area was covered by the high-density array by adding 200 FT-counters more. Finally we set up 56 FT-counters around the 36,900 m² high density array and equipped 8 D-counters with FT-PMT in 2003. At present, the Tibet air shower array consists of 761 FT-counters (249 of which have a D-PMT) and 28 D-counters as in Fig. 1.

The performance of the Tibet air shower array has been well examined by observing the Moon's shadow (approximately 0.5 degrees in diameter) in cosmic rays. The deficit map of cosmic rays around the Moon demonstrates the angular resolution to be around 0.9° at a few TeV for the Tibet III array. The pointing error is estimated to be better than $\sim 0.01^\circ$, as shown in Fig. 2, by displacement of the shadow's center from the apparent center in the north-south direction, as the east-west component of the geomagnetic field is very small at the experimental site. On the other hand, the shadow center displacement in the east-west direction due to the geomagnetic field enables us to spectroscopically estimate the energy scale uncertainty at $\pm 12\%$ level, as shown in Fig. 3. Thus, the Tibet air shower experiment introduces a new method for energy scale calibration other than the conventional estimation by the difference between the measured cosmic-ray flux by an air shower experiment and the higher-energy extrapolation of cosmic-ray flux measured by direct measurements by balloon-borne or satellite experiments.

Physics Results

TeV gamma-ray astrophysics

Using this HD array, in 1999, we succeeded in observing multi-TeV gamma-ray signals from the Crab Nebula. This was the first detection of multi-TeV γ -ray signals by a conventional air shower array. Then, using the Tibet-III dataset collected by this array from 1999 November through 2005 November, we obtained the energy spectrum of γ -rays from the Crab Nebula[11], expressed by a power law as $(dJ/dE) = (2.09 \pm 0.32) \times 10^{-12} (E/3 \text{ TeV})^{-2.96 \pm 0.14} \text{ cm}^{-2} \text{ s}^{-1} \text{ TeV}^{-1}$ in the energy range of 1.7 to 40 TeV. This result is consistent with other independent γ -ray obser-

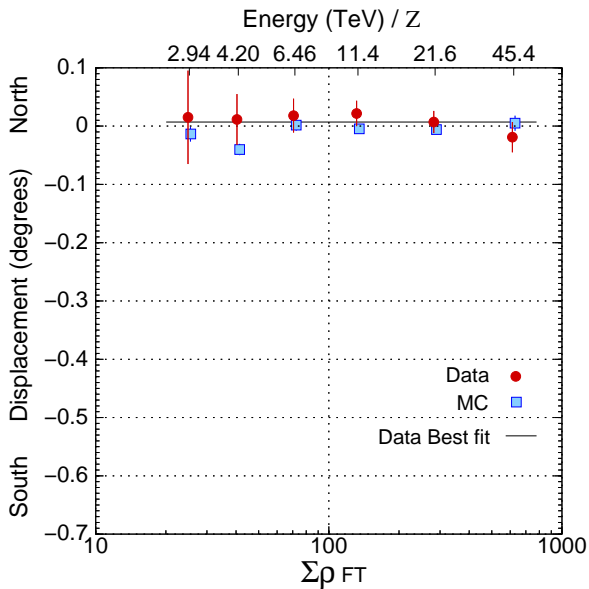


Fig. 2. From [11]. The Moon's shadow center displacement from the apparent position in the north-south direction as a function of energy, observed by Tibet III.

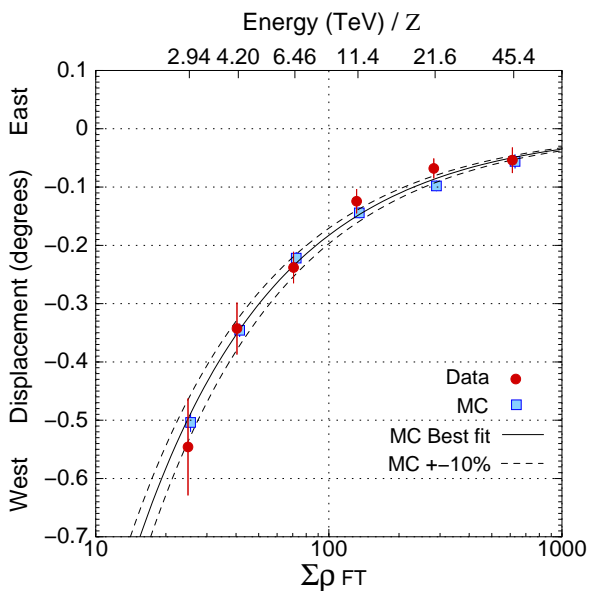


Fig. 3. From [11]. The Moon's shadow center displacement from the apparent position in the east-west direction as a function of energy, observed by Tibet III.

vations by imaging air Cherenkov telescopes. We also search for gamma rays from the Crab pulsar with 33 ms periodicity and find no significant signal. Accordingly, we set flux upper limits on the pulsed gamma-ray flux, as shown in Fig. 4.

The *Fermi* Gamma-ray Space Telescope (*Fermi*), successor of the Energetic Gamma Ray Experiment (EGRET), was launched in June 2008 to measure the energy range between 20 MeV and 300 GeV, approximately a hundred times sensitive

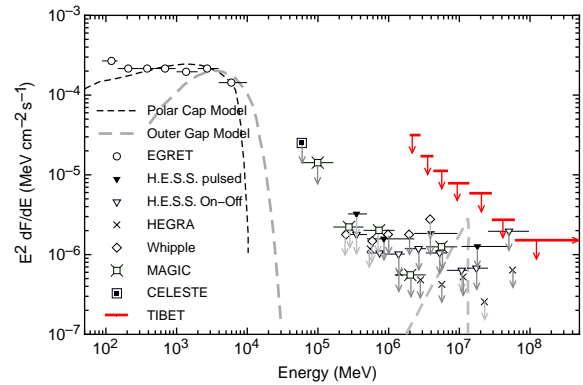


Fig. 4. From [11]. Upper limits on the pulsed γ -ray flux from the Crab pulsar observed by the Tibet-III array (arrows with thick solid line), together with results from other experiments. The long-dashed curve and dashed curve represent the fluxes expected from the outer gap and polar cap models, respectively. For more detail and references, see [11].

than EGRET. The Large Area Telescope (LAT) on board the *Fermi* surveys the entire sky for 3 months, after which the 205 most significant sources were published as a bright source list above 100 MeV at a significance greater than $\sim 10\sigma$. This survey detected many new γ -ray pulsars. A typical 95% uncertainty radius of source position in this list is approximately 10 arcmin and the maximum is 20 arcmin; these values are greatly improved compared to those of EGRET. This provides a more accurate, unbiased search for common sources across multi wavelengths, compared with the EGRET era. Recently, the Milagro experiment observed 14 of the 34 *Fermi* sources selected from the list at a false-positive significance of 3σ or more at the representative energy of 35 TeV. Accordingly, we search for TeV γ -ray sources in the *Fermi* bright source list with the Tibet-III air shower array. Using the Tibet-III air shower array, we search for TeV γ -rays from 27 potential Galactic sources in the early list of bright sources obtained by the *Fermi* Large Area Telescope at energies above 100 MeV. Among them, we observe 7 sources instead of the expected 0.61 sources at a significance of 2σ or more excess. The chance probability from Poisson statistics would be estimated to be 3.8×10^{-6} , as is seen in Fig. 5. If the excess distribution observed by the Tibet-III air shower array has a density gradient toward the Galactic plane, the expected number of sources may be enhanced in chance association. Then, the chance probability rises slightly, to 1.2×10^{-5} ,

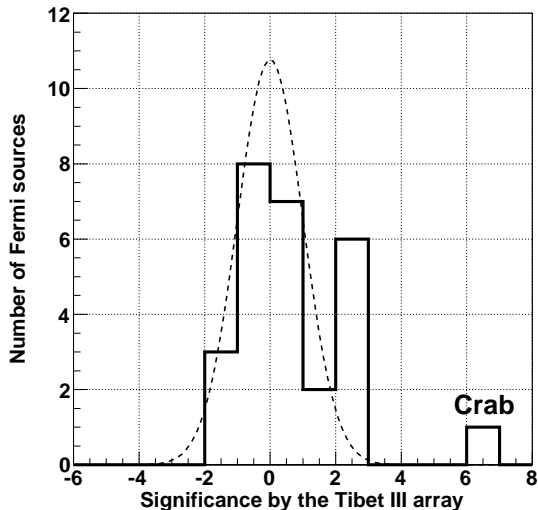


Fig. 5. From [15]. Shown are histograms of significance distribution of the *Fermi* bright sources observed by the Tibet-III air shower array. The dashed curve is the expected normal Gaussian distribution.

based on a simple Monte Carlo simulation. These low chance probabilities clearly show that the *Fermi* bright Galactic sources have statistically significant correlations with TeV γ -ray excesses. We also find that all 7 sources are associated with pulsars, and 6 of them are coincident with sources detected by the Milagro experiment at a significance of 3σ or more at the representative energy of 35 TeV. The significance maps observed by the Tibet-III air shower array around the *Fermi* sources, which are coincident with the Milagro $\geq 3\sigma$ sources, are consistent with the Milagro observations. Besides, the maximum significance positions obtained by both the Tibet-III air shower array and the Milagro experiment might be shifted from the pulsar positions. In fact, recent imaging air Cherenkov telescopes also discovered many candidates for TeV pulsar wind nebulae (PWNe), which are displaced within a few tenths of degree from the pulsars in the southern sky. Thus, these observations would imply that the excesses are possible candidates for TeV PWNe. This is the first result of the northern sky survey of the *Fermi* bright Galactic sources in the TeV region.

Chemical composition and energy spectrum of primary cosmic rays

As shown in Fig. 6, we obtain an updated all-particle energy spectrum of primary cosmic rays in a wide range from 10^{14} eV to 10^{17} eV using

5.5×10^7 events collected in the period from 2000 November through 2004 October by the Tibet-III air-shower array. The energy spectrum exhibits a sharp knee at a corresponding primary energy around 4 PeV. This work uses increased statistics and new simulation calculations for the analysis. We performed extensive Monte Carlo calculations and discuss the model dependence involved in the final result assuming interaction models of QGSJET01c and SIBYLL2.1 and primary composition models of heavy dominant (HD) and proton dominant (PD) ones. Pure proton and pure iron primary models are also examined as extreme cases. The detector simulation was also made to improve the accuracy of determining the size of the air showers and the energy of the primary particle. We confirmed that the all-particle energy spectra obtained under various plausible model parameters are not significantly different from each other as expected from the characteristics of the experiment at the high altitude, where the air showers of the primary energy around the knee reaches near maximum development and their features are dominated by electromagnetic components leading to the weak dependence on the interaction model or the primary mass. This is the highest-statistical and the best systematics-controlled measurement covering the widest energy range around the knee energy region.

The primary proton and helium spectrum around the knee region, being inaccessible by any direct observations, are obtained by an ANN analysis of the 3-year EC ($80m^2$ emulsion chambers) + air shower data[1]. The absolute fluxes of protons and helium nuclei are estimated within 30% systematic errors depending on the hadronic interaction models used in our Monte Carlo simulation. This is the first measurement of the differential energy spectra of primary protons and heliums by selecting them event by event at the knee energy region. The (all-particle - (proton+He))/all-particle flux ratio is shown in Fig. 7, indicating that the knee is composed of nuclei heavier than helium. This is the first conclusive (i.e., inclusion of systematic errors) evidence that the chemical composition of cosmic rays in the knee energy region is heavy-nucleus dominant, while the proton-dominant chemical composition was widely believed. It should be noted that the flux ratio largely cancels out the systematic energy scale uncertainty in the air

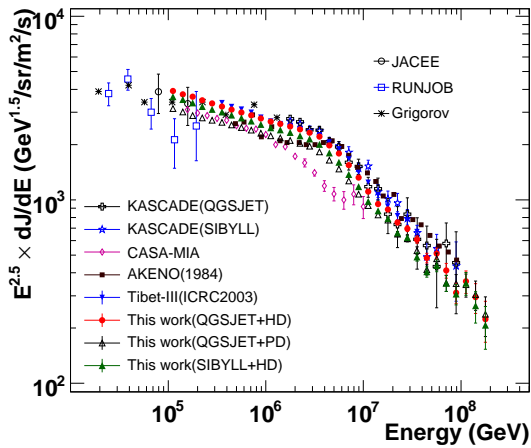


Fig. 6. From [9]. The differential energy spectra of all particles obtained by the present work using mixed composition models compared with other experiments. For the following references; JACEE (Asakimori et al. 1998), RUNJOB (Apanasenko et al. 2001), Grigorov (Grigorov et al. 1971), KASCADE (Antoni et al. 2005), CASA-MIA (Glasmacher et al. 1999), AKENO(1984) (Nagano et al. 1984), Tibet-III(ICRC2003) (Amenomori et al. 2003a), see [9].

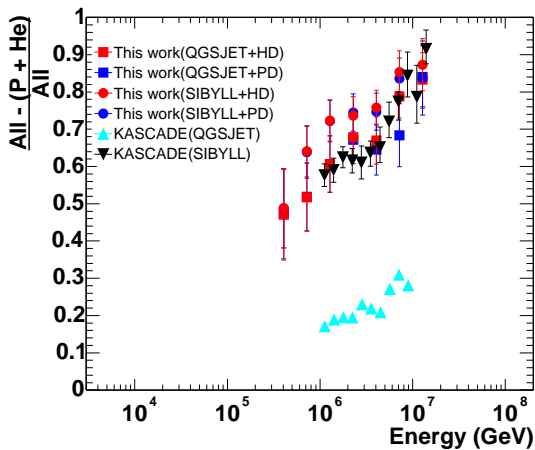


Fig. 7. From [1]. Primary (all-particle - (proton+helium)) / all-particle flux ratio in the knee energy region, assuming the QGSJET and SIBYLL hadronic interaction models (two extreme cases).

shower energy determination.

We observed the shadowing of galactic cosmic rays in the direction of the Moon, what we call the Moon's shadow. As almost all the cosmic rays are positively charged, they are bent by the geomagnetic field, thereby shifting the Moon's shadow westward. Cosmic rays will also produce a shadow additionally in the eastward direction of the Moon, if they contain negatively charged

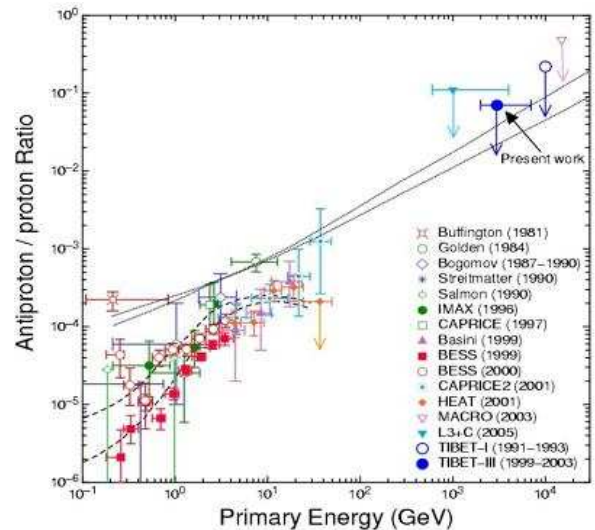


Fig. 8. From [5]. The antiproton/proton ratio at the atmosphere.

particles, such as antiprotons, according to their fraction. We selected 1.5×10^{10} air shower events with energy beyond 3 TeV approximately from the dataset accumulated by the Tibet air shower array. With the dataset, we detected the Moon's shadow at $\sim 40\sigma$ level. The center of the Moon was in the direction away from its apparent center of the Moon by 0.23° to the west. Comparison between the Moon's shadow data and a full Monte Carlo simulation enables us to search for the existence of the shadow produced by antiprotons at multi-TeV energies. We found no evidence for the existence of antiprotons in this energy region. As is shown in Fig. 8, we set an upper limit of 7 % on the flux ratio of antiprotons to protons at the 90 % confidence level in the multi-TeV energy region[5].

Cosmic-ray anisotropy in the multi-TeV region with high precision

The 2-dimensional anisotropy in the equatorial coordinates are obtained with high-precision [2] in the multi-TeV energy range, thanks to high statistics, as shown in Fig. 9. The "Tail-in" (hump) and "Loss-cone" (dip) structures are impressive. We find that the observed anisotropy tends to be faint over 300 TeV region. This implies that cosmic rays corotate with our galaxy.

Furthermore, we discovered a very interesting large-scale excess in the Cygnus region, as shown in Fig. 9a)&b), although we cannot judge currently whether it is caused by gamma rays and/or a local

cosmic-ray anisotropy. Meanwhile, The Milagro group capable of hadron/gamma-ray discrimination claimed detection of TeV diffuse gamma-ray signal in the Cygnus region along the galactic plane¹. The estimated flux may be plotted under the Tibet-III sensitivity by a factor of 3 approximately.

A closer view of the Cygnus region shows the large-scale excess is composed of a few spatially separated excesses with a smaller scale ($\sim 2^\circ$), as shown in Fig. 9e). Some of them were later confirmed by the Milagro experiment as gamma-ray emitting sources.

We also model the observed two-dimensional cosmic-ray anisotropy at sidereal time frame[17]. The relative intensity map obtained in $5^\circ \times 5^\circ$ pixels is modeled in terms of two components as:

$$RI_{n,m} = RI_{n,m}^{GA} + RI_{n,m}^{MA}, \quad (1)$$

where $RI_{n,m}^{GA}$ and $RI_{n,m}^{MA}$, respectively, denote the relative intensities of the Global Anisotropy (GA) and the Midscale Anisotropy (MA) of the (n, m) pixel in the equatorial coordinate system. The model gives a reasonable fit to the data[17].

Another interesting cosmic-ray anisotropy is the one at solar time frame. The cosmic-ray anisotropy at solar time frame due to terrestrial orbital motion of the Earth (i.e. Compton Getting anisotropy of the order of $\sim 0.01\%$) was also measured with high-precision by the Tibet air shower array[8]. The amplitude of the Compton-Getting (CG) anisotropy $\Delta I/I$ contains the power-law index of the cosmic-ray energy spectrum:

$$\Delta I/I = (\alpha + 2)(v/c)\cos\theta, \quad (2)$$

where I denotes the cosmic-ray intensity, α the power-law index of the cosmic-ray energy spectrum, v the orbital velocity of the Earth, c the speed of light in vacuum, and θ the angle between the arrival direction of cosmic-rays and the moving direction of the observer. Based on this relation and with the Tibet air-shower array data shown in Fig. 10, we measure the cosmic-ray spectral index to be $-3.03 \pm 0.55_{stat} \pm 0.62_{syst}$ between 6 TeV and 40 TeV, consistent with -2.7 from direct energy spectrum measurements. Potentially, this CG anisotropy analysis can be utilized to confirm the astrophysical origin of the ‘‘knee’’ against

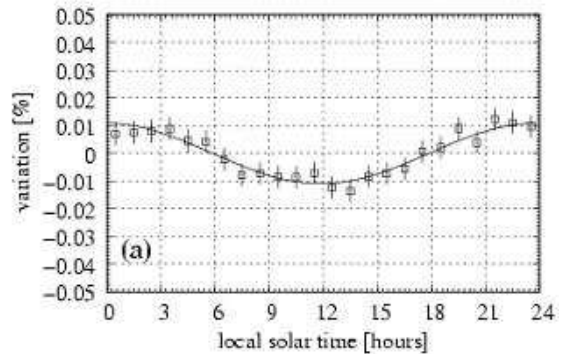


Fig. 10. From [8]. The differential variation of relative CR intensity in the local solar time. The solid lines are the sinusoidal curves best fitted to the data. The error bars are statistical only. For more detail, see [8].

models for non-standard hadronic interactions in the atmosphere.

Global 3-dimensional structure of the solar and interplanetary magnetic fields by observing the Sun’s shadow in cosmic rays

The Tibet air shower array is very powerful to get new information on the relation between time variation of the large-scale structure of the solar and interplanetary magnetic fields and the solar activities by the sun’s shadow in cosmic rays, since high-statistics data taken by the Tibet air shower array can follow up the movement of the Sun’s shadow at every one-two months. The depth and displacement of the center position in the Sun’s shadow are expected to have an anti-correlation with the 11-year-period solar activities which affect the solar and interplanetary magnetic fields, as the charged cosmic rays are bent by them.

A clear solar-cycle variation of the Sun’s shadow in 10 TeV cosmic rays are observed by the Tibet air shower array covering a full solar cycle from 1996 to 2009, as is shown in Fig. 11

Numerical simulations of the Sun’s shadow are developed, employing the Potential Field Source Surface (PFSS) model and the Current Sheet Source Surface (CSSS) model for the coronal magnetic field, to interpret the physical implications of the observed solar cycle variation. It is found that the intensity deficit in the simulated Sun’s shadow is very sensitive to the coronal magnetic field structure, and the observed variation of the Sun’s shadow is better reproduced by the CSSS model than the

*1 R. Atkins et al., Phys. Rev. Lett. 95, 251103 (2005)

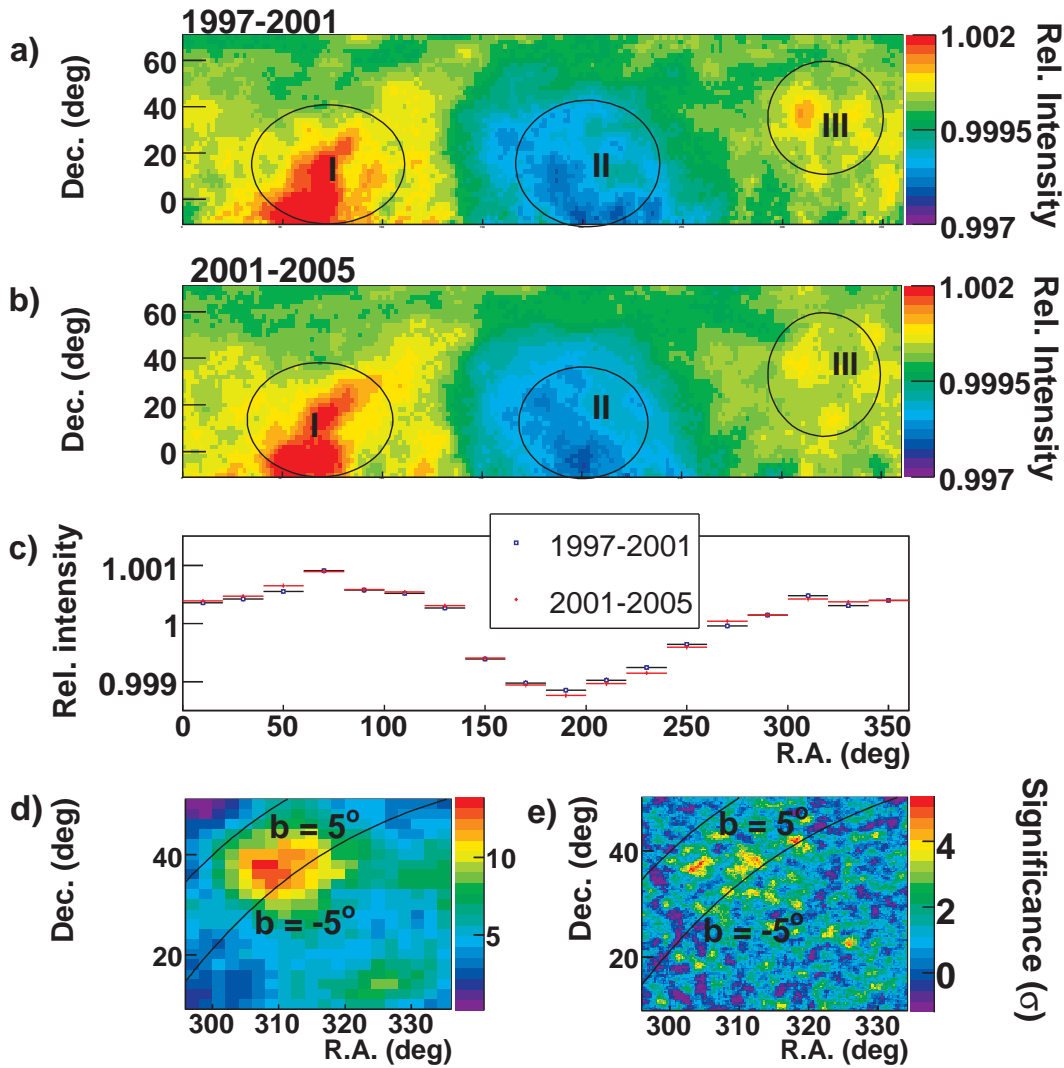


Fig. 9. From [2]. Two-dimensional relative intensity map of multi-TeV cosmic-ray anisotropy at sidereal time frame, a) for data taken from 1996 to 2001, b) for data from 2001 to 2005. The circled regions labeled by I, II and III are tail-in, loss cone and newly discovered anisotropy around the Cygnus region, respectively. c) The one-dimensional projection of a) and b). d) and e) show the significance maps around the Cygnus region, where the pixel size in e) is 0.9° sampled over square grids with 0.25° window.

PFSS model, as is shown in Fig. 12. This is the first successful attempt to evaluate the coronal magnetic field models by means of the Sun's shadow observed in 10 TeV cosmic rays .

Future Plans

Chemical composition of primary cosmic rays making the knee in the all-particle energy spectrum

We have measured the energy spectra of primary cosmic-ray protons, heliums, all particles around the knee energy region. The main component responsible for making the knee structure in the all particle energy spectrum is heavier nuclei than helium. The next step is to identify the chemical component making the knee in the all particle energy

spectrum. We have a plan to install an Yangbajing Air shower Core detector array (YAC) around the center of Tibet III to distinguish the chemical component making the knee. We set up YAC2 (~ 100 detectors over $\sim 1000\text{m}^2$ in area) in 2012 to mainly study the energy spectra of proton and helium components in the knee energy region. Currently, we are planning to set up YAC3 (~ 400 detectors over $\sim 5000\text{m}^2$ in area) to measure the iron flux in the knee energy region.

Gamma-ray astronomy in the 100 TeV region

We have a plan[14] to construct a large ($\sim 10,000\text{ m}^2 \times 1.5\text{m}$ deep) underground ($\sim 2.5\text{ m}$ soil+concrete overburden) water Cherenkov muon detector array (Tibet MD) around an extended ver-

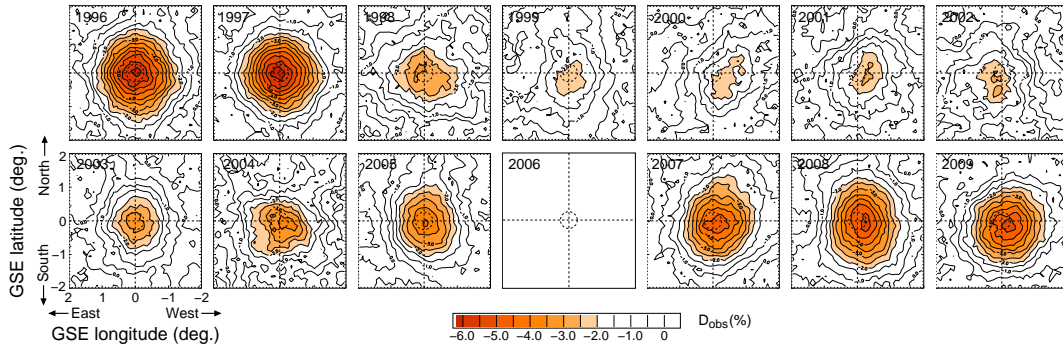


Fig. 11. Year-to-year variation of the observed Sun's shadow between 1996 and 2009. Each panel displays a 2 dimensional contour map of the observed flux deficit (D_{obs}) due to the Sun's shadow as a function of GSE longitude and latitude (horizontal and vertical axes, respectively). The map in 2006 is omitted because of insufficient statistics for drawing a map.

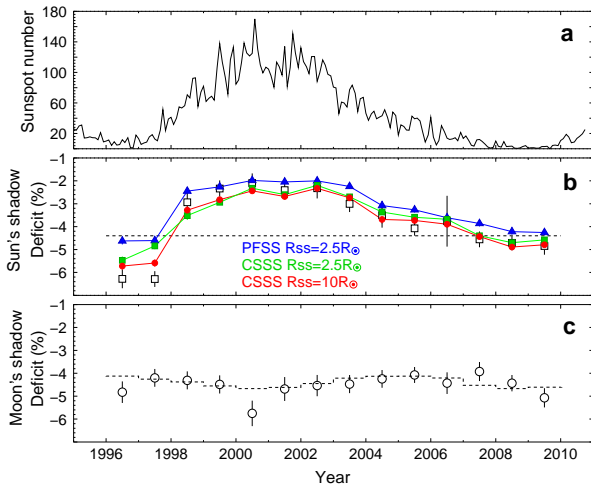


Fig. 12. Yearly variation of (a) sunspot numbers, (b) the deficit intensity in the Sun's shadow and (c) the deficit intensity in the Moon's shadow. The open squares in the panel (b) are the observed central deficit (D_{obs}) by the Tibet air shower array. The blue triangles, green squares and red circles indicate the central deficits (D_{MC}) by the MC simulations assuming the PFSS ($R_{ss} = 2.5R_{\odot}$), the CSSS ($R_{ss} = 2.5R_{\odot}$) and the CSSS ($R_{ss} = 10.0R_{\odot}$) models, respectively. The dashed lines in the panels (b) and (c) are the deficits expected from the apparent angular size of the Sun and the Moon.

sion (Tibet AS, $\sim 83,000 \text{ m}^2$) of Tibet III. By Tibet AS + MD, we aim at background-free detection of celestial point-source gamma rays in the 100 TeV region (10 TeV – 1000 TeV) with world-best sensitivity and at locating the origins of cosmic rays accelerated up to the knee energy region in the northern sky. The measurement of cut off energies in the energy spectra of such gamma rays in the 100 TeV region may contribute significantly to understanding of the cosmic-ray acceleration limit at SNRs. Search for extremely diffuse gamma-ray sources by Tibet AS + MD, for example, from the galactic

plane or from the Cygnus region may be very intriguing as well. Above 100 TeV, the angular resolution of Tibet AS with 2-steradian wide field of view is 0.2° and the hadron rejection power of Tibet MD is 1/10000. The proposed Tibet AS + MD, demonstrated in Fig. 13, has the world-best sensitivity in the 100 TeV region, superior to HESS and HAWC above 10-20 TeV and to CTA above 30-40 TeV. HAWC in Mexico will start in a few years, competing in terms of schedule with the Tibet AS + MD. However, The Tibet AS + MD is complementary in energy to HAWC aiming at low-energy ($< 10 \text{ TeV}$) gamma-ray astronomy.

In addition to unknown point-like sources, we expect to detect established sources in the 100 TeV region: TeV J2032+4130, HESS J1837-069, Crab, MGRO J2019+37, MGRO J1908+06, Milagro candidate sources, Mrk421, Mrk501 are sufficiently detectable and Cas A, HESS J1834-087, LS I+63 303, IC443 and M87 are marginal.

Furthermore, our integral flux sensitivity to diffuse gamma rays will be the world-best as well. The diffuse gamma rays from the Cygnus region reported by the Milagro group and also diffuse gamma-rays from the galactic plane will be clearly detected. Diffuse gamma-rays of extragalactic origin may be an interesting target as well.

In addition to gamma-ray astronomy, the MD will play an important role in measuring the chemical composition of cosmic-ray energy spectrum in the knee energy region. As an iron nucleus gives approximately 3 times as many muons as a proton, we can group the chemical composition into several groups of nuclei. This is a complementary approach to the YAC experiment which separates nuclear species by the air shower core distri-

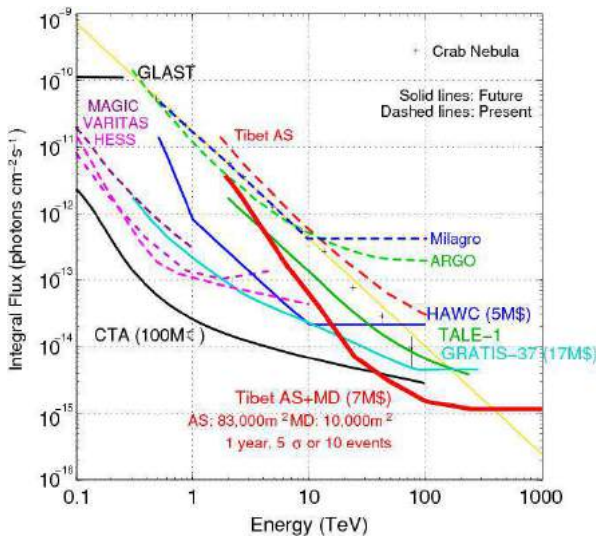


Fig. 13. Tibet AS + MD (red curve) integral flux sensitivity (5σ or 10 events/1yr) for a point source.

Contributions of the electromagnetic component induced by cosmic rays. Thanks to the altitude of the Tibet AS γ experiment, we can measure cosmic rays down to a few TeV where the chemical composition of cosmic rays has been measured by various direct measurements. This uniquely allows us to tune the hadronic interaction models which seriously affects various muon distributions in a cosmic-ray induced air showers, decoupling the chemical composition ambiguity in the knee energy region.

In fall, 2007, a prototype underground muon detector, composed of two 52m² water pools, was successfully constructed in Tibet to demonstrate the technical feasibility, cost estimate, validity of our Monte Carlo simulation. Data analyses demonstrate that our MC simulation reproduces real data quite reasonably.

In 2010, construction of 5/12 of the full-scale MD started and the concrete-based water pools were successfully completed. The remaining works are under way.

Summary

During the period from 2006 to 2012, the Tibet AS γ experiment contributed significantly to the cosmic-ray physics field in various aspects, thanks to unique features of the Tibet air shower array located at 4300 m above sea level, Yangbajing, Tibet, in China. Some part of the next plan, i.e., the Tibet AS+MD+YAC project has been funded and under construction now. We are looking forward to new results from the part (hopefully full scale) of the Ti-

bet AS+MD+YAC project during the forthcoming 6 years.

THE TIBET AS γ COLLABORATION

Spokespersons:

Masato Takita (ICRR),

Hongbo Hu (IHEP, Beijing)

Institute	Country	(*)
ICRR, Univ. of Tokyo	Japan	5
Hirosaki Univ.	Japan	2
Institute of High Energy Physics	China	25
Hebei Normal Univ.	China	2
Tibet Univ.	China	8
Shandong Univ.	China	5
SouthWest Jiaotong Univ.	China	4
Kanagawa Univ.	Japan	4
Utsunomiya Univ.	Japan	1
Konan Univ.	Japan	3
Waseda Univ.	Japan	3
Yokohama National Univ.	Japan	3
Shinshu Univ.	Japan	3
Shandong Agriculture Univ.	China	1
Saitama Univ.	Japan	1
National Institute of Informatics	Japan	1
Sakushin Gakuin Univ.	Japan	1
Tokyo Metropolitan College of Industrial Technology	Japan	1
Max-Planck-Institut für Physik	Germany	1
Nihon Univ.	Japan	1
Shonan Institute of Technology	Japan	1
RIKEN	Japan	1
Total		77

(*) Number of participants as of February 2012.

Members

Staffs

Masato Takita, Associate Professor, February 2001 to the present

Munehiro Ohnishi, Research Associate, April 1993 to the present

Takahide Kobayashi, Technical Staff, from 1967 to the present

Postdoctoral Fellows

Atsushi Shiomi, from April 1999 to March 2008
 Kazumasa Kawata, from April 2002 to March 2012
 Jing Huang, from July 2003 to December 2008
 Zhitao Yan, from May 2005 to May 2007
 Xiao Wang, from October 2005 to October 2007
 Ding Chen, from November 2008 to April 2012

Graduate Students

One student was awarded a doctor degree and 6 students earned master degrees during 2006–2012, supervised by ICRR staff members.

List of Publications

Papers in Refereed Journals

- [1] “Are protons still dominant at the knee of the cosmic-ray energy spectrum?”, M. Amenomori *et al.*, *Physics Letters*, **B632**, 58-64 (2006).
- [2] “Anisotropy and Corotation of Galactic Cosmic Rays”, M. Amenomori *et al.*, *Science*, **314**, 439-443 (2006).
- [3] “Variation of Sun shadow in the solar cycle 23 observed with the Tibet air shower array”, M. Amenomori *et al.*, *Advances in Space Research*, **38**, 936-941 (2006).
- [4] “Underground water Cherenkov muon detector array with the Tibet air shower array for gamma-ray astronomy in the 100 TeV region”, M. Amenomori *et al.*, *Astrophysics and Space Science*, **309**, 435-439 (2007).
- [5] “Moon Shadow by Cosmic Rays under the Influence of Geomagnetic Field and Search for Antiprotons at Multi-TeV Energies”, M. Amenomori *et al.*, *Astroparticle Physics*, **28**, 137-142 (2007).
- [6] “Implication of the sidereal anisotropy of ~ 5 TeV cosmic ray intensity observed with the Tibet III air shower array”, M. Amenomori *et al.*, *AIP Conf. Proc.*, **932**, 283-289 (2007).
- [7] “A solar neutron telescope in Tibet and its capability examined by the 1998 November 28th event”, Y. Muraki *et al.*, *Astroparticle Physics*, **28**, 119-131 (2007).
- [8] “New Estimation of the Spectral Index of High-Energy Cosmic Rays as Determined by the Compton-Getting Anisotropy”, M. Amenomori *et al.*, *ApJL*, **672**, L53-L56 (2008).
- [9] “The all-particle spectrum of primary cosmic rays in the wide energy range from 10^{14} eV to 10^{17} eV observed with the Tibet-III air-shower array”, M. Amenomori *et al.*, *ApJ*, **678**, 1165-1179 (2008).
- [10] “The energy spectrum of all-particle cosmic rays around the knee region observed with the Tibet-III air-shower array”, M. Amenomori *et al.*, *Advances in Space Research*, **42**, 467-472 (2008).
- [11] “Multi-TeV Gamma-Ray Observation from the Crab Nebula Using the Tibet-III Air Shower Array Finely Tuned by the Cosmic-Ray Moon’s Shadow”, M. Amenomori *et al.*, *ApJ*, **692**, 61-72 (2009).
- [12] “Chemical Composition of Cosmic Rays around the Knee Observed by the Tibet Air Shower-Core Detector”, M. Amenomori *et al.*, *J. Phys. Soc. Jpn*, **78**, 206-209 (2009).
- [13] “Recent results on gamma-ray observation by the Tibet air shower array and related topics”, M. Amenomori *et al.*, *J. Phys. Soc. Jpn*, **78**, 88-91 (2009).
- [14] “Exploration of a 100 TeV gamma-ray northern sky using the Tibet air-shower array combined with an underground water-Cherenkov muon-detector array”, T.K. Sako *et al.*, *Astroparticle Physics*, **32**, 177-184 (2009).
- [15] “Observation of TeV Gamma Rays from the Fermi Bright Galactic Sources with the Tibet Air Shower Array”, M. Amenomori *et al.*, *ApJL*, **709**, L6-L10 (2010).
- [16] “On Temporal Variations of the Multi-TeV Cosmic Ray Anisotropy Using the Tibet III Air Shower Array”, M. Amenomori *et al.*, *ApJ*, **711**, 119-124 (2010).
- [17] “Heliospheric signatures seen in the sidereal anisotropy of high-energy galactic cosmic ray intensity”, M. Amenomori *et al.*, *AIP Conf. Proc.*, **1302**, 285-290 (2010).

- [18] “Cosmic-ray energy spectrum around the knee observed with the Tibet air-shower experiment”, M. Amenomori *et al.*, *Astrophysics and Space Sciences Transactions*, **7**, 15-20 (2011).
- [19] “Observation of the Fermi pulsar catalog at TeV energies with the Tibet air shower experiment”, M. Amenomori *et al.*, *Astrophysics and Space Sciences Transactions*, **7**, 211-215 (2011).
- [20] “Cosmic-ray energy spectrum around the knee obtained by the Tibet experiment and future prospects”, M. Amenomori *et al.*, *Advances in Space Research*, **47**, 629-639 (2011).
- Papers in Conference Proceedings**
- [21] “Primary cosmic-ray energy spectrum around the knee energy region measured by the Tibet hybrid experiment”, M. Amenomori *et al.*, *Physics at the End of Cosmic Ray Spectrum*, *Journal of Physics: Conference Series* **47** pp 51-58 (2006).
- [22] “Tibet Air Shower Array: Results and Future Plan”, M. Amenomori *et al.*, *TAUP2007*, *Journal of Physics: Conference Series* **120** 062024 pp 1-3 (2008).
- [23] “A large underground water Cherenkov muon detector array with the Tibet air shower array for the gamma-ray astronomy in the 100 TeV region: detector design and simulation”, M. Amenomori *et al.*, *ISVHECR2006*, *Nuclear Physics B (Proc. Suppl.)* vol. 175-176, pp 480-483 (2008).
- [24] “A large underground water Cherenkov muon detector array with the Tibet air shower array for the gamma-ray astronomy in the 100 TeV region: Overview and physics goal”, M. Amenomori *et al.*, *ISVHECR2006*, *Nuclear Physics B (Proc. Suppl.)* vol. 175-176, pp 476-479 (2008).
- [25] “Northern Sky Survey for Gamma-ray Point Sources in 100 TeV Region with the Tibet Air Shower Array”, M. Amenomori *et al.*, *ISVHECR2006*, *Nuclear Physics B (Proc. Suppl.)* vol. 175-176, pp 431-434 (2008).
- [26] “Spectral index of high-energy cosmic rays by the Compton-Getting effect at solar time frame with the Tibet air shower array”, M. Amenomori *et al.*, *ISVHECR2006*, *Nuclear Physics B (Proc. Suppl.)* vol. 175-176, pp 427-430 (2008).
- [27] “The cosmic-ray energy spectrum around the knee measured by the Tibet-III air-shower array”, M. Amenomori *et al.*, *ISVHECR2006*, *Nuclear Physics B (Proc. Suppl.)* vol. 175-176, pp 318-321 (2008).
- [28] “Cosmic ray data and their interpretation: about the Tibet Air Shower Array-Chemical Composition of Cosmic Rays at the Knee Viewed from the Tibet Air Shower Experiment”, M. Shibata for the Tibet ASgamma experiment, *ISVHECR2006*, *Nuclear Physics B (Proc. Suppl.)* vol. 175-176, pp 318-321 (2008).
- [29] “Analysis of primary cosmic ray proton and helium components at the knee energy region with the Tibet hybrid experiment”, M. Amenomori *et al.*, *Proceedings in the 30th International Cosmic Ray Conference*, (3-11 July 2007, Merida, Mexico), vol. 2, pp 112-120 (2008).
- [30] “Chemical composition of cosmic rays at the knee measured by the Tibet air-shower-core detector”, M. Amenomori *et al.*, *Proceedings in the 30th International Cosmic Ray Conference*, (3-11 July 2007, Merida, Mexico), vol. 2, pp 121-124 (2008).
- [31] “Chemical composition of cosmic rays at the knee measured by the Tibet air-shower-core detector”, M. Amenomori *et al.*, *Proceedings in the 30th International Cosmic Ray Conference*, (3-11 July 2007, Merida, Mexico), vol. 2, pp 121-124 (2008).
- [32] “Future plan for observation of cosmic gamma rays in the 100 TeV energy region with the Tibet air shower array : physics goal and overview”, M. Amenomori *et al.*, *Proceedings in the 30th International Cosmic Ray Conference*, (3-11 July 2007, Merida, Mexico), vol. 2, pp 353-356 (2008).
- [33] “Future plan for observation of cosmic gamma rays in the 100 TeV energy region with the

- Tibet air shower array : simulation and sensitivity”, M. Amenomori *et al.*, Proceedings in the 30th International Cosmic Ray Conference, (3-11 July 2007, Merida, Mexico), vol. 2, pp 357-360 (2008).
- [34] “A search for 100 TeV celestial gamma rays with the Tibet air shower array and a future prospect”, M. Amenomori *et al.*, Proceedings in the 30th International Cosmic Ray Conference, (3-11 July 2007, Merida, Mexico), vol. 2, pp 575-578 (2008).
- [35] “Seven-year observation of multi-TeV gamma rays from the Crab Nebula with the Tibet air shower array”, M. Amenomori *et al.*, Proceedings in the 30th International Cosmic Ray Conference, (3-11 July 2007, Merida, Mexico), vol. 2, pp 799-802 (2008).
- [36] “Search for pulsed multi-TeV gamma rays from the Crab pulsar with the Tibet III air shower array”, M. Amenomori *et al.*, Proceedings in the 30th International Cosmic Ray Conference, (3-11 July 2007, Merida, Mexico), vol. 2, pp 783-786 (2008).
- [37] “Gamma-hadron separation of parent particles of air showers above several 10 TeV energies using Tibet-III air-shower array”, M. Amenomori *et al.*, Proceedings in the 30th International Cosmic Ray Conference, (3-11 July 2007, Merida, Mexico), vol. 2, pp 583-583 (2008).
- [38] “Study of discrimination between cosmic gamma rays and protons at multi-TeV energies with the Tibet air shower array”, M. Amenomori *et al.*, Proceedings in the 30th International Cosmic Ray Conference, (3-11 July 2007, Merida, Mexico), vol. 3, pp 1493-1493 (2008).
- [39] “The cosmic ray all-particle spectrum in the wide energy range from 10^{14} eV to 10^{17} eV observed with the Tibet-III air shower array”, M. Amenomori *et al.*, Proceedings in the 30th International Cosmic Ray Conference, (3-11 July 2007, Merida, Mexico), vol. 4, pp 103-106 (2008).
- [40] “Zenith angle dependence of the size spectrum of air showers around the knee observed with the Tibet air shower array”, M. Amenomori *et al.*, Proceedings in the 30th International Cosmic Ray Conference, (3-11 July 2007, Merida, Mexico), vol. 4, pp 99-102 (2008).
- [41] “Sun’s Shadow in the Solar Cycle 23 Observed with the Tibet Air Shower Array and Comparison with Simulation Studies”, M. Amenomori *et al.*, Proceedings in the 30th International Cosmic Ray Conference, (3-11 July 2007, Merida, Mexico), vol. 5, pp 529-532 (2008).
- [42] “Implication of the sidereal anisotropy of ~ 10 TeV cosmic ray intensity observed with the Tibet III air shower array”, M. Amenomori *et al.*, Proceedings in the 30th International Cosmic Ray Conference, (3-11 July 2007, Merida, Mexico), vol. 5, pp 593-596 (2008).
- [43] “Study on TeV gamma Ray Emission from Cygnus Region Using the Tibet Air Shower”, M. Amenomori *et al.*, Proceedings in the 30th International Cosmic Ray Conference, (3-11 July 2007, Merida, Mexico), vol. 2, pp 695-698 (2008).
- [44] “Two-dimensional observation on TeV Cosmic-ray solar diurnal variation using the Tibet Air Shower Array”, M. Amenomori *et al.*, Proceedings in the 30th International Cosmic Ray Conference, (3-11 July 2007, Merida, Mexico), vol. 5, pp 577-580 (2008).
- [45] “The study of Periodic Variation of Cosmic Ray intensity with the Tibet III Air Shower Array”, Li A. F. *et al.* for the Tibet ASgamma collaboration, Proceedings in the 30th International Cosmic Ray Conference, (3-11 July 2007, Merida, Mexico), vol. 1, pp 609-612 (2008).
- [46] “A Monte Carlo study to measure the energy spectra of the primary heavy components at the knee using a new Tibet AS core detector array and a large underground muon detector array”, J. Huang *et al.* for the Tibet ASgamma collaboration, Proceedings in the 30th International Cosmic Ray Conference, (3-11 July 2007, Merida, Mexico), vol. 2, pp 329-332 (2008).
- [47] “A northern sky survey for PeV gamma rays using the Tibet air shower array with

- water-Cherenkov-type underground muon detectors”, M. Amenomori *et al.*, Proceedings in the 31st International Cosmic Ray Conference, (7-15 July 2009, Lodz, Poland), ID=293, (2009).
- [48] “Tibet AS+MD Project”, M. Amenomori *et al.*, Proceedings in the 31st International Cosmic Ray Conference, (7-15 July 2009, Lodz, Poland), ID=297, (2009).
- [49] “Demonstration of hadronic cosmic-ray rejection power by a water Cherenkov underground muon detector with the Tibet air shower array”, M. Amenomori *et al.*, Proceedings in the 31st International Cosmic Ray Conference, (7-15 July 2009, Lodz, Poland), ID=810, (2009).
- [50] “Interpretation of the cosmic-ray energy spectrum and the knee inferred from the Tibet air-shower experiment”, M. Amenomori *et al.*, Proceedings in the 31st International Cosmic Ray Conference, (7-15 July 2009, Lodz, Poland), ID=294, (2009).
- [51] “Large-scale sidereal anisotropy of multi-TeV galactic cosmic rays and the heliosphere”, M. Amenomori *et al.*, Proceedings in the 31st International Cosmic Ray Conference, (7-15 July 2009, Lodz, Poland), ID=296, (2009).
- [52] “New estimation of the power-law index of the cosmic-ray energy spectrum as determined by the Compton-Getting anisotropy at solar time frame”, M. Amenomori *et al.*, Proceedings in the 31st International Cosmic Ray Conference, (7-15 July 2009, Lodz, Poland), ID=303, (2009).
- [53] “Sun’s Shadow in changing phase from the Solar Cycle 23 to 24 Observed with the Tibet Air Shower Array”, M. Amenomori *et al.*, Proceedings in the 31st International Cosmic Ray Conference, (7-15 July 2009, Lodz, Poland), ID=751, (2009).
- [54] “About the cosmic-ray energy spectrum around the knee”, M. Shibata, Proceedings in the 31st International Cosmic Ray Conference, (7-15 July 2009, Lodz, Poland), (2009).
- [55] “The sidereal anisotropy of multi-TeV cosmic rays in an expanding Local Interstellar Cloud”, Y. Mizoguchi *et al.*, Proceedings in the 31st International Cosmic Ray Conference, (7-15 July 2009, Lodz, Poland), ID=388, (2009).
- [56] “The TIBET AS+MD Project; progress report 2011”, M. Amenomori *et al.*, Proceedings in the 32nd International Cosmic Ray Conference, (11-18 August 2011, Beijing, China), ID=351, (2011).
- [57] “Correlation between Solar Activity and the Sun’s Shadow Observed by the Tibet Air Shower Array”, M. Amenomori *et al.*, Proceedings in the 32nd International Cosmic Ray Conference, (11-18 August 2011, Beijing, China), ID=352, (2011).
- [58] “Air-shower core detector array to study the mass composition of cosmic rays beyond 100 TeV by Tibet hybrid experiment”, M. Amenomori *et al.*, Proceedings in the 32nd International Cosmic Ray Conference, (11-18 August 2011, Beijing, China), ID=356, (2011).
- [59] “Modeling of the galactic cosmic-ray anisotropy at TeV energies”, M. Amenomori *et al.*, Proceedings in the 32nd International Cosmic Ray Conference, (11-18 August 2011, Beijing, China), ID=361, (2011).
- [60] “Time Dependence of Loss Cone Amplitude measured with the Tibet Air-shower Array”, M. Amenomori *et al.*, Proceedings in the 32nd International Cosmic Ray Conference, (11-18 August 2011, Beijing, China), ID=379, (2011).
- [61] “Observation of atmospheric charged particles associated with thunderstorms at Tibet”, M. Amenomori *et al.*, Proceedings in the 32nd International Cosmic Ray Conference, (11-18 August 2011, Beijing, China), ID=497, (2011).
- [62] “Observation of Sub-PeV Gamma Rays from the Galactic Plane Using the Tibet Air Shower Array”, M. Amenomori *et al.*, Proceedings in the 32nd International Cosmic Ray Conference, (11-18 August 2011, Beijing, China), ID=748, (2011).

- [63] “Variability of TeV Gamma-ray Flux from the Crab Nebula with the Tibet Air Shower Array”, M. Amenomori *et al.*, Proceedings in the 32nd International Cosmic Ray Conference, (11-18 August 2011, Beijing, China), ID=786, (2011).
- [64] “Tibet AS+MD detector simulation using GEANT4”, M. Amenomori *et al.*, Proceedings in the 32nd International Cosmic Ray Conference, (11-18 August 2011, Beijing, China), ID=1058, (2011).
- [65] “On temporal variations of the multi-TeV cosmic ray anisotropy using the Tibet III Air Shower Array”, M. Amenomori *et al.*, Proceedings in the 32nd International Cosmic Ray Conference, (11-18 August 2011, Beijing, China), ID=1167, (2011).
- [66] “Study of the large Tyvek bag technique for the water Cherenkov detector in TIBET AS+MD”, M. Amenomori *et al.*, Proceedings in the 32nd International Cosmic Ray Conference, (11-18 August 2011, Beijing, China), ID=1168, (2011).
- [67] “Calibration of the Yangbajing air-shower core detector (YAC) using the beam of BEPC”, M. Amenomori *et al.*, Proceedings in the 32nd International Cosmic Ray Conference, (11-18 August 2011, Beijing, China), ID=1217, (2011).
- [68] “Test of the hadronic interaction models at around 10 TeV with Tibet EAS core data”, M. Amenomori *et al.*, Proceedings in the 32nd International Cosmic Ray Conference, (11-18 August 2011, Beijing, China), ID=1238, (2011).
- [69] “A Monte Carlo study to measure the energy spectra of the primary proton and helium components at the knee using a new Tibet AS core detector array”, M. Amenomori *et al.*, Proceedings in the 32nd International Cosmic Ray Conference, (11-18 August 2011, Beijing, China), ID=1239, (2011).
- [70] “Measurement of some properties of EAS-cores using new air-shower core detectors array developed for the Tibet hybrid experiment”, M. Amenomori *et al.*, Proceedings in the 32nd International Cosmic Ray Conference, (11-18 August 2011, Beijing, China), ID=1241, (2011).
- [71] “The forward particle production in the energy range of 10^{15} eV as seen with the Tibet hybrid experiment”, M. Amenomori *et al.*, Proceedings in the 32nd International Cosmic Ray Conference, (11-18 August 2011, Beijing, China), ID=1251, (2011).
- [72] “TeV Gamma Ray Survey on the Direction of Fermi-LAT Pulsars with the Tibet Air Shower Array”, M. Amenomori *et al.*, Proceedings of the First Session of the Sant Cugat Forum on Astrophysics, (12-16 April 2010, Sant Cugat, Spain), Spriger, ed. by Nanda Rea and Diego F. Torres, pp491-495 (2011).

HIGH ENERGY ASTROPHYSICS GROUP

Introduction

Group History

The high energy astrophysics group was created recently in December 2009. The first $2\frac{1}{3}$ fiscal years of the group (December 2009 - March 2012) were devoted for the start up of the research activity. Since April 2012, two postdoctoral fellows have joined and contributed to widen the coverage of the research areas by the group. From April 2013 a new Assistant Professor position will be made available for this group by the administration of the University of Tokyo. The selection procedure for this position is now under way.

Science Targets

The high energy astrophysics group aims at making theoretical and observational studies of violent astrophysical phenomena in which nonthermal cosmic ray particles are being accelerated. Targets of the group's study include high energy astrophysical objects such as supernova explosions/shocks, neutron star (NS) magnetospheres, giant flares and repeating bursts of magnetars, relativistic jets from black holes (BH), which are expected to exist in the center of active galactic nuclei (AGN) and mysterious gamma ray bursts (GRB). In addition, studies have been made also for nonthermal phenomena within the heliosphere [19, 20], such as interplanetary shocks and the earth's bow shock, magnetic reconnection, the interaction processes between the solar wind and the lunar surface. While these heliospheric phenomena are limited in their energy coverage, their studies have been proved to give a theoretical basis to interpret distant high energy phenomena. For example, Hillas' well known argument¹ about the origin of ultra high energy cosmic rays is that the maximum energy E_{\max} of particles of charge Ze accelerated in the region with a characteristic plasma velocity v , a magnetic field B , and a spatial scale L , is regulated by a simple relation,

$$E_{\max} = ZevBL \quad (1)$$

We see in Figure 1 (from [20]) that in various heliospheric regions there is close agreement between

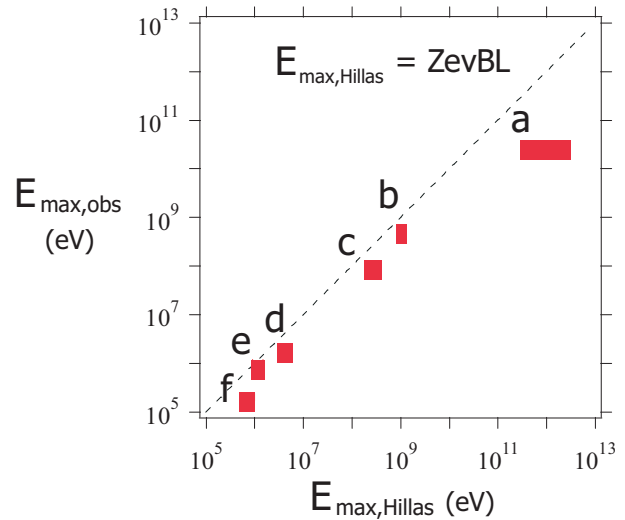


Fig. 1. Heliospheric Hillas' relation. The horizontal and vertical axes show E_{\max} expected from the Hillas relation and E_{\max} from observations from a: solar flares, b: the Van Allen belt of the earth, c: heliospheric shocks, d the earth's bow shock and kinks of the interplanetary magnetic field, e: the magnetotail of the earth, and f: the foreshock region of the earth's bow shock.

theoretical values of E_{\max} from eq.(1) and the observed maximum energies. In this way, we can 'calibrate' various astrophysical formulae in the heliospheric 'laboratory'.

Reevaluation of acceleration processes

While the diffusive shock acceleration process has been accepted as the standard model of astrophysical particle acceleration, interests are being renewed on other processes such as magnetic reconnection and second-order stochastic acceleration. In [2], we have presented a new result on the contribution of the second order acceleration to the formation of the X-ray photon spectrum from GRBs. We have also performed numerical simulation of the stochastic acceleration process in a relativistic turbulence, which is created through the Kelvin-Helmholtz instability in a relativistic velocity shear layer as expected in colliding plasmas in the environments around AGNs and GRBs (Figure 2, Obi et al., in preparation).

Both in diffusive shock acceleration and second-order acceleration processes, cyclotron resonant in-

*¹ Hillas, A. M., Ann. Rev. Astron. Astrophys., **22**, 425 (1984).

interaction between particles and turbulence plays the dominant role, whose condition is given by,

$$\omega - k_{\parallel} v_{\parallel} = n \frac{\Omega_c}{\gamma} \quad (2)$$

where (ω, k_{\parallel}) define the properties of turbulence, namely the frequency and wavenumber parallel to the background magnetic field \vec{B}_0 . v_{\parallel} is the particle velocity component parallel to \vec{B}_0 , γ the Lorentz factor, and Ω_c the nonrelativistic cyclotron frequency. In eq.(2) the choice of n is named as follows: $n = +1$ the fundamental cyclotron resonance, $n = -1$ the anomalous cyclotron resonance, $n = 0$ the transit-time resonance (or Landau resonance), and $n = \pm 2, \pm 3, \dots$ the cyclotron higher harmonic resonance. Since the middle 60's when the above definitions were made, there seem to have been some confusion and misunderstanding about their interpretation. By presenting a unified review of the cyclotron resonant interaction process [16], we have contributed to clarify the interpretation.

It is noted that particle acceleration theory in astrophysics has been generally focused onto fully ionized collisionless plasmas. Only recently, the importance of the neutral component of the interstellar gas on the particle acceleration process has been noticed. To this new trend, [1] is our contribution, where the modification of the supernova shock structure as well as shock-acceleration efficiency by the pick-up interstellar neutrals is studied.

Pulsars and Magnetars

Millisecond Pulsars

A spinning magnetized neutron star (pulsar) generates huge electric fields in the magnetosphere via unipolar induction, and accelerates particles to produce electron/positron pairs. Then, almost all the spin-down energy is transferred to the outflows of relativistic electron/positron, resulting in the lepton component of cosmic rays. We study the particle acceleration in the pulsar magnetosphere and the observational verifications of them. As an example, we have shown the possibility that cosmic-ray electrons/positrons from millisecond pulsars (MSPs), which have a higher angular frequency and a lower surface magnetic field than that of canonical pulsars, may contribute significantly to the observed spectrum. Our results are shown in Figure 3 (from [22]). Recent observations suggest that the MSP

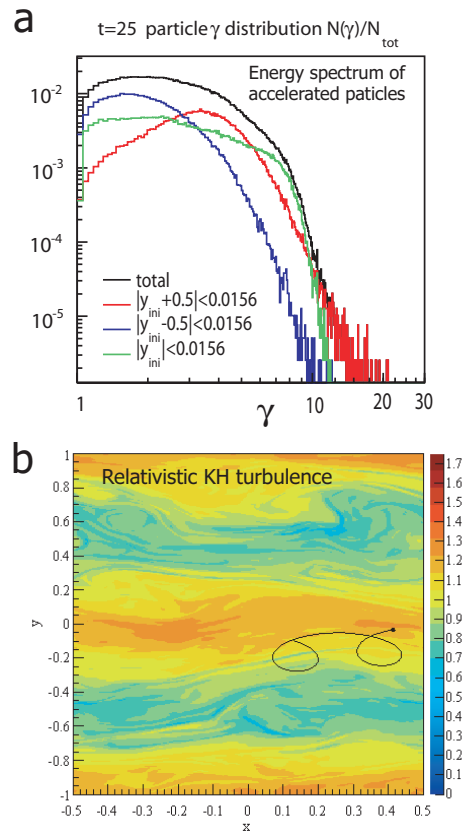


Fig. 2. Particle acceleration in a simulated turbulence in relativistic Kelvin-Helmholtz instability for the plasma layer with an initial velocity shear of $\pm 0.6c$. (a) Energy spectra of accelerated particles depend on their initial positions (blue, green, and red) with respect to the velocity shear layer, where the maximum acceleration efficiency (red) was seen for those from the layer with a maximum negative vorticity ($|\gamma + 0.5| < 0.0156$). (b) An example of the orbits of accelerated particles, superposed onto the color map of the magnetic field component B_z , shows the gradient-B drift motion within the magnetic inhomogeneity generated in the turbulence.

population is separated into two subclasses with respect to the number of ejected electrons/positrons (multiplicity). In Figure 3 (a), the electron/positron flux from multiple MSPs with low multiplicity is shown. There is a large peak at 10–50 TeV energy range. Even if the fraction of their MSPs is as small as 10 per cent, this peak would be detectable in future missions such as CALET (see the later subsection) and CTA. On the other hand, MSPs with high multiplicity are expected to contribute to the excess in the energy spectrum between 100 GeV and several TeV (Figure 3 (b)).

Crab Pulsar

Crab pulsar, the remnant of the supernova explosion in 1054 A.D., is one of the well-known neu-

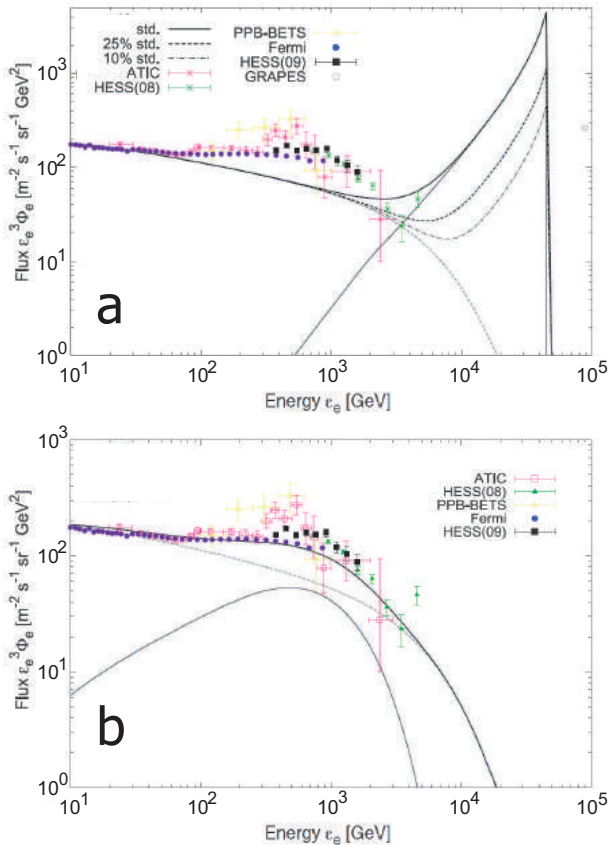


Fig. 3. (a) Predicted cosmic ray electron/positron spectrum from MSPs. A thin solid line shows the MSP contribution if 100% of MSPs are with *low* multiplicity. A thick solid line shows the total spectra, namely the sum of the MSP contribution and the background cosmic rays electron/positron. Thick-dashed and dot-dashed lines show the total spectra, if 25% and 10% of MSPs are with low multiplicity and contribute to the spectra. (b) A thin solid line shows the MSP contribution if 100% of MSPs are with *high* multiplicity. A thick solid line shows the total spectra.

tron stars. While its physical properties have been studied for more than 40 years since its discovery, there remains an enigma about the origin of giant radio pulses (GRPs). While for a long time the GRPs had been regarded as a phenomenon limited to the radio frequency pulsar emission, a 3% enhancement of the optical emission at the GRP timing was discovered recently (Shearer et al., 2003). Since only a very loose upper limit ($<250\%$) was obtained for the enhancement, if any, of the hard X-ray emission at the GRP timing², we have started a correlational study³ between the radio and hard X-ray observations collaborating with radio and X-ray astronomers at National Institute of Informa-

*² Lundgren et al., *Astrophys. J.*, **453**, 433 (1995).

*³ Nagata, K., Master thesis, Department of Physics, Tokyo Institute of Technology (2011).

tion and Communications Technology, Tokyo Institute of Technology, and Institute of Space and Astronautical Science in Japan Aerospace Exploration Agency. Figure 4 shows the preliminary result of our analysis based on the simultaneous observations of radio and X-ray signals from the Crab pulsar in three opportunities on 6 April 2010, 22 March 2011, and 1-2 September 2011. The superposed X-ray photon count rates (red dots with error bars) at the main-pulse GRP phase (180°) were marginally enhanced (by 2.9σ) above the average X-ray photon count rates obtained with normal (namely, non-giant) radio pulses (a black curve). To obtain statistically significant results, we are waiting for further opportunities of the simultaneous radio and X-ray observations to improve the photon statistics.

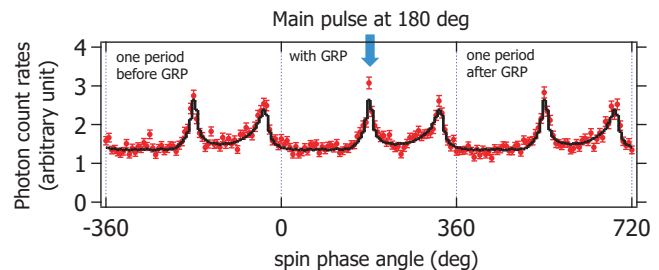


Fig. 4. A black curve shows the X-ray intensity profile (SUZAKU/HXD, 15-75 keV) superposed over the periods of normal radio pulses from the Crab pulsar. Red dots show the X-ray intensity profile superposed over three adjacent periods (from -360° to $+720^\circ$) around main-pulse GRPs (at 180°). The error bars are drawn according to the photon count statistics with 6-degree binning boxes.

Magnetars

Magnetars, slowly-rotating neutron stars with strong magnetic field of 10^{13-15} G, occasionally show giant-flare (GF) activities with peak gamma-ray luminosities reaching to 10^{47} erg s^{-1} , which are as strong as the luminosities of AGNs. The detailed physics of magnetars have been under extensive investigations both theoretically and observationally. Our previous contribution to the magnetar study was the definite determination of the peak luminosities and fluences for two GFs in 1998 and 2004 based on the GEOTAIL measurements^{4,5}. In addition we have reported the first clear detection of transient Extremely-Low-Frequency (ELF) radio waves caused by the largest-ever-known GF from the magnetar, SGR 1806-20, on 27 December 2004

*⁴ Terasawa et al., *Nature*, **434**, 1110 (2005).

*⁵ Tanaka et al., *Astrophys. J.*, **655**, L55 (2007).

(Figure 5 from [12]). Although the excitation mechanism of these ELF waves has not been uniquely identified, this provides a new monitoring method for magnetar GFs.

Along with rare GFs, magnetars show burst activities, much weaker than GFs but repeating many times. We have also discovered ionospheric disturbances caused by repeating bursts from the magnetar SGR J1550-5418 in January 2009 [10]. Such ionospheric disturbance can be used as another monitoring method for magnetar activities.

Interaction process between supersonic flow and solid objects

It is expected that the interactions between supersonic plasma flows and surfaces of solid bodies play important roles in many astrophysical environments. The nearest example found recently is in the solar-wind-moon interaction [3, 4, 5, 8, 9, 11], where detailed studies of kinetic properties of plasmas can be made.

From multi-spacecraft observation of the earth's bow shock around the moon, it is shown that the shape of the bow shock is deformed in the lunar wake region [11]. It is noted that the size of the moon ($R_M = 1738\text{km}$) is several times of the characteristic kinetic scale of the plasma (the ion gyro-radius $\sim 250\text{km}$). The above observations of the lunar perturbation on the bow shock shape teaches us that down to this spatial scale the magnetohydrodynamics description is applicable to the plasma-solid body interaction process.

On the other hand, kinetic behavior beyond the magnetohydrodynamic description is also found important: Figure 6a-f shows the time series data from SELENE, the Japanese lunar orbiter, between 12:00 and 18:00 UT on 4 April 2008, showing quiet (# 1) and active (# 3) conditions of the wake in the near-Moon space. From these observations, a new model of the near-Moon wake environment is proposed ([8], Figure 6g), where the electromagnetic acceleration of the solar wind particles and the kinetic plasma instability (two stream instability) are playing the dominant role.

R/D studies

CALET project

CALET (CALorimetric Electron Telescope, Figure 7a) is a new observatory for the International Space Station to search for signatures of dark

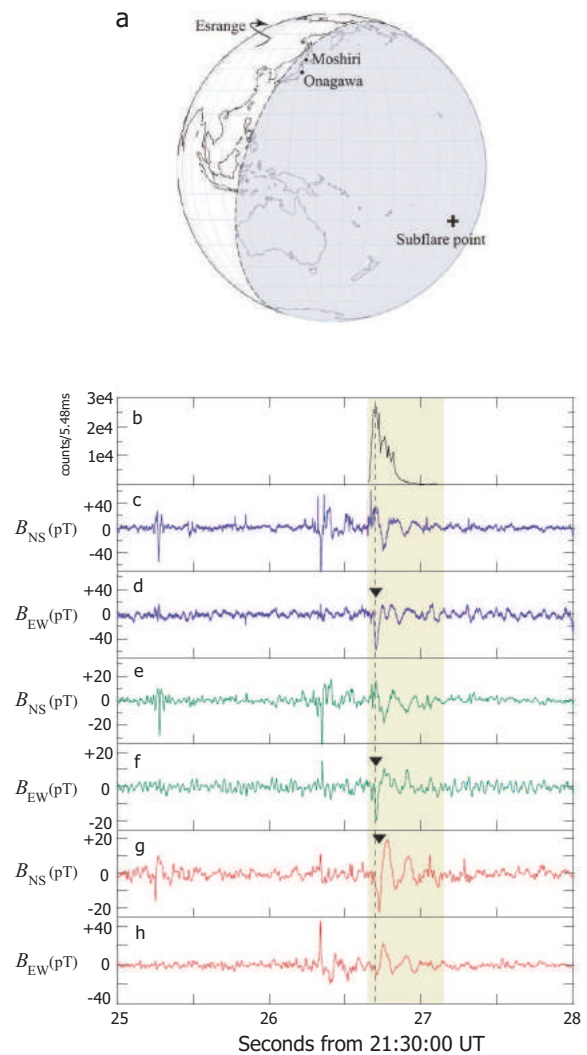


Fig. 5. (a) The shaded hemisphere indicates the part of the earth illuminated by the giant gamma-ray flare of SGR 1806-20 on 27 December 2004. The positions of the three relevant ELF observing stations (Moshiri, Onagawa, and Esrange) are depicted by filled circles. (b) GEOTAIL gamma-ray light curve ($E > 50$ keV) during the most intense period of this flare (a yellow bar). (c), (e) and (g) are the North-South components of the ELF magnetic field recorded at these three stations. (d), (f) and (h) are similar to (c), (e) and (g) but for the East-West components of the ELF magnetic field at these stations. Triangles in the panels (d), (f) and (g) indicate the onsets of the ELF signals at these stations, just corresponding to the peak time of the giant flare at 21:30:26.70 UT, which is shown by a vertical dashed line.

matter and nearby cosmic ray sources. CALET is designed to perform direct measurements of electrons from 1 GeV to 20 TeV, gamma rays from 10 GeV to 10 TeV, and nuclei from several 10 GeV to 1000 TeV. With its imaging and deep calorimeter, CALET provides excellent particle identification and high energy resolution, which will enables

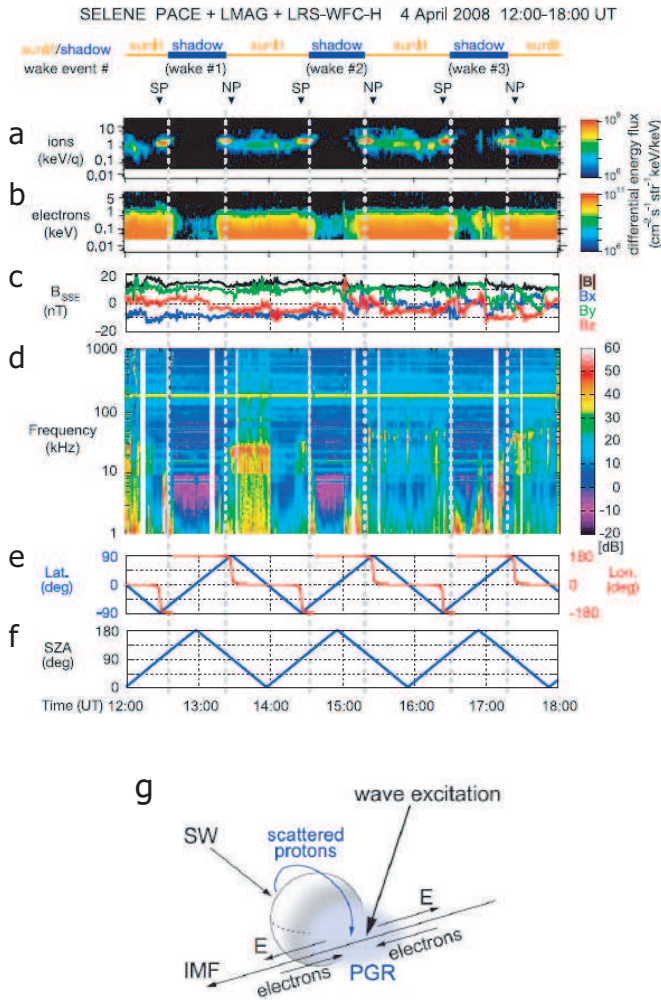


Fig. 6. Energy-time spectra of (a) protons and (b) electrons, (c) magnetic field in the SSE (Selenocentric Solar Ecliptic) coordinate, (d) frequency-time spectrogram of the plasma wave detector, and (e and f) spacecraft locations in the SSE coordinates and solar zenith angle (SZA) are shown [8]. Intervals of sunlit/shadow regions are indicated by orange/blue bars at the top of the figure, where the wake was observed within the shadow region. (g) A new model of the near-Moon wake environment where the protons of the solar wind origin scattered at the sunlit region of the Moon and accelerated by the $-V \times B$ electric field are penetrating deeply into the middle of the wake region and forming the proton governed region (PGR) [8]. Vectors in the figure, SW, E, and IMF, show directions of the solar wind flow, the ambipolar electric field, and the interplanetary magnetic field, respectively.

us to detect a distinctive feature in the energy spectrum caused from dark matter or nearby astrophysical sources. To achieve the expected CALET performance, we have performed simulation studies and a beam test at CERN-SPS with a CALET prototype [21]. Comparing the measured data (Figure 7b) with simulation results (Figure 7c), we have improved the accuracy of the analysis method and

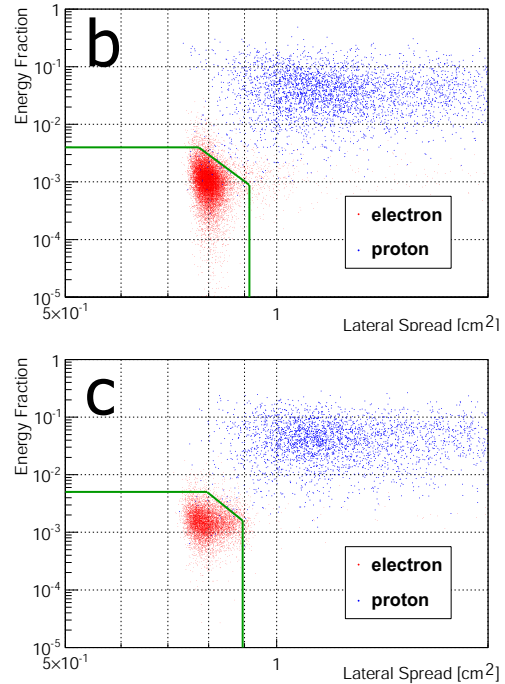
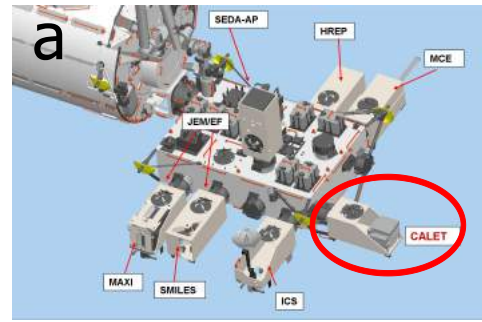


Fig. 7. (a) The CALET instrument attached to the Japan Exposure Module on the International Space Station. We distinguish electrons from protons, which are the largest source of background for electron observation, by the difference of each shower development within the CALET instrument. Panels (b) and (c) respectively show measured and simulated scatter plots of the shower profile for 150 GeV electrons and 350 GeV protons in a CALET prototype for CERN-SPS beam test. Energy fraction means the ratio of the deposit energy at the bottom calorimeter layer to the total deposit energy. Events in the bottom-left region bordered by green solid lines are regarded as electrons. In both cases of beam test and simulation, the proton contamination to the bottom-left region was only a few out of 4×10^5 events while electrons are survived there with 90% efficiency.

simulations, and confirmed the basic performance such as energy and angular resolutions.

Radio detection of UHECRs and extraterrestrial grains

Wide attention has been attracted to the detection of ultra high energy cosmic rays (UHE-

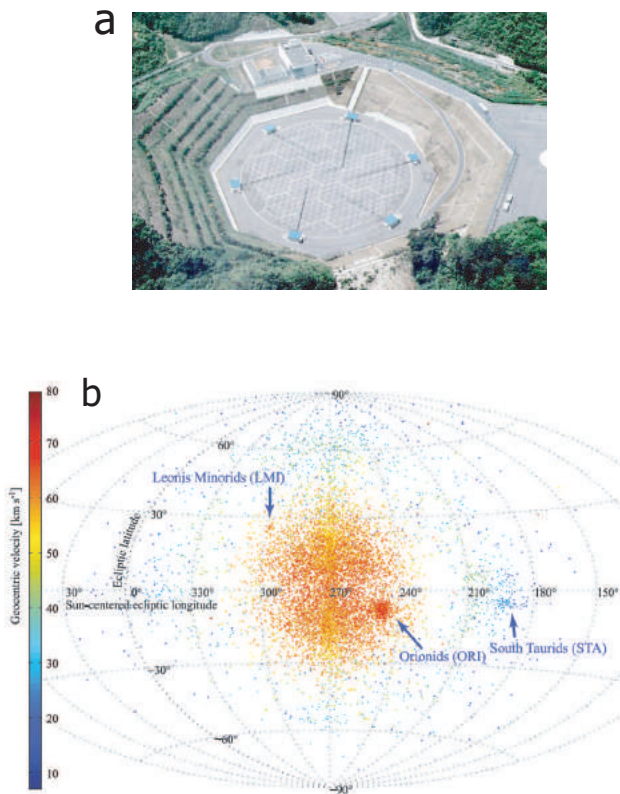


Fig. 8. (a) The MU radar in Shigaraki, Japan. This is a high-power (peak:1 MW, average:50 kW) mono-static pulse Doppler radar with the central frequency $f = 46.5$ MHz operated by the Research Institute for Sustainable Humanosphere (RISH) of Kyoto University. (b) The radiant distribution of the ~ 10000 meteors detected during the 33-h MU radar experiment plotted in Sun-centered ecliptic coordinates [13]. In addition to the known sporadic meteor radiants scattered around the longitude $\sim 270^\circ$, there is a significant enhancement in the Orionids radiant region (ORI) as well as less significant enhancements around Leonis Minorids (LMI) and South Taurids (STA).

CRs) with radio techniques, either passive and active, towards future large-scale UHECR observatory on the ground. Collaborating with the TA group of the high energy cosmic ray division of the ICRR, we have made a R/D study of the active method, namely, the detection of radar echoes from extensive air showers of UHECRs (UHECR echoes, hereafter) [17, 18]. Parallel to the above R/D study, we have also joined a radar research project for extraterrestrial grains (meteors) collaborating with radar physicists and planetary physicists at National Institute for Polar Research, Research Institute for Sustainable Humanosphere in Kyoto University, and Department of Earth Planetary Sciences in the University of Tokyo. Despite more than three orders of magnitude difference in the echo du-

ration between UHECR echoes ($< \sim \mu\text{s}$, expected but not yet identified) and meteor echoes (several - several tens of ms, observed), the know-how developed in the latter project (e.g., [13, 14], Figure 8) provides a technical basis for the former. It is further noted that the radar meteor project involves a search for the grains of the interstellar origin, and that there is a suggestion⁶ that a general enhancement of refractory elements to volatile elements in low energy galactic cosmic rays (GCR) is due to the injection of interstellar grains to the acceleration process. Therefore, the radar observation of the interstellar grain flux, if realized, can contribute to the quantitative modeling of GCR refractory elements.

Prospect

The research activity of the high energy astrophysics group closely couples with those in the other groups in the ICRR (Table 1). Firstly, we share common research interests on observational targets of the experimental groups in the high energy cosmic ray division. In addition, possibilities of collaboration extend to the groups in the other divisions: For example, the next generation neutrino detector, *Hyper Kamiokande*, is being planned, with which the detection of solar *flare* neutrinos may become a feasible research target. In our group, preliminary Geant-4 simulations of neutrino generation in X-class solar flares have been started.

The last line in Table 1 is for *KAGRA*, with which the gravitational wave signals from merger events of NS-NS or NS-BH binaries will be searched. It is noted that such merger events are believed to cause short GRB, one category of GRB of relatively short duration ($< \sim 1\text{sec}$). To clarify the physical nature of gravitational wave events, once identified, close collaboration among gravitational physicists, multi-wavelength astronomers, and high-energy astrophysicists is essential.

Members

Staff

Toshio Terasawa, Professor, December 2009 to the present

Research Associate, to be assigned in April 2013

*6 Meyer, J.P., L. O'C. Drury, and D. C. Ellison, *Astrophys. J.*, **487**, 182 (1997).

Division in ICRR	Group/Project	Examples of topics
High Energy Cosmic Ray Division	Telescope Array Group	origin/propagation of UHECR radio detection of UHECR
	Cherenkov Cosmic Gamma Ray Group	high energy γ ray emission from SNR, pulsars, Galactic Center, GRB, AGN, ... origin of GCR origin of diffuse gamma rays
	Tibet AS γ Group	anisotropy/composition of GCR origin of diffuse gamma rays
Neutrino and Astroparticle Division	Hyper-Kamiokande Project	solar <i>flare</i> neutrino
Astrophysics and Gravity Division	Primary Cosmic Ray Group	solar modulation of GCR
	Observational Cosmology Group	origin of cosmic magnetic field source of reionization (GRB, AGN, ...)
	KAGRA ^a Project	merger events (NS-NS, NS-BH)

Table 1. Topics of common interest. KAGRA^a=KAmioka GRAvitational wave detector.

Postdoctoral Fellows

Yosui Akaike, JSPS fellow, April 2012 to the present

Shota Kisaka, ICRR researcher, April 2012 to the present

Collaboration researcher

Hideaki Miyamoto, April 2012 to the present

Graduate students

Three students earned master degrees during 2011-2012, supervised by the ICRR staff member.

List of Publications

Papers in Refereed Journals

[1] Ohira, Y., T. Terasawa, and F. Takahara, “Plasma instabilities as a result of charge exchange in the downstream region of supernova

remnant shocks”, *Astrophys. J. Lett.* **703**, L59-L62 (2009).

[2] Asano, K., and T. Terasawa, “Slow heating model of gamma-ray burst: Photon spectrum and delayed emission”, *Astrophys. J.* **705**, 1714-1720 (2009).

[3] Yokota, S., et al., “First direct detection of ions originating from the Moon by MAP-PACE IMA onboard SELENE(KAGUYA)”, *Geophys. Res. Lett.* **36**, L11201.1-4 (2009).

[4] Nishino, M. N., et al., “Pairwise energy gain-loss feature of solar wind protons in the near-Moon wake”, *Geophys. Res. Lett.* **36**, L12108.1-4 (2009).

[5] Nishino, M. N., et al., “Solar-wind proton access deep into the near-Moon wake”, *Geophys. Res. Lett.* **36**, L16103.1-4 (2009).

- [6] Tanaka, T., et al., “First in situ observation of the Moon-originating ions in the Earth’s Magnetosphere by MAP-PACE on SELENE(KAGUYA)” *Geophys. Res. Lett.* **36**, L22106.1-4 (2009).
- [7] Masada, Y., et al., “Solar-type magnetic reconnection model for magnetar giant flares”, *Pub. Astron. Soc. Japan* **104**, 1093-1102 (2010).
- [8] Nishino, M. N., et al., “Effect of the solar wind proton entry into the deepest lunar wake”, *Geophys. Res. Lett.* **37**, L12106.1-4 (2010).
- [9] Saito, Y., et al., “In-flight performance and initial results of plasma energy angle and composition experiment (PACE) on SELENE (Kaguya)”, *Space Sci. Rev.* **154**, 265-303 (2010).
- [10] Tanaka, Y. T., et al., “First very low frequency detection of short repeated bursts from magnetar SGR J1550-5418”, *Astrophys. J.* **721**, L24-L27 (2010).
- [11] Nishino, M. N., et al., “Anomalous deformation of the Earth’s bow shock in the lunar wake: Joint measurement by Chang’E-1 and SELENE”, *Planet. Space Sci.* **59**, 378-386 (2011).
- [12] Tanaka, Y. T., et al., “Detection of transient ELF emission caused by the extremely intense cosmic gamma-ray flare of 27 December 2004”, *Geophys. Res. Lett.* **38**, L08805.1-4 (2011).
- [13] Kero., J., et al., “First results from the 2009-2010 MU radar head echo observation programme for sporadic and shower meteors: the Orionids 2009”, *Mon. Not. R. Astron. Soc.* **416**, 2550-2559 (2011).
- [14] Kero., J., et al., “A meteor head echo analysis algorithm for the lower VHF band”, *Annales Geophys.* **30**, 639-659 (2012).
- [15] Murase, K., et al., “The Role of Stochastic Acceleration in the Prompt Emission of Gamma-Ray Bursts: Application to Hadronic Injection”, *Astrophys. J.*, **746**, 164-175 (2012).
- [16] Terasawa, T., and S. Matsukiyo, “Cyclotron resonant interactions in cosmic particle accelerators”, *Space Sci. Rev.*, in press (2012).
- Papers in Conference Proceedings/Books
- [17] Terasawa, T., et al., “Search for radio echoes from EAS with the MU radar, Shigaraki, Japan”, *Proceedings of 31st International Cosmic Ray Conference*, session H.E.1.6, paper #0199 (2009).
- [18] Othman, M. A., et al., “Air Shower Detection by Bistatic Radar, International Symposium on the recent progress of ultra-high energy cosmic ray observation”, *AIP Conference Proceedings* **1367**, 143-146 (2011).
- [19] Terasawa, T., “Shocks in the heliosphere”, Chapter 12, *IAGA Special Sopron Book Series vol. 4, “The Sun, the Solar Wind, and the Heliosphere”*, ed. by M. P. Miralles and J. S. Almeida, Springer (2011).
- [20] Terasawa, T., “Collisionless shocks and particle acceleration: Lessons from studies of heliospheric shocks”, *IAU Symposium, Volume 274*, p. 214-219 (2011).
- [21] Akaike, Y., et al. “Performance of a CALET prototype calorimeter at the CERN-SPS”, 39th COSPAR Scientific Assembly, *Cosmic Ray Origins: the Viktor Hess Centennial Anniversary* (2012).
- [22] Kisaka, S., and N. Kawanaka “TeV cosmic ray electrons from millisecond pulsars”, *IAU symposium 291 Neutron Stars and Pulsars: Challenges and Opportunities after 80 years* (2012).

ASHRA

Introduction

Ashra (*All-sky Survey High Resolution Air-shower detector*)¹ [8, 15, 24] is a project to build an unconventional optical telescope complex that images very wide field of view (FOV), covering 77% of the sky, yet with the angle resolution of a few arcmin, sensitive to the blue to UV light with the use of image intensifier and CMOS technology. The project primarily aims to observe Cherenkov and fluorescence lights from the lateral and longitudinal developments of very-high energy cosmic rays in the atmosphere. It can also be used to monitor optical transients in the wide field of sky. The observatory will firstly consist of one main station having 12 detector units and two sub-stations having 8 and 4 detector units. One detector unit has a few light collecting systems with segmented mirrors. The main station and one of the sub stations were constructed on Mauna Loa (3,300 m) on Hawaii Island in 2007 as shown in Fig.1.

Project

Main Technical Features

The key technical feature of the Ashra detector rests on the use of electrostatic lenses to generate convergent beams rather than optical lens systems. This enables us to realise a high resolution over a wide FOV. This electron optics requires:

- *photoelectric lens imaging-tube*[21]; the world's largest imaging-tube uses electrostatic lens in addition to an optical system to generate convergent beams from photocathode of 20-in. diameter to output phosphor window of 1-in. diameter, enabling a very low cost and high performance image sensor providing a high resolution over a wide FOV, and
- *image pipeline*[2]; the image transportation from imaging-tube (image intensifier) to a trigger device and image sensors of fine pixels (CCD+CMOS), with high gain and resolution, enabling very fine images with parallel self-trigger systems that trigger separately for



Fig. 1. The Ashra main and sub stations at the Mauna Loa site (top), and a light collector towards Mauna Kea (bottom).

optical flash, atmospheric Cherenkov and fluorescence lights.

Observational Objectives

Optical transients; Ashra will acquire optical images every 1 s with 1-s exposure without deadtime. An example of a 42° FOV image taken by the Ashra light collector is shown in Figure 2. This enables us to explore optical transients, possibly associated with gamma ray bursts (GRBs), flares of soft gamma-ray repeaters (SGRs), supernovae explosion, and so on, in so far as they are brighter than $B \simeq 13$ mag, for which we expect 3- σ signals. The unique advantage is the on-time detection of the events without resorting to usual satellite alerts. In each detector unit FOV, 1~2 events per year are expected in coincidence with the Swift gamma-ray events. The total Ashra FOV that is wider than satellite instruments allows to detect more optical transients, including an interesting possibility for an optical flash, not visible with gamma-rays.

*1 <http://www.icrr.u-tokyo.ac.jp/~ashra>

TeV gamma rays; Atmospheric Cherenkov radiation is imaged by Ashra. Requiring the signal-to-noise ratio (SNR) >5 , the system will allow to explore VHE gamma-ray sources with the energy threshold of several TeV at the limiting flux sensitivity of 5% Crab for 1-year observation.

EeV cosmic rays; For fluorescence lights from VHE cosmic rays the effective light gathering efficiency is comparable with that of the High Resolution Fly's Eye detector (HiRes). The arcmin pixel resolution of Ashra provides finer images of longitudinal development profiles of EeV cosmic ray (EeV-CR) air-showers. The resolution of arrival direction with the stereo reconstruction is thus significantly improved and it is better than one arcmin for the primary energy of EeV and higher [1]. This is useful to investigate events clustered around the galactic and/or extragalactic sources. This in turn would give us information as to the strength and coherence properties of the magnetic field ². The great advantage of the fine image of Ashra can be applied to the detection of Cherenkov light emitted from the primary particle in the energy range around PeV prior to its first interaction in the atmosphere. The charge of the primary particle (Z) is estimated from the intensity of this light which is proportional to Z^2 . A typical emission angle for the direct Cherenkov light is 0.15° to 0.3° , whereas most of the air-shower light is emitted at angle greater 0.4° from the shower axis ^{3, 4}. The Ashra image resolution of a few arcmin is useful for the discrimination between the direct Cherenkov and the air-shower lights.

PeV-EeV neutrinos; Ashra may detect Cherenkov and/or fluorescence signals generated from tau-particle induced air-showers that is generated from interactions of tau neutrinos with the mountain and/or the earth. This is identified by peculiar geometry of the air-shower axis. The 1-year detection sensitivity with the full configuration of Ashra is 5 and 2 times larger than the Waxman-Bahcall limit for mountain-produced event (Cherenkov) and earth-skimming event (fluorescence), respectively ^{5, 6}. The most sensitive energy of around 100 PeV

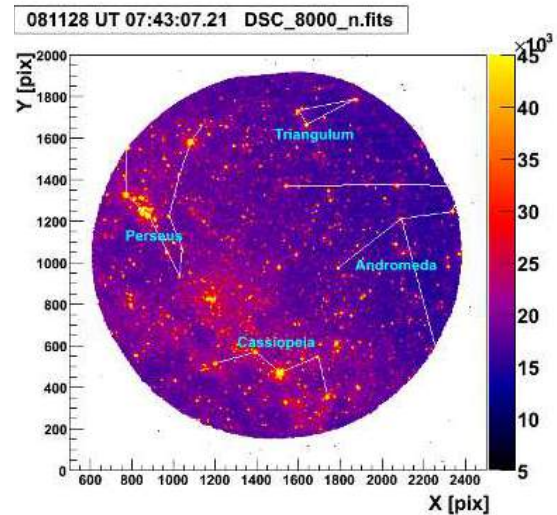


Fig. 2. An example of a 42° FOV image taken by the Ashra light collector (4-s exposure). The solid lines are drawn to indicate constellations.

is suitable for the detection of neutrinos originating from hadrons accelerated to EeV at astronomical objects.

Brief History

The basic concept of the Ashra project was presented firstly [7] in ICRR2000 Satellite Symposium (Comprehensive Study of High Energy Universe) by M. Sasaki. After the Ashra collaboration distributed copies of its proposal based on the conceptual design and basic R&D works [1, 2, 8], the Ashra project was funded by the Coordination Fund for Promoting Science and Technology (157-20004100) from 2003 to 2005. In 2004, University of Hawaii joined in the Ashra collaboration as a local host institute and the site use permit was granted to Department of Physics and Astronomy of the University of Hawaii at Hilo by the state of Hawaii in 2005. The brief history from 2006 is summarized as follows:

- *August, 2007;* The civil engineering construction of light collectors in shelters at the Mauna Loa site was completed.
- *June, 2008;* We started observation of optical transients and commissioning observation of VHE tau neutrinos (see the left panel of Fig.3) with some of the light collectors (Obs01). In this observation period, we submitted an op-

*2 D. Harari, S. Mollerach and E. Roulet, JHEP 0207 (2002) 006

*3 D. Kieda, S. P.Swordy, and S.P. Wakely, Astropart.Phys. 15, 287 (2001)

*4 F. Aharonian et al., Physical Rev. D75, 042004 (2007)

*5 G.W.S. Hou and M.A. Huang, astro-ph/0204145.

*6 E. Waxman and J.N. BahCall, Phys. Rev. D59 (1998) 023002.

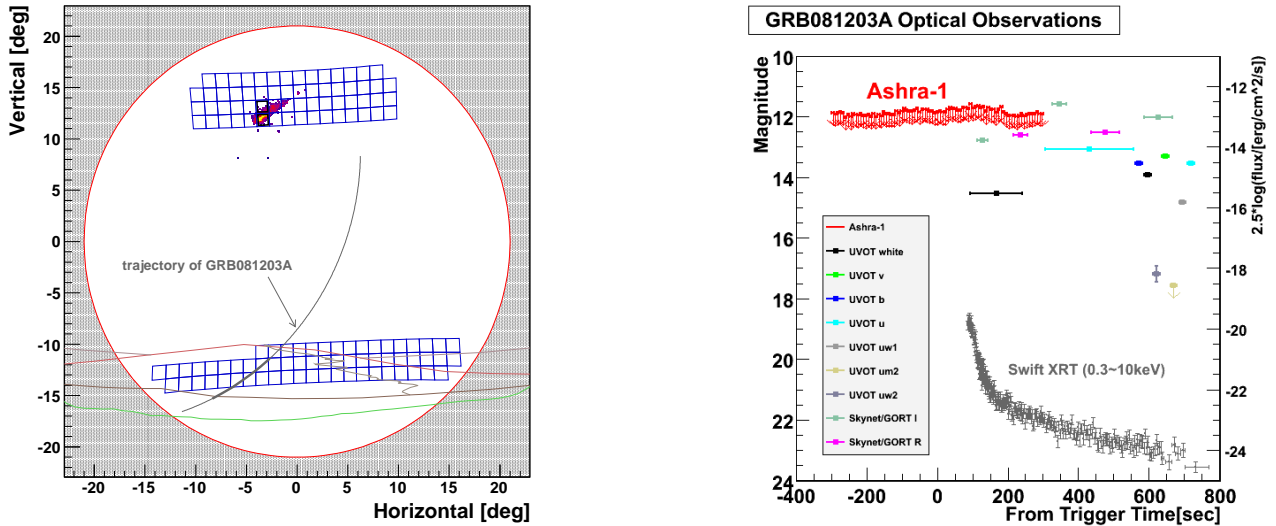


Fig. 3. (*Left*) Boundary (large red circle) between the inside (open circle) and outside (hatched area) of the FOV of the Ashra-1 light collector, which faces Mauna Kea, and the layout of trigger pixel FOVs (blue boxes) for Cherenkov τ shower observation [22]. Repositioned array of the trigger pixel FOVs (upper blue boxes) to check the detection sensitivity with ordinary cosmic-ray air showers at a higher elevation. Firing trigger pixels (thick blue boxes) of an observed image of a cosmic-ray air shower readout along the trigger (points). An extended portion of the trajectory of GRB081203A counterpart (circular arc), the segment of this trajectory used in the v_τ search (thick circular arc), the ridge lines of Mauna Kea (red) and Mauna Loa (green) mountains, the horizon, and Mauna Kea access road are shown. (*Right*) Summarized lightcurve for GRB081203A [19] around the trigger time. 3-sigma limiting magnitudes of our observation (labeled as Ashra-1) and other observations are compared as a function of time after GRB. The horizontal axis is in linear scale. The vertical axis in the right is only for the data by Swift XRT (gray data), where the scale is arbitrary.

tical observation report of GRB081203A [19] as shown in the right panel of Fig. 3.

- *October, 2009*; We restarted observation of optical transients after three-month shut down (Obs02). In this observation period, we submitted a report of GRB100906A observation [20].
- *June, 2011*; We published the paper about PeV–EeV tau neutrino search from GRB081203A [22] in *Astrophysical Journal Letters*.
- *June, 2011*; The permit for the 10 year extension of the Ashra Mauna Loa site was granted.
- *January, 2012*; We started observation of optical transients VHE CRs, and VHE tau neutrinos after upgrading our detectors for both targets (Obs03).

Observation

As a first step, we have started the observation of optical transients. During observation, optical images were constantly collected every 6 s after 4-s

exposure. We have accumulated 3780 hours of observation time in two years of highly efficient observation.

Ashra-1 observation of early optical emissions: GRB081203A and GRB100906A [19, 20]

We searched for optical emission in the field of GRB081203A [19] around the BAT-triggered GRB time (T_0) with one light collector unit in the Ashra-1 detector. The Ashra-1 light collector unit used in this analysis has the achieved resolution of a few arcmin, viewing 42° circle region of which center is located at $\text{Alt} = 11.7^\circ$, $\text{Azi} = 22.1^\circ$. The sensitive region of wavelength is similar with the B-band. From our analysis, we detected no new optical object within the PSF resolution around the GRB081203A determined by Swift-UVOT during the observation between T_0-300 s and T_0+300 s. As a result, the 3-sigma limiting magnitudes were estimated in comparison with stars in Tycho-2 Catalog to be distributed between 11.7 and 12.0, as shown in the right panel of Fig. 3. Our observation also covered the Swift-BAT error circle at the time of GRB100906A in the other light collector towards $\text{Alt} = 60^\circ$, $\text{Azi} = 0^\circ$, and the result of our optical

transient search was reported in Ref.[20].

Observational search for PeV–EeV tau neutrino from GRB081203A [22]

The earth-skimming tau neutrino (ν_τ) technique⁷ has the advantage of a large target mass, since it uses air showers produced by decay particles of tau leptons (τ s) in the atmosphere as the observed signals. τ s emerge out of the side of the mountain or the ground facing the detector; they are the product of interactions between VHE ν_τ and the earth matter they traverse. No air Cherenkov observation was made to date based on the earth-skimming ν_τ technique with air showers induced by τ decays (hereafter referred to as the Cherenkov τ shower method). However, it can achieve sufficient detection sensitivity in the PeV–EeV region to be useful in the search for ν s originating from hadrons accelerated to EeV at astronomical objects. Additional advantages of the Cherenkov τ shower method are its perfect shielding of cosmic-ray secondary particles, highly precise arrival direction determination for primary ν_τ and negligible background contamination by atmospheric ν s in the PeV–EeV energy range.

As shown in Fig. 4, one of the Ashra light collectors built on Mauna Loa has two geometrical advantages: (1) it faces Mauna Kea, allowing it to encompass the large target mass of Mauna Kea in the observational FOV, (2) it has an appropriate distance of ~ 30 km from Mauna Kea, yielding good observational efficiency when imaging air-shower Cherenkov lights which are directional with respect to the air-shower axis. Using the advanced features, we performed commissioning search for Cherenkov τ showers in 2008. We served limited 62 channels of photomultiplier tubes (PMTs) as trigger sensors prepared for the commissioning runs to cover the view of the surface area of Mauna Kea, as shown in Fig.3 (left). Adjacent-two logic was adopted to

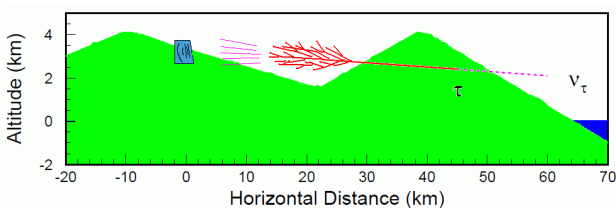


Fig. 4. Concept of Cherenkov τ shower method. The right mountain is Mauna Kea and the left is Mauna Loa.

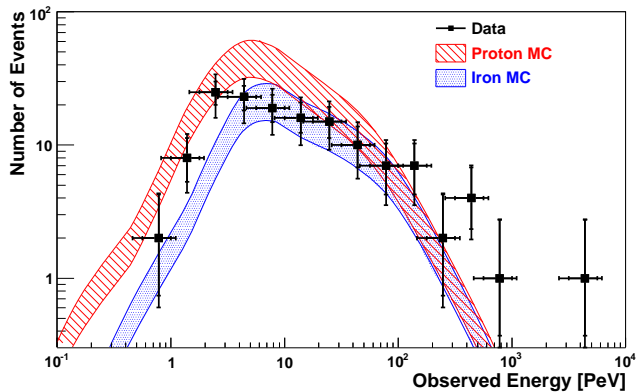


Fig. 5. Observed cosmic-ray flux spectrum (filled box) with bars indicating statistical and systematic errors and the MC predictions for proton primary (hatched band) and iron primary (shaded band) assumptions [22]. The width of the bands shows the evaluated systematic error of 30% of the MC prediction.

trigger the fine imaging, by judging discriminated waveform signals from each pixel of the multi-PMT trigger sensor. During the search period, ~ 2 hr before the trigger of GRB081203A. GRB counterpart (R.A. 15:32:07.58, decl. $+63:31:14.9$) passed behind Mauna Kea, as viewed from the Ashra-1 observatory.

To investigate the features, selection criteria, detection efficiency, and background rate for the observation of Cherenkov τ shower images, intensive Monte Carlo (MC) studies were performed considering all the results of the photometric and trigger sensitivity calibration. To confirm the detection sensitivity and gain calibration for the Cherenkov τ shower, we detected and analyzed 140 events of normal cosmic-ray air-shower Cherenkov images for a total of 44.4 hr using the same instruments used in neutrino observation, but after rearranging the trigger pixel layout to view the sky field above Mauna Kea (Fig.3 (left)). The observed and MC cosmic-ray flux spectra are shown in Fig. 5, in which the MC prediction used the typically observed cosmic-ray flux in the knee region⁸. Since the primary cosmic-ray components are observationally undefined, we present the MC prediction of cosmic-ray flux spectra, assuming either only protons or irons as the primary cosmic rays in Fig. 5. In both cases, the observed data and the MC prediction agreed well on the normalization and the shape of the distribution within the expected errors. The

^{*7} D. Fargion, ApJ **570**, 909 (2002).

^{*8} T. Antoni *et al.*, Astropart. Phys. **24**, 1 (2005), M. Amenomori *et al.*, ApJ **678**, 1165 (2008).

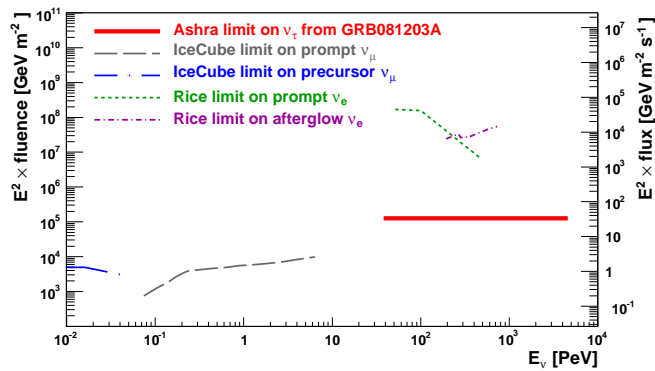


Fig. 6. Ashra 90% CL limit (thick continuous line (red)) on ν_τ fluence of precursor and afterglow emissions from the GRB081203A counterpart in the PeV–EeV region [22]. For comparison, IceCube limits in the prompt (long dashed dotted (gray)) and precursor (long dashed dotted (blue)) phases and RICE limits in the prompt (dashed (green)) and afterglow (dashed dotted (magenta)) phases are shown. The energy ranges were defined as containing 90%, 90%, and 80% of the expected signals from assumed spectrum for Ashra, IceCube, and RICE, respectively.

estimation of the detection sensitivity of the Ashra light collector and the validity of the reconstruction procedure were well demonstrated.

For the ν_τ search, we used image data acquired using the trigger for 197.1 hr in only case of the data status defined as good out of the total observation time of 215.8 hr. Detailed data analysis yielded a null ν_τ candidate [22]. On the basis of the above null result and the estimated effective areas, we placed 90% confidence level (CL) upper limits on the ν_τ fluence of precursor and afterglow emissions in the PeV–EeV region, for two 3780 s periods, the first between 2.83 and 1.78 hr before GRB081203A and the second between 21.2 and 22.2 hr after it, as shown in Fig. 6, where we assumed a typical E_ν^{-2} flux to ensure unbiased constraints on observationally undefined physical mechanisms of a GRB.

For comparison, Fig. 6 shows other observational limits on the ν fluence from point sources⁹. Our results are the most stringent in the PeV–EeV region and complementary to the IceCube results for the sub-PeV energy region, and indicate the advanced instantaneous sensitivity of the system even during this commissioning phase. Our first search for PeV–EeV ν_τ reported in Ref. [22] complements other experiments in energy range and detection method, and implies the prologue of “multi-particle astronomy” [7] with a precise determination of time

⁹R. Abbasi *et al.*, *ApJ* **710**, 346 (2010), D. Besson, S. Razzaque, J. Adams, and P. Harris, *Astropart. Phys.* **26**, 367 (2007).

and location.

Prospects

In this Ashra-1 experiment, we were performing device installation and specific observation in a step-by-step way to enhance the scientific impacts as shown in the previous sections. We have already made a refereed journal publication of PeV–EeV tau neutrino search [22] as important physics results with the Ashra-1 detector unit adding to publications on the detector or methodological developments and circulations [21, 19, 20]. We are now preparing for a few physics publications from the optical observation data of the 2.5 years from the Obs01 to Obs02 as well as keeping highly efficient observation runs in Obs03 for optical transients, VHE CRs and tau neutrinos. Adding that, the R&D for the direct Cherenkov method applied to Ashra-1 has been granted and under development.

The full Ashra observatory (Ashra-2) will consist of three peripheral sites separated by about 25 km at Mauna Loa (3,300 m), Camp Kilohana (2,014 m) on the side of Mauna Kea, and Hualalai (2,320 m) and one central site among them on the island of Hawaii. The full configuration emphasizes the hybrid stereoscopic observation with Cherenkov and fluorescence lights from air-showers with two or three stations at separated sites as well as the effective detection area for air-showers. The parallax observation for optical transients with two or more stations is also useful for rejecting local background events.

Ashra Collaboration

Spokesperson: Makoto Sasaki (ICRR)

Institute	Country	(*)
ICRR, Univ. of Tokyo	Japan	7
Toho Univ.	Japan	7
Univ. Hawaii Manoa	USA	2
Univ. Hawaii Hilo	USA	3
Nagoya Univ.	Japan	1
Chiba Univ.	Japan	1
Ibaraki Univ.	Japan	1
Kanagawa Univ.	Japan	1
Total		23

(*) Number of participants as of June 2012.

Members

Staffs

Makoto Sasaki, Assoc. Professor, April 1996 to the present

Yoichi Asaoka, Research Associate, April 2002 to the present

Postdoctoral Fellows

Holger Motz, April 2012 to the present

Graduate Students

One student was awarded doctor degrees and six students earned master degrees during 2006–2012, supervised by ICRR staff members.

List of Publications

Before Year 2006

Papers in Refereed Journals

- [1] M. Sasaki, A. Kusaka and Y. Asaoka, “Design of UHECR telescope with 1 arcmin resolution and 50° field of view”, *Nucl. Instrum. Methods Phys. Res. A* **492**, 49 (2002).
- [2] M. Sasaki, Y. Asaoka and M. Jobashi, “Self-triggered image intensifier tube for high resolution UHECR imaging detector”, *Nucl. Instrum. Methods Phys. Res. A* **501**, 359 (2003).
- [3] M. Sasaki *et al.*, “GRB041211: Ashra Prototype optical observation”, *GCN Circ.* 2846, (2004).
- [4] M. Sasaki *et al.*, “GRB050504: Ashra-P2/3 monitor and Ashra-AFT response”, *GCN Circ.* 3499, (2005).
- [5] M. Sasaki, N. Manago, K. Noda, Y. Asaoka, “GRB050502b: Early Observation”, *GCN Circ.* 3421, (2005).
- [6] Y. Asaoka, Y. Aita, T. Aoki, M. Sasaki, “Development of a 16-inch UV-ray image intensifier tube”, *IEEE Trans. Nucl. Sci.*, *IEEE*, **52**, 1773-1778, (2005).

Papers in Conference Proceedings

- [7] M. Sasaki, in *Proc. ICRR2000 Satellite Symposium: Workshop of Comprehensive Study of the High Energy Universe*, edited by T. Kifune, J. Okada, T. Kajita, and M. Sasaki (ICRR, the University of Tokyo, Kashiwa, 2000), p. 110.
- [8] M. Sasaki, “Very High Energy Particle Astronomy with All-sky Survey High Resolution Air-shower Detector (Ashra)”, *Progress of Theoretical Physics Supplement*, **151**, 192 (2003).
- [9] H. Kuze, S. Fukagawa, N. Takeuchi, Y. Asaoka, and M. Sasaki, “Development of a wide-area imaging lidar for atmospheric monitoring”, *29th SICE Remote Sensing Symposium (Tsukuba)*, 61-64 (2003).
- [10] Y. Arai *et al.*, “ASHRA Trigger and Readout Pixel Sensors”, *Proc. 28th Intl. Cosmic Ray Conf. (Tsukuba)*, pp. 961–964, 2003.
- [11] Y. Aita *et al.*, “The ASHRA Detector”, *ibid.*, pp. 1061-1064.
- [12] K. Kohri *et al.*, “Particle Physics in ASHRA”, *ibid.*, pp. 1747-1750.
- [13] Y. Aita *et al.*, “High Energy Astrophysics by ASHRA”, *ibid.*, pp. 2991-2994.
- [14] M. Sasaki, “Very High Energy Particle Astronomy with All-Sky Survey High Resolution Air-shower Detector (Ashra)”, *Modern Physics Letters A* **19**, 1107-1115, 2004.
- [15] M. Sasaki *et al.*, “Status of Ashra project”, *Proc. 29th Int. Cosmic Ray Conf. (Pune, India)*, Vol. 8, 197-200, 2005.
- [16] M. Sasaki *et al.*, “Observation of Optical Transients with the Ashra prototype”, *ibid.*, Vol. 5, 319-322, 2005.
- [17] S. Fukagawa, I. Kouga, H. Kuze, N. Takeuchi, M. Sasaki, Y. Asaoka, S. Ogawa, “Simulation study for aerosol distribution retrieval from bistatic, imaging lidar data”, *Conference on Laser and Electro Optics / Pacific Rim 2005*, C15, July 14, 2005.
- [18] S. Fukagawa, I. Kouga, H. Kuze, N. Takeuchi, M. Sasaki, Y. Asaoka, S. Ogawa, “Environmental application of the all-sky survey

high-resolution air-shower (Ashra) telescope - aerosol distribution measurement using a bistatic, imaging lidar”, Proceedings of the CERESe international symposium on radiation budget and atmospheric parameters studied by satellite and ground observation data, P-3, pp.196-199 (2005.2).

After Year 2006

Papers in Refereed Journals

- [19] Y. Aita *et al.*, “GRB081203A: Ashra-1 observation of early optical and VHE-neutrino emission”, GCN Circ., 8632 (2008).
- [20] Y. Asaoka *et al.*, “GRB100906A: Ashra-1 observation of early optical emission”, GCN Circ., 11291 (2010).
- [21] Y. Asaoka and M. Sasaki, “Performance of a 20-in. photoelectric lens image intensifier tube”, Nucl. Instrum. Methods Phys. Res. A **647**, 34 (2011).
- [22] Y. Aita *et al.*, “Observational Search For PeV–EeV Tau Neutrino From GRB081203A”, ApJ **736**, L12 (2011).
- [23] Y. Asaoka and M. Sasaki, “Cherenkov τ shower earth-skimming method for PeV–EeV ν_τ observation with Ashra”, Astropart. Phys. (2012), <http://dx.doi.org/10.1016/j.astropartphys.2012.10.001>

Papers in Conference Proceedings

- [24] M. Sasaki *et al.*, “The Ashra Project”, 30th Intl. Cosmic Ray Conf. (Merida), ID1232, 2007.
- [25] Y. Aita *et al.*, “Ashra Mauna Loa Observatory and Slow Control System”, *ibid.*, ID684.
- [26] Y. Aita *et al.*, “Hybrid Photo Detector as the Ashra Trigger Sensor”, *ibid.*, ID1279.
- [27] Y. Aita *et al.*, “VHE neutrino pilot observation with the Ashra detector”, 31th Intl. Cosmic Ray Conf. (Lodz), ID313, 2009.
- [28] Y. Aita *et al.*, “Ashra Optical Transient Observation”, *ibid.*, ID1410.

CTA (R & D)

Introduction

During the past few years, Very High Energy (VHE) gamma ray astronomy has made spectacular progress and has established itself as a vital branch of astrophysics. To advance this field even further, we propose the Cherenkov Telescope Array (CTA), the next generation VHE gamma ray observatory, in the framework of a worldwide, international collaboration. CTA is the ultimate VHE gamma ray observatory, whose sensitivity and broad energy coverage will attain an order of magnitude improvement above those of current Imaging Atmospheric Cherenkov Telescopes (IACTs). By observing the highest energy photons known, CTA will clarify many aspects of the extreme Universe, including the origin of the highest energy cosmic rays in our Galaxy and beyond, the physics of energetic particle generation in neutron stars and black holes, as well as the star formation history of the Universe. CTA will also address critical issues in fundamental physics, such as the identity of dark matter particles and the nature of quantum gravity.

VHE gamma rays from 100GeV to 10TeV can be observed with ground-based IACTs. The history of VHE gamma ray astronomy begun with the discovery of VHE gamma rays from the Crab Nebula by the Whipple Observatory in 1989. The current generation IACTs featuring new technologies, such as H.E.S.S., MAGIC, VERITAS, and CANGAROO, have discovered more than 100 Galactic and extragalactic sources of various types to date.

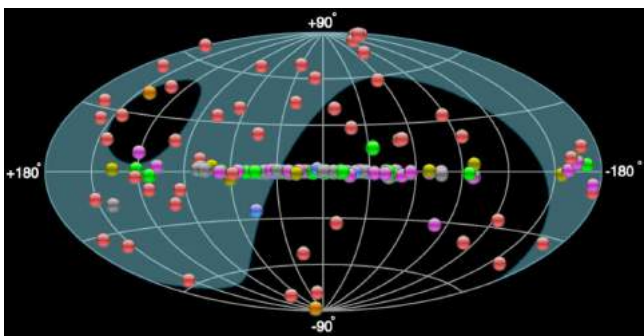


Fig. 1. Very High Energy Gamma Ray Sky ($> 100\text{GeV}$). More than 150 Galactic and extragalactic sources have been discovered by H.E.S.S., MAGIC, VERITAS and CANGAROO.



Fig. 2. The current generation VHE gamma ray observatories, the MAGIC, VERITAS, H.E.S.S. and CANGAROO telescopes. The Cherenkov Cosmic Gamma Ray group operates MAGIC on La Palma, Canary Islands, and CANGAROO (closed in 2011) at Woomera in Australia.

CTA Project

CTA is designed to achieve superior sensitivity and performance, utilizing established technologies and experience gained from the current IACTs. The project is presently in its preparatory phase, with international efforts from Japan, US and the EU. It will consist of several 10s of IACTs of three different sizes (Large Size Telescopes, Mid Size Telescopes, and Small Size Telescopes). With a factor of 10 increase in sensitivity ($1\text{m Crab} \sim 10^{-14} \text{ erg cm}^{-2} \text{ s}^{-1}$), together with much broader energy coverage from 20GeV up to 100TeV, CTA will bring forth further dramatic advances for VHE gamma ray astronomy. The discovery of more than 1000 Galactic and extragalactic sources is anticipated with CTA.

CTA will allow us to explore numerous, diverse topics in physics and astrophysics. The century-old question of the origin of cosmic rays is expected to be finally settled through detailed observations of supernova remnants and other Galactic objects along with the diffuse Galactic gamma ray emis-

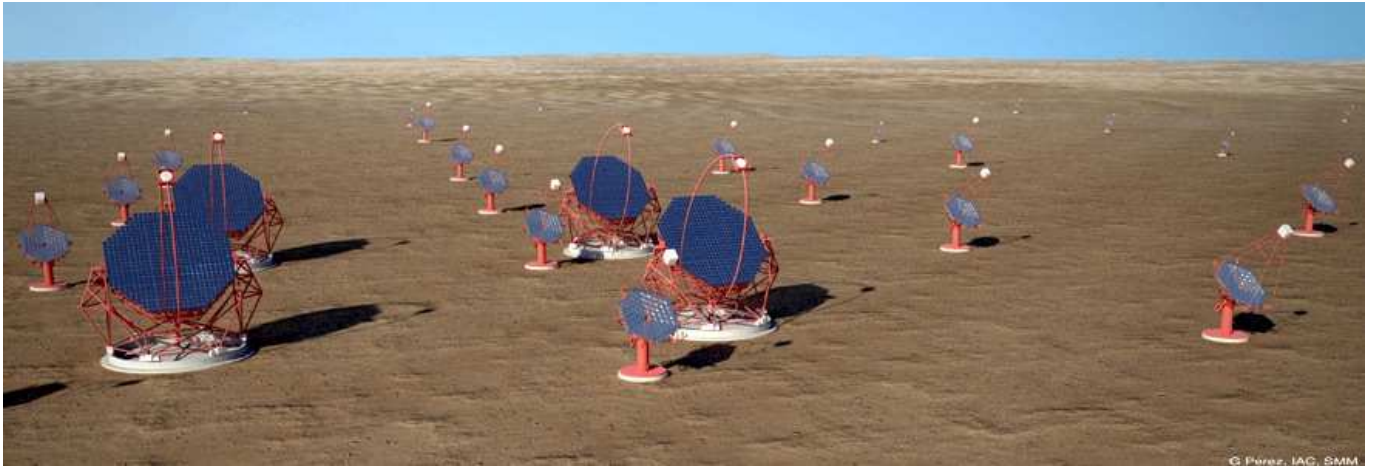


Fig. 3. Artist view of the CTA observatory. CTA consists of three types of telescopes, Large Size Telescopes (23m diameter), Mid Size Telescopes (12m) and Small Size Telescopes (6m), and covers the broad energy band from 20GeV to 100TeV.

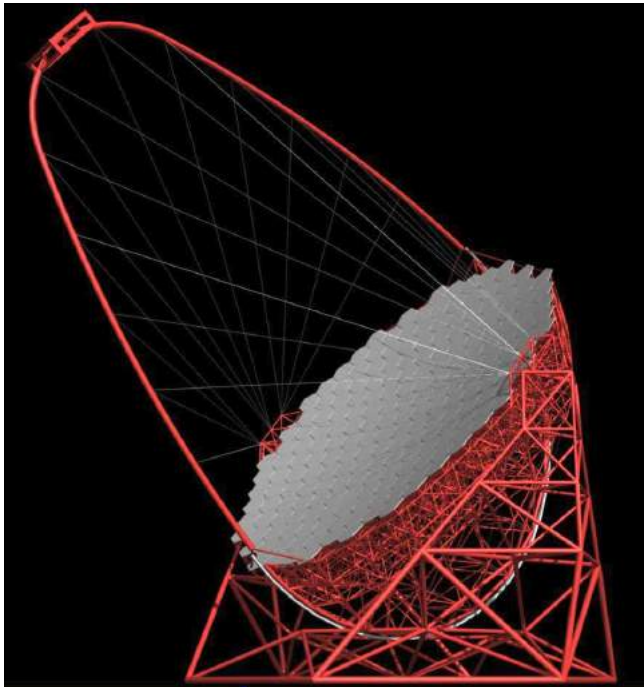


Fig. 4. Large Size Telescope (23m diameter) designed by Max-Planck-Institute for Physics. CTA Japan is contributing to the design and prototyping of the imaging camera at the focal plane, ultrafast readout electronics, and high precision segmented mirrors.

sion, which will also shed light on the physics of the interstellar medium. Observing pulsars and associated pulsar wind nebulae will clarify physical processes in the vicinity of neutron stars and extreme magnetic fields. The physics of accretion onto supermassive black holes, the long-standing puzzle of the origin of ultrarelativistic jets emanating from them, as well as their cosmological evolution will

be addressed by extensive studies of active galactic nuclei (AGN). Through dedicated observing strategies, CTA will also elucidate many aspects of the mysterious nature of gamma ray bursts (GRBs), the most energetic explosions in the Universe. Detailed studies of both AGNs and GRBs can also reveal the origin of the highest energy cosmic rays in the Universe, probe the cosmic history of star formation including the very first stars, as well as provide high precision tests of theories of quantum gravity. Finally, CTA will search for signatures from elementary particles constituting dark matter with the highest sensitivity yet. Realization of the rich scientific potential of CTA is very much feasible, thanks to the positive experience gained from the current IACTs.

Structure of the large size telescope (LST)

The structure of the large size telescope (LST) as shown in figure 4 was designed by the MPI Munich group together with the company MERO-TSK. The major part of the telescope consists of the space frame structure with carbon fiber reinforced plastic (CFRP) tubes. The total weight of the telescope is designed to be about 50 tons and allows the fast rotation of the telescope, 180 degrees in 20 seconds, for fast follow-up observations of gamma ray bursts using the location determined by gamma ray satellites.

The telescope geometry is optimized to maximize the cost performance by Monte Carlo simulations and toy models. The baseline parameters are defined with the dish size of 23m, the focal length

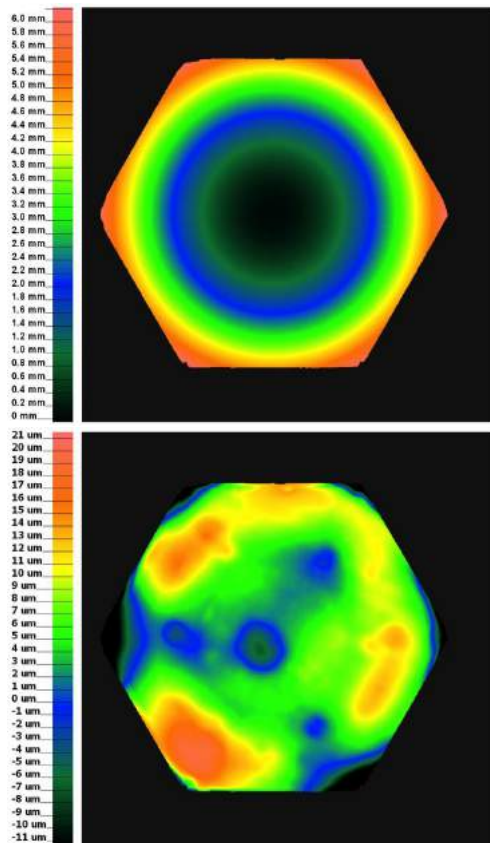


Fig. 6. Surface measurement of mirror prototypes produced by Sanko with Phase Measurement Deflectometry (PMD). Top: Global profile of the segmented mirror surface. Bottom: Deviation from the ideal mirror surface. The RMS of deviation is $6.6 \mu\text{m}$.

of 28m and then $F/D = 1.2$, and the camera FoV of 4.5 degrees with a pixel size of 0.1 degrees.

Activities of CTA-Japan

The CTA-Japan consortium is aiming to contribute particularly to the construction of the Large Size Telescopes (LSTs) and is involved in their development. The LST covers the low energy domain from 20GeV to 1000GeV and is especially important for studies of high redshift AGNs and GRBs. The diameter and area of the mirror is respectively 23m and 400m^2 to achieve the lowest possible energy threshold of 20GeV. All optical elements/detectors require high specifications, for example, high reflectivity, high collection efficiency, high quantum efficiency and ultra fast digitization of signal and so on. For this purpose, CTA-Japan is developing high quantum efficiency photomultipliers, ultrafast readout electronics and high precision segmented mirrors.

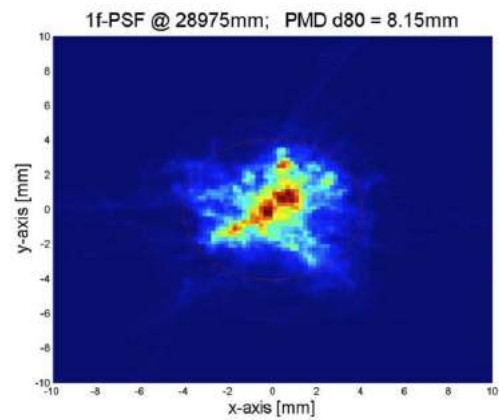


Fig. 7. The expected Point Spread Function (PSF) obtained by the ray trace with PMD method. D80 (the diameter containing 80% of total light) is 8.1mm, which is well smaller the LST specification of 20mm.

Segment Mirrors for LST

The reflector with its diameter of 23m consists of 206 units of hexagonal shape 1.5m flat to flat segmented mirrors of 2m^2 . The total area of the reflector is about 400m^2 . The individual segmented mirror is attached to the knots of the space frame structure with a universal joint and two actuators. The segmented mirrors have a sandwich structure consisting of glass sheet of 2.7mm thickness - aluminum honeycomb of 60mm thickness - glass sheet. The weight of a segmented mirror is 45kg. The reflective layer of the mirror is coated with Cr and Al on the surface of the glass sheet with a protective multi-coat layer of SiO_2 , HfO_2 and SiO_2 . By adjusting the thickness of individual layers with SiO_2 and HfO_2 , we can optimize the reflectivity to about 95% due to the interference effect of multi-layers.

Permanent Active Mirror Control

We will define the optical axis (OA) of the LST optics with two infra-red lasers at the center of the dish constantly shining two targets left and right of the imaging camera. The individual segmented mirror will also have an infra-red laser at the edge of the mirror (MIR) which makes the spot at the target near the imaging camera confirm the direction of the mirror facet relative to the OA laser (optical axis). The directional offset of the mirror facets will be estimated by taking pictures of the MIR-laser and OA-laser spots on the target near the Camera with a high resolution IR CCD camera viewing from the center of the dish. If any significant offsets



Fig. 5. Hexagonal shape mirrors of 1510mm size prototyped by Sanko LTD. The area is about 2m^2 and the focal length is 28m. Mirrors are produced with the cold slump technique. The mirror surface is protected with the multi-layer coating with SiO_2 and HfO_2 which are produced by sputtering method.

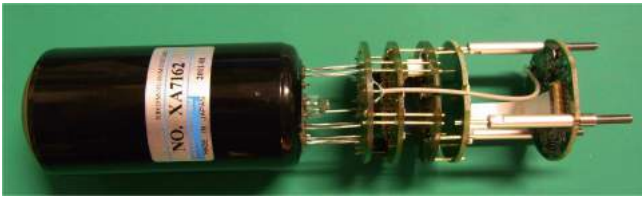


Fig. 8. R11920-100-20 PMT module. This module consists of Hamamatsu Photomultiplier R11920, Cockcroft-Walton HV, and Ultra fast Preamplifier. CTA-Japan has developed this PMT module together with Hamamatsu photonics.



Fig. 9. PMT Cluster consists of seven photomultipliers, CW-HVs, Preamplifiers, readout electronics, and trigger system. Signals are digitized in this module and sent to DAQ camera server system via Ethernet.

are found, the direction of the corresponding mirror facets will be corrected by actuators. The mirror directional calibrations over 206 mirrors will be done sequentially and performed within one minute. This calibration and control will be done continuously during the observation. After the first rotation for the GRB follow-up observation, or at the beginning of the observation of any source, we will use the look-up table corresponding to the zenith angle of the target source as the initial value of actuators and then move to the mode of permanent active mirror control loop.

Imaging Camera

The imaging camera has a FOV of 4.5 degrees and a pixel size of 0.1 degrees. The actual size of the image plane will be about 2.2m in diameter. The signals from the photomultipliers will be read with 1G samples/sec speed and be stored in the ring capacitors of 4096 depth, which corresponds to 4 micro-seconds.

The camera will be sealed to resist the humidity and dust in the field. The front side (entrance win-

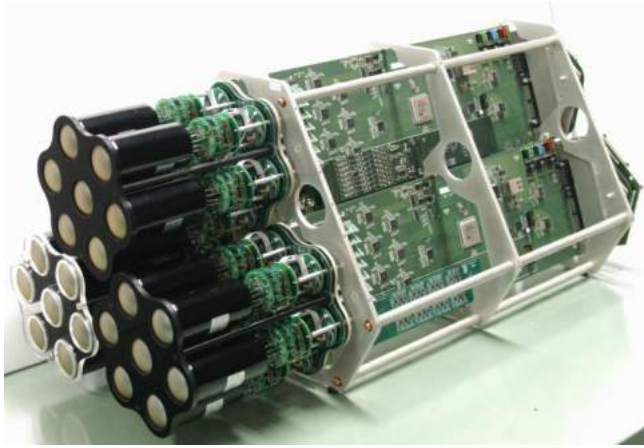


Fig. 10. Mini Camera with three PMT clusters for testing triggers between neighbouring clusters. In the LST camera, we will have 1855 PMTs and 265 clusters.

dow) of the imaging camera will be covered with uv-transparent plexiglass. Two water cooling plates are used to keep the temperature of the camera and the electronics constant. As a part of the Camera mechanical structure they will also serve as a support for the PMT/electronics clusters. The readout electronics and the auxiliary electronics (HV, and amplifiers) will dissipate a heat of 2W/ch. 7-PMTs and readout electronics are mechanically bundled as a PMT/electronics cluster. The total number of pixels and clusters will be 1855 and 265, respectively. The total heat dissipation inside camera will amount to 4-5kW.

Summary

As mentioned above, CTA-Japan will have important responsibilities on segmented mirrors, active mirror control system, focal plane instruments and readout electronics of the first Large Size Telescopes (LSTs). CTA-Japan will deliver these elements with the budget, the JSPS Grant-in-Aid for the special promoted research.

The final site for CTA north and south will be decided in the end of 2013, and then sites will be developed in 2014 and 2015. All elements of the first Large Size Telescope will be prepared and well tested before 2015 and the final integration test is foreseen in the first half of 2015 and shipped to the final site. The construction will start in the middle of 2015. The commissioning and the first light of the first Large Size Telescope is expected in the end of 2015. For the full construction (four LSTs in north and another four in south), we need more

efforts to secure the finance and manpower.

CTA-Japan Consortium

CTA is the international collaboration consisting of 985 scientists and 163 institutions from 26 countries as of May 2012. Here we just show members of the CTA-Japan consortium. The spokesperson of the CTA-Japan Consortium is Masahiro Teshima (ICRR).

Institute	Country	(*)
ICRR, Univ. of Tokyo	Japan	13
Aoyama Gakuin Univ.	Japan	6
Ibaraki Univ.	Japan	7
Osaka Univ.	Japan	2
Kitazato Univ.	Japan	1
Kyoto Univ.	Japan	9
Kinki Univ.	Japan	5
Kumamoto Univ.	Japan	1
KEK	Japan	4
Konan Univ.	Japan	2
Saitama Univ.	Japan	3
Tokai Univ.	Japan	5
Univ. of Tokyo	Japan	1
Tokyo Inst. Tech.	Japan	1
Univ. of Tokushima	Japan	2
Nagoya Univ.	Japan	9
Hiroshima Univ.	Japan	4
Miyazaki Univ.	Japan	1
Yamagata Univ.	Japan	3
Yamanashi Gakuin Univ.	Japan	2
Waseda Univ.	Japan	2
Total		84

(*) Number of participants as of May 2012.

Members

Staffs

Teshima M, Professor, 2010 -
 Yoshikoshi T, Assoc. Professor, 2004 -
 Ohishi M, Research Associate, 2006 -

Postdoctoral Fellows

Saito K, 2012-2014

List of Publications

Papers in Refereed Journals

- [1] “Design concepts for the Cherenkov Telescope Array CTA: An advanced facility for ground-based high-energy gamma-ray astronomy”,
CTA Consortium Collaboration (M. Actis, K. Ioka, H.Kubo, R. Orito, H. Tajima, M. Teshima, T. Totani, T. Yoshida, T. Yoshikoshi, 60 other CTA-Japan members *et al.*). *Exper.Astron.* **32**, 193 (2011).

Papers in Conference Proceedings

- [2] “Monte Carlo Study on the Large Imaging Air Cherenkov Telescopes for > 10 GeV gamma ray astronomy”
M.Teshima *et al.* *Proc. of ICRC 2009 at Lodz, Poland*, arXiv: 0906.4633
- [3] “Design Study of a CTA Large Size Telescope”,
M. Teshima *et al.*, *Proc. of ICRC2011 at Beijing China*, arXiv:1111.2183
- [4] “Development of PMT Clusters for CTA-LST Camera”,
R. Orito *et al.*, *Proc. of ICRC2011 at Beijing China*, arXiv:1111.2183
- [5] “Development of the Readout System for CTA Using the DRS4 Waveform Digitizing Chip”,
H. Kubo *et al.*, *Proc. of ICRC2011 at Beijing China*, arXiv:1111.2183

ASTROPHYSICS AND GRAVITY DIVISION

GRAVITATIONAL WAVE GROUP

Introduction

The detection of gravitational wave has been a persistent dream for physicists for long time after J. Weber initiated the challenge by his resonant antenna in 1960s¹. Although his result was denied by the end of 1970s, many successors began to take over his work. In place of resonant antennae, detection by a laser interferometer was pursued and developed. Construction of practical detectors to detect real gravitational waves started by the initial LIGO and Virgo². At the same time, German physicists and Japanese researchers had made a break in this field by developing intermediate scale laser interferometers, which were operated by early in 2000s. These interferometric gravitational wave detectors³ are categorized as detectors that belong to the first generation.[1] The coverage distance of these detectors in the Universe is from 1 Mpc to 20 Mpc (1 pc=3.3 light year). The estimation of detection rate is not a practical number.

The R&D by 2005 was the main subject presented in the previous external review. Since 2006, we were trying to achieve sensitivity limit of Cryogenic Laser Interferometer Observatory (CLIO) that is the first cryogenic mirror interferometer placed underground at Kamioka. And also we did our best to obtain the funding for constructing the large scale gravitational wave telescope (LCGT)[2, 82], which is now called KAGRA⁴. In overseas projects, LIGO and Virgo ceased its operation and entered into an period of replacement & improvement. Including KAGRA, these detectors are called as “advanced” and belong to the second generation detectors.

KAGRA has been funded in 2010 to firstly detect a gravitational wave event. The construction and manufacturing apparatus are being conducted as scheduled. We plan to operate the most simple interferometer optical configuration by 2015 and to improve by advanced cryogenic mirror and optical configuration until 2016. We will begin the ob-

servation by 2017 with full specification sensitivity. We are going to promote technical collaboration with overseas projects for construction and plan to advance scientific collaboration in future.

This report summarizes the effort of construction of KAGRA after brief summary of CLIO project, which is the technical basis of cryogenic KAGRA interferometer.

CLIO Project

Overview of CLIO

CLIO is a 100 m-baseline underground cryogenic interferometer at the Kamioka mine. CLIO forms a bridge connecting the CLIK (7 m prototype cryogenic interferometer at Kashiwa campus) and the KAGRA (3 km cryogenic interferometer at Kamioka). The site of CLIO, near the Super-Kamiokande neutrino detector, is shown in Fig. 1. The tunnel was dug in 2002, and a strain meter for geophysics was installed in 2003 [3]. The construction of CLIO began in late 2003, and installation of the mode cleaner vacuum system was finished in 2004. Four sets of cryostats and whole vacuum system were installed in 2004-2005. We started the operation of CLIO in 2006 (Fig. 2).



Fig. 2. Overview of the CLIO interferometer.

The prime purpose of CLIO is to demonstrate mirror thermal noise reduction with cryogenic mirrors (Fig. 3). We achieved the design sensitivity at the room temperature after noise hunting taken in 2008 [4, 5]. After then, we started out cooling the mirrors and noise hunting with the mirrors under

*1 J. Weber: Phys. Rev. Lett. 22 (1969) 1320

*2 recent reports are in B. Abbott et al.(LIGO Scientific Collaboration), Rep. Prog. Phys. 72 (2009) 076901 for LIGO: F. Acernese et al. (Virgo Collaboration), Class. Quantum Grav. 25 (2008) 114045 for Virgo

*3 M. Prijatelj, et al.:Class. Quantum Grav. 29 (2012) 055009.

*4 <http://gwcenter.icrr.u-tokyo.ac.jp/en/>

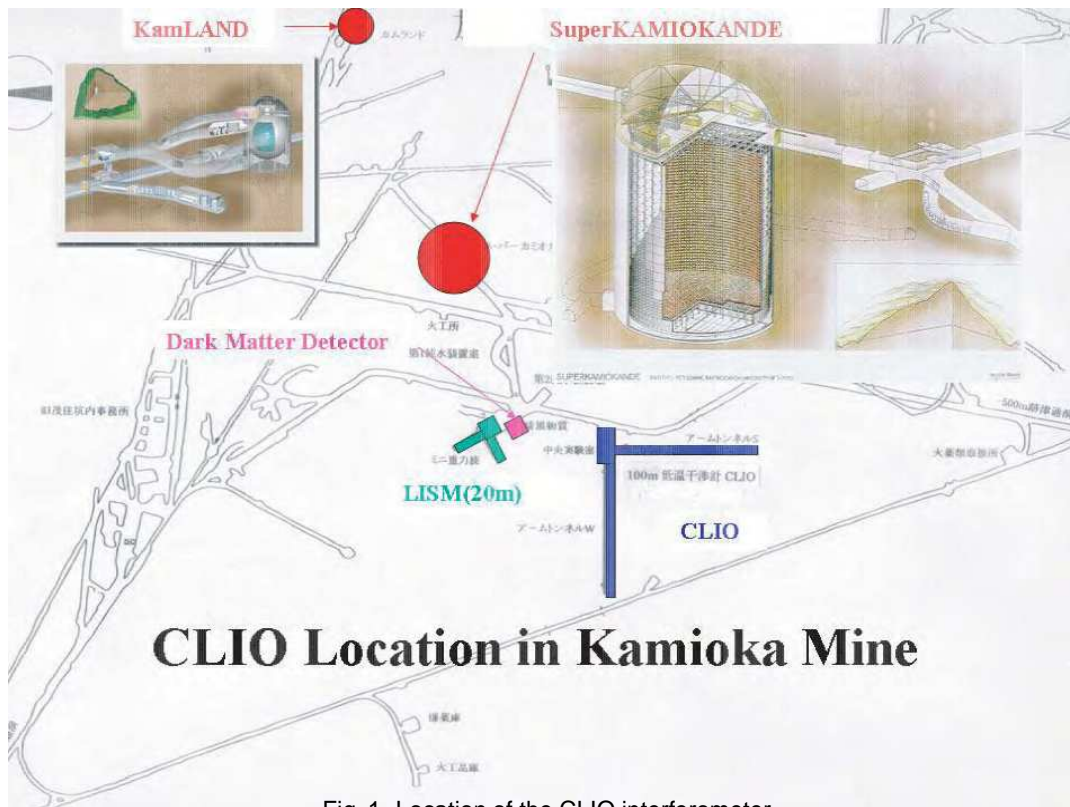


Fig. 1. Location of the CLIO interferometer.

20K had been done. We firstly observed the sensitivity improvement due to the mirror thermal noise reduction.

CLIO sensitivity curve with cooled mirrors (cryogenic sensitivity) and without cooling (300K sensitivity) are shown in Fig. 4 with estimation curves of the mirror thermal noise. The 300K sensitivity and the cryogenic sensitivity were measured at 2008/11/5 and at 2010/03/20, respectively. When the cryogenic sensitivity was measured, two front mirrors were cooled and the rest of two end mirrors were at the room temperature. Temperature of the front mirrors were 17K and 18K. Modifications possibly affecting the sensitivity at the cryogenic sensitivity measurement are exchange of final suspension wires and addition of heat link wires to the suspension systems. Cooling the mirror took about 250 hours and vacuum pressure was better than 10^{-4} Pa for both sensitivity measurements.

The noise floor⁵ level of the cryogenic sensitivity from 90Hz to 240Hz is below the 300K sensitivity. Observation range for GWs from neutron star binary coalescence was also improved to 159kpc from 148kpc for the optimum direction.

This is the first observation of sensitivity improvement by the cryogenic mirrors. The noise floor at 165Hz was reduced to $2.2 \times 10^{-19} \text{ m}/\sqrt{\text{Hz}}$ from $3.1 \times 10^{-19} \text{ m}/\sqrt{\text{Hz}}$ after cooling the front mirrors. Amount of this noise floor reduction is consistent with the estimation of mirror thermal noise reduction due to cooling. This achievement has been published in 2012 [6].



Fig. 3. A sapphire mirror and cryogenic suspension system

*⁵ Power spectrum of the output signal defines the sensitivity of the detector. The most sensitive part is the bottom of the curve and called by the word "floor."

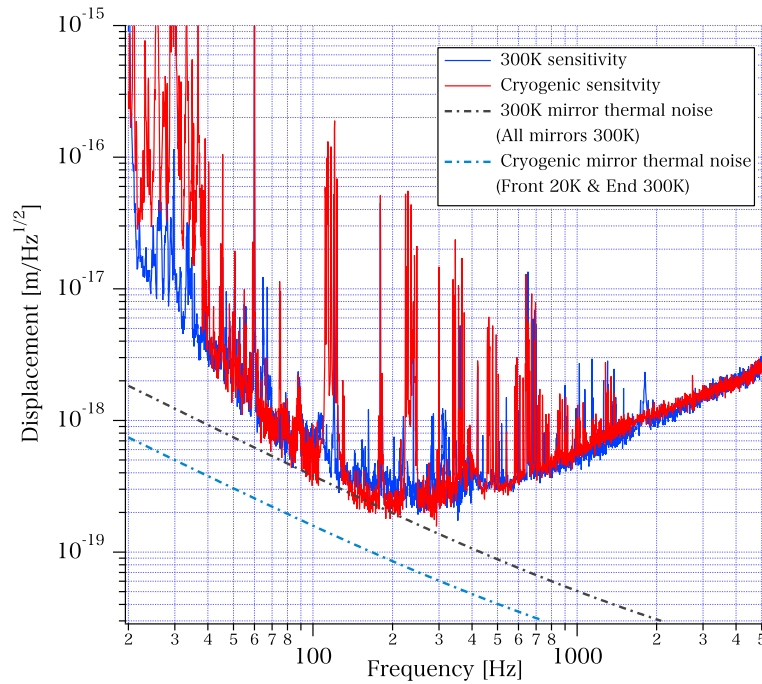


Fig. 4. Comparison of CLIO sensitivity curves. 300K sensitivity (solid blue line) and Cryogenic sensitivity (solid red line) show CLIO sensitivity curves without cooling mirrors measured at 2008/11/05 and with front mirrors under 20K measured at 2010/03/20, respectively. 300K mirror thermal noise (dot dash gray line) and Cryogenic mirror thermal noise (dot dash blue line) show estimation curve of mirror thermal noise corresponding to the each sensitivity measurements.

MC Locking Demonstration Using NQD method

We tried to demonstrate the Mode Cleaner (MC) lock acquisition using a newly developed method, which utilizes the expansion of linear range of the feedback loop in locking Fabry-Perot cavity with adjusting the demodulation phase to near Quadrature phase (NQD) [7]. CLIO has two RF sidebands, one is 11.97 MHz for the Mode Cleaner (MC) control and 15.804MHz(f_1) for 100m-FP arm cavity control. To obtain the NQD signal for MC whose FSR was same with f_1 , we shifted the RF sideband frequency f_1 to 15.844MHz(f_2) by 40kHz (in other words, $f_2 = FSR + 40\text{kHz}$), and we used f_2 as a demodulation frequency. In this manner, we could obtain the beat signal of 40kHz between the f_2 sideband and the laser frequency.

We verified that the expected NQD signals could be obtained and also succeeded to lock the MC using the NQD signal. Because of small offset in the error signals, the offset locking was sometimes observed. In addition to this, we also compared the lock acquisition under the condition that the PDH signal⁶ had beating wave forms because of the MC end mirror swing motion that was driven by addi-

tional force. We obtained preliminary results that lock acquisition success rate by NQD signals was much higher than that by the normal PDH signals, which showed the effectiveness of NQD method. However, for application to KAGRA interferometer we should consider that this time MC control loop that had 300kHz UGF helped a lot for the successful lock acquisition rate.

CLIO Collaboration

The spokesperson of CLIO is Masatake Ohashi, ICRR, Univ. of Tokyo.

Institute	Country	(*)
ICRR, University of Tokyo (abbreviated as UT)	Japan	10
Earthquake Research Institute (UT)	Japan	2
Department of Physics (UT)	Japan	1
Department of Engineering (UT)	Japan	2
High Energy Accelerator Research Organization (KEK)	Japan	4

^{*6} Pound-Drever-Hall method to extract modulated signal from the cavity: R. W. P. Drever, *et al.*, Appl. Phys. B **31** (1983) 97-105.

Institute	Country	(*)
National Astronomical Observatory (NAOJ)	Japan	7
Department of Physics (Osaka City University)	Japan	1
Metrology and Measurement Science (National Institute of AIST)	Japan	1
California Institute of Technology	USA	1
Department of Physics (Tokyo Institute of Technology)	Japan	1
TERC, University of Tsukuba	Japan	1
Department of Earth and Space Science (Osaka University)	Japan	1
Department of Physics (Kyoto University)	Japan	1
Department of Humanities (Yamanashi Eiwa College)	Japan	1
Advanced Research Institute for the Sciences and Humanities (Nihon University)	Japan	1
Total		35

(*) Number of participants as of March 2012.

Members (as of July 2012)

Staffs

Kazuaki Kuroda, Professor, April 1992 to the present

Seiji Kawamura, Project Associate Professor, November 2010 to June 2011; Professor, July 2011 to the present

Masatake Ohashi, Assoc. Professor, March 1999 to the present

Shinji Miyoki, Research Associate, April 1998 to June 2012/Assoc. Professor, July 2012 to the present

Ryutaro Takahashi, Project Research Associate, November 2010 to the present

Takashi Uchiyama, Research Associate, February 2003 to the present

Kazuhiro Yamamoto, Project Research Associate, April 2011 to the present

Osamu Miyakawa, Project Research Associate, November 2008 to the present

Naoko Ohishi, Project Research Associate, November 2009 to March 2012

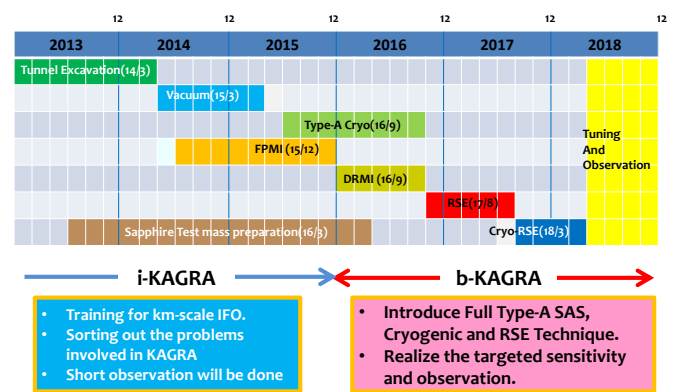


Fig. 5. Planned schedule of KAGRA. Beginning two years of iKAGRA are omitted in this figure. That is, 5 year iKAGRA corresponds to 2015.

Graduate Students

Two students were awarded doctor degrees and three students earned master degrees during 2006–2012, supervised by ICRR staff members.

KAGRA project

Overview of KAGRA

KAGRA (The new nickname has been given for LCGT : Large-scale Cryogenic Gravitational wave Telescope), as one of the world network of gravitational wave detectors, aims at the detection of gravitational waves by a 3 km baseline laser interferometer with cryogenic mirror subsystem placed underground at Kamioka.

The development of KAGRA started as a 6.5 year project in October 2010, but later it was rescheduled as a 7.5 year project due to the suspension of the budget for the start of tunnel excavation as a result of the Great East Japan Earthquake which occurred on March 11, 2011. The KAGRA development is divided into two stages: initial KAGRA (iKAGRA) and baseline KAGRA (bKAGRA) (shown in Fig. 5). In the 5 year iKAGRA stage the mirror subsystem will be kept at room temperature without SAS (Seismic Attenuation System) and RSE (Resonant Sideband Extraction) in operation while the bKAGRA is the latter 2.5 year development stage where the final goal is to be pursued with full equipment in operation including SAS, cryogenic subsystem and RSE.

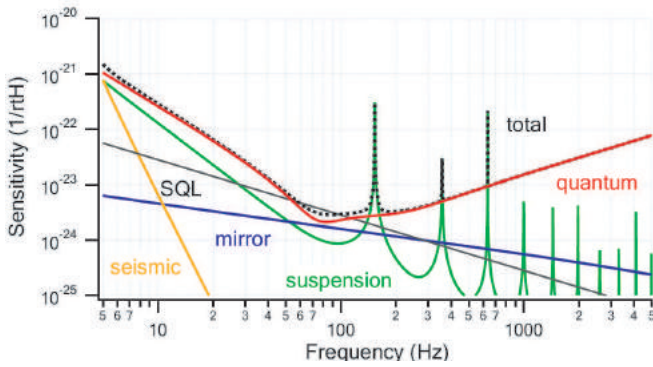


Fig. 6. Ultimate sensitivity limit of KAGRA.

The host organization to conduct the KAGRA project is the Institute for Cosmic Ray Research, the University of Tokyo with a number of organizations both domestic and international involved. Up to now 31 Japanese and 32 overseas universities and research institutes have joined the KAGRA collaboration and still increasing. The official agreements to establish international collaborations have been exchanged between ICRR and 7 foreign institutes.

KAGRA, in the final configuration of bKAGRA, is designed to achieve the aim to detect gravitational-wave signals. Among several expected gravitational-wave sources, the primary observation target is selected to be an inspiral and merger of neutron-star binary. This is because it is the most certain source: its existence has been proved by radio-pulsar surveys, and its event rate has been theoretically estimated from astronomical observation results.

It is required that the KAGRA sensitivity be high enough to realize more than one detection of gravitational waves from neutron-star binaries in a one-year observation run with probability 90% or higher. For the requirement, the KAGRA duty factor must be higher than 80% and the observation range must be larger than 180 Mpc. Here the signal-to-noise ratio is 8 and the normal incidence of gravitational waves on to the detector is assumed.

Figure 6 shows the estimated ultimate sensitivity limits of KAGRA where incoherent sum of the fundamental noise sources is assumed. The observation range with the ultimate sensitivity limit of KAGRA is 280 Mpc.

With the currently-practical design parameter set for bKAGRA, the sensitivity limited by fundamental noise sources gives the observation range of 240Mpc. The requirement allocation to each sub-

system is determined in such a way as not to deteriorate the sensitivity more than 10% in total. It is also required to each subsystem that the duty factor of KAGRA during the observation run be 80% or higher in total. More detailed requirement allocation is shown in the Interface Control Document (ICD).

The requirement for KAGRA is to be flowed down into that for each of the subsystems. Required values for the subsystem components are determined in such a way that the KAGRA target sensitivity be achieved with all the noise curves summed up in the spectrum. Some of the setup parameters are shared by multiple subsystems and those interface parameters shall be controlled by the System Engineer Office (SEO), where the manpower organization of KAGRA project is shown in Fig. 7.

The following is the summary of major advancement of KAGRA project.

Tunnel

KAGRA interferometer will be placed underground at Kamioka with two 3km arms. Those arms cross perpendicularly at the center of Beam Splitter (BS) chamber in center area. Schematic design view of the center area is shown in Fig. 8, where two arms called by X arm and Y arm. The location of the center of the BS chamber is latitude of 36.41°N and longitude of 137.31° . Altitude of the floor of the BS chamber from the sea level is 372m. Y arm is rotated by 28.31° from the North to the West. KAGRA has three important areas, center, Xend (end side of the X arm) and Yend (end side of the Y arm), where the test mass vacuum chambers will be placed. Those areas are located to be inside more than 200m from the surface of the mountain for the small seismic motion.

The tunnel design was made with Suncoch consultant for the bid of tunnel construction. Kajima corporation won the bid and is responsible for the tunnel construction. After the excavation, construction of a drainage system, splaying concrete on the tunnel surface, and making floors will be done as the finish of the tunnel construction.

The tunnel excavation has started in May, 2012, where two teams are digging from the Y arm end and the new Atotsu entrance, respectively. By September, 2012, the Y end experimental room has been finished and 400 m tunnel has been excavated in the new Atotsu entrance.

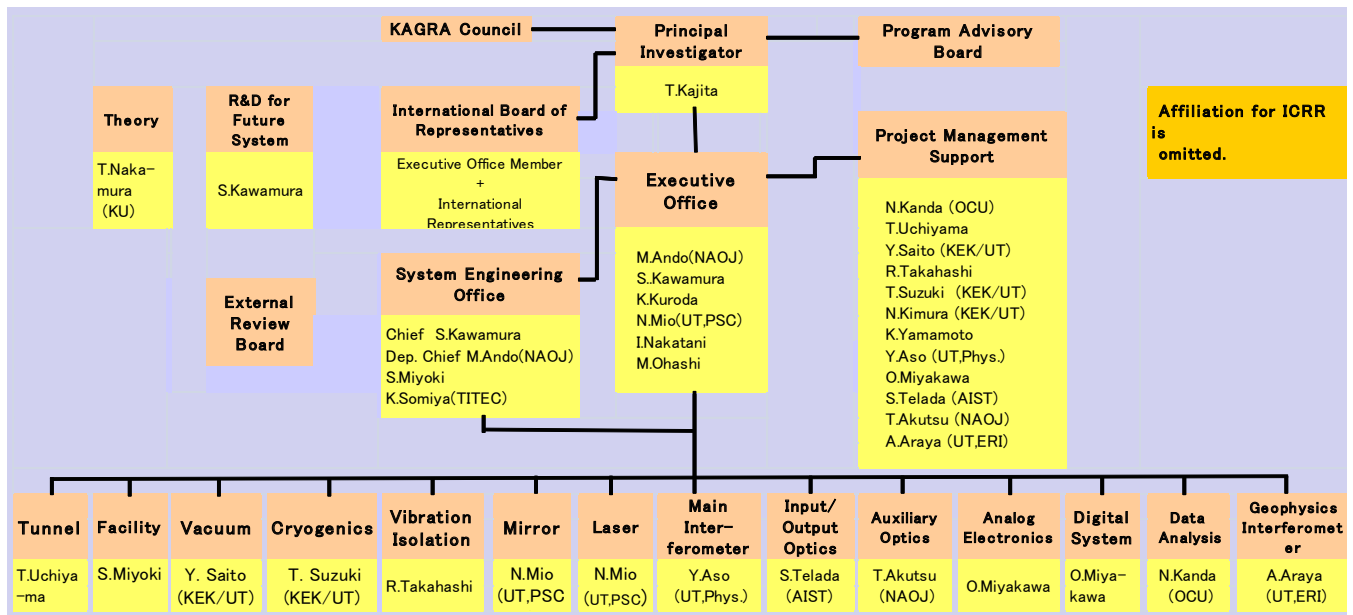


Fig. 7. Manpower organization chart of KAGRA project.

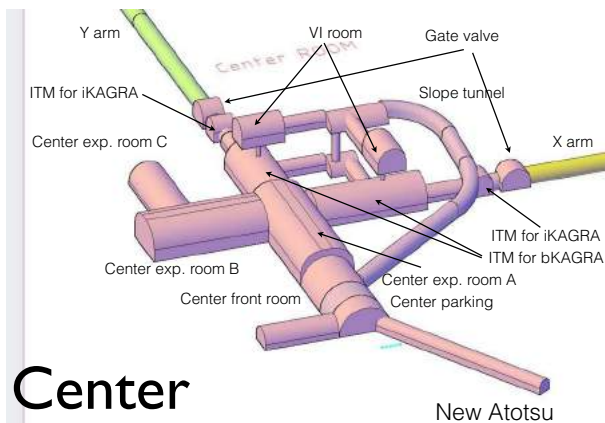


Fig. 8. Schematic view of center area at underground location of KAGRA.

Vacuum subsystem

The substantial items of the KAGRA Vacuum Subsystem are manufacturing and installing the two beam tubes of 3-km long and 800 mm in diameter, as well as 21 of chambers for the mirrors with suspension and vibration isolation devices. Optical baffles installed at every 12 m in the beam tube for suppressing small angle scattering from the main mirrors are also to be designed so that the structure and surface-finish are optimized for optical and vacuum performance. Further, overall layout of the vacuum chambers and interconnecting tubes and Gate Valves are to be managed by the vacuum group[8].

In order to realize the ultra-high vacuum, the outgassing rate of the materials for component use is to be reduced to the order of $10^{-8} \text{ Pa m}^3 \text{ s}^{-1} \text{ m}^{-2}$, or lower, for 50 hours pumping. The stainless-steel material SS314L and 316 are chosen for beam tube and bellows, respectively. The inner surface of the unit tube (12-m long and 800 mm in diameter) after welding flanges and bellows is processed by electropolishing so as to remove $30 \mu\text{m}$ of the surface degraded layer. A pre-baking process at 200°C for 20 hours is finally performed to the unit tube in order to passivate the surface layer. The result of outgassing rate measured for a tube shows a value of the order of $10^{-9} \text{ Pa m}^3 \text{ s}^{-1} \text{ m}^{-2}$ for 100 hours of pumping. For fiscal years of 2010 and 2011, 320 of 500 beam tubes are manufactured and transferred to a storage place at Kamioka (Fig. 9).

Cryogenic subsystem

Subject of the subsystem is to carry out designing, prototype test, manufacture inspection, storage, transportation, installation and adjustment for those equipments of cryochambers, cryocooler units, shield ducts, monitoring instruments and cryogenic payloads.

Specifications of chambers accord with the instruction of vacuum subsystem. Decision to use a new material was made after passing the measurement of outgassing rate. For example, measurements were made for a new type of thermal insu-



Fig. 9. Tube delivery to the storage tunnel.

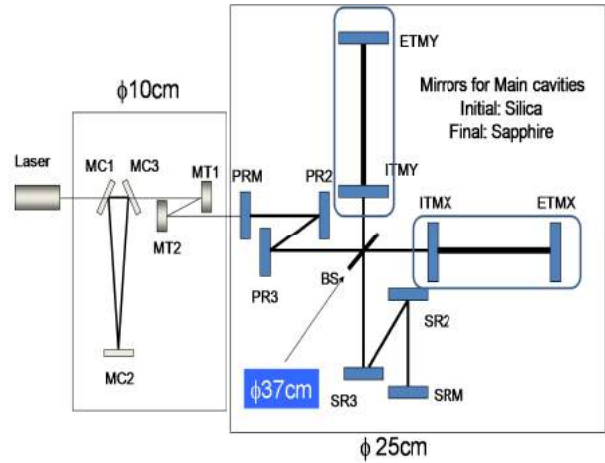


Fig. 12. Mirrors for Main cavities with input & output recycling cavities.

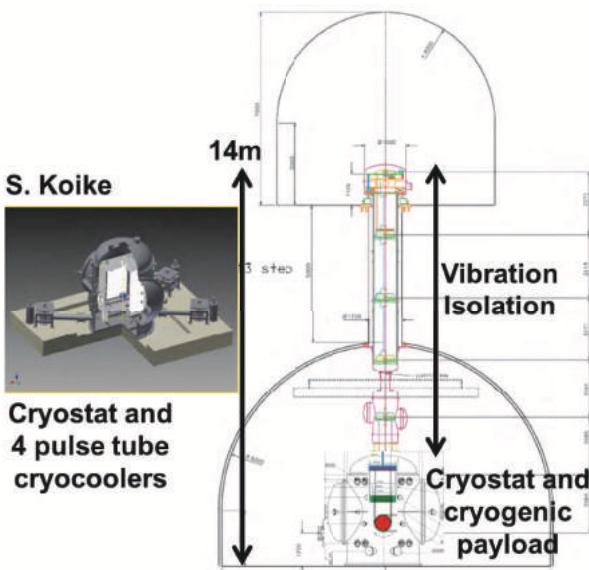


Fig. 10. Cryogenic subsystem consists of a large cryostat with 4 cryocoolers and a cryogenic suspension system.

lation film and bulk of polyimide.[9] Tolerances of machining accord with JIS B0405 standard.

The schematic design of cryogenic subsystem is shown in Fig. 10, which is compatible with vibration isolation subsystem in a vacuum. Design of cryochambers and 4K cryocooler units were finished.[83] Those equipments are in manufacturing.

The heat radiation coming from the vacuum duct maintained at room temperature was shown to be suppressed by infrared optical baffles placed in front of the cooled mirror. We measured the surface emissivity of the material used for radiation shield.[10]

Vibration Isolation

All mirrors used in KAGRA are suspended through vibration isolation system. There are two purposes required for this isolation subsystem. One is attenuation of seismic noise in the observation band (less than 4×10^{-20} m/ $\sqrt{\text{Hz}}$ at 10 Hz). The other is reduction of RMS displacement or RMS velocity of mirrors (less than $0.1 \mu\text{m}$ or $0.1 \mu\text{m/s}$). Three kinds of system are disposed to 21 vacuum chambers to accomplish their purposes. Main mirrors are isolated by Type-A system, which consists of an inverted pendulum (IP), five stage geometric anti-spring (GAS) filters and a cryogenic mirror suspension. Other core optics is isolated by Type-B system, which consists of an IP, three stage GAS filters and a mirror suspension. Small optics is isolated by Type-C system, which consists of three stages stack and a mirror suspension. Schematic view of Type-A/B system is shown in figure 11. The mirror suspension is called “payload.” Type-A test mass is a sapphire mirror of 22 cm in diameter, 15 cm in thickness and 23 kg in weight. Type-B test mass is a silica mirror of 25 cm in diameter, 10 cm in thickness and 10 kg in weight. GAS filters are linked by connection wires each other. The GAS blades and the connection wires are made of maraging steel. The top part is called “pre-isolator” which consists of IP and top filter. The diameter of the top filter is larger than that of standard filter’s to reach lower resonant frequencies and to suspend a larger total mass.[11]

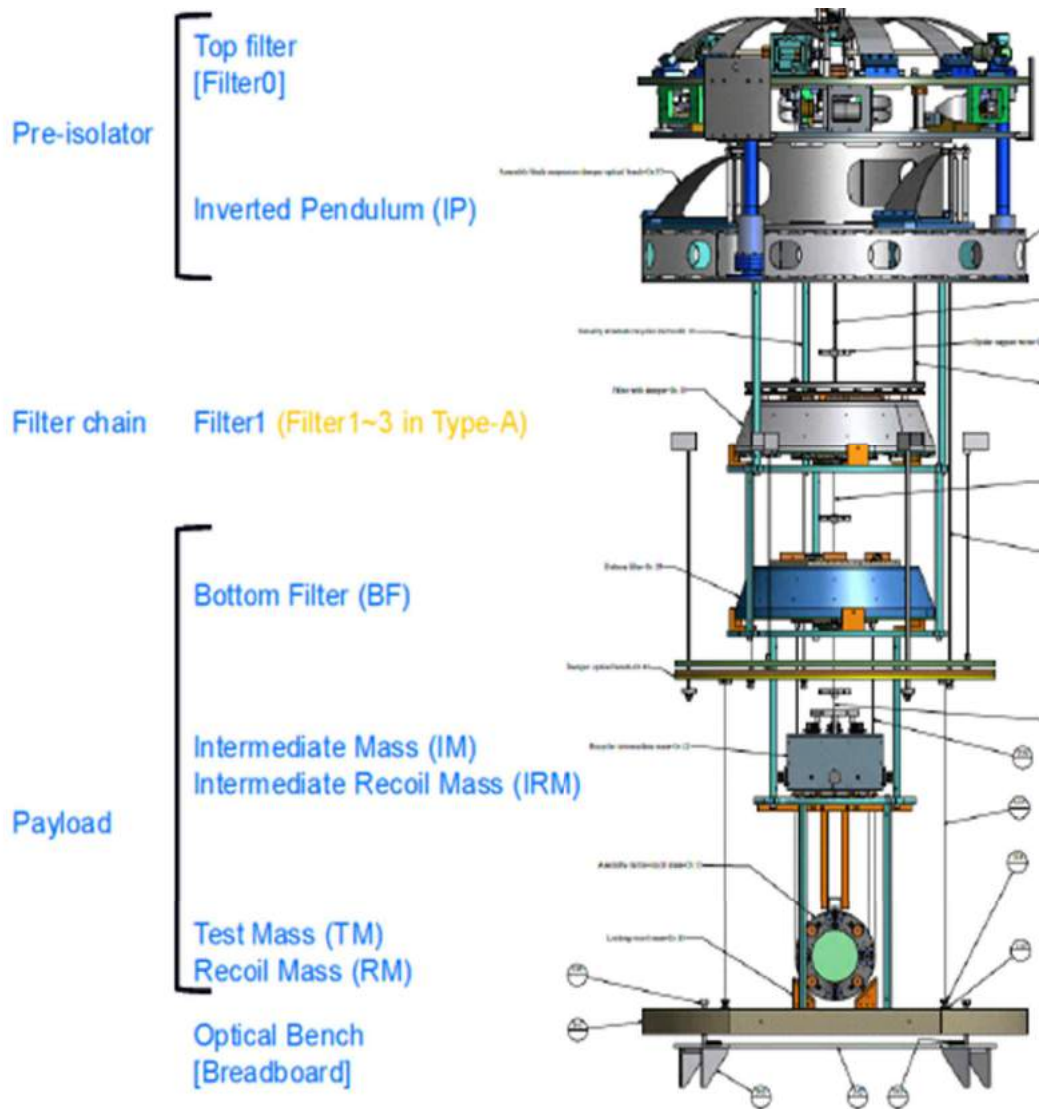


Fig. 11. Schematic view of Type-A/B system. Type-A system has additional two filters (Filter2 and 3). The payload for Type-A system is cryogenic (see Fig. 10).

Mirror

Mirrors for the main cavities are initially made of silica for iKAGRA and will be changed to sapphire for bKAGRA. The beam splitter and mirrors that will be used in room temperature are all made of silica. The diameter of the mirrors is set to 25 cm in order to suppress the diffraction loss; the size is the same as that of initial LIGO mirrors. As for sapphire mirrors, the diameter is limited to 22 cm because of the size of the sapphire mono-crystal. The diameter of the beam-splitter (BS) is also the same as that of aLIGO in order to reduce the cost for fabrication. For small mirrors such as mirrors for the mode-matching telescope and the mode cleaner, the diameter is 10 cm.

The basic design of the optics for bKAGRA is

the same as that of iKAGRA. The most significant difference is that sapphire is used for the test masses. The absorption of sapphire is 30 ppm/cm at present. It is not enough for the initial requirements of KAGRA. However, these issues might be solved before the installation of bKAGRA. We will be making efforts to realize the requirements.

Main Interferometer

The main interferometer (MIF) is a subsystem which is responsible for converting gravitational waves into electronic signals on a photodetector (PD). It includes two arm cavities, the power recycling cavity and the signal recycling cavity. The MIF subsystem also provides specifications for out-

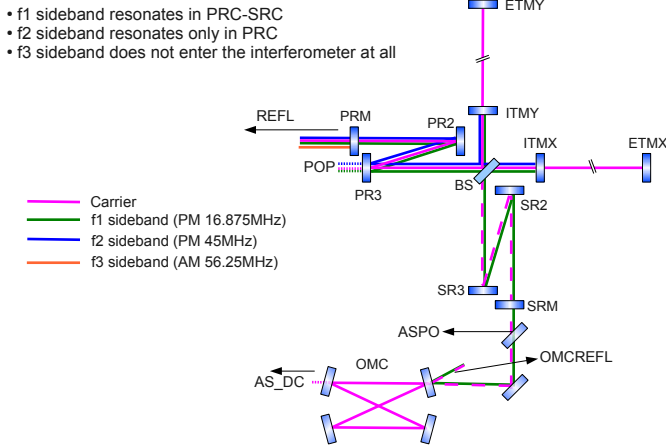


Fig. 13. Sideband resonant conditions and signal ports in bK-AGRA interferometer design.

put mode cleaner, which will be manufactured by the input/output optics subsystem. The MIF team is also responsible for the development of the robust interferometer sensing and control schemes, both for length and alignment. The team will design the necessary electronic circuits, such as PDs, demodulation boards etc. After the mirrors are installed in the vacuum system, the MIF team will be mostly responsible for the commissioning of the interferometer to achieve the target sensitivity as early as possible.

The minimum goal of iKAGRA is to lock a Fabry-Perot Michelson interferometer. Although we will do our best to operate the iKAGRA interferometer in the best condition, we plan not to consume much time and manpower in pursuing higher duty factor and better sensitivity. The design of iKAGRA is set to be a natural pass point to bKAGRA. Details of the design are explained in **JGW-T1200913**, which is found at <http://gwdoc.icrr.u-tokyo.ac.jp/cgi-bin/DocDB/DocumentDatabase>.

The main goal of the bKAGRA interferometer is to achieve the target sensitivity while keeping the duty factor of the interferometer above 90%.

The optical configuration, parameters and the control scheme for the bKAGRA interferometer have been almost fully determined by Spring, 2012. The design is documented in detail in the KAGRA document (at the above web-site).

Figure 13 shows the design of the main interferometer on sideband resonant conditions and signal ports.

Input/output subsystem

Input Output Optics (IOO) subsystem provides the input optics system, located between the laser and the power recycling mirror, and the output optics system. Some parts of the output optics systems are assigned to the Auxiliary Optics Subsystem (AOS). IOO prepares various optical components excluding the core optics and is also in charge of the facility for the laser.

An optical design of input optics system is shown in Fig. 14. Optics components in front of the mode cleaner are placed on an optical table in the laser room. The mode cleaner, the Faraday isolator and mirrors for the mode matching telescope are placed in vacuum. Frequency stabilization and intensity stabilization of laser beam is performed by the reference cavity, the pre-mode cleaner and the mode cleaner.

Digital subsystem

Digital subsystem is in charge of development of a whole real time control system for a km scale interferometer with flexible human interfaces. Digital subsystem is a key system to operate interferometer and all subsystems for control/monitor/diagnostic/tuning (Fig. 15).

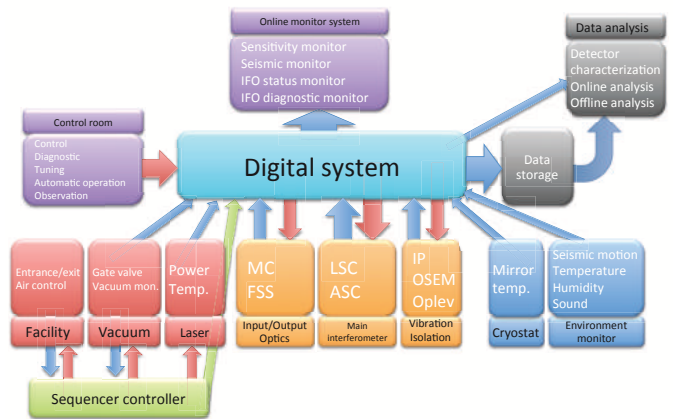


Fig. 15. Interferometer is controlled by Digital Subsystem

We started a prototype test for single Real Time (RT) PC at CLIO from 2009. The channel numbers was not so many, but we tested important basic functions for IFO operation like lock acquisition, calibration, noise performance check. Then we decided to deliver standalone(STDA) systems for development subsystem with a digital control. This STDA system is based on experiences at CLIO prototype test. By the end of FY2011 we distributed

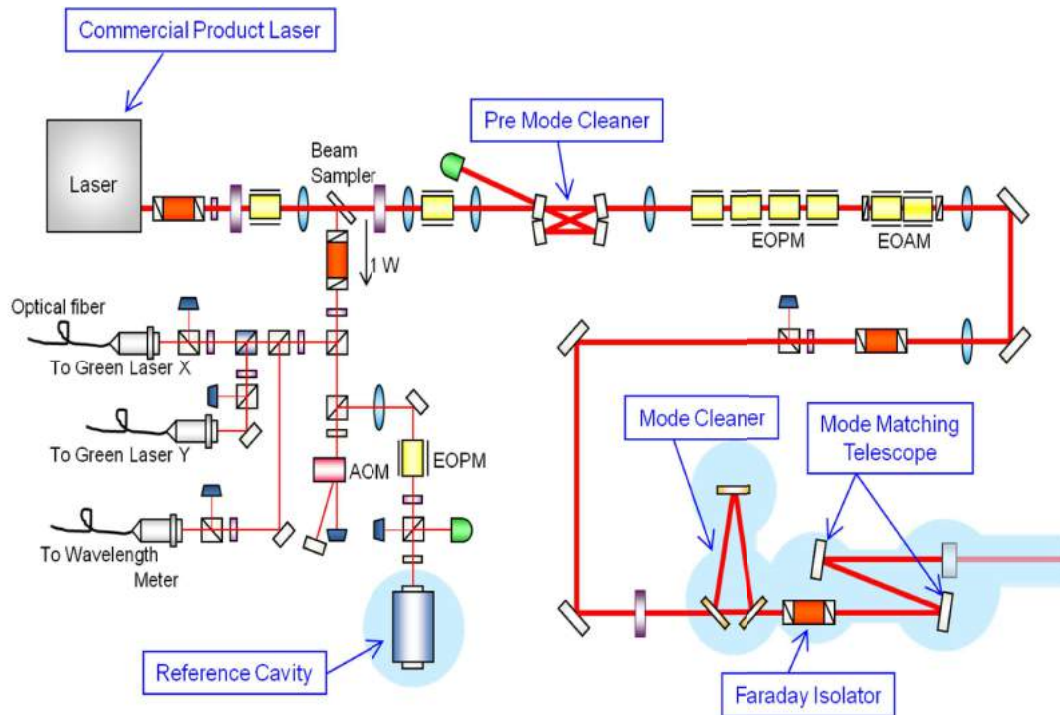


Fig. 14. Optical design of input optics system.

two STDA systems. One is to data analysis group for testing frame data and data analysis software, and another one is to vibration isolation subsystem for controlling a Pre-Isolator. We are preparing another STDA system for monitoring temperatures in a cryostat.

In parallel with delivering STDA system, we tested a network connection using 2 or 3 RT control computers in FY2011. Real time control using a single computer is not so difficult, but when two or more computers are connected, real time control will be much more difficult due to network bandwidth, latency, synchronization etc. This setup will be extended to a large scale network system in FY2012 with 7-10 server PCs and 5 RT PCs for an important test as a full network operation with enough network bandwidth, latency and redundancy. This large scale test is performed on the new floor of Hokubu-Kaikan at Kamioka. This large network system will be moved and installed into mine directly and it will be an actual full system for commissioning.

Data taking & analysis

Coordination of “Data Analysis Subsystem (DAS)” covers the acquisition, the storage and the management of observational data. The outline of this subsystem is illustrated in Fig. 16.

DAS subsystem introduce two preprocess servers at Kamioka facility. One is for the data acquisition and the data transfer, and the other is for the detector characterization and backup of the 1st system. The rate of data produced by KAGRA is about 70 GB/hour. For the one month science mode observation of iKAGRA, 50 TB of data are produced. Beside those science mode data, data are produced during the commissioning phase. For the detector characterization and the commissioning, we want to store the several months of data at the detector’s site and the main storage system. For this purpose, three data storage systems will be introduced. Two systems are introduced to the above pre-process servers and each has 200 TB. The 3rd system is the master data storage system with storage size of 500 TB and is introduced at ICRR-Kashiwa. The 3rd system is used for the off-line data analysis and the data archive.

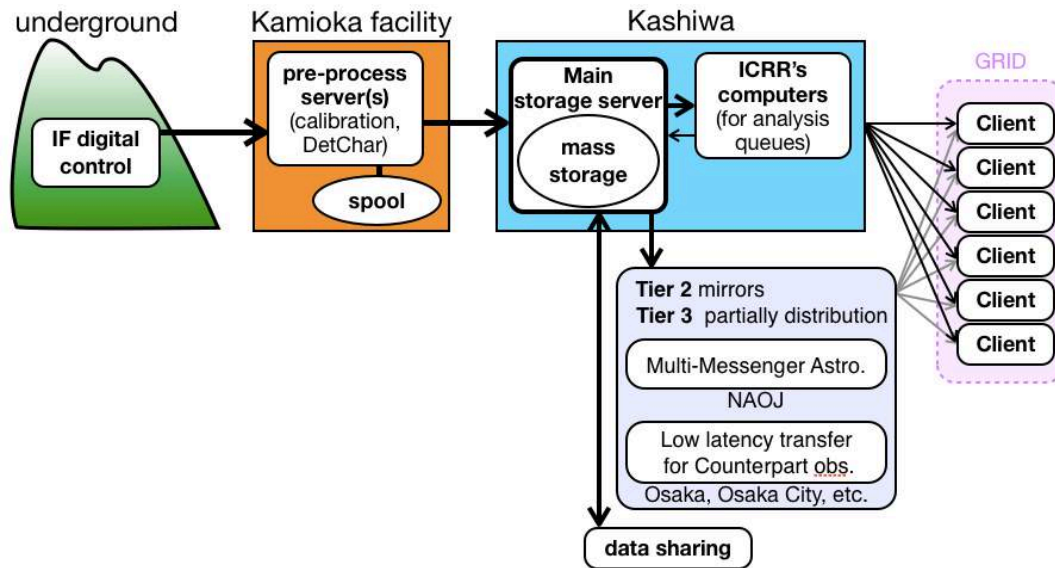


Fig. 16. Schematic outline of the Data Analysis Subsystem

For iKAGRA observation, DAS subsystem will have to provide the continuous and stable data acquisition, storage and pipelines for gravitational wave event searches. Raw data rate is estimated about 70 GB/hour. Network transfer and the pre-process server throughput must be faster than this. Main data storage will be placed at ICRR-Kashiwa. Roughly 1 PByte/year is needed for the storage of KAGRA experimental data only (more than 600TByte raw data + simulation data×effective duty time of the operation×mirroring). International data sharing (5sites = KAGRA + LIGO*2 +Virgo + “fifth-site”) will reach to 5PB/year.

Outreach activity

The rapidly changing status of KAGRA is presented in several international conferences.[82] There are also special articles presented in journals of academic societies.[2] We also present activity in our web-page.⁷

Summary

After the long time of R&D for LCGT (now, KAGRA), funding for construction was approved in 2010. The achievement of CLIO cryogenic sensitivity contributed to this funding. Organization of manpower was restructured by involving KEK and NAOJ for the success of the KAGRA project. Planning and detailed design stages have been almost

finished. Tunnel excavation started in May, 2012 and manufacturing vacuum pipes has been completed about 80% by September, 2012. We plan to assemble the basic structure of the KAGRA detector and let it be in operation as the detector of iKAGRA by 2015 and after improvement with cryogenic system and advanced optical configuration, observation by bKAGRA with the objective sensitivity will be initiated in FY 2017. Hiring the resources and manpower of overseas projects is constructively pursued and strategy to collaborate in data-analysis is being considered.

KAGRA Collaboration

The spokesperson of KAGRA is Takaaki Kajita, ICRR, Univ. of Tokyo. The project manager is Ichiro Nakatani, one of guest professors of ICRR from Aichi University of Technology.

Institute	Country	(*)
ICRR, University of Tokyo (abbreviated as UT)	Japan	22
National Astronomical Observatory (NAOJ)	Japan	13
High Energy Accelerator Research Organization (KEK)	Japan	7
Department of Physics (UT)	Japan	11
Research Center for the Early Universe (UT)	Japan	3

^{*7} <http://gwcenter.icrr.u-tokyo.ac.jp/en/>

Institute	Country	(*)	Institute	Country	(*)
Institute for Laser Science (University of Electro-Communications)	Japan	4	Faculty of Science (University of the Ryukyu)	Japan	1
Department of Advanced Materials Science (UT)	Japan	6	Max Planck Institute for Gravitational physics (AEI)	Germany	1
Earthquake Research Institute (UT)	Japan	2	California Institute of Technology	USA	4
Department of Astronomy (UT)	Japan	1	Department of Physics (University of Western Australia)	Australia	5
Department of Physics (Osaka City University)	Japan	3	Department of Physics (Louisiana State University)	USA	1
Faculty of Engineering (Hosei University)	Japan	4	Center for Computational Relativity and Gravitation (Rochester Institute of Technology)	USA	1
Metrology and Measurement Science (National Institute of AIST)	Japan	3	Department of Physics (Glasgow University)	UK	1
Space-Time Standards Group (National Institute of Information and Communication Technology)	Japan	1	Columbia Astrophysics Laboratory (Columbia University in the city of New York)	USA	1
Department of Earth and Space Science (Osaka University)	Japan	4	Department of Astronomy (Beijing Normal University)	China	1
Department of Physics (Kyoto University)	Japan	3	Information Science and Technology (Tsinghua University)	China	1
Yukawa Institute for Theoretical Physics (Kyoto University)	Japan	6	Inter University Center for Astronomy & Astrophysics (Pune University)	India	3
Department of Humanities (Yamanashi Eiwa College)	Japan	1	Sternberg State Astronomical Institute (Moscow University)	Russia	1
Sokendai	Japan	1	LATMOS (CNRS)	France	1
School of Science and Engineering (Teikyo University)	Japan	1	Center for Astrophysics (University of Science and Technology of China)	China	1
Graduate School of Humanities and Sciences (Ochanomizu University)	Japan	2	Shanghai United Center for Astrophysics (Shanghai Normal University)	China	3
Advanced Research Institute for the Sciences and Humanities (Nihon University)	Japan	1	Center for Astrophysics (Tsinghua University)	Taiwan	1
Department of Advanced Physics (Hirosaki University)	Japan	1	Center for Measurement Standards (Industrial Technology Research Institute)	Taiwan	2
Astronomical Institute (Tohoku University)	Japan	2	ARTEMIS (CNRS)	France	1
Department of Physics (Niigata University)	Japan	1	Department of Astronomy (Maryland University)	USA	1
Department of Physics (Rikkyo University)	Japan	2	Department of Engineering (University of Sannio at Benevento)	Italy	2
College of Industrial Technology (Nihon University)	Japan	1	Department of Physics (Korea University)	Korea	1
Department of Physical Science (Hiroshima University)	Japan	1			

Institute	Country	(*)
College of Natural Science (Inje University)	Korea	1
Department of Physics and Astronomy (Seoul University)	Korea	1
Department of Physics (Myongji National University)	Korea	1
Quantum Optics Center (Korea Atomic Energy Research Institute)	Korea	1
Department of Physics (Hanyang University)	Korea	1
Department of Physics (Pusan National University)	Korea	1
Korea Institute of Science and Technology of Information	Korea	1
National Institute of Mathematical Sciences	Korea	2
Department of Astronomy and Atmospheric Sciences (Kyungpook National University)	Korea	1
Department of Physics (Gunsan National University)	Korea	1
Korean Institute for Advanced Study	Korea	1
Shanghai Institute of Ceramics (Chinese Academy of Sciences)	China	3
Total		156

(*) Number of participants as of March 2012.

Members (as of July 2012)

Staffs

Kazuaki Kuroda, Professor, April 1992 to the present

Seiji Kawamura, Project Associate Professor, November 2010 to June 2011; Professor, July 2011 to the present

Masatake Ohashi, Assoc. Professor, March 1999 to the present

Shinji Miyoki, Research Associate, April 1998 to June 2012/Assoc. Professor, July 2012 to the present

Ryutaro Takahashi, Project Research Associate, November 2010 to the present

Takashi Uchiyama, Research Associate, February 2003 to the present

Kazuhiro Yamamoto, Project Research Associate, April 2011 to the present

Osamu Miyakawa, Project Research Associate, November 2008 to the present

Postdoctoral Fellows

Eiichi Hirose, April 2011 to the present

Daniel Friedrich, March 2012 to the present

Graduate Students

Four students were awarded doctor degrees and five students earned master degrees during 2006–2012, supervised by ICRR staff members.

List of Publications

Before Year 2006

Papers in Refereed Journals

- [1] “Stable Operation of A 300-m Laser Interferometer with Sufficient Sensitivity To Detect Gravitational-wave Events within our Galaxy”, M. Ando et al., *Phys. Rev. Lett.* **86** (2001) 3950.

After Year 2006

Papers in Refereed Journals

- [2] K. Kuroda, “Large-scale Cryogenic Gravitational wave Telescope (LCGT) -Construction Status of LCGT project-”, *J. Cryo. Super. Soc. Jpn* **46** (2011) 385 (in Japanese).
- [3] “A 100 m laser strainmeter system in the Kamioka Mine, Japan, for precise observations of tidal strains”, S. Takemoto, *et al.*, *Journal of Geodynamics* **41** (2006) 23.
- [4] “Underground Cryogenic Laser Interferometer CLIO”, S. Miyoki, *et al.*, *Journal of Physics: Conference Series* **203** (2010) 012075.
- [5] T. Uchiyama and S. Miyoki, “Experimental Demonstration of Cryogenic Mirror Technique - Achievements of CLIO-”, *J. Cryo. Super. Soc. Jpn.*, **46** (2011) 392-399.

- [6] Takashi Uchiyama, Shinji Miyoki, Souichi Telada, Kazuhiro Yamamoto, Masatake Ohashi, Kazuhiro Agatsuma, Koji Arai, Masa-Katsu Fujimoto, Tomiyoshi Haruyama, Seiji Kawamura, Osamu Miyakawa, Naoko Ohishi, Takanori Saito, Takakazu Shintomi, Toshikazu Suzuki, Ryutaro Takahashi, Daisuke Tatsumi, "Reduction of thermal fluctuations in a cryogenic laser interferometric gravitational wave detector", *Phys. Rev. Lett.* **108**, 141101 (2012).
- [7] S. Miyoki, S. Telada and T. Uchiyama, "Expansion of linear range of Pound-Drever-Hall signal", *Applied Optics*, **49**, Issue 28, pp.5217-5225 (2010).
- [8] R. Takahashi, Y. Saito, "Vacuum-system Design for the Large-scale Cryogenic Gravitational wave Telescope", *Vacuum* **84** (2010) 709-712.
- [9] T. Ohmori *et al.*, "Vacuum and Insulation Technology for Large-scale Cryogenic Gravitational wave Telescope (LCGT)", *J. Cryo. Super. Soc. Jpn* **46** (2011) 408 (in Japanese).
- [10] Y. Sakakibara *et al.*, "Emissivity of radiation shield metal in cryogenic temperature at wavelength $10\mu\text{m}$ for Large scale Cryogenic Gravitational wave Telescope", *J. Cryo. Super. Soc. Jpn* **46** (2011) 434 (in Japanese).
- [11] R. Takahashi, "Vibration Isolation System for Mirrors", *J. Vac. Jpn* **54** (2011) 24-27.
- [12] Seiji Kawamura, et al., "The Japanese space gravitational wave antenna: DECIGO", *Class. Quantum Grav.* **28** (2011) 094011.
- [13] Shinji Miyoki, LCGT Collaboration, "Quest for Direct Detection of Gravitational Waves and Large-scale Cryogenic Gravitational wave Telescope (LCGT) Project in Japan", *Journal of the Vacuum Society of Japan*, **54** (2012) 587-596 (in Japanese).
- [14] Yoichi Aso, LCGT Collaboration, "Optical Configuration and Control of Ultra-sensitive Gravitational Wave Detectors", *Journal of the Vacuum Society of Japan*, **54** (2012) 597-603 (in Japanese).
- [15] Noriaki Ohmae, Norikatsu Mio, "Characteristics of Laser System Used in Large-Scale Cryogenic Gravitational Wave Telescope", *Journal of the Vacuum Society of Japan*, **54** (2012) 604-609 (in Japanese).
- [16] Ryutaro Takahashi, "Vibration Isolation System for Mirrors", *Journal of the Vacuum Society of Japan*, **54** (2012) 610-613 (in Japanese).
- [17] Takanori Saito, Souichi Telada, Takashi Uchiyama, Shinji Miyoki, Osamu Miyakawa, Masatake Ohashi, "Development of Cryogenic Laser Interferometer Observatory (CLIO) and Local Suspension Point Interferometer (LSPI) in Kamioka", *Journal of the Vacuum Society of Japan*, **54** (2012) 614-620 (in Japanese).
- [18] Yoshio Saito, Ryutaro Takahashi, "Production Process of the Interferometer Beam Tubes in LCGT Project", *Journal of the Vacuum Society of Japan*, **54** (2012) 621-626 (in Japanese).
- [19] H. H. Lim, T. Katagai, S. Kurimura, T. Shimizu, K. Noguchi, N. Ohmae, N. Mio, I. Shoji, "Thermal performance in high power SHG characterized by phase-matched calorimetry", *OPTICS EXPRESS* **19** (23) (2011) 22588-22593.
- [20] Takayuki Tomaru, Hiroaki Hoshikawa, Hiroshi Tabuchi, Takakazu Shintomi, "Conduction Cooling Using Ultra-pure Fine Metal Wire I -Pure Aluminum-", *J. Cryo. Super. Soc. Jpn*, **46** (2011) 415-420 (in Japanese).
- [21] Takakazu Shintomi, Takayuki Tomaru, Kenji Yajima, "Conduction Cooling Using Ultra-pure Fine Metal Wire II -Pure Copper-", *J. Cryo. Super. Soc. Jpn*, **46** (2011) 421-425 (in Japanese).
- [22] Kazuhiro Yamamoto, "Cryogenic Mirror: The State-of-the-art in Interferometric Gravitational Wave Detectors-", *J. Cryo. Super. Soc. Jpn*, **46** (2011) 426-433 (in Japanese).
- [23] J. Abadie, B.P. Abbott, R. Abbott, et al., "Search for gravitational waves associated with the August 2006 timing glitch of the Vela pulsar", *Physical Review D* **83** (2011) 042001.

- [24] S. Hild, M. Abernathy, F. Acernese et al., “Sensitivity studies for third-generation gravitational wave observatories”, *Classical and Quantum Gravity* **28** (2011) 094013.
- [25] J. Abadie, B.P. Abbott, R. Abbott, et al., “Search for gravitational waves from binary black hole inspiral, merger, and ringdown”, *Physical Review D* **83** (2011) 122005.
- [26] J. Abadie, B.P. Abbott, R. Abbott, et al., “SEARCH FOR GRAVITATIONAL WAVE BURSTS FROM SIX MAGNETARS”, *Astrophysical Journal Letters* **734** (2011) L35.
- [27] J. Abadie, B.P. Abbott, R. Abbott, et al., “BEATING THE SPIN-DOWN LIMIT ON GRAVITATIONAL WAVE EMISSION FROM THE VELA PULSAR”, *Astrophysical Journal* **737** (2011) 93.
- [28] D. Heinert, A. G. Gurkovsky, R. Nawrodt, S. P. Vyatchanin, and K. Yamamoto, “Thermorefractive noise of finite-sized cylindrical test masses”, *Physical Review D* **84** (2011) 062001.
- [29] D. Friedrich, H. Kaufer, T. Westphal, K. Yamamoto, A. Sawadsky, F. Ya Khalili, S. L. Danilishin, S. Goebel, K. Danzmann and R. Schnabel “Laser interferometry with translucent and absorbing mechanical oscillators”, *New Journal of Physics* **13** (2011) 093017.
- [30] J. Abadie, B.P. Abbott, R. Abbott, et al., “Directional Limits on Persistent Gravitational Waves Using LIGO S5 Science Data”, *Physical Review Letters* **107** (2011) 271102.
- [31] J. Abadie, B.P. Abbott, R. Abbott, et al., “All-sky search for periodic gravitational waves in LIGO S5 the full data”, *Physical Review D* **85** (2012) 022001.
- [32] J. Abadie, B.P. Abbott, R. Abbott, et al., “Search for gravitational waves from low mass compact binary coalescence in LIGO’s sixth science run and Virgo’s science runs 2 and 3”, *Physical Review D* **85** (2012) 082002.
- [33] Sanjeev Dhurandhar, Hideyuki Tagoshi, Yuta Okada, Nobuyuki Kanda, and Hirotaka Takahashi, “The cross-correlation search for a hot spot of gravitational waves”, *Phys. Rev. D* **84** (2011) 083007.
- [34] Maurice H.P.M. van Putten, Nobuyuki Kanda, Hideyuki Tagoshi, Daisuke Tatsumi, Fujimoto Masa-Katsu and Massimo Della Valle, “Prospects for true calorimetry on Kerr black holes in core-collapse supernovae and mergers”, *Phys Rev D* **83** (2011) 044046.
- [35] Yi Pan, Alessandra Buonanno, Ryuichi Fujita, Etienne Racine, Hideyuki Tagoshi, “Post-Newtonian factorized multipolar waveforms for spinning, non-precessing black-hole binaries”, *Phys. Rev. D* **83** (2011) 064003.
- [36] Koji Ishidoshiro, Masaki Ando, Akiteru Takamori, Hideyuki Tagoshi, Kenshi Okada, Nobuyuki Matsumoto, Wataru Kokuyama, Nobuyuki Kanda, Yoichi Aso, and Kimio Tsubono, “First observational upper limit on gravitational wave backgrounds at 0.2 Hz with a torsion-bar antenna”, *Phys Rev Letter* **106** (2011) 161101.
- [37] K. Takeno, N. Ohmae, N. Mio, T. Shirai, “Determination of wavefront aberrations using a Fabry-Perot cavity”, *OPTICS COMMUNICATIONS* **284** (13) (2011) 3197-3201.
- [38] N. Ohmae, S. Moriwaki and N. Mio, “High-efficiency electro-optic amplitude modulation with delayed coherent addition”, *Opt. Lett.* **36** (2) (2011) 238-240.
- [39] M. Tokunari, et al., “Optical properties measurement of an Al₂O₃ mirror substrate for the Large-Scale Cryogenic Gravitational Wave Telescope (LCGT),” *Class. Quantum Grav.* **27**, 185015 (2010).
- [40] N. Ohmae, S. Moriwaki and N. Mio, “Wide-band and high-gain frequency stabilization of a 100-W injection-locked Nd:YAG laser for second-generation gravitational wave detectors”, *Rev. Sci. Instrum.* **81** (7) (2010) 073105.
- [41] Araya, A., A. Takamori, W. Morii, H. Hayakawa, T. Uchiyama, M. Ohashi, S. Telada and S. Takemoto, “Analyses of far-field coseismic crustal deformation observed by a new laser distance measurement system”, *Geophys. J. Int.*, **181**, 127-140, 2010.

- [42] Kazuhiro Agatsuma, Takashi Uchiyama, Kazuhiro Yamamoto, et al., “Direct measurement of thermal fluctuation of high-Q pendulum”, *Phys. Rev. Lett.*, **104**, 040602 (2010).
- [43] K. Arai *et al.*, “Status of Japanese gravitational wave detectors”, *Class. Quantum Grav.* **26** (2009) 204020-1-9.
- [44] T. Hori, A. Araya, S. Moriwaki, N. Mio, “Formulation of frequency stability limited by laser intrinsic noise in feedback systems”, *Appl. Opt.* **48** (2) (2009)429-435.
- [45] K. Machida, S. Moriwaki, and N. Mio, “High-Speed Mechanical Actuator for Precision Optical Path Length Control”, *Jpn. J. Appl. Phys.* **48** (1) (2009) 010212-1-3.
- [46] S. Moriwaki, T. Mori, K. Takeno and N. Mio, “Frequency Discrimination Method Making Use of Polarization Selectivity of Triangular Optical Cavity”, *Appl. Phys. Express* **2** (1) (2009) 016501-1-3.
- [47] W. Sun, S. Okubo, G. Fu and A. Araya, “General formulations of global co-seismic deformations caused by an arbitrary dislocation in a spherically symmetric earth model applicable to deformed earth surface and space-fixed point”, *Geophys. J. Int.*, **177**, 817-833, 2009.
- [48] K. Yamamoto, et al., “Current status of the CLIO project”, *J. Phys :Conference Series* **122**, 012002, 2008.
- [49] T. Tomaru, et al., “Reduction of Heat Load of LCGT Cryostat”, *ibid*, 012009,
- [50] K. Yamamoto, et al., “Parametric instabilities in the LCGT arm cavity”, *ibid*, 012015.
- [51] N. Mio, H. Takahashi and S. Moriwaki, “High-power photo-detection system for next-generation gravitational wave detectors”, *ibid*, 012014-1-6.
- [52] K. Agatsuma, R. Takahashi, K. Arai, D. Tatsumi, M. Fukushima, T. Yamazaki, M. Fujimoto, Y. Arase, N. Nakagawa, A. Takamori, K. Tsubono, K. Kuroda, M. Ohashi, R. DeSalvo, A. Bertolini, S. Márka, V. Sannibale, “Control system for the seismic attenuation system (SAS) in TAMA300”, *ibid*, 12013-1-6.
- [53] Y. Arase, R. Takahashi, K. Arai, D. Tatsumi, M. Fukushima, T. Yamazaki, M. Fujimoto, K. Agatsuma, N. Nakagawa, “Damping system for torsion modes of mirror isolation filters in TAMA300”, *ibid*, 12027-1-6.
- [54] R. Takahashi, K. Arai, D. Tatsumi, M. Fukushima, T. Yamazaki, M.-K. Fujimoto, K. Agatsuma, Y. Arase, N. Nakagawa, A. Takamori, K. Tsubono, R. DeSalvo, A. Bertolini, S. Márka, V. Sannibale and the TAMA Collaboration, “Operational status of TAMA300 with the Seismic Attenuation System (SAS)”, *Class. Quantum Grav.* **25** (2008) 114036-1-8.
- [55] K. Yamamoto, et al., “Effect of energy deposited by cosmic-ray particles on interferometric gravitational wave detectors”, *Phys. Rev. D* **78**, 022004, 2008.
- [56] T. Tomaru, et al., “Conduction Effect of Thermal Radiation in a Metal Shield Pipe in a Cryostat for a Cryogenic Interferometric Gravitational Wave Detector”, *Jpn. J. App. Phys.* **47**, 1771, 2008.
- [57] T. Akutsu, et al., “Search for continuous gravitational waves from PSR J0835-4510 using CLIO data”, *Class. Quantum Grav.* **25**, 184013, 2008.
- [58] N. Ohmae, K. Takeno, S. Moriwaki, and N. Mio, “Wideband Frequency Stabilization of a 100-W Injection-Locked Nd:YAG Laser Using an External Electrooptic Modulator”, *Appl. Phys. Express* **1** (9) (2008) 092601-1-3.
- [59] T. Mori, S. Moriwaki, N. Mio, “Mechanical Q-factor Measurement of a Quartz Oscillator at Cryogenic Temperature”, *Appl. Phys. Express* **1** (7) (2008) 077002-1-3.
- [60] S. V. Tovstonog, S. Kurimura, I. Suzuki, K. Takeno, S. Moriwaki, N. Ohmae, N. Mio and T. Katagai, “Thermal effects in high-power CW second harmonic generation in Mg-doped stoichiometric lithium tantalite”, *Opt. Express.* **16** (15) (2008) 11294-11299.

- [61] N. Ohmae, K. Takeno, S. Moriwaki, N. Mio, “Development of electrooptic modulator for advanced ground-based gravitational wave telescopes using stoichiometric MgO-doped LiNbO₃ crystals”, *Appl. Phys. Express* **1** (1) (2008) 012005-1-3.
- [62] S. Márka, R. DeSalvo, V. Sannibale, H. Tariq, A. Bertolini, G. Cella, N. Viboud, K. Numata, R. Takahashi, M. Fukushima, A. Takamori, P. Raffai, “Inverted pendulum as low-frequency pre-isolation for advanced gravitational wave detectors”, *Nucl. Instrum. Meth. A* **582** (2007) 683-692.
- [63] Norikatsu Mio, Takafumi Ozeki, Kosuke Machida, and Shigenori Moriwaki, “Laser Intensity Stabilization System Using Laser-Diode-Pumped Nd:YAG Rod-Laser Amplifier”, *Jpn. J. Appl. Phys.* **46** (8A) (2007) 5338-5341.
- [64] T. Hori, A. Araya, S. Moriwaki and N. Mio, “Development of a wavelength-stabilized distributed Bragg reflector laser diode to the Cs-D2 line for field use in accurate geophysical measurements”, *Rev. Sci. Instrum.* **78** (2) (2007) 026105-1-3.
- [65] Araya, A., W. Morii, H. Hayakawa, A. Takamori, T. Uchiyama, M. Ohashi, I. Yamada, S. Telada, and S. Takemoto, “Broadband observation with laser strainmeters and a strategy for high resolution long-term strain observation based on quantum standard”, *J. Geod. Soc. Japan*, **53**(2) 81-97, 2007.
- [66] T. Akutsu, et al., “Veto analysis for gravitational wave burst signals in TAMA300 data using ALF filter”, *Class. Quantum Grav.* **23** (2006)S23.
- [67] S. Miyoki, et al., “The CLIO project”, *Class. Quantum Grav.* **23** (2006)S231.
- [68] K. Kuroda and the LCGT Collaboration, “The status of LCGT”, *Class. Quantum Grav.* **23** (2006)S215.
- [69] N. Nakagawa, et al., “Influence of radio frequency harmonics to TAMA300 sensitivity”, *J Phys. Conf. series* **32** (2006) 99.
- [70] T. Uchiyama, et al., “Cryogenic systems of the Cryogenic Laser Interferometer Observatory”, *ibid*, 259.
- [71] K. Yamamoto, et al., “Measurement of vibration of the top of the suspension in a cryogenic interferometer with operating cryocoolers”, *ibid*, 418.
- [72] M. Tokunari, et al., “Development of an automatic birefringence measuring device of mirror substrates for gravitational wave detectors”, *ibid*, 432.
- [73] A. Okutomi, et al., “Development of a radiation pressure noise interferometer”, *ibid*, 327.
- [74] Z. Yan, et al., “Rayleigh scattering, absorption, and birefringence of large-size bulk single-crystal sapphire”, *Appl. Optics* **45** (2006) 2631.
- [75] K. Kuroda and LCGT Collaboration, “Experimental effort to detect gravitational waves”, *Progress on Theor. Phys. Suppl.* **163** (2006) 54.
- [76] K. Yamamoto, et al., “Measurement of the mechanical loss of a cooled reflective coating for gravitational wave detection”, *Phys. Rev. D* **74** (2006) 022002.
- [77] T. Akutsu *et al.*, “Results of the search for inspiraling compact star binaries from TAMA300’s observation in 2000-2004”, *Phys. Rev. D* **74** (12): Art. No. 122002.
- [78] T. Tanji, T. Kawanami, S. Moriwaki, N. Mio, F. Yin and A. Matsushita, “Study of a nonlinear mechanical response of reentrant spin glass antiferromagnet Mn-Cu alloys”, *J. Appl. Phys.* **100** (6) (2006) 073508-1-6.
- [79] K. Somiya, Y. Chen, S. Kawamura, N. Mio, “Frequency noise and intensity noise of next-generation gravitational-wave detectors with RF/DC readout schemes”, *Phys. Rev. D* **73** (12) (2006) 122005-1-17.
- [80] B. Abbott *et al.*, “Joint LIGO and TAMA300 search for gravitational waves from inspiralling neutron star binaries”, *Phys. Rev. D* **73** (10) (2006) 102002-1-10.

- [81] K. Takeno, T Ozeki, S Moriwaki and N Mio, “Development of a 100-W, single-frequency Nd:YAG laser for large-scale cryogenic gravitational wave telescope”, *J. Phys.: Conf. Series* **32** (2006) 276-281.
- Papers in Conference Proceedings
- [82] “Current Status of LCGT project”, S. Miyoki and LCGT collaboration, TAUP 2011 in Minich, Munchen.
- [83] N. Kimura *et al.*, “Refrigerator and Cryostat Design for LCGT”, GWADW 2011, 22-28 May, 2011, La Biodola, Isola d’Elba, Italy.
- [84] “Cryogenic system of LCGT”, S.Miyoki and KAGRA Cryogenic group, Korea-Japan Workshop on KAGRA (Korea, Seoul), 13 Jan., 2012.
- [85] S. Miyoki and LCGT collaboration, “The Present Status of LCGT Project”, ICGAC10 in Qui Nhon (Vietnam, Qui Nhon), 20 Dec., 2011.
- [86] Nobuyuki Kanda, “Frontier of Gravitational Wave Astronomy - Opening New Window of Astrophysics and Cosmology”, JSPS-DST Asia Academic Seminar, 26 September - 1 October 2011, Hyogo, Japan.
- [87] N. Kimura, S. Koike, T. Kume, T. Ohmori, Y. Saito, Y. Sakakibara, K. Sasaki, Y. Sato, T. Suzuki, T. Uchiyama, K. Yamamoto, H. Yamaoka and LCGT Collaboration, “Cryogenic System design of LCGT”, Italy-Japan workshop, Kashiwa, 5 Oct., 2011.
- [88] K. Kuroda, “Gravitational Waves: Current and future experiments”, TAUP2011 in Minich (Germany, Munchen) 5-9 Sept. 2011.
- [89] Hideyuki Tagoshi, et al., “Ground-based GW Detectors and the Status of LCGT”, Gravitational Wave Astrophysics, Binary Supermassive Black Holes, and Galaxy Mergers, Lijiang, Yunnan, China, 1-5 August, 2011.
- [90] Nobuyuki Kanda, “LCGT and the Global Network of Gravitational Wave Detectors”, 11th Asian-Pacific Regional IAU Meeting, July 26-29, 2011, Chiang Mai, Thailand.
- [91] Nobuyuki Kanda, “The cross-correlation search for a hot spot of gravitational waves”, 9th Edoardo Amaldi Conference on Gravitational Waves, and the 2011 Numerical Relativity - Data Analysis meeting, July 10-15 2011, Cardiff (UK).
- [92] Yoichi Aso, et al., “Length sensing and control strategies for the LCGT interferometer”, 9th Amaldi conference on gravitational waves, Cardiff university, Cardiff, Wales, UK, 10-15, July, 2011.
- [93] N. KIMURA, Y. SAKAKIBARA, S. KOIKE, T. SUZUKI, H. YAMAOKA, and LCGT Collaboration, “Present Design of LCGT Cryogenics Payload- Status of cryogenics design”, GWADW 2011, 22-28 May, 2011, La Biodola, Isola d’Elba, Italy. <http://agenda.infn.it/conferenceDisplay.py?confId=3351>
- [94] N. KIMURA, T. SUZUKI, S. KOIKE, T. KUME, T. OHMORI, K. SASAKI, Y. SAITO, Y. SATO, H. YAMAOKA and LCGT Collaboration, “Refrigerator and Cryostat Design for LCGT”, *ibid.*
- [95] Kentaro Somiya, Erina Nishida, et al., “Detector Configuration and Control System for LCGT”, *ibid.*
- [96] Riccardo DeSalvo, et al., “LCGT-SAS Design and R&D”, *ibid.*
- [97] K. Kuroda on behalf of LCGT Collaboration, “Underground Gravitational Wave Detector —LCGT—”, APPC11, Shanghai, November, 2010.
- [98] K. Kuroda, et al., “Status of LCGT project”, LSC&Virgo meeting, Krakov, September, 2010.
- [99] K. Kuroda, et al., “Cryogenic Advanced Gravitational Wave Detector”, 1st Galilei-Xu International Conference, Shanghai, October, 2009.
- [100] K. Kuroda, et al., “LCGT project in Japan”, ICGA 9, Wuhang, June 2009.

- [101] K. Kuroda, et al., “Status of LCGT”, 8th Edoardo Amaldi Conference (Amaldi8) New York, June, 2009.
- [102] K. Agatsuma, et al., “Thermal-noise-limited underground interferometer CLIO”, *ibid.*
- [103] K. Kuroda, et al., “LCGT”, Fujihara Seminar, Hayama, May, 2009.
- [104] K. Kuroda, et al., “CLIO”, GWADW 9, Florida, May, 2009.
- [105] K. Kuroda and LCGT Collaboration, “CLIO and LCGT”, Proceedings of XLIIInd Rencontres de Moriond, 2007: “Gravitational Waves and Experimental Gravity”, ed. Jacques Dumarchez and Jean Tran Thanh Van, pp.15 and pp.45, THE GIOI, Vietnam, 2007.
- [106] M. Ohashi, “Current Status of LCGT and CLIO”, TAUP2007, 11-15, September, 2007, Sendai, Japan.
- [107] K. Kuroda, “Status of Japanese Projects”, LSC-Virgo Meeting, 22-25 October, 2007, Hannover, Germany.
- [108] K. Kuroda and LCGT Collaboration, “CLIO and LCGT”, XLIIInd Rencontres de Moriond, March 11-18, 2007, La Thuile, Italy.
- [109] K. Kuroda, “Status of Japanese Project”, LSC-Virgo Joint Meeting, 22-25 May, 2007, Cascina, Italy.
- [110] K. Kuroda and LCGT Collaboration, “Current Status of LCGT”, 7th Edoardo Amaldi Conference on Gravitational Waves, 8-14 July 2007, Sydney, Australia.
- [111] K. Yamamoto and CLIO Collaboration, “Current Status of CLIO”, *ibid.*
- [112] K. Kuroda, “PI in Cryogenic Cavities”, Parametric Instability Workshop, 16-18 July 2007, Gingin, Perth, Australia.
- [113] K. Kuroda, “LCGT Project”, LSC-Virgo Joint Meeting, 24-27 July, 2007, Boston, USA.
- [114] K. Kuroda, “Status of Japanese Projects”, LSC-Virgo Meeting, 22-25 October, 2007. Hannover, Germany.

OBSERVATIONAL COSMOLOGY GROUP

Introduction

We study observational cosmology with optical-infrared telescopes. We conducted Sloan Digital Sky Survey (SDSS) under the SDSS collaboration and completed the survey in 2008. After 2008, efforts for data analyses and paper publications were made. Having this completion of SDSS survey, we have started new observational cosmology programs with new deep surveys with the world largest optical-infrared-radio telescope facilities. These activities of SDSS and new deep survey programs are presented in the following two subsections.

Research Activities

Sloan Digital Sky Survey

The SDSS was a nearly-20-years project with its preparation commenced in 1992 (including our Japanese team), its survey operation begun from April 2000, and finally ended in July 2008. The contribution of the Japanese team was from the beginning, perhaps, most importantly to instrumentation, designing, production, testing, and verification of the instruments mostly for the photometric survey. In the beginning, there were only 5 institutions (one being our JCG) and only some 20 people worked for the project. The tests were done meticulously in laboratories, so that imaging was done successfully as designed from the first night. After it got to the survey mode the numbers of participating institutes and participants drastically increased by an order of magnitude, while the Japanese participation stayed to be unchanged, or even shrunk down. The SDSS facility itself can still be valid, and is being used for SDSS-III after upgrades of the spectrograph. This defines a new project with the goal shifted from the original plan, rather than a continuation. No group of ICRR has directly involved in the SDSS-III.

The data taken with the SDSS were all reduced and catalogued as SDSS Data Release 7 (DR7: [33]), which stands for the final catalogue of the SDSS project. The catalogue contains images and parameters of 360 million objects over 11663 square degrees of sky and spectra of 1.62

million objects over 9380 square degrees, approximately 1/4 the entire sky. Not only these numbers are unprecedented but important with the catalogue is its high accuracy, especially in photometry. The entries in the catalogues are used as the standard reference for various observational projects outside the SDSS.

Primary science analyses were also carried out, which fulfilled more than 95% of the science goals contemplated in the beginning of the projects, all at a satisfactory level. In addition, we obtained significant outcomes that had not been seriously considered as goals of the survey in the beginning. They include the discovery of baryon acoustic oscillation, discovery of reionization of the Universe at $z > 6$, gravitational weak-lensing that gives the mass distribution of galaxies, even to the scale beyond their virial radii, and evidence for continued mass assembly of the Milky Way. In short, SDSS has made a great contribution that tightens our understanding of the Universe and its evolution, summarised as establishing “the Standard Cosmology”. The data are, and will be, used as the fundamental data-base to study a variety of the astrophysical science probably as long as for a century.

Our work in 2006 onward pertaining to SDSS may be summarised as follows: We measured the photometric response function from time to time during the survey, the results of which were made publicly available without delay through the web. The final results were published in [41]. The photometric accuracy and characters were studied in detail using the DR7 final catalogue [52].

There were also a number of science projects that continued from the years before 2006. The representative examples that were finalised and published after 2007 include: (i) Morphological classification of galaxies with visual inspection [17], and the investigation of properties of discs and bulges [34]; (ii) Updates of galaxy correlation functions and of the measurement of baryon acoustic oscillation with DR7 [40, 39]; (iii) A study of type Ia supernovae and their host galaxies [38]; (iv) Search for strong lenses of quasar images [63, 62]. The final quasar catalogue [42] contains 105783 quasars, among which a half are taken. The search was made

for multiple images: 19 lenses (among total of 62) with the well defined selection criterion resulted in $\Omega_\Lambda = 0.79$, $\Omega_m = 0.21$, which agree with CMB and others. The lensing test we (Fukugita, Futamase and Kasai 1990, and Turner 1990) proposed twenty years ago finally yielded the result [63].

High photometric accuracy and a huge amount of data have made some photometric studies that could not be conceived in the past possible. Our example is the discovery of dust in galactic haloes, perhaps expelled from galaxies. The analysis rested on the unique feature of SDSS, large data sets, 24 million galaxies and 200 thousand quasars used, stacked and extremely accurate photometry, as one has to resolve variations of brightness at an accuracy of 0.001 magnitude [37]. The amount of dust outside galaxies is nearly as much as that in discs. When the two components are added, they give the amount that is expected from the star formation history of galaxies, which means the closure of the inventory. A similar example is the detection of dust in Mg II absorbers. Using the similar stacking technique, we detected dust and heavy atoms that causes 0.001 magnitude of extinction behind the Mg II cloud. This requires that the photometric errors decrease as $1/\sqrt{N}$ when N data are coadded, and that other systematics are removed to this high accuracy with SDSS photometry. The result of the detection of dust means that Mg II clouds must be a product of galaxies (outflows) and not primordial objects [64].

Another example is the measurement of the mass density distribution around the galaxy. High accuracy of photometry has enabled the detection of tiny magnification of quasar brightness. This in turn has made possible to detect the lensing signal even in the middle to the neighbouring galaxies [64]. With the aid of dark-matter-only N body simulations, which are known to be reliable, we deconvolve the components that contribute to the column mass density. We find that the mass distribution of galaxy continues to far beyond the galaxy, to the middle of the neighbouring galaxies in an organised way. The Universe is nowhere empty. It is filled with the material all the way [55]. This, at the same time, resolved the discrepancy in the old argument that luminosity times the M/L gives only half the global mass density.

15 years ago Jim Peebles, Craig Hogan and Fukugita (1998) uncovered that 80% (the modern

value is 90%) of baryons ought to be present in the universe are missed from observations (the problem now termed “missing baryons”). Around 2004 Peebles and I extended this consideration to include all forms of the energy present in the universe. The table, that we call the cosmic energy inventory, turned out to be very useful to know what we have already understood and what we have not, either theoretically or observationally. In fact, the search for dust outside galaxy was one of the problems we noticed in the inventory consideration. This “missing dust” problem prompted us to search for the presence of dust outside galaxies: we found it. The missing galaxy mass above was another problem found in the inventory argument.

Brief history of the work by the Japanese team for the SDSS is reviewed in Fukugita, Butsuri: Bull. Phys. Soc. Japan, 2010, **65**, 524.

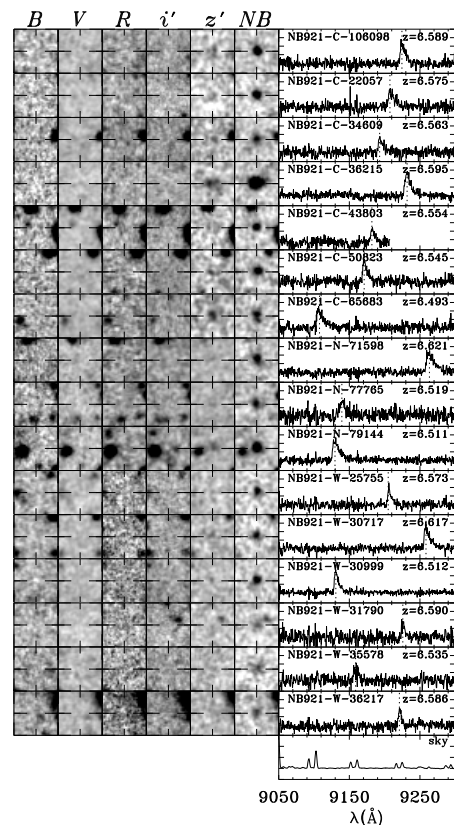


Fig. 1. Spectra and snapshots of some of our $z = 6.6$ LAEs confirmed with Keck/DEIMOS. Each object has a spectrum in the right panel and snapshots of B , V , R , i' , z' , and $NB921$ images in the left panels. Each snapshot is presented in a $6'' \times 6''$ box. The right bottom panel shows a typical DEIMOS spectrum of the sky background that is obtained in the process of sky subtraction.

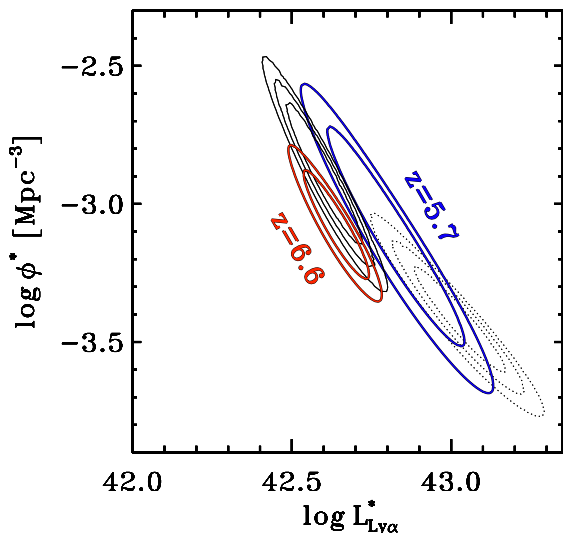


Fig. 2. Error ellipses of our Schechter parameters, $L_{\text{Ly}\alpha}^*$ and ϕ^* . Red contours represent the fit of $z = 6.6$ LF with the fixed slope of $\alpha = -1.5$ based on SXDS and SDF data. The inner and outer contours indicate 68% and 90% confidence levels, respectively, which include cosmic variance errors. Blue contours denote $z = 5.7$ LFs, which are similarly derived with cosmic variance errors. The error ellipses of the $z = 5.7$ LF are larger than those of our $z = 6.6$ LF. This is because the data of $z = 5.7$ LF have more uncertainties of cosmic variance. Black solid and dotted lines indicate 1, 2, and 3 sigma confidence levels of $z = 6.6$ and $z = 5.7$ LFs with no cosmic variance errors previously derived solely with the smaller data of SDF.

New Observational Cosmology Programs

New observational cosmology programs have started since 2010, addressing the issues of cosmic reionization and early galaxy formation that are missing pieces of our understanding of cosmic history. The outstanding scientific questions are the unknown reionization physical process, the missing ionizing photon problem, the formation of first star, and the structural/dynamical/chemical evolutions of galaxies at the early epoch of cosmic history. Our basic strategy is to carry out deep surveys with the world largest telescope facilities that have a sensitivity good enough for probing the distant universe. The key component of our programs is the next generation Subaru wide-field optical imager, Hyper Suprime-Cam (HSC), whose first light is planned in the summer of 2012. Since 2010, preparatory and supporting observations of our HSC exploration have been performed with various facilities from optical to radio, such as Subaru and Keck telescopes, Hubble space telescope, and Atacama Large Millimeter/submillimeter Array (ALMA).

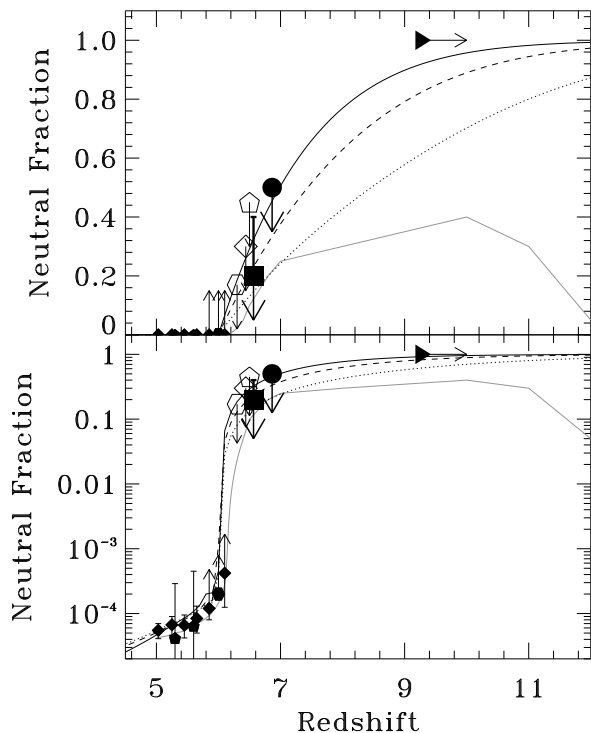


Fig. 3. Neutral hydrogen fraction, x_{HI} , of IGM as a function of redshift. Top and bottom panels are the same, but with a vertical axis of linear and log scales, respectively. Filled square and circle are the upper limits of x_{HI} that we obtain from the evolution of Ly α LF and clustering, respectively. Open symbols denote the upper limits from Ly α LF and Ly α damping wing of GRB given by the previous studies. Filled hexagon and pentagons indicate constraints given by GRB spectra and QSO dark gap statistics, respectively. Filled diamonds represent the measurements from GP optical depth of SDSS QSOs. Triangle plots the 1σ lower-limit of redshift of a neutral universe given by WMAP7 in the case of instantaneous reionization. Avoiding overlapping symbols, we give a small offset along redshift to the positions of the filled circle and the open diamond. Dotted, dashed, and solid lines show the evolution of x_{HI} for mini-halo, small, and large halo cases, respectively, predicted by the semi-analytic models. Gray solid line presents the prediction in the double reionization scenario suggested by the theoretical model.

Using Subaru and Keck telescopes, we have investigated Ly α luminosity function (LF), clustering, and Ly α line profiles based on the largest sample, to date, of 207 Ly α emitters (LAEs) at $z = 6.6$ on the 1-deg² sky of Subaru/XMM-Newton Deep Survey (SXDS) field ([48]; Fig. 1). Our $z = 6.6$ Ly α LF including cosmic variance estimates yields the best-fit Schechter parameters of $\phi^* = 8.5_{-2.2}^{+3.0} \times 10^{-4} \text{Mpc}^{-3}$ and $L_{\text{Ly}\alpha}^* = 4.4_{-0.6}^{+0.6} \times 10^{42} \text{erg s}^{-1}$ with a fixed $\alpha = -1.5$, and indicates a decrease from $z = 5.7$ at the $\gtrsim 90\%$ confidence level (Fig. 2), suggesting an increase of Ly α damping wing absorption

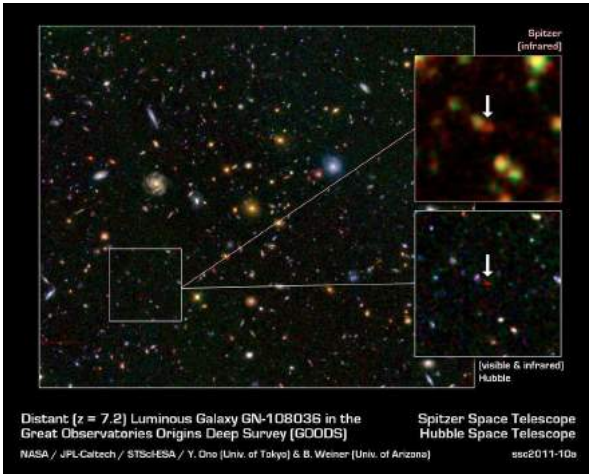


Fig. 4. The NASA and JPL press-release image of GN-108036 at $z = 7.213$. This is a color composite image of optical and infrared data taken by Hubble and Spitzer space telescopes, respectively. This is a remarkable object with the very high star-formation activity at the early epoch of the universe.

given by neutral hydrogen in inter-galactic medium (IGM). However, this decrease is not large, only $\simeq 30\%$ in $\text{Ly}\alpha$ luminosity, which is too small to be identified in the previous studies. A clustering signal of $z = 6.6$ LAEs is detected for the first time. We obtain the correlation length of $r_0 = 2 - 5 h_{100}^{-1}$ Mpc and bias of $b = 3 - 6$, and find no significant boost of clustering amplitude by reionization at $z = 6.6$. The average hosting dark-matter halo mass inferred from clustering is $10^{10} - 10^{11} M_{\odot}$, and the fraction of active LAE population in dark-matter halos is roughly $\sim 1\%$ albeit with large uncertainties. The average of our high-quality Keck spectra shows an FWHM velocity width of $251 \pm 16 \text{ km s}^{-1}$. We find no large evolution of $\text{Ly}\alpha$ line profile from $z = 5.7$ to 6.6 , and no anti-correlation between $\text{Ly}\alpha$ luminosity and line width at $z = 6.6$. The combination of various reionization models and our observational results about the LF, clustering, and line profile indicates that there would exist a small decrease of IGM's $\text{Ly}\alpha$ transmission owing to reionization, but that the hydrogen IGM is not very highly neutral at $z = 6.6$ (Fig. 3). Our neutral-hydrogen fraction constraint implies that the major reionization process took place at $z \sim 7$ and beyond.

These results provide a clue for our understanding of cosmic reionization. However, the decrease of $\text{Ly}\alpha$ LF could be produced by galaxy evolution. Because $\text{Ly}\alpha$ emission is weakened not only by the absorption of neutral hydrogen of intergalactic medium (IGM) at the epoch of reioniza-

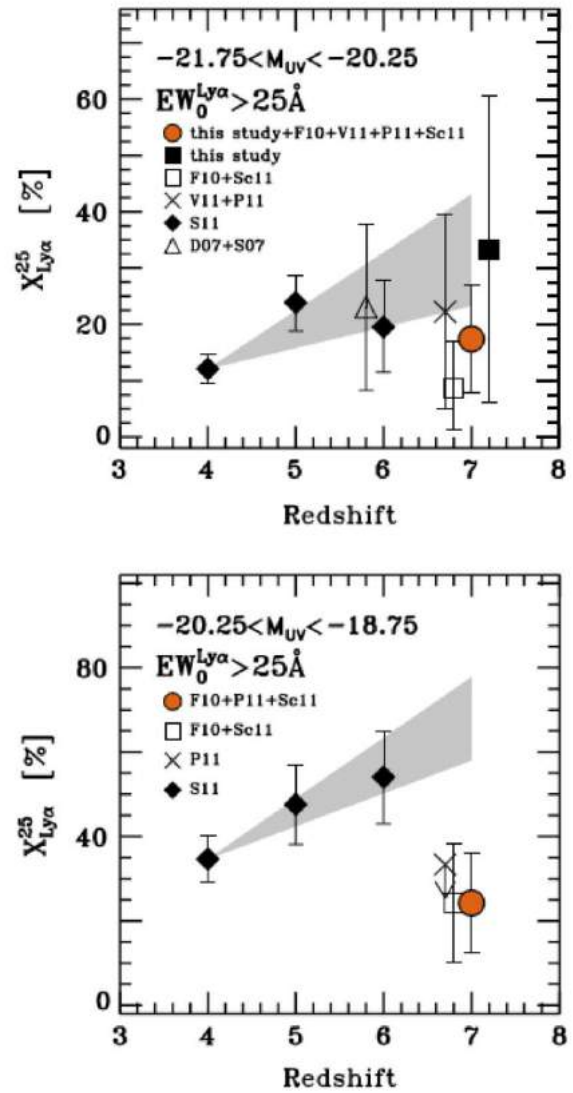


Fig. 5. Evolution in the fraction of $\text{Ly}\alpha$ emitting galaxy ($EW > 25\text{\AA}$) with $-21.75 < M_{\text{UV}} < -20.25$ (top panels) and $-20.25 < M_{\text{UV}} < -18.75$ (bottom panels) over $4 < z < 7$. The filled red circles are the composite results of our studies and previous programs. The rest of symbols are those in the literature. The shaded area is derived by extrapolating the trend seen in lower redshifts to $z \sim 7$.

tion (EoR), but by a less active star-formation in galaxies at EoR. We, thus, extend this study with the z -dropout galaxies that are selected with a UV ($> 121.6 \text{ nm}$) continuum with no IGM absorption. We have conducted ultra-deep Keck spectroscopy for z -dropout galaxies in the SDF and GOODS-N [65]. For 3 out of 11 objects, we detect an emission line at $\sim 1 \mu\text{m}$ with a signal-to-noise ratio of ~ 10 . The lines show asymmetric profiles with high weighted skewness values, consistent with being $\text{Ly}\alpha$, yielding redshifts of $z = 7.213$, 6.965 , and 6.844 . Specifically, we confirm the $z = 7.213$ object, GN-108036, in two independent Keck ob-

servicing runs with different spectroscopic configurations. This particular object has a star-formation rate of $\sim 100M_{\odot} \text{ yr}^{-1}$ that is about an order of magnitude higher than those found at the similar redshifts. It is not clear that such a remarkably active galaxy can be produced under the standard hierarchical structure formation. With the importance of this discovery, NASA, JPL, University of Tokyo, and NAOJ have issued a press-release (Figure 4), and the stories of this discovery were featured in various mass media all over the world including BBC, ABC, and major Japanese news papers/TV programs. The three z -dropouts found in our study have $\text{Ly}\alpha$ fluxes of $3 \times 10^{-17} \text{ erg s}^{-1} \text{ cm}^{-2}$ and rest-frame equivalent widths $\text{EW}_0^{\text{Ly}\alpha} = 33 - 43\text{\AA}$. Based on the largest spectroscopic sample of 43 z -dropouts that is the combination of our and previous data, we find that the fraction of $\text{Ly}\alpha$ -emitting galaxies ($\text{EW}_0^{\text{Ly}\alpha} > 25\text{\AA}$) is low at $z \sim 7$; $17 \pm 10\%$ and $24 \pm 12\%$ for bright ($M_{\text{UV}} \simeq -21$) and faint ($M_{\text{UV}} \simeq -19.5$) galaxies, respectively. The fractions of $\text{Ly}\alpha$ -emitting galaxies drop from $z \sim 6$ to 7 and the amplitude of the drop is larger for faint galaxies than for bright galaxies (Figure 5). These two pieces of evidence would indicate that the neutral hydrogen fraction of the IGM increases from $z \sim 6$ to 7, and that the reionization proceeds from high- to low-density environments, as suggested by an inside-out reionization model.

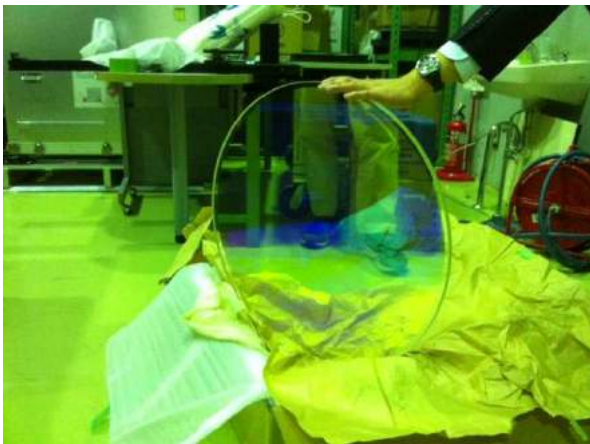


Fig. 6. Test filter of HSC NB921 with a physical size of 600mm diameter. This picture was taken in March 2012.

On-Going Projects and Future Prospects

Although these preparatory studies provide various implications about the early epoch of cosmic history, large uncertainties raised by the small

statistics do not allow us to obtain conclusive results. One example is shown in Figure 3 that presents four competing theoretical models of cosmic reionization; the models of major ionizing sources of large, small and mini-halo galaxies, and ‘double reionization’ model driven by an early Population III starburst period followed by normal Population II galaxy formation. The current observational constraints cannot distinguish these various possibilities. Another example is the physical process of reionization that is poorly understood. Until recently, theoretical studies favor a simple inside-out process of reionization; high-density regions ionized first then extend to void regions, but there is an on-going debate with other possibilities such as an opposite outside-in process. Moreover, a complex reionization process is suggested by more recent studies with sophisticated physical models. A combination of radiative transfer and hydrodynamic simulations shows that both overdense regions and voids are ionized earlier than intermediate-density regions of filaments, owing to their high recombination rate and low emissivity. Although our preparatory study supports the idea of inside-out reionization models, it is still a speculative picture emerged from the combination of circumstance evidence.

To address these open questions, we are working on the Subaru HSC project. The HSC project will obtain samples of high- z galaxies about 30 times larger than the currently available samples, which will provide physical measurements with an unprecedented accuracy that is good enough to distinguish the competing models shown above. After the first light of HSC scheduled in 2012, we plan to start the HSC survey from the fall 2013 under the large collaboration of Physics department, IPMU, NAOJ, Princeton University, and Taiwanese institutions etc. This is a 5-year survey program that will be completed in 2017. We plan to publish preliminary results in 2015, with the first 2-year data taken by the time. Our contribution to the HSC survey is to supply two narrowband (NB) filters that will be used to identify high- z galaxies. These two NB filters have central wavelengths of $0.9\mu\text{m}$ (NB921) and $1\mu\text{m}$ (NB973) with a 1% bandwidth that are realized by multi-layer coatings of two kinds of material with different refraction indexes, Ta_2O_5 and SiO_2 via magnetron sputtering. With a support of nearly 40 million yen from KAK-

ENHI (23244025: Ouchi et al.) Grant-in-Aid for Scientific Research(A) through JSPS, the basic design and tests for the NB921 filter have been completed, and fabricated in Materion Corporation. A test product of NB921 filter is shown in Figure 6. We expect to produce the NB921 and NB973 with the satisfactory specification no later than the end of fiscal year 2013.

The Subaru HSC survey is the promising project to address the questions that require large statistics. However, the optical imaging program of HSC survey cannot reveal stellar morphology and molecular hydrogen distribution that are key for understanding early galaxy formation; i.e. how molecular gas is converted to stars. Thus, we work on the UDF12 project of ultra-deep imaging with Hubble Space Telescope (HST) at the near-infrared wavelengths with the US, UK, and French colleagues (PI. R. Ellis). The observations of UDF12 project is starting in August 2012, and the first results are planned to be published this winter. Similarly, we lead the program of deep ALMA observations at 1.2mm wavelengths for atomic carbon in high- z galaxies at $z \sim 6 - 7$ found by our Subaru survey (PI. M. Ouchi) with colleagues in NAOJ, California institute of technology etc. The first ALMA observations of our program are scheduled in the summer of 2012. We expect to obtain some preliminary results within the fiscal year of 2012. In this way, having the main project of HSC survey, we are extending our studies with complementary facilities of Hubble and ALMA.

Summary

We have conducted SDSS under the international collaboration whose observations were completed in 2008. SDSS has produced a number of significant results resolving the key problems of cosmology that include the discovery of baryon acoustic oscillation, the discovery of reionization of the Universe at $z > 6$, gravitational weak-lensing that gives the mass distribution of galaxies, and evidence for continued mass assembly of the Milky Way. In 2006-2011, the group of ICRR especially contributed to the discoveries of cosmic dust and extended distribution of dark matter out to the intergalactic space from a galaxy via the gravitational lensing technique.

After the completion of SDSS project, we started new observational cosmology programs

with Subaru telescope, in conjunction with the complementary facilities of Keck, HST, and ALMA, to uncover the physical processes of cosmic reionization and galaxy formation that are getting important questions in cosmology and astrophysics today. Our Subaru, Keck, and HST programs have revealed that there exist an increase of neutral hydrogen fraction beyond $z \sim 6$, free from systematic bias given by galaxy evolution effects. Moreover, our observational results provide the first hint for inside-out reionization scenario. Our findings from the program were featured in the various mass media all over the world via NASA, JPL, U. Tokyo, and NAOJ press releases. Although these studies provide a number of implications about the early epoch of cosmic history, there remain open questions for the physical process of cosmic reionization and cosmic reionization history tightly related to galaxy formation. To address these issues, we are working on the Subaru HSC project that will obtain samples of high- z galaxies about 30 times larger than the currently available samples, which will provide physical measurements with an unprecedented accuracy good enough to distinguish the competing physical models. The HSC survey will start in 2013, and complete in 2017 under the large international collaboration. The ICRR group is developing two HSC-NB filters of NB921 and NB973 with a support of nearly 40 million yen given by JSPS. At the same time, we are conducting the large HST UDF12 program and ALMA observations for cosmic reionization and early galaxy formation with the superb sensitivities and the capabilities for identifying molecular hydrogen distribution, respectively, which complement our on-going efforts of large-area optical survey of the HSC-NB program.

HSC-NB/UDF12 collaborations

HSC-NB spokespersons:

Masami Ouchi (ICRR, The University of Tokyo)

Kazuhiro Shimasaku (The University of Tokyo)

UDF12 spokespersons:

Richard Ellis (California Institute of Technology)

Ross McLure (University of Edinburgh)

UDF12 Tokyo group leader:

Masami Ouchi (ICRR, The University of Tokyo)

Institute	Country	(*)
ICRR, Univ. of Tokyo	Japan	6
Kavli IPMU, U. of Tokyo	Japan	8
School of Science, U. of Tokyo	Japan	15
NAOJ	Japan	29
JAXA	Japan	5
Tohoku Univ.	Japan	6
Tsukuba Univ.	Japan	4
Kyoto Univ.	Japan	4
Osaka Sangyo Univ.	Japan	1
Ehime Univ.	Japan	4
ASIAA	Taiwan	12
NCU	Taiwan	5
NTNU	Taiwan	2
Princeton Univ.	USA	19
Caltech	USA	2
Univ. of Arizona	USA	3
UCLA	USA	2
STScI	USA	2
Carnegie	USA	1
Swinburne Univ.	Australia	4
Univ. of Edinburgh	UK	8
Durham Univ.	UK	1
IAP	France	1
Total		144

(*) Number of participants as of April 2012.

Members

Staffs

Masataka Fukugita, Professor, April 1996 to March 2012

Naoki Yasuda, Assoc. Professor, October 2003 to February 2009

Masami Ouchi, Assoc. Professor, July 2010 to the present

Yoshiaki Ono, Research Associate, April 2012 to the present

Postdoctoral Fellows

Rieko Momose, April 2012 to the present

Suraphong Yuma, May 2012 to the present

Graduate Students

One student was awarded a doctor degree and one student earned a master degree during 2006–2012, supervised by Naoki Yasuda. Note that the group has suspended the graduate student education for

a while but resumed the educational activities since April 2012 when Masami Ouchi accepted two graduate students. Strong emphasis is placed on graduate student education after the arrival of Masami Ouchi.

List of Publications

Papers in Refereed Journals

- [1] “The Ly α Forest Power Spectrum from the Sloan Digital Sky Survey”
P. McDonald *et al.*, *Astrophys. J. Suppl.* **163**, 80–109 (2006).
- [2] “Massive Coronae of Galaxies”
M. Fukugita & P. J. E. Peebles *et al.*, *Astrophys. J.* **639**, 590–599 (2006).
- [3] “The Fourth Data Release of the Sloan Digital Sky Survey”
J. K. Adelman-McCarthy *et al.*, *Astrophys. J. Suppl.* **162**, 38–48 (2006).
- [4] “Erratum: “A Snapshot Survey for Gravitational Lenses among $z \geq 4.0$ Quasars. II. Constraints on the $4.0 < z < 5.4$ Quasar Population””
G. T. Richards *et al.*, *Astron. J.* **131**, 49–54 (2006). [Erratum: *Astron. J.* **132**, 967–967 (2006).]
- [5] “The White Dwarf Luminosity Function from Sloan Digital Sky Survey Imaging Data”
H. C. Harris *et al.*, *Astron. J.* **131**, 571–581 (2006).
- [6] “SDSS J103913.70+533029.7: A Super Star Cluster in the Outskirts of a Galaxy Merger”
G.R. Knapp *et al.*, *Astron. J.* **131**, 859–865 (2006)
- [7] “A Survey of $z > 5.7$ Quasars in the Sloan Digital Sky Survey. IV. Discovery of Seven Additional Quasars”
X. Fan *et al.*, *Astron. J.* **131**, 1203–1209 (2006).
- [8] “Constraining the Evolution of the Ionizing Background and the Epoch of Reionization with $z \sim 6$ Quasars. II. A Sample of 19 Quasars”
X. Fan *et al.*, *Astron. J.* **132**, 117–136 (2006).

- [9] “The Sloan Digital Sky Survey Quasar Survey: Quasar Luminosity Function from Data Release 3”
G. T. Richards *et al.*, *Astron. J.* **131**, 2766–2787 (2006).
- [10] “The History of Cosmological Star Formation: Three Independent Approaches and a Critical Test Using the Extragalactic Background Light”
K. Nagamine *et al.*, *Astrophys. J.* **653**, 881–893 (2006).
- [11] “The Sloan Digital Sky Survey monitor telescope pipeline”
D. L. Tucker *et al.*, *Astr. Nachr.* **327**, 821–843 (2006).
- [12] “Limit on the neutrino mass from the WMAP three-year data”
M. Fukugita *et al.*, *Phys. Rev. D* **74**, 027302-1–3 (2006).
- [13] “The Sloan Digital Sky Survey Quasar Lens Search. I. Candidate Selection Algorithm”
M. Oguri *et al.*, *Astron. J.* **132**, 999–1013 (2006).
- [14] “The rest-frame optical colours of 99000 Sloan Digital Sky Survey galaxies”
V. Smolčić *et al.*, *Mon. Not. Roy. astr. Soc.* **371**, 121–137 (2006).
- [15] “Cosmological constraints from the SDSS luminous red galaxies”
M. Tegmark *et al.*, *Phys. Rev. D* **74**, 123507-1–34 (2006).
- [16] “SDSS J1029+2623: A Gravitationally Lensed Quasar with an Image Separation of 22.5”
N. Inada *et al.*, *Astrophys. J. Lett.* **653**, L 97–L 100 (2006).
- [17] “A Catalog of Morphologically Classified Galaxies from the Sloan Digital Sky Survey: North Equatorial Region”
M. Fukugita *et al.*, *Astron. J.* **134**, 579–593 (2007).
- [18] “Measuring the Matter Density Using Baryon Oscillations in the SDSS”
W. J. Percival *et al.*, *Astrophys. J.* **657**, 51–55 (2007).
- [19] “The Shape of the Sloan Digital Sky Survey Data Release 5 Galaxy Power Spectrum”
W. J. Percival *et al.*, *Astrophys. J.* **657**, 645–663 (2007).
- [20] “Spatial Variations of Galaxy Number Counts in the Sloan Digital Sky Survey. II. Test of Galactic Extinction in High-Extinction Regions”
N. Yasuda *et al.*, *Astron. J.* **134**, 698–705 (2007).
- [21] “The Fifth Data Release of the Sloan Digital Sky Survey”
J. K. Adelman-McCarthy *et al.*, *Astrophys. J. Suppl.* **172**, 634–644 (2007).
- [22] “Sloan Digital Sky Survey Standard Star Catalog for Stripe 82: The Dawn of Industrial 1% Optical Photometry”
Ivezić *et al.*, *Astron. J.* **134**, 973–998 (2007).
- [23] “The Sloan Digital Sky Survey Quasar Catalog. IV. Fifth Data Release”
D. P. Schneider *et al.*, *Astron. J.* **134**, 102–117 (2007).
- [24] “Exploring the Variable Sky with the Sloan Digital Sky Survey”
B. Sesar *et al.*, *Astron. J.* **134**, 2236–2251 (2007).
- [25] “Life Products of Stars”
A. M. Serenelli *et al.*, *Astrophys. J. Suppl.* **172**, 649–662 (2007).
- [26] “Supernovae in the Subaru Deep Field: an initial sample and Type Ia rate out to redshift 1.6”
D. Poznanski *et al.*, *Mon. Not. Roy. astr. Soc.* **382**, 1169–1186 (2007).
- [27] “The Milky Way Tomography with SDSS. I. Stellar Number Density Distribution”
M. Jurić *et al.*, *Astrophys. J.* **673**, 864–914 (2008).
- [28] “The Sloan Digital Sky Survey Quasar Lens Search. II. Statistical Lens Sample from the Third Data Release”
N. Inada *et al.*, *Astron. J.* **135**, 496–511 (2008).
- [29] “The Sloan Digital Sky Survey Quasar Lens Search. III. Constraints on Dark Energy from

- the Third Data Release Quasar Lens Catalog”
M. Oguri *et al.*, *Astron. J.* **135**, 512–519 (2008)
- [30] “The Sixth Data Release of the Sloan Digital Sky Survey”
J. K. Adelman-McCarthy *et al.*, *Astrophys. J. Suppl.* **175**, 297–313 (2008).
- [31] “The Milky Way Tomography with SDSS. II. Stellar Metallicity”
Ž. Ivezić *et al.*, *Astrophys. J.* **684**, 287–325 (2008).
- [32] “Luminosity Function Constraints on the Evolution of Massive Red Galaxies since $z \sim 0.9$ ”
R. J. Cool *et al.*, *Astrophys. J.* **682**, 919–936 (2008).
- [33] “The Seventh Data Release of the Sloan Digital Sky Survey”
K. N. Abazajian *et al.*, *Astrophys. J. Suppl.* **182**, 543–558 (2009).
- [34] “Properties of Disks and Bulges of Spiral and Lenticular Galaxies in the Sloan Digital Sky Survey”
N. Oohama *et al.*, *Astrophys. J.* **705**, 245–254 (2009).
- [35] “Cross-correlation Weak Lensing of SDSS Galaxy Clusters. I. Measurements”
E. S. Sheldon *et al.*, *Astrophys. J.* **703**, 2217–2231 (2009).
- [36] “The Greater Impact of Mergers on the Growth of Massive Galaxies: Implications for Mass Assembly and Evolution since $z \sim 1$ ”
K. Bundy *et al.*, *Astrophys. J.* **697**, 1369–1383 (2009).
- [37] “Measuring the galaxy-mass and galaxy-dust correlations through magnification and reddening”
B. Ménard *et al.*, *Mon. Not. Roy. astr. Soc.* **405**, 1025–1039 (2010).
- [38] “Luminosity Functions of Type Ia Supernovae and Their Host Galaxies from the Sloan Digital Sky Survey”
N. Yasuda *et al.*, *Astron. J.* **139**, 39–52 (2010).
- [39] “Cosmological constraints from the clustering of the Sloan Digital Sky Survey DR7 luminous red galaxies”
B. A. Reid *et al.*, *Mon. Not. Roy. astr. Soc.* **404**, 60–85 (2010).
- [40] “Baryon acoustic oscillations in the Sloan Digital Sky Survey Data Release 7 galaxy sample”
W. J. Percival *et al.*, *Mon. Not. Roy. astr. Soc.* **401**, 2148–2168 (2010).
- [41] “Photometric Response Functions of the Sloan Digital Sky Survey Imager”
M. Doi *et al.*, *Astron. J.* **139**, 1628–1648 (2010).
- [42] “The Sloan Digital Sky Survey Quasar Catalog. V. Seventh Data Release”
D. P. Schneider *et al.*, *Astron. J.* **139**, 2360–2373 (2010)
- [43] “Effects of massive neutrinos on the structure formation of the universe”
M. Fukugita *et al.*, *Prog. in Particle and Nucl. Phys.* **64**, 360–362 (2010).
- [44] “The Milky Way Tomography with SDSS. III. Stellar Kinematics”
N. A. Bond *et al.*, *Astrophys. J.* **716**, 1–29 (2010).
- [45] “The Sloan Digital Sky Survey Quasar Lens Search. IV. Statistical Lens Sample from the Fifth Data Release”
N. Inada *et al.*, *Astron. J.* **140**, 403–415 (2010).
- [46] “Stellar Populations of Ly α Emitters at $z = 4.86$: A Comparison to $z \sim 5$ Lyman Break Galaxies”
S. Yuma *et al.*, *Astrophys. J.*, **720**, 1016–1029 (2010).
- [47] “Ly α Emitters at $z = 7$ in the Subaru/XMM-Newton Deep Survey Field: Photometric Candidates and Luminosity Functions”
K. Ota *et al.*, *Astrophys. J.* , **722**, 803–811 (2010).
- [48] “Statistics of 207 Ly α Emitters at a Redshift Near 7: Constraints on Reionization and Galaxy Formation Models”
M. Ouchi *et al.*, *Astrophys. J.* , **723**, 869–894 (2010).

- [49] “Keck spectroscopy of faint $3 < z < 7$ Lyman break galaxies - I. New constraints on cosmic reionization from the luminosity and redshift-dependent fraction of Lyman α emission”
D. P. Stark *et al.*, *Mon. Not. Roy. astr. Soc.* , **408**, 1628–1648 (2010).
- [50] “Stellar Populations of Ly α Emitters at $z \sim 6 - 7$: Constraints on the Escape Fraction of Ionizing Photons from Galaxy Building Blocks”
Y. Ono *et al.*, *Astrophys. J.* , **724**, 1524–1535 (2010).
- [51] “Lyman- α Emitters and Lyman-Break Galaxies at $z = 3-6$ in Cosmological SPH Simulations”
K. Nagamine *et al.*, *Publ. of Astr. Soc. Japan*, **62**, 1455–1472 (2010).
- [52] “Characterization of Sloan Digital Sky Survey Stellar Photometry”
M. Fukugita *et al.*, *Astron. J.* , **141**, 47–58 (2011).
- [53] “Microwave Emission from the Edgeworth-Kuiper Belt and the Asteroid Belt Constrained from the Wilkinson Microwave Anisotropy Probe”
K. Ichikawa *et al.*, *Astrophys. J.* **736**, 122–128 (2011).
- [54] “Supernovae in the Subaru Deep Field: the rate and delay-time distribution of Type Ia supernovae out to redshift 2”
O. Graur *et al.*, *Mon. Not. Roy. astr. Soc.* **417**, 916–940 (2011).
- [55] “Matter Distribution around Galaxies”
S. Masaki *et al.*, *Astrophys. J.* **746**, 38–43 (2012).
- [56] “The Subaru Ly α blob survey: a sample of 100-kpc Ly α blobs at $z = 3$ ”
Y. Matsuda *et al.*, *Mon. Not. Roy. astr. Soc.* , **410**, L13–L17 (2011).
- [57] “Keck Spectroscopy of Faint $3 < z < 7$ Lyman Break Galaxies: A High Fraction of Line Emitters at Redshift Six”
D. P. Stark *et al.*, *Astrophys. J.* , **728**, L2–L6 (2011).
- [58] “MOIRCS Deep Survey. VII. NIR morphologies of star-forming galaxies at redshift $z \sim 1$ ”
M. Konishi *et al.*, *Publ. of Astr. Soc. Japan*, **63**, 363–377 (2011).
- [59] “MOIRCS Deep Survey. IX. Deep Near-Infrared Imaging Data and Source Catalog”
M. Kajisawa *et al.*, *Publ. of Astr. Soc. Japan*, **63**, 379–401 (2011).
- [60] “Completing the Census of Ly α Emitters at the Reionization Epoch”
N. Kashikawa *et al.*, *Astrophys. J.*, **734**, 119–137 (2011).
- [61] “Keck Spectroscopy of Lyman-break Galaxies and Its Implications for the UV-continuum and Ly α Luminosity Functions at $z > 6$ ”
L. Jiang *et al.*, *Astrophys. J.* , **743**, 65–74 (2011).
- [62] “The Sloan Digital Sky Survey Quasar Lens Search. V. Final Catalog from the Seventh Data Release”
N. Inada *et al.*, *Astron. J.* **143**, 119–133 (2012).
- [63] “The Sloan Digital Sky Survey Quasar Lens Search. VI. Constraints on Dark Energy and the Evolution of Massive Galaxies”
M. Oguri *et al.*, *Astron. J.* **143**, 120–133 (2012).
- [64] “Cosmic Dust in Mg II Absorbers”
B. Ménard *et al.*, *Astrophys. J.* , **754**, 116–123 (2012).
- [65] “Spectroscopic Confirmation of Three z -dropout Galaxies at $z = 6.844 - 7.213$: Demographics of Ly α Emission in $z \sim 7$ Galaxies”
Y. Ono *et al.*, *Astrophys. J.* , **744**, 83–95 (2012).
- [66] “Average Metallicity and Star Formation Rate of Ly α Emitters Probed by a Triple Narrow-band Survey”
K. Nakajima *et al.*, *Astrophys. J.* , **745**, 12–30 (2012).

Papers in Conference Proceedings

- [67] “Massive Neutrinos in Cosmology”
M. Fukugita, *The 7th International Workshop on Neutrino Factories and Superbeams*, **155**, 10–17 (2006).

- [68] “Probing the Cosmic Reionization with High- z Galaxies”
M. Ouchi *et al.*, Astronomy with Megastructures. Joint Science with the E-ELT and SKA, 63–67 (2010).
- [69] “Reionization History and Physical Processes Indicated from the Census of Ly α Emitters at $z \sim 7$ ”
M. Ouchi *et al.*, American Astronomical Society, 220th AAS Meeting, 512.01 (2012).

PRIMARY COSMIC RAY GROUP

Introduction

Earth's climate system responds to both internal and external forcing. One of the most important sources of external forcing is solar activity variations at monthly to millennial time scales accompanied by the changes in total solar irradiance (TSI), ultra violet (UV) radiation, and solar wind. Solar wind affects the state of heliosphere, and thus the modulation of galactic cosmic rays. Possible connections between solar activity and climate at a wide range of time scales have been found by paleoclimate proxy records. The physics behind is, however, still not fully understood and is under debate. The objectives of this research group are to understand the features and the physics of long-term variations of solar activity and the consequent changes in the modulation of galactic cosmic rays in the heliosphere. Also, we aim to understand the mechanisms of solar influence on climate change. Especially, the influence through modulating the galactic cosmic rays is poorly understood and thus needs focused investigation. For those purposes, we are now conducting the measurements of cosmogenic nuclides in (1) tree rings and (2) ice cores with annual time resolution, (3) reconstruction of paleoclimate based on stable isotopes in tree rings, and the comparison of those records especially for the 22-year time scale, at which period the impact of galactic cosmic rays can be explicitly traced. Also, we analyze (4) cloud parameters obtained from satellite-based observations to examine the detailed physical mechanisms of cosmic ray impact on cloud formation and the atmospheric circulation. Variations of galactic cosmic rays caused by solar flares and current sheet passages can be utilized to trace the recipient and the propagation of cosmic ray impacts. For further investigating the impacts of high energy cosmic ray particles on cloud micro physics, we have started to plan (5) observations at around the equatorial region. Our research interests also cover the topic of (6) the variability of total solar irradiance. We are now planning to conduct borehole experiment on the moon.

Measurement of carbon-14 in tree rings

We have measured carbon-14 content in tree rings (Figure 1) with the precision of 0.3% using the Accelerator Mass Spectrometer (AMS) at Yamagata University, Nagoya University and MALT (Micro Analysis Laboratory, Tandem accelerator), the University of Tokyo. Carbon-14 is produced in the atmosphere by the capture of secondary cosmic rays (neutrons) by nitrogen nuclei, and is absorbed in trees by photosynthesis. Temporal variations of carbon-14 content in tree rings reflect the variations of solar wind and heliospheric magnetic field. We have so far focused on the grand solar minima such as the Maunder (AD1645-1715) and Spörer (AD1415-1534) minima, and the long-term activity maxima around BC5200 and AD300. We have reconstructed the changes in solar cycle length during the times as well as their transitions around the onset. We have found a tendency of lengthening of solar cycles to 13-14 years at the periods of low solar activity level. Importantly, the lengthening starts at least two cycles ahead of the onset of the events, suggesting a gradual change in the meridional circulation in solar convection zone around the onset. The reconstruction of solar cycle lengths in the past can be useful also for constraining the history of absolute solar activity level. Low resolution records of carbon-14 are often contaminated by the information on the changes of geomagnetic field intensity and the carbon cycle. Detection of lengthening/shortening of solar cycles can be an independent methodology for retrieving the history of solar activity levels. Imprints of solar decadal cycles in fossil corals and shells might be also utilized to trace the longer history, e.g. to challenge the faint young sun paradox.

Measurement of beryllium-10 in ice cores

Since 2007, we have conducted measurements of beryllium-10 content in Antarctic ice core obtained at Dome Fuji station. Beryllium-10 is produced through the spallation of atmospheric nuclei by cosmic rays. The typical energy of cosmic rays to produce beryllium-10 is about 1 GeV, and thus the production rate of beryllium-10 reflect the state of



Fig. 1. Annual rings of trees retaining the history of the Sun, cosmic rays, and climate.

solar modulation of cosmic rays. Annual measurements were conducted for the Maunder minimum in order to understand the feature of solar dynamo and the heliospheric environment in detail. Together with the independently obtained beryllium-10 record obtained by NGRIP¹, we have analyzed the record and found that 28-year cycles become dominant at the Maunder Minimum (Figure 3-c). This period is the double length of 14-year solar cycle found by carbon-14 data. This 28-year cycle is the manifestation of the Hale cycle during the time, suggesting that the drift effect of cosmic rays in the heliosphere had become prominent at this suppressed solar activity, and that the heliospheric environment had been changed. The analyses of beryllium-10 record based on the result of numerical simulation of drift effect² suggest that the tilt of heliospheric current sheet was totally flattened at this period (Figure 2). It was suggested that the flattened current sheet resulted in the spikes of incident cosmic rays at the Earth at around the solar minima of negative polarity. The flux of incident cosmic rays at those periods is 30-50% higher compared to the solar minima of positive polarity. In 2011, we started high precision measurements of carbon-14 in annual tree rings to determine the absolute ages of those cosmic ray events, and to examine the precise flux at the Earth. In order to utilize the AMS facility installed at the Yamagata University in 2009,

*1 Berggren et al., *Geophys. Res. Lett.* **36**, L11801 (2009).

*2 Kota and Jokipii, *Adv. Space Res.* **27**, 529-534 (2001)

our group has been trying to achieve 0.1% precision, higher precision than usual precision of AMS.

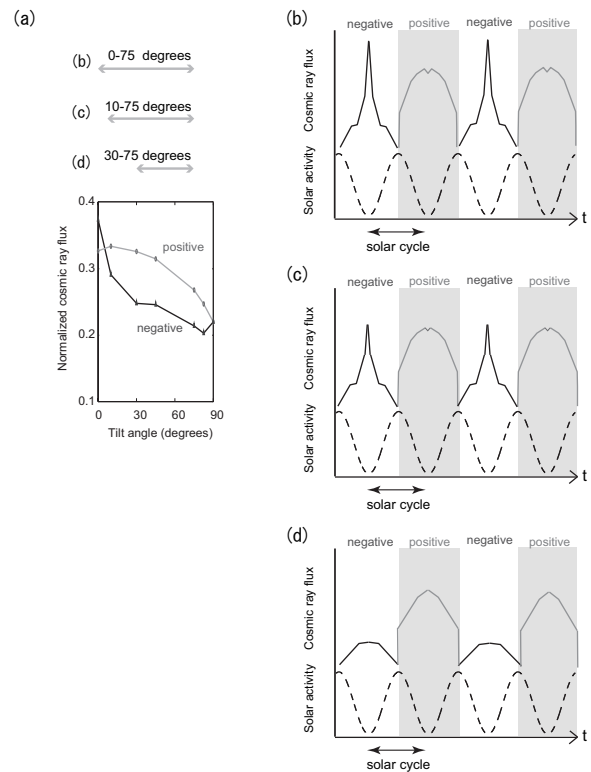


Fig. 2. Profiles of cosmic ray 22-year variations under different heliospheric conditions. (a) Flux of cosmic rays at the Earth against the tilt angle of solar magnetic neutral line and the polarity of solar dipole magnetic field (based on Kota and Jokipii, 2001). (b) Time profile of cosmic ray variation when the range of the tilt angle over solar cycles is 0-75 degrees. (c) Same as (b) but for 5-75 degrees. (d) Same as (b) but for 30-75 degrees.

Reconstruction of paleo-climate

In 2008, we have found that the characteristic variations of cosmic rays with 22-year period are reflected in northern hemispheric climate variations (Figure 3-a,b). For example, lengthening and shortening of 22-year cycles as well as the phase transitions of 22-year cycles are found in climate proxy records. Phase transition of 22-year cycle is related to the drift effect of cosmic rays in the heliosphere. Generally, the flux of incident cosmic rays tends to be higher at the periods of positive solar magnetic polarity, however, the intensity becomes much higher at negative magnetic polarity only around

*3 Vinther et al., *Geophys. Res. Lett.* **30**, 1387-1390 (2003).

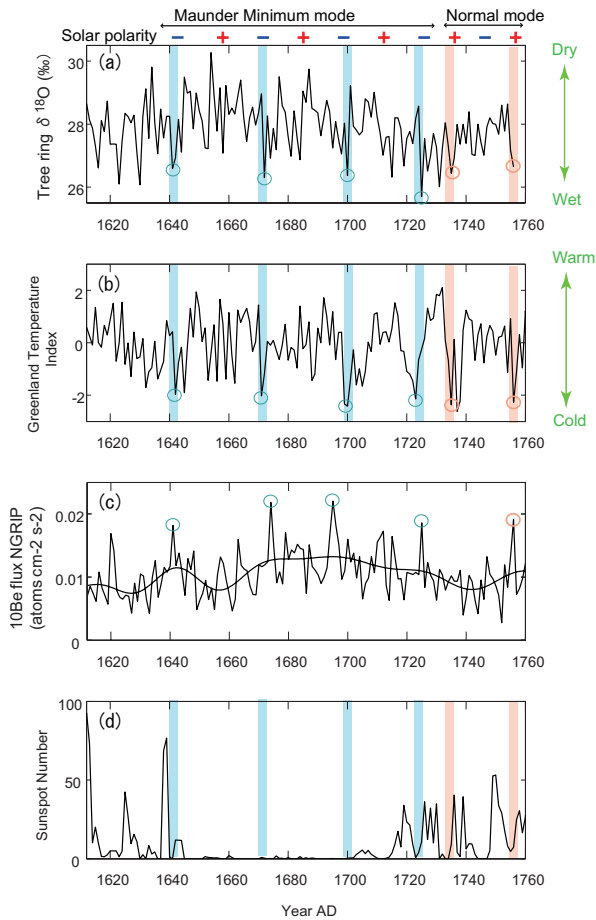


Fig. 3. Comparison of reconstructed cosmic rays and climate around the Maunder Minimum. (a) Reconstructed relative humidity in Japan around June. (b) Reconstructed temperature based on oxygen-18/oxygen-16 ratio in the Greenland ice cores³. (c) Beryllium-10 record from Greenland ice core (Berggren et al., 2009). (d) Record of sunspot number. The blue shaded areas correspond to the solar cycle minima of polarity negative determined by carbon-14 record.

the grand solar minima (Figure 2). The manifestation of 22-year cycles and their phase transitions in climate records suggest that cosmic rays are one of the important external forcing of climate change. The galactic cosmic rays have been considered to promote cloud formation, however the detailed physical mechanism is not fully understood. Although the physical mechanisms should be clarified through both laboratory experiment such as the CLOUD experiment at CERN and the direct observations in the actual atmosphere, the anomalous spikes of cosmic rays found at the Maunder Minimum (Figure 1-c) can be also utilized to trace the response of climate system to cosmic rays. The cos-

mic ray spikes are 1-year durations respectively and four events are identified in total. We are now measuring stable isotopes in tree rings obtained from Japan and Asian countries to trace the response of Asian monsoon to 1-year cosmic ray enhancements. So far we have found decrease in northern hemispheric temperatures, enhancement of relative humidity in Japan around the rainy season, and the decrease in the winter temperature in Japan. Mapping of such temperature and precipitation records over the globe at the cosmic ray spikes can shed light on the response of monsoonal activities as well as the response of overall climate system.

Tracing the impact of solar rotations on cloud activities

Since 2006, we have conducted the analyses of cloud data obtained by satellite based observations. It is known that lightning activity often show 27-day variation, which is close to the time scale of solar rotations. It is also known that the 27-day signal in lightning activity tends to be enhanced at around the 11-year solar activity maxima. In order to examine the impact of 27-day solar rotational period on meteorological phenomena, we analyzed the Outgoing Long-wave Radiation (OLR) data, available since AD1974. Continuous record is available only since AD1979, but it covers at least three solar decadal cycles. In 2010, we found that the monthly variations in cloud height around the tropical regions are under the influence of solar rotations. 27-day period was found in cloud activity around the Indian Ocean and the western Pacific Ocean (Figure 4), only around the maximal period of solar cycles. The appearance of sunspots and faculae around solar cycle maxima changes the total solar irradiance and ultra violet radiation. Large solar flares caused by sunspot activities also cause the changes in incident cosmic rays at the Earth. Although the actual parameter to mediate the connection between solar rotations and cloud activities is not clear, it is suggested that solar impact is also present at this monthly time scale. Further investigations on this phenomenon would improve the predictability of weather and climate. We have also investigated the impact of Quasi-Biennial Oscillation (QBO) in the stratosphere on the 27-day solar rotational signal in cloud activities around the equatorial region. As a result, we found that QBO is affecting the spatial distribution of 27-day sig-

nal around the tropics (Figure 4) at around solar maxima. It may be suggesting that the interaction between the stratosphere and the troposphere is strengthened at high solar activity levels and that QBO is changing the sensitive location in the troposphere to the external forcing at such periods.

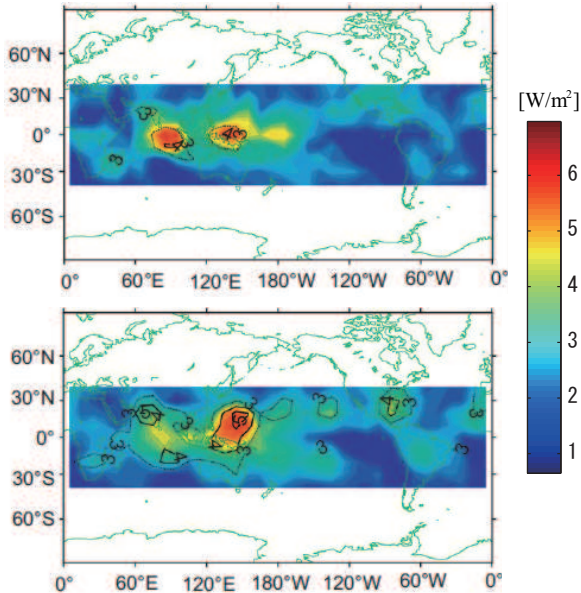


Fig. 4. Distribution map of the 27-day variability in Outgoing Long-wave Radiation at around the maxima of 11-year solar cycles. Upper panel is for the QBO westerly phases and the lower panel is for the QBO easterly phases.

Planning future observations

Apart from the examinations based on paleo-solar and climate reconstructions, we are now planning to conduct cloud and aerosol measurements at the equatorial region at which sensitive response to solar rotations were found. The problem of satellite based observations is that the data are often limited to one snapshot per day, and thus cannot be used to examine the impact of cosmic rays on the cloud micro physics. Also, most of the records obtained by the missions so far do not have altitude distributions, which would be essential to trace the cosmic ray impacts. We are now discussing the possibility to conduct measurements with 1 km altitude distribution. There are two steps in cosmic ray impacts. One is the production of Cloud Condensation Nuclei (CCN) by ionizing the atmospheric molecules. The other is the promotion of coagulation between the pre-existing cloud droplets and aerosols. For the latter part, it is suggested that the sign of cosmic ray impacts could be different by altitudes. LIDAR ob-

servations, ground-based observations at high altitude mountain, aircraft measurements, and aerosol sonde are the candidates for the methodology. Possible observational sites are now under consideration (Figure 5).



Fig. 5. View from the meteorological station at the Mt. Kenya (3678m a.s.l.).

Lunar borehole experiment

Extent of long-term variability of total solar irradiance is also an important issue. Since 2006, we have been discussing the possibility of reconstructing the long-term changes in total solar irradiance since Galileo's time by the lunar borehole experiment. Lunar surface temperature is determined by simple radiative balance and thus it is controlled by the changes in solar irradiance and the distance to the Sun. The changes in the thermal properties at lunar surface diffuse in the lunar regolith, and are stored due to the very low thermal diffusivity. Numerical simulation using the thermal properties obtained by Apollo project in the 1970's suggests that 10 meters of lunar regolith still retains the information of solar irradiance since AD1600 (Figure 6). Although the borehole measurements were achieved only for the upper 2 meters of lunar regolith during the Apollo time, new technique developed since then can reach at least 3-5 meters depth and possibly 10 meters in the near future. We are now discussing to conduct preliminary experiment at the next Japanese lunar landing mission.

Summary

Cosmogenic nuclides are powerful tools to understand the long-term variations of solar magnetic

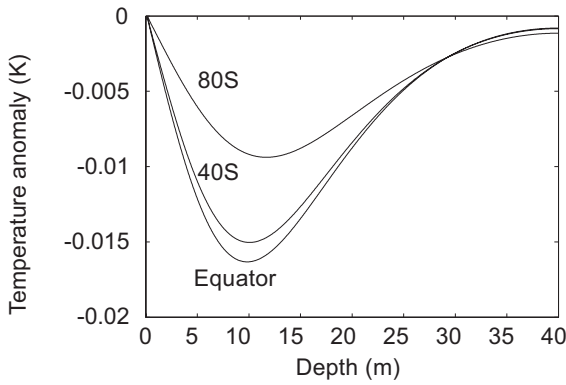


Fig. 6. Temperature anomalies in lunar regolith as response to $2W/m^2$ difference in total solar irradiance at the Maunder Minimum, at the equator, mid-latitude (40S) and near the south pole (80S).

activity, heliospheric environment, and the characteristics of incident primary cosmic rays. Reconstruction of solar cycle lengths based on carbon-14, for example, has shed light on the mechanism of long-term reduction of solar activity level, such as the Maunder Minimum. Realistic numerical modeling of solar dynamo based on such observational data would enable us to better predict near future solar activity. Records of cosmogenic nuclides also allow us to understand the lively discussed sun-climate connection. Comparison of cosmogenic nuclides and paleo-climate data are strongly suggesting that solar and heliospheric magnetic field is playing an important role in climate change through modulation of galactic cosmic rays. Satellite-based observations of clouds suggest that external forcing of climate might be playing an important role, especially in equatorial cloud activities. Further observations of cloud properties such as Cloud Condensation Nuclei and cloud droplet radii, associated with cosmic ray events such as Forbush Decreases (FDs) and Ground Level Enhancements (GLEs), would help us to understand the influence of charged particles on cloud microphysics.

Collaborating Members

Institute	Country	(*)
ICRR, Univ. of Tokyo	Japan	6
Univ. of Tokyo	Japan	4
Tokyo Inst. of Tech.	Japan	4
Yamagata Univ.	Japan	4
GSFC, NASA	USA	3
Jomo-Kenyatta Univ.	Kenya	3
Nagoya Univ.	Japan	2
Osaka City Univ.	Japan	2
KUCT	Kenya	2
Aichi Univ. of Tech.	Japan	1
Chubu Univ.	Japan	1
Hirosaki Univ.	Japan	1
JAMSTEC	Japan	1
NAOJ	Japan	1
NIPR	Japan	1
Osaka Pref. Univ.	Japan	1
Tata Inst.	India	1
Total		37

(*) Number of participants as of September 2012.

Research projects described above have been conducted by Hiroko Miyahara (ICRR) as a co-ordinator.

Members

Staffs

Hiroko Miyahara, Project Research Associate, October 2008 to present

List of Publications

Papers in Refereed Journals

- [1] “9,400 years of cosmic radiation and solar activity from ice cores and tree rings”
F. Steinhilber, J. Abreu, J. Beer, I. Brunner, M. Christl, H. Fischer, U. Heikkila, P. Kubik, M. Mann, H. Miller, H. Miyahara, K.G. McCracken, H. Oerte, and F. Wilhelms, Proc. Natl. Acad. Sci. **vol. 109**, 5967–5971 (2012).
- [2] “A decade of the Moderate Resolution Imaging Spectroradiometer: is a solar - cloud link detectable?”
B. Laken, E. Palle, and H. Miyahara, Journal of Climate, doi:http://dx.doi.org/10.1175/JCLI-D-11-00306.1., (2012).

- [3] “Implications for the low latitude cloud formations from solar activity and the Quasi-Biennial Oscillation”
P.K. Hong, H. Miyahara, Y. Yokoyama, Y. Takahashi, and M. Sato, *Journal of Atmospheric and Solar-Terrestrial Physics* **vol. 73**, 587–591 (2011).
- [4] “Synchronized Northern Hemisphere Climate Change and Solar Magnetic Cycles during the Maunder Minimum”
Y. T. Yamaguchi, Y. Yokoyama, H. Miyahara, K. Sho and T. Nakatsuka, *Proc. Natl. Acad. Sci.*, doi: 10.1073/pnas.1000113107, (2010).
- [5] “Explosive volcanic eruptions triggered by cosmic rays: volcano as a bubble chamber”
T. Ebisuzaki, H. Miyahara, R. Kataoka, T. Sato, and Y. Ishimine, *Gondwana Research*, doi:10.1016/j.gr.2010.11.004, (2010).
- [6] “Is the Sun heading for another Maunder Minimum? –Precursors of the grand solar minima”
H. Miyahara, K. Kitazawa, K. Nagaya, Y. Yokoyama, H. Matsuzaki, K. Masuda, T. Nakamura, and Y. Muraki, *Journal of Cosmology* **vol. 8**, 1970–1982 (2010).
- [7] “Variations of Solar Activity and Climate during the Past 1200 Years”
H. Miyahara, *Journal of Geography* **vol. 119**, 510–518 (2010).
- [8] “27-day variation in cloud amount and relationship to the solar cycle”
Y. Takahashi, Y. Okazaki, M. Sato, H. Miyahara, K. Sakanoi, and P.K. Hong, *Atmos. Chem. Phys.* **vol. 10**, 1577–1584 (2010).
- [9] “Cosmogenic Radiocarbon and the Solar Activity”
K. Masuda, K. Nagaya, H. Miyahara, Y. Muraki, and T. Nakamura, *Proc. Int. Workshop Advances in Cosmic Ray Science*, *J. Phys. Soc. Jpn.* **vol. 78**, Suppl. A, 1–6 (2009).
- [10] “Possible link between multi-decadal climate cycles and periodic reversals of solar magnetic field polarity”
H. Miyahara, Y. Yokoyama and K. Masuda, *Earth Planet. Sci. Lett.* **vol. 272**, 290–295 (2008).
- [11] “Deriving Historical Total Solar Irradiance from Lunar Borehole Temperatures”
H. Miyahara, G. Wen, R. Cahalan and A. Ohmura, *Geophys. Res. Lett.* **vol. 35** L02716 (2008).
- [12] “Transition of solar cycle length in association with the occurrence of grand solar minima indicated by radiocarbon content in tree-rings”
H. Miyahara, K. Masuda, T. Nakamura, H. Kitagawa, K. Nagaya and Y. Muraki, *Quaternary Geochronology* **vol. 3**, 208–212 (2008).
- [13] “High precision ^{14}C measurements and application to wiggle-match dating of wood materials at Nagoya University”
T. Nakamura, H. Miyahara, K. Masuda, H. Menjo, K. Kuwana, K. Kimura, M. Okuno, M. Minami, H. Oda, A. Rakowski, T. Ohta, A. Ikeda and E. Niu, *Nucl. Instrum. Methods. Phys. Res., Sect. B*, **vol. 259**, 408–413 (2007).
- [14] “Variation of solar activity from the Spoerer to the Maunder minima indicated by radiocarbon content in tree-rings”
H. Miyahara, K. Masuda, K. Nagaya, K. Kuwana, Y. Muraki and T. Nakamura, *Adv. Space Res.* **vol. 40**, 1060–1063 (2007).
- [15] “The solar cycle at the Maunder minimum epoch”
H. Miyahara, D. Sokoloff and I. G. Usoskin, *Adv. Geosciences* **vol. 2**, 1–20 (2006).
- [16] “Variation of solar cyclicity during the Spoerer Minimum”
H. Miyahara, K. Masuda, Y. Muraki, H. Kitagawa and T. Nakamura, *J. Geophys. Res.* **vol. 111**, A03103 (2006).
- Papers in Conference Proceedings
- [17] “Influence of the Schwabe/Hale solar cycles on climate change during the Maunder Minimum”
H. Miyahara, Y. Yokoyama, Y.T. Yamaguchi, *IAU XXVII General Assembly* **vol. 264**, 427–433 (2009).

THEORY GROUP

Introduction

The main interests of the theory group are particle physics phenomenology and particle cosmology. The group has been conducted by three staff members, Kawasaki (May 2004 till present), Hisano (March 2002 – June 2010), and Ibe (March 2011 till present). After 2006, the group hosted fourteen PDs. The research led to the publications of 158 papers in refereed journals, 23 papers in conference proceedings, and 20 papers under referee. The group also conducted the education in the graduate school in collaboration with the Department of Physics. The group accepted twenty six graduate-school students after 2006, and nine of them have acquired Ph-D.

Research Activities: Particle Phenomenology

The supersymmetric (SUSY) extension of the standard model (SM) in the particle physics is considered to be one of the most promising models beyond the standard model. In the minimal version, the Higgs boson mass is interrelated to the gauge coupling constants, and hence, the Higgs boson mass is predictable. The supersymmetric standard model is also favored since it is compatible with the grand unified theories (GUTs). A lot of theoretical and experimental efforts to search for the signature are put into now. Our group are studying phenomenological aspects of the SUSY models as follows.

Flavor Physics

The Standard Model (SM) predictions for the lepton flavor-violating (LFV) processes like $\mu \rightarrow e\gamma$ are well far from any realistic experimental resolution, thus, the appearance of $\mu \rightarrow e\gamma$ at the running MEG experiment would unambiguously point towards a New Physics (NP) signal. In Ref. [80], we discussed the phenomenological implications in case of observation/improved upper bound on $\mu \rightarrow e\gamma$ at the running MEG experiment for supersymmetric (SUSY) scenarios with a see-saw mechanism accounting for the neutrino masses. We outlined the role of related observables to $\mu \rightarrow e\gamma$ in

shedding light on the nature of the SUSY LFV sources providing useful tools to reconstruct some fundamental parameters of the neutrino physics and to test whether an underlying SUSY Grand Unified Theory (GUT) is at work. The perspectives for the detection of LFV signals in tau decays were also discussed (Fig. 1).

In Ref. [45], we discussed the μ - e transition processes induced by non-holomorphic Yukawa interactions in the minimal supersymmetric standard model (MSSM). When supersymmetry is broken, the coupling structures between Higgs doublets and leptons are modified and flavor-changing neutral currents could be generated. In the framework of the MSSM, we calculated those effects to the rates for $\mu \rightarrow e\gamma$, $\mu \rightarrow eee$, and μ - e conversion in nuclei. We performed more detailed calculations of the lepton flavor violating (LFV) operators in the heavy Higgs decoupling limit than previous works, and show the accurate $\tan\beta$ dependence of them. Furthermore, we compared the contribution to the LFV operators mediated by Higgs bosons with the one generated gaugino/slepton exchange, and discussed the competition between these two effects.

The Standard Model predictions for the hadronic and leptonic electric dipole moments (EDMs) are well far from the present experimental resolutions, thus, the EDMs represent very clean probes of NP effects. Especially, within supersymmetric frameworks with flavor-violating soft terms large and potentially visible effects to the EDMs are typically expected. In Refs. [86, 116, 145], we evaluated the predictions for the EDMs at the beyond-leading-order (BLO). In fact, we showed that BLO contributions to the EDMs dominate over the leading-order (LO) effects in large regions of the supersymmetric parameter space. Hence, their inclusion in the evaluation of the EDMs is unavoidable. As an example, we showed the relevance of BLO effects to the EDMs for a SUSY SU(5) model with right-handed neutrinos.

Dark Matter

Existence of the dark matter in the universe has been established by cosmological observation, while nature of the dark matter is still mystery.

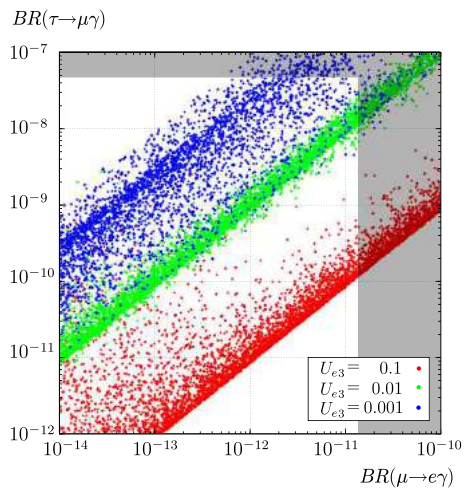


Fig. 1. $BR(\mu \rightarrow e\gamma)$ vs $BR(\tau \rightarrow \mu\gamma)$ in SUSY SU(5) GUT with right-handed neutrinos. Here, U_{e3} in the MNS matrix are 0.1, 0.01, and 0.001. Grey regions are excluded by experimental upper bounds on $BR(\mu \rightarrow e\gamma)$ and $BR(\tau \rightarrow \mu\gamma)$.

Weakly-interacting massive particles (WIMPs) are attractive candidates for the dark matter, and many models are proposed to predict WIMPs.

In Ref. [158] we pointed out that thermal relic abundance of the dark matter is strongly altered by a non-perturbative effect called the Sommerfeld enhancement, when constituent particles of the dark matter are non-singlet under the $SU(2)_L$ gauge interaction and much heavier than the weak gauge bosons. Typical candidates for such dark matter particles are the heavy wino- and higgsino-like neutralinos. We investigated the non-perturbative effect on the relic abundance of dark matter for the wino-like neutralino as an example. We showed that its thermal abundance is reduced by 50% compared to the perturbative result. The wino-like neutralino mass consistent with the observed dark matter abundance turns out to be $2.7 \text{ TeV} < m < 3.0 \text{ TeV}$ (see Fig. 2).

The direct search of the dark matter on the earth is to detect recoiled nuclei from the elastic scattering with dark matter. In Refs. [44, 46] we calculated the spin-independent cross section of nucleon-dark matter scattering process at loop level, which is relevant to the dark matter direct detection. Paying particular attention to the scattering of gluon with dark matter, which contributes as leading order in the perturbation, we systematically evaluated loop diagrams with tracking the characteristic loop momentum which dominates in the loops. Here loop diagrams whose typical loop momentum scales are the masses of quarks and other heavier particles are

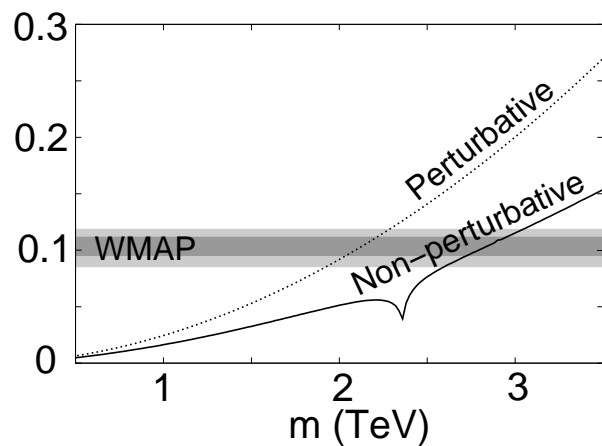


Fig. 2. Thermal relic abundance of the dark matter in the current universe as a function of wino-like neutralino mass. Solid (Dashed) line comes from dark matter annihilation cross section with (without) the Sommerfeld enhancement. Allowed region by the WMAP at 1(2) σ levels are also shown as dark (light) shaded area.

separately presented. Then, we properly took into account each contribution to give the cross section. We assume that the dark matter is pure bino or wino in the supersymmetric models. The application to other models is straightforward.

The excess of cosmic-ray electron and positron fluxes was reported by the PAMELA satellite and ATIC balloon experiments on 2008. It might be interpreted as the signals of the dark matter annihilation or decay into leptons. First, we showed that the dark matter annihilation/decay which reproduces the electron/positron excess may yield a significant amount of high-energy neutrinos from the Galactic center [74, 87]. In the case, future kilometer-square size experiments may confirm such a scenario, or even the Super-Kamiokande results already put constraints on some dark matter models. Next, we showed that the dark matter annihilation in the big-bang nucleosynthesis epoch affects the light element abundances, and it gives stringent constraints on such annihilating dark matter scenarios for the case of hadronic annihilation [84, 92].

Higgs Boson Mass

The recent discovery of the Higgs-like boson at the Large Hadron Collider (LHC) at an essentially 5σ level is not only completing the Standard Model but also opens new frontiers in particle physics. Especially, the Higgs boson mass, which is now observed at around 125 GeV, plays a role of a strong discriminator of models beyond the Standard Model physics. For example, in the models

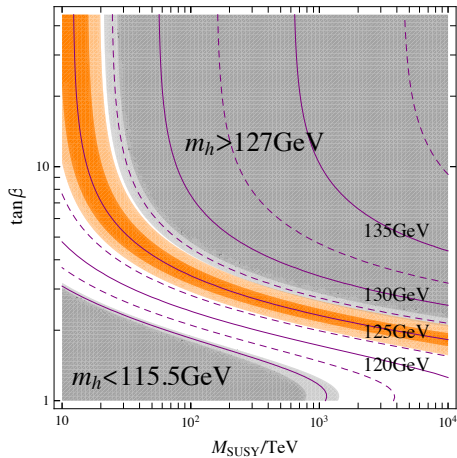


Fig. 3. The contour plot of the lightest Higgs boson mass. Here, we have fixed $m_{3/2} = 50 \text{ TeV}$ and taken $\mu_H = M_{\text{SUSY}}$. The orange band shows the Higgs boson mass $124 \text{ GeV} < m_h < 126 \text{ GeV}$ hinted by the ATLAS and CMS collaborations for the central value of the Top quark mass. The light orange band is the one including the 1σ error of the Top quark mass.

with the Higgs boson emerging as a composite particle, the Higgs boson mass tends to be much larger than the Z-boson masses, while it does not highly exceed the Z-boson mass in the models with the elementary Higgs boson.

In response to this situation (and in fact slightly proceeding to the announcement of the discovery of the Higgs-like boson at the LHC experiments), we proposed a model of the MSSM, the pure gravity mediation model (refs. [8, 11]), which successfully predicts the elementary Higgs boson mass in the above range (Fig. 3). In the model, the scalar partners of the matter fields in the Standard Model are predicted to have masses in the range of tens to hundred TeV range, which is far above the reach of the LHC experiments. The fermionic partners of the gauge bosons are, on the other hand, predicted to have masses below the TeV range which allows us to detect them at the LHC experiments. Interestingly, the model predicts a meta stable charged particle (chargino) which decays into a pair of a charged pion and a neutral stable particle (neutralino). Such a meta stable particle enables us to detect the events involving supersymmetric particles by looking for charged tracks disappearing inside the detectors. We also studied the neutralino dark matter properties and found that the scenario can be tested by the future observation of the cosmic ray anti-proton flux (Fig. 4).

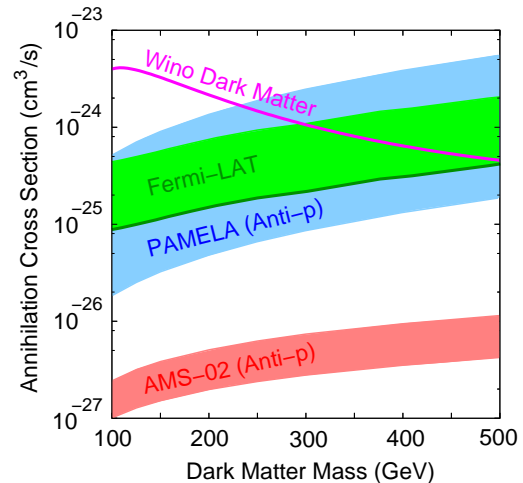


Fig. 4. Constraints and future prospects of indirect detection experiments of dark matter. Theoretical prediction of the neutral wino dark matter is also shown. Here, the expected sensitivity of AMS-02 is the one for the one year operation. It should be noted that AMS-02 has an excellent sensitivity to the anti-protons up to 250 – 500 GeV which is capable of picking-up the anti-protons from the decays of the W-bosons in the final state for the dark matter annihilation with a mass up to 1 TeV.

Research Activities: Astroparticle Physics

The progress in particle physics such as grand unification theories and supersymmetry leads us to more insight into the fundamental aspects of the early universe. On the other hand, cosmology and astrophysics are used to test new theories in particle physics. Such particle cosmology is one of main subjects of our group.

Big Bang Nucleosynthesis and Gravitino Problem

The predicted abundances of the light elements in Big Bang Nucleosynthesis (BBN) are sensitive to the cosmological scenario. Exotic cosmological scenarios based on physics beyond the standard model would modify the light-element abundances too much to be consistent with the observations. Thus, the BBN provides significant constraints on the new particles which change the cosmological evolution at the cosmic time $t \sim 10^{-2} - 10^{12} \text{ sec}$.

In Ref. [128] we derived general constraints on the relic abundances of a long-lived particle which mainly decays into a neutrino at cosmological time scales. We also studied BBN constraints on both unstable and stable gravitino taking account of recent progress in theoretical study of the BBN processes as well as observations of primordial light-element abundances [105, 131, 139]. In the case of unstable gravitino, we set the upper limit on the

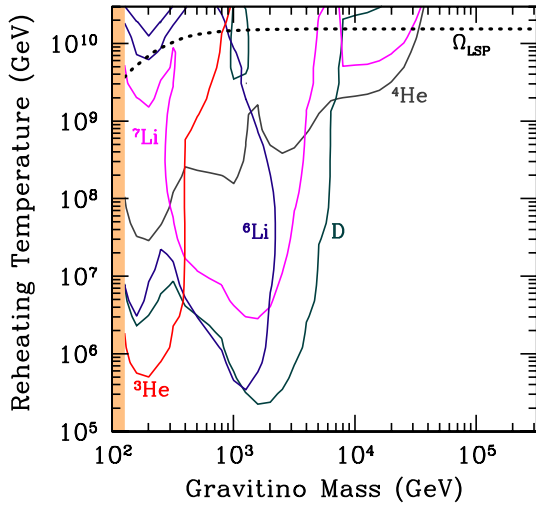


Fig. 5. BBN constraints for unstable gravitino. Each solid line shows the upper bound on the reheating temperature from D, ^3He , ^4He , ^6Li , or ^7Li . The dotted line is the upper bound on the reheating temperature from the overclosure of the Universe.

reheating temperature assuming that the primordial gravitinos are mainly produced by the scattering processes of thermal particles (fig. 5). For stable gravitino, we considered B-ino, stau, and sneutrino as the next-to-the-lightest supersymmetric particle and obtained constraints on their properties.

In Ref. [147, 153] we pointed out that there is a new gravitino problem beside due to the thermal production of the gravitino. An inflaton field has non-vanishing supersymmetry (SUSY)-breaking auxiliary field in most of inflation models in SUGRA, which gives rise to an enhanced decay of the inflaton into a pair of gravitinos. This gravitino production in inflaton decay is more effective for lower reheating temperature while the production by particle scatterings in the thermal bath is more important for higher temperature. Therefore, the direct gravitino production is complementary to the thermal gravitino production, and the former may put severe constraints on inflation models together with the latter.

Baryogenesis and Q ball

Baryogenesis is one of the main issues in the theories of the early universe. Among many baryogenesis scenarios proposed so far, the mechanism proposed by Affleck and Dine is a promising candidate since it can be realized in the SUSY standard model. It is known that the Affleck-Dine mechanism is complicated by the formation of Q balls which is a non-topological soliton in the SUSY

standard model.

In Ref. [50] we studied Q-ball formation in the expanding universe on 1D, 2D and 3D lattice simulations and obtained detailed Q-ball charge distributions (fig 6). We also investigated a scenario of simultaneous production of the baryon asymmetry and the dark matter of the universe through the Q-ball decay in the gauge-mediated SUSY breaking model [20]. In this scenario the Q-balls with charge $Q \simeq 10^{23}$ decay mainly into nucleons to create baryon number of the Universe and they also decay partially into gravitinos with mass $m_{3/2} \simeq 0.01 - 0.1$ GeV which account for the dark matter of the universe.

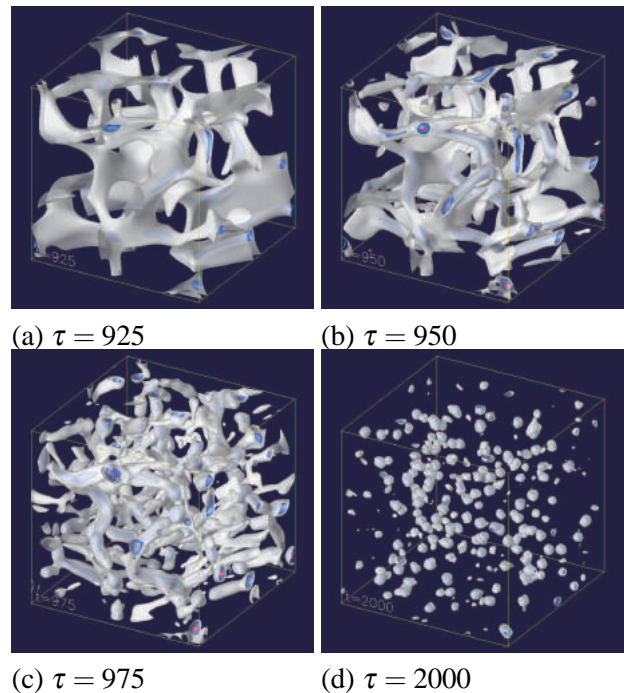


Fig. 6. Time evolution of the isosurfaces of charge density.

Cosmology of Topological Defects

Topological defects such as domain walls and cosmic strings can be produced in the early universe at the phase transition associated with spontaneous symmetry breaking. Topological defects have various effects on thermal and dynamical evolution of the universe and hence they can be a clue to particle physics beyond the standard model and the history of the early universe.

Domain walls are surface-like defects produced when a discrete symmetry is spontaneously broken in the early universe. In Ref. [31, 54] we studied production of gravitational waves from domain walls. If stable domain walls exist, they eventu-

ally dominate the energy density of the universe, and lead to cosmological disasters. However, this problem can be avoided if the discrete symmetry is only approximate. In such a case, domain walls become unstable and annihilate before they overclose the universe.

We investigated the cosmological evolution of unstable domain walls based on the lattice simulation of the scalar field. Using the result of the numerical simulations, we calculated the spectrum of gravitational waves produced by unstable domain walls. Extrapolating the numerical results, we found that the signal of gravitational waves produced by domain walls whose energy scale is around 10^{10} - 10^{12} GeV would be observable in the next generation gravitational wave interferometric experiments.

Cosmic strings, line-like defects, are formed at breaking of a $U(1)$ symmetry. We studied the observational signature of a cosmic string network on the weak lensing experiment [16, 17, 192]. We showed that the string-lensed spectra decay more slowly on small scales compared with primordial scalar perturbations, and the non-vanishing signals for B-mode cosmic shear and curl-mode deflection angle naturally arise. We found that the weak lensing signals are shown to be potentially detectable from the upcoming cosmic shear and cosmic microwave background lensing observations.

Axion Cosmology

The axion is a pseudo Nambu-Goldstone (NG) boson of the Peccei-Quinn (PQ) symmetry, which is introduced to the standard model as a solution to the Strong CP problem in quantum chromodynamics (QCD). The axion has rich implications for astrophysics and cosmology.

When the spontaneous breaking of $U(1)_{\text{PQ}}$ occurs in the universe, a cosmological network of axionic strings is formed. The produced axionic strings lose their energy by emitting axions and follow the so-called scaling solution. How much the emitted axions contribute to the present dark matter density crucially depends on their energy spectrum. However, there was a controversy about the energy spectrum of the axions radiated from axionic strings. We estimated the energy spectrum precisely by using field-theoretic simulations in a box of 512^3 grids and a pseudo power spectrum estimator and found that the spectrum has a sharp

peak at the horizon scale. From our spectrum we obtained constraint on the axion decay constant $f_a < 3 \times 10^{11}$ GeV.

Axion models also predict a formation of domain walls, when the temperature of the universe becomes comparable to \sim GeV. At that time, N_{DW} domain walls are attached to strings, where N_{DW} is an integer number whose value depends on models. The subsequent history of the universe is different between models with $N_{\text{DW}} = 1$ and $N_{\text{DW}} > 1$.

In Ref. [4], we studied the scenario with $N_{\text{DW}} = 1$ where domain walls are bounded by strings and they immediately collapse due to the tension of walls. We investigated the formation and annihilation of string-wall networks by performing field-theoretic lattice simulations (fig 7). We analyzed the spectrum of axions radiated from collapse of domain walls and found that axions produced by the decay of domain walls give significant contribution to the cold dark matter abundance. On the other hand, the string-wall networks become long-lived for the models with $N_{\text{DW}} > 1$. In Ref. [34], we investigated the evolution of such long-lived domain walls and estimated their decay rate. We found that such models are constrained by various cosmological and astrophysical observations.

When the PQ symmetry is broken during (or before) inflation, the axionic strings and domain walls are diluted away by inflation. However, in this case the axion field acquires fluctuations during inflation, which leads to isocurvature density perturbations. In Ref. [127] we derived constraints on the axion model parameters from observation of the cosmic microwave background (CMB). Furthermore, the axion isocurvature fluctuations can have large non-Gaussianity. We derived generic formulae for non-Gaussianity of isocurvature perturbations and applied it to axion models [96]

Non-Gaussianity in Density Perturbations

Simple single field inflation models predict nearly scale invariant, pure adiabatic and Gaussian density perturbations, which is consistent with the current observational data. However, significant non-Gaussianity can be generated when other light scalars exist during inflation.

In Ref. [110] we studied non-Gaussianity in models where fluctuations from the inflaton and the curvaton can both contribute to the present cosmic density fluctuations and found that large non-

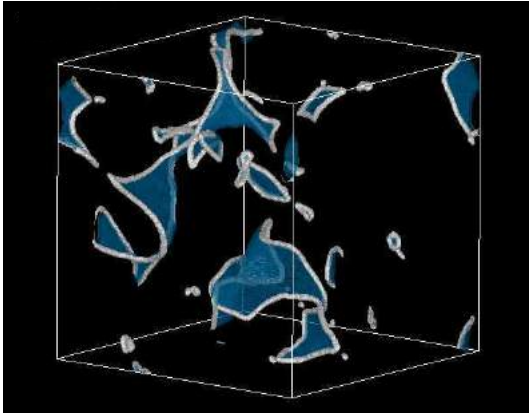


Fig. 7. Visualization of the lattice simulation of axionic string-wall networks. The white lines correspond to the position of strings, while the blue surfaces correspond to the position of the center of domain walls.

Gaussianity can be produced. Furthermore, we studied the inflationary parameters such as the spectral index and the tensor-to-scalar ratio in this kind of models and discussed in what cases models predict the spectral index and tensor modes allowed by the current data while generating large non-Gaussianity.

Non-Gaussianity can also exist in the isocurvature perturbations. We developed a formalism for studying non-Gaussianity in both curvature and isocurvature perturbations [94, 96]. It was shown that non-Gaussianity in the isocurvature perturbation between dark matter and photons leaves distinct signatures in the cosmic microwave background temperature fluctuations, which may be confirmed in future experiments. Using the formalism we studied non-Gaussianities of isocurvature perturbations generated in the axion model and Affleck-Dine mechanism [95, 96].

The existence of an extra radiation component in the universe beyond the standard three neutrino species is indicated by measurements of the CMB anisotropy and the primordial helium abundance. We explored the possibility that the extra radiation has isocurvature fluctuations and developed a general formalism to evaluate isocurvature perturbations in the extra radiation in the mixed inflaton-curvaton system [19]. Furthermore, we studied non-Gaussian properties of the isocurvature perturbations in the dark radiation [5]

Formation of Primordial Black Holes

We studied formation of primordial black holes in a double inflation model [6, 55, 117, 149]. The

transition from one inflation to another could enhance the spectrum of density perturbations on some specific scale, which could lead to formation of primordial black holes with a very narrow range of masses. The produced black holes with mass $\lesssim 10^{-7}M_{\odot}$ can account for the dark matter of the universe while they are seeds for supermassive black holes if their mass is $\simeq 10^5M_{\odot}$.

Members

Staffs

Masahiro Kawasaki, Professor, 2004–present
 Masahiro Ibe, Assoc. Professor, 2011–present
 Junji Hisano, Assoc. Professor, 2002–2010

Postdoctoral Fellows

Shuichiro Yokoyama, 2012–present
 Shohei Sugiyama, 2011–present
 Daisuke Yamauchi, 2011–present
 Sachiko Kuroyanagi, 2010–2012
 Toyokazu Sekiguchi, 2010–2011
 Koji Ishiwata, 2010
 Motohiko Kusakabe, 2009–2012
 Masato Yamanaka, 2009–2010
 Michihisa Takeuchi, 2009
 Takashi Hiramatsu, 2008–2010
 Masaki Asano, 2008–2009
 Mayumi Aoki, 2007–2008
 Teruaki Suyama, 2007–2008
 Masato Senami, 2005–2007

Graduate Students

Nine students were awarded doctor degrees and nineteen students earned master degrees during 2006–2012, supervised by ICRR staff members.

List of Publications

Note 1: The symbol * indicates the authors belonging to ICRR.

Note 2: Seventeen papers, [77], [84], [87], [92], [96], [105], [108], [110], [121], [126], [131], [138], [139], [147], [148], [151], and [153] are cited more than fifty times.

Papers in Refereed Journals

[1] Stochastic Approach to Flat Direction during Inflation,

- M. Kawasaki* and T. Takesako*,
JCAP **1208**, 031 (2012) [arXiv:1207.1165 [hep-ph]].
- [2] Seesaw Mechanism with Occam's Razor
K. Harigaya, M. Ibe* and T. T. Yanagida
Phys. Rev. D **86**, 013002 (2012) [arXiv:1205.2198 [hep-ph]].
- [3] The Lightest Higgs Boson Mass in the MSSM with Strongly Interacting Spectators
J. L. Evans, M. Ibe* and T. T. Yanagida
Phys. Rev. D **86**, 015017 (2012) [arXiv:1204.6085 [hep-ph]].
- [4] Production of dark matter axions from collapse of string-wall systems
T. Hiramatsu, M. Kawasaki*, K. Saikawa* and T. Sekiguchi
Phys. Rev. D **85**, 105020 (2012) [arXiv:1202.5851 [hep-ph]].
- [5] Non-Gaussian isocurvature perturbations in dark radiation
E. Kawakami*, M. Kawasaki*, K. Miyamoto*, K. Nakayama and T. Sekiguchi
JCAP **1207**, 037 (2012) [arXiv:1202.4890 [astro-ph.CO]].
- [6] Primordial seeds of supermassive black holes
M. Kawasaki*, A. Kusenko and T. T. Yanagida
Phys. Lett. B **711**, 1 (2012) [arXiv:1202.3848 [astro-ph.CO]].
- [7] Forecast constraints on cosmic string parameters from gravitational wave direct detection experiments
S. Kuroyanagi*, K. Miyamoto*, T. Sekiguchi, K. Takahashi and J. Silk
Phys. Rev. D **86**, 023503 (2012) [arXiv:1202.3032 [astro-ph.CO]].
- [8] Pure Gravity Mediation with $m_{3/2} = 10 - 100\text{TeV}$
M. Ibe*, S. Matsumoto and T. T. Yanagida
Phys. Rev. D **85**, 095011 (2012) [arXiv:1202.2253 [hep-ph]].
- [9] A 125GeV Higgs Boson and Muon $g-2$ in More Generic Gauge Mediation
J. L. Evans, M. Ibe*, S. Shirai and T. T. Yanagida
Phys. Rev. D **85**, 095004 (2012) [arXiv:1201.2611 [hep-ph]].
- [10] Hubble Induced Mass in Radiation Dominated Universe
M. Kawasaki* and T. Takesako*
Phys. Lett. B **711**, 173 (2012) [arXiv:1112.5823 [hep-ph]].
- [11] The Lightest Higgs Boson Mass in Pure Gravity Mediation Model
M. Ibe* and T. T. Yanagida
Phys. Lett. B **709**, 374 (2012) [arXiv:1112.2462 [hep-ph]].
- [12] Resonant annihilation of long-lived massive colored particles through hadronic collisions
M. Kusakabe* and T. Takesako*
Phys. Rev. D **85**, 015005 (2012) [arXiv:1112.0860 [hep-ph]].
- [13] The GeV-scale dark matter with B-L asymmetry
M. Ibe*, S. Matsumoto and T. T. Yanagida
Phys. Lett. B **708**, 112 (2012) [arXiv:1110.5452 [hep-ph]].
- [14] Multi-field open inflation model and multi-field dynamics in tunneling
K. Sugimura, D. Yamauchi* and M. Sasaki
JCAP **1201**, 027 (2012) [arXiv:1110.4773 [gr-qc]].
- [15] Prospects for determination of thermal history after inflation with future gravitational wave detectors
S. Kuroyanagi*, K. Nakayama and S. Saito
Phys. Rev. D **84**, 123513 (2011) [arXiv:1110.4169 [astro-ph.CO]].
- [16] Weak lensing of CMB by cosmic (super-)strings
D. Yamauchi*, K. Takahashi, Y. Sendouda and C. -M. Yoo
Phys. Rev. D **85**, 103515 (2012) [arXiv:1110.0556 [astro-ph.CO]].
- [17] Full-sky lensing reconstruction of gradient and curl modes from CMB maps
T. Namikawa, D. Yamauchi* and A. Taruya
JCAP **1201**, 007 (2012) [arXiv:1110.1718 [astro-ph.CO]].
- [18] Non-Gaussianity from Curvatons Revisited
M. Kawasaki*, T. Kobayashi and F. Takahashi
Phys. Rev. D **84**, 123506 (2011) [arXiv:1107.6011 [astro-ph.CO]].

- [19] Isocurvature perturbations in extra radiation
M. Kawasaki*, K. Miyamoto*, K. Nakayama
and T. Sekiguchi
JCAP **1202**, 022 (2012) [arXiv:1107.4962
[astro-ph.CO]].
- [20] Gravitino dark matter and baryon asymmetry
from Q-ball decay in gauge mediation
S. Kasuya and M. Kawasaki*
Phys. Rev. D **84**, 123528 (2011)
[arXiv:1107.0403 [hep-ph]].
- [21] Relatively Heavy Higgs Boson in More
Generic Gauge Mediation
J. L. Evans, M. Ibe* and T. T. Yanagida
Phys. Lett. B **705**, 342 (2011)
[arXiv:1107.3006 [hep-ph]].
- [22] Higher Order Corrections to the Primordial
Gravitational Wave Spectrum and its Impact
on Parameter Estimates for Inflation
S. Kuroyanagi* and T. Takahashi
JCAP **1110**, 006 (2011) [arXiv:1106.3437
[astro-ph.CO]].
- [23] R-symmetry Matching In SUSY Breaking
Models
J. Goodman, M. Ibe*, Y. Shirman and F. Yu
Phys. Rev. D **84**, 045015 (2011)
[arXiv:1106.1168 [hep-th]].
- [24] Constraints on Direct Gauge Mediation Mod-
els with Complex Representations
K. Hanaki, M. Ibe*, Y. Ookouchi and
C. S. Park
JHEP **1108**, 044 (2011) [arXiv:1106.0551
[hep-ph]].
- [25] Open inflation in the landscape
D. Yamauchi*, A. Linde, A. Naruko,
M. Sasaki and T. Tanaka
Phys. Rev. D **84**, 043513 (2011)
[arXiv:1105.2674 [hep-th]].
- [26] Differentiating CDM and Baryon Isocurvature
Models with 21 cm Fluctuations
M. Kawasaki*, T. Sekiguchi* and T. Takahashi
JCAP **1110**, 028 (2011) [arXiv:1104.5591
[astro-ph.CO]].
- [27] Time Dependent Quark Masses and Big Bang
Nucleosynthesis Revisited
M. -K. Cheoun, T. Kajino, M. Kusakabe* and
G. J. Mathews
Phys. Rev. D **84**, 043001 (2011)
[arXiv:1104.5547 [astro-ph.CO]].
- [28] Cosmological Aspects of Inflation in a Super-
symmetric Axion Model
M. Kawasaki*, N. Kitajima* and
K. Nakayama
Phys. Rev. D **83**, 123521 (2011)
[arXiv:1104.1262 [hep-ph]].
- [29] Direct Detection of Electroweak-Interacting
Dark Matter
J. Hisano, K. Ishiwata, N. Nagata* and
T. Takesako*
JHEP **1107**, 005 (2011) [arXiv:1104.0228
[hep-ph]].
- [30] Simplified R-Symmetry Breaking and Low-
Scale Gauge Mediation
J. L. Evans, M. Ibe*, M. Sudano and
T. T. Yanagida
JHEP **1203**, 004 (2012) [arXiv:1103.4549
[hep-ph]].
- [31] Study of gravitational radiation from cosmic
domain walls
M. Kawasaki* and K. Saikawa*
JCAP **1109**, 008 (2011) [arXiv:1102.5628
[astro-ph.CO]].
- [32] Cosmological constraints on dark matter
models with velocity-dependent annihilation
cross section
J. Hisano, M. Kawasaki*, K. Kohri, T. Moroi,
K. Nakayama and T. Sekiguchi*
Phys. Rev. D **83**, 123511 (2011)
[arXiv:1102.4658 [hep-ph]].
- [33] Improved estimation of radiated axions from
cosmological axionic strings
T. Hiramatsu, M. Kawasaki*, T. Sekiguchi*,
M. Yamaguchi and J. Yokoyama
Phys. Rev. D **83**, 123531 (2011)
[arXiv:1012.5502 [hep-ph]].
- [34] Evolution of String-Wall Networks and Ax-
ionic Domain Wall Problem
T. Hiramatsu, M. Kawasaki* and K. Saikawa*
JCAP **1108**, 030 (2011) [arXiv:1012.4558
[astro-ph.CO]].
- [35] Quantum Statistical Corrections to Astro-
physical Photodisintegration Rates

- G. J. Mathews, Y. Pehlivan, T. Kajino, A. B. Balantekin and M. Kusakabe*
Astrophys. J. **727**, 10 (2011)
[arXiv:1012.0519 [astro-ph.SR]].
- [36] Destruction of ${}^7\text{Be}$ in big bang nucleosynthesis via long-lived sub-strongly interacting massive particles as a solution to the Li problem
M. Kawasaki* and M. Kusakabe*
Phys. Rev. D **83**, 055011 (2011)
[arXiv:1012.0435 [hep-ph]].
- [37] The Japanese space gravitational wave antenna: DECIGO
S. Kawamura, M. Ando, N. Seto, S. Sato, T. Nakamura, K. Tsubono, N. Kanda, T. Tanaka, . . . , Kuroyanagi* *et al.*
Class. Quant. Grav. **28**, 094011 (2011).
- [38] Running Spectral Index from Inflation with Modulations
T. Kobayashi* and F. Takahashi
JCAP **1101**, 026 (2011) [arXiv:1011.3988 [astro-ph.CO]].
- [39] Prospects for Direct Detection of Inflationary Gravitational Waves by Next Generation Interferometric Detectors
S. Kuroyanagi*, T. Chiba and N. Sugiyama
Phys. Rev. D **83**, 043514 (2011)
[arXiv:1010.5246 [astro-ph.CO]].
- [40] Kahler moduli double inflation
M. Kawasaki* and K. Miyamoto*
JCAP **1102**, 004 (2011) [arXiv:1010.3095 [astro-ph.CO]].
- [41] Inflation from a Supersymmetric Axion Model
M. Kawasaki*, N. Kitajima* and K. Nakayama
Phys. Rev. D **82**, 123531 (2010)
[arXiv:1008.5013 [hep-ph]].
- [42] Decaying Dark Matter in Supersymmetric Model and Cosmic-Ray Observations
K. Ishiwata*, S. Matsumoto and T. Moroi
JHEP **1012**, 006 (2010) [arXiv:1008.3636 [hep-ph]].
- [43] Non-Gaussianity from Lifshitz Scalar
K. Izumi, T. Kobayashi* and S. Mukohyama
JCAP **1010**, 031 (2010) [arXiv:1008.1406 [hep-th]].
- [44] Gluon contribution to the dark matter direct detection
J. Hisano*, K. Ishiwata* and N. Nagata*
Phys. Rev. D **82**, 115007 (2010)
[arXiv:1007.2601 [hep-ph]].
- [45] Reevaluation of Higgs-mediated mu-e transition in the MSSM
J. Hisano*, S. Sugiyama, M. Yamanaka and M. J. S. Yang
Phys. Lett. B **694**, 380 (2011)
[arXiv:1005.3648 [hep-ph]].
- [46] A complete calculation for direct detection of Wino dark matter
J. Hisano*, K. Ishiwata* and N. Nagata*
Phys. Lett. B **690**, 311 (2010)
[arXiv:1004.4090 [hep-ph]].
- [47] Signals of the cosmological reionization in the radio sky through C and O fine structure lines
M. Kusakabe* and M. Kawasaki*
arXiv:1004.1087 [astro-ph.CO].
- [48] B-mode polarization induced by gravitational waves from kinks on infinite cosmic strings
M. Kawasaki*, K. Miyamoto* and K. Nakayama*
Phys. Rev. D **82**, 103504 (2010)
[arXiv:1003.3701 [astro-ph.CO]].
- [49] WIMP dark matter in gauge-mediated SUSY breaking models and its phenomenology
J. Hisano*, K. Nakayama*, S. Sugiyama*, T. Takesako* and M. Yamanaka*
Phys. Lett. B **691**, 46 (2010) [arXiv:1003.3648 [hep-ph]].
- [50] Numerical study of Q-ball formation in gravity mediation
T. Hiramatsu*, M. Kawasaki* and F. Takahashi
JCAP **1006**, 008 (2010) [arXiv:1003.1779 [hep-ph]].
- [51] A new idea to search for charged lepton flavor violation using a muonic atom
M. Koike, Y. Kuno, J. Sato and M. Yamanaka*
Phys. Rev. Lett. **105**, 121601 (2010)
[arXiv:1003.1578 [hep-ph]].

- [52] Effects of Light Fields During Inflation
T. Kobayashi* and S. Mukohyama
Phys. Rev. D **81**, 103504 (2010)
[arXiv:1003.0076 [astro-ph.CO]].
- [53] Gravitational waves from kinks on infinite cosmic strings
M. Kawasaki*, K. Miyamoto* and K. Nakayama*
Phys. Rev. D **81**, 103523 (2010)
[arXiv:1002.0652 [astro-ph.CO]].
- [54] Gravitational Waves from Collapsing Domain Walls
T. Hiramatsu*, M. Kawasaki* and K. Saikawa*
JCAP **1005**, 032 (2010) [arXiv:1002.1555 [astro-ph.CO]].
- [55] Primordial Black Holes as All Dark Matter
P. H. Frampton, M. Kawasaki*, F. Takahashi and T. T. Yanagida
JCAP **1004**, 023 (2010) [arXiv:1001.2308 [hep-ph]].
- [56] New results on catalyzed BBN with a long-lived negatively-charged massive particle
M. Kusakabe*, T. Kajino, T. Yoshida and G. J. Mathews
Phys. Rev. D **81**, 083521 (2010)
[arXiv:1001.1410 [astro-ph.CO]].
- [57] Stau relic density at the Big-Bang nucleosynthesis era consistent with the abundance of the light element nuclei in the coannihilation scenario
T. Jittoh, K. Kohri, M. Koike, J. Sato, T. Shimomura and M. Yamanaka*
Phys. Rev. D **82**, 115030 (2010)
[arXiv:1001.1217 [hep-ph]].
- [58] Production of the p-Process Nuclei in the Carbon Deflagration Model for Type Ia Supernovae
M. Kusakabe*, N. Iwamoto and K. 'i. Nomoto
Astrophys. J. **726**, 25 (2011)
[arXiv:1001.0145 [astro-ph.SR]].
- [59] Forecast Constraints on Inflation from Combined CMB and Gravitational Wave Direct Detection Experiments
S. Kuroyanagi*, C. Gordon, J. Silk and N. Sugiyama
Phys. Rev. D **81**, 083524 (2010) [Erratum-ibid. D **82**, 069901 (2010)] [arXiv:0912.3683 [astro-ph.CO]].
- [60] Right-handed sneutrino dark matter and big-bang nucleosynthesis
K. Ishiwata, M. Kawasaki*, K. Kohri and T. Moroi
Phys. Lett. B **689**, 163 (2010)
[arXiv:0912.0781 [hep-ph]].
- [61] Implications of CDMS II result on Higgs sector in the MSSM
J. Hisano*, K. Nakayama* and M. Yamanaka*
Phys. Lett. B **684**, 246 (2010)
[arXiv:0912.4701 [hep-ph]].
- [62] Probing the primordial power spectra with inflationary priors
M. Kawasaki* and T. Sekiguchi*
JCAP **1002**, 013 (2010) [arXiv:0911.5191 [astro-ph.CO]].
- [63] Neutrino mass from cosmology: Impact of high-accuracy measurement of the Hubble constant
T. Sekiguchi*, K. Ichikawa, T. Takahashi and L. Greenhill
JCAP **1003**, 015 (2010) [arXiv:0911.0976 [astro-ph.CO]].
- [64] Density Fluctuations in Thermal Inflation and Non-Gaussianity
M. Kawasaki*, T. Takahashi and S. Yokoyama
JCAP **0912**, 012 (2009) [arXiv:0910.3053 [hep-th]].
- [65] Gravitational Wave Background and Non-Gaussianity as a Probe of the Curvaton Scenario
K. Nakayama* and J. Yokoyama
JCAP **1001**, 010 (2010) [arXiv:0910.0715 [astro-ph.CO]].
- [66] On some hybrid-types of Q balls in the gauge-mediated supersymmetry breaking
S. Kasuya and M. Kawasaki*
Phys. Rev. D **80**, 123529 (2009)
[arXiv:0910.0694 [hep-ph]].
- [67] A numerical study of primordial magnetic field amplification by inflation-produced gravitational waves

- S. Kuroyanagi*, H. Tashiro and N. Sugiyama
Phys. Rev. D **81**, 023510 (2010)
 [arXiv:0909.0907 [astro-ph.CO]].
- [68] Effects of Dark Matter Annihilation on the Cosmic Microwave Background
 T. Kanzaki*, M. Kawasaki* and K. Nakayama*
Prog. Theor. Phys. **123**, 853 (2010)
 [arXiv:0907.3985 [astro-ph.CO]].
- [69] Cosmological Constraints on a Massive Neutrino
 M. Kawasaki* and K. Sato
Prog. Theor. Phys. **122**, 205 (2009)
 [arXiv:0907.2007 [astro-ph.CO]].
- [70] The R-axion and non-Gaussianity
 K. Nakayama* and F. Takahashi
Phys. Lett. B **679**, 436 (2009)
 [arXiv:0907.0834 [hep-ph]].
- [71] Non-linear Evolution of Baryon Acoustic Oscillations from Improved Perturbation Theory in Real and Redshift Spaces
 A. Taruya, T. Nishimichi, S. Saito and T. Hiramatsu*
Phys. Rev. D **80**, 123503 (2009)
 [arXiv:0906.0507 [astro-ph.CO]].
- [72] Curvatons in Warped Throats
 T. Kobayashi* and S. Mukohyama
JCAP **0907**, 032 (2009) [arXiv:0905.2835 [hep-th]].
- [73] Constraining Light Gravitino Mass from Cosmic Microwave Background
 K. Ichikawa, M. Kawasaki*, K. Nakayama*, T. Sekiguchi* and T. Takahashi
JCAP **0908**, 013 (2009) [arXiv:0905.2237 [astro-ph.CO]].
- [74] Upward muon signals at neutrino detectors as a probe of dark matter properties
 J. Hisano*, K. Nakayama* and M. J. S. Yang*
Phys. Lett. B **678**, 101 (2009)
 [arXiv:0905.2075 [hep-ph]].
- [75] Cosmological Constraints on Rapid Roll Inflation
 T. Kobayashi*, S. Mukohyama and B. A. Powell
JCAP **0909**, 023 (2009) [arXiv:0905.1752 [astro-ph.CO]].
- [76] Non-Gaussianity from Isocurvature Perturbations : Analysis of Trispectrum
 E. Kawakami*, M. Kawasaki*, K. Nakayama* and F. Takahashi
JCAP **0909**, 002 (2009) [arXiv:0905.1552 [astro-ph.CO]].
- [77] Phenomenological Aspects of Horava-Lifshitz Cosmology
 S. Mukohyama, K. Nakayama*, F. Takahashi and S. Yokoyama
Phys. Lett. B **679**, 6 (2009) [arXiv:0905.0055 [hep-th]].
- [78] Axion isocurvature fluctuations with extremely blue spectrum
 S. Kasuya and M. Kawasaki*
Phys. Rev. D **80**, 023516 (2009)
 [arXiv:0904.3800 [astro-ph.CO]].
- [79] Diffuse gamma-ray background and cosmic-ray positrons from annihilating dark matter
 M. Kawasaki*, K. Kohri and K. Nakayama*
Phys. Rev. D **80**, 023517 (2009)
 [arXiv:0904.3626 [astro-ph.CO]].
- [80] Waiting for $\mu \rightarrow e\gamma$ from the MEG experiment
 J. Hisano*, M. Nagai, P. Paradisi and Y. Shimizu
JHEP **0912**, 030 (2009) [arXiv:0904.2080 [hep-ph]].
- [81] Axion braneworld cosmology
 C. Bambi, M. Kawasaki* and F. R. Urban
Phys. Rev. D **80**, 023533 (2009)
 [arXiv:0903.4516 [hep-ph]].
- [82] Chasing the non-linear evolution of matter power spectrum with numerical resummation method: solution of closure equations
 T. Hiramatsu* and A. Taruya, *Phys. Rev. D* **79**, 103526 (2009) [arXiv:0902.3772 [astro-ph.CO]].
- [83] Non-linear Evolution of Matter Power Spectrum in Modified Theory of Gravity
 K. Koyama, A. Taruya and T. Hiramatsu*
Phys. Rev. D **79**, 123512 (2009)
 [arXiv:0902.0618 [astro-ph.CO]].
- [84] Cosmic Rays from Dark Matter Annihilation and Big-Bang Nucleosynthesis
 J. Hisano*, M. Kawasaki*, K. Kohri, T. Moroi

- and K. Nakayama*
 Phys. Rev. D **79**, 083522 (2009)
 [arXiv:0901.3582 [hep-ph]].
- [85] Discriminating electroweak-ino parameter ordering at the LHC and its impact on LFV studies
 J. Hisano*, M. M. Nojiri and W. Sreethawong
 JHEP **0906**, 044 (2009) [arXiv:0812.4496 [hep-ph]].
- [86] Flavor effects on the electric dipole moments in supersymmetric theories: A beyond leading order analysis
 J. Hisano*, M. Nagai and P. Paradisi
 Phys. Rev. D **80**, 095014 (2009)
 [arXiv:0812.4283 [hep-ph]].
- [87] Neutrino Signals from Annihilating/Decaying Dark Matter in the Light of Recent Measurements of Cosmic Ray Electron/Positron Fluxes
 J. Hisano*, M. Kawasaki*, K. Kohri and K. Nakayama*
 Phys. Rev. D **79**, 043516 (2009)
 [arXiv:0812.0219 [hep-ph]].
- [88] Leptogenesis Scenarios via Non-Thermally Produced Right-handed Neutrino and Sneutrino in Supersymmetric Seesaw Model
 M. Senami and T. Takayama*
 JCAP **0906**, 007 (2009) [arXiv:0812.0120 [hep-ph]].
- [89] Cosmological Moduli Problem from Thermal Effects
 K. Nakayama* and F. Takahashi
 Phys. Lett. B **670**, 434 (2009)
 [arXiv:0811.0444 [hep-ph]].
- [90] A realistic extension of gauge-mediated SUSY-breaking model with superconformal hidden sector
 M. Asano*, J. Hisano*, T. Okada* and S. Sugiyama*
 Phys. Lett. B **673**, 146 (2009)
 [arXiv:0810.4606 [hep-ph]].
- [91] Efficient diagrammatic computation method for higher order correlation functions of local type primordial curvature perturbations
 S. Yokoyama, T. Suyama* and T. Tanaka
 JCAP **0902**, 012 (2009) [arXiv:0810.3053 [astro-ph]].
- [92] Positron/Gamma-Ray Signatures of Dark Matter Annihilation and Big-Bang Nucleosynthesis
 J. Hisano*, M. Kawasaki*, K. Kohri and K. Nakayama*
 Phys. Rev. D **79**, 063514 (2009) [Erratum-ibid. D **80**, 029907 (2009)] [arXiv:0810.1892 [hep-ph]].
- [93] Hilltop Non-Gaussianity
 M. Kawasaki*, K. Nakayama* and F. Takahashi
 JCAP **0901**, 026 (2009) [arXiv:0810.1585 [hep-ph]].
- [94] A General Analysis of Non-Gaussianity from Isocurvature Perturbations
 M. Kawasaki*, K. Nakayama*, T. Sekiguchi*, T. Suyama* and F. Takahashi
 JCAP **0901**, 042 (2009) [arXiv:0810.0208 [astro-ph]].
- [95] Non-Gaussianity from Baryon Asymmetry
 M. Kawasaki*, K. Nakayama* and F. Takahashi
 JCAP **0901**, 002 (2009) [arXiv:0809.2242 [hep-ph]].
- [96] Non-Gaussianity from isocurvature perturbations
 M. Kawasaki*, K. Nakayama*, T. Sekiguchi*, T. Suyama* and F. Takahashi
 JCAP **0811**, 019 (2008) [arXiv:0808.0009 [astro-ph]].
- [97] Light Higgs boson scenario in the SUSY seesaw model
 M. Asano*, T. Kubo, S. Matsumoto and M. Senami
 Phys. Rev. D **80**, 095017 (2009)
 [arXiv:0807.4922 [hep-ph]].
- [98] Exact gravitational lensing by cosmic strings with junctions
 T. Suyama*
 Phys. Rev. D **78**, 043532 (2008)
 [arXiv:0807.4355 [astro-ph]].
- [99] Primordial Curvature Fluctuation and Its Non-Gaussianity in Models with Modulated Reheating
 K. Ichikawa, T. Suyama*, T. Takahashi and M. Yamaguchi

- Phys. Rev. D **78**, 063545 (2008) [arXiv:0807.3988 [astro-ph]].
- [100] Direct/indirect detection signatures of non-thermally produced dark matter
M. Nagai and K. Nakayama*
Phys. Rev. D **78**, 063540 (2008) [arXiv:0807.1634 [hep-ph]].
- [101] Neutrino mass, Dark Matter and Baryon Asymmetry via TeV-Scale Physics without Fine-Tuning
M. Aoki*, S. Kanemura and O. Seto
Phys. Rev. Lett. **102**, 051805 (2009) [arXiv:0807.0361 [hep-ph]].
- [102] Isocurvature fluctuations in Affleck-Dine mechanism and constraints on inflation models
S. Kasuya, M. Kawasaki* and F. Takahashi
JCAP **0810**, 017 (2008) [arXiv:0805.4245 [hep-ph]].
- [103] Electron and Photon Energy Deposition in Universe
T. Kanzaki* and M. Kawasaki*
Phys. Rev. D **78**, 103004 (2008) [arXiv:0805.3969 [astro-ph]].
- [104] CP violation in B_s mixing in the SUSY SU(5) GUT with right-handed neutrinos
J. Hisano* and Y. Shimizu
Phys. Lett. B **669**, 301 (2008) [arXiv:0805.3327 [hep-ph]].
- [105] Big-Bang Nucleosynthesis and Gravitino
M. Kawasaki*, K. Kohri, T. Moroi and A. Yotsuyanagi
Phys. Rev. D **78**, 065011 (2008) [arXiv:0804.3745 [hep-ph]].
- [106] Upperbound on squark masses in gauge-mediation model with light gravitino
J. Hisano*, M. Nagai*, S. Sugiyama* and T. T. Yanagida
Phys. Lett. B **665**, 237 (2008) [arXiv:0804.2957 [hep-ph]].
- [107] Probing reheating temperature of the universe with gravitational wave background
K. Nakayama*, S. Saito, Y. Suwa and J. Yokoyama
JCAP **0806**, 020 (2008) [arXiv:0804.1827 [astro-ph]].
- [108] Non-Gaussianity from Symmetry
T. Suyama* and F. Takahashi
JCAP **0809**, 007 (2008) [arXiv:0804.0425 [astro-ph]].
- [109] Probing the Effective Number of Neutrino Species with Cosmic Microwave Background
K. Ichikawa, T. Sekiguchi* and T. Takahashi
Phys. Rev. D **78**, 083526 (2008) [arXiv:0803.0889 [astro-ph]].
- [110] Non-Gaussianity, Spectral Index and Tensor Modes in Mixed Inflaton and Curvaton Models
K. Ichikawa, T. Suyama*, T. Takahashi and M. Yamaguchi
Phys. Rev. D **78**, 023513 (2008) [arXiv:0802.4138 [astro-ph]].
- [111] Solving Cosmological Problems of Supersymmetric Axion Models in Inflationary Universe
M. Kawasaki* and K. Nakayama*
Phys. Rev. D **77**, 123524 (2008) [arXiv:0802.2487 [hep-ph]].
- [112] Space laser interferometers can determine the thermal history of the early Universe
K. Nakayama*, S. Saito, Y. Suwa and J. Yokoyama
Phys. Rev. D **77**, 124001 (2008) [arXiv:0802.2452 [hep-ph]].
- [113] Primordial Helium Abundance from CMB: a constraint from recent observations and a forecast
K. Ichikawa, T. Sekiguchi* and T. Takahashi
Phys. Rev. D **78**, 043509 (2008) [arXiv:0712.4327 [astro-ph]].
- [114] Unitarity bounds in the Higgs model including triplet fields with custodial symmetry
M. Aoki* and S. Kanemura
Phys. Rev. D **77**, 095009 (2008) [arXiv:0712.4053 [hep-ph]].
- [115] Probing Majorana Phases and Neutrino Mass Spectrum in the Higgs Triplet Model at the CERN LHC
A. G. Akeroyd, M. Aoki* and H. Sugiyama
Phys. Rev. D **77**, 075010 (2008) [arXiv:0712.4019 [hep-ph]].

- [116] Electric dipole moments from flavor-changing supersymmetric soft terms
J. Hisano*, M. Nagai* and P. Paradisi
Phys. Rev. D **78**, 075019 (2008)
[arXiv:0712.1285 [hep-ph]].
- [117] Formation of intermediate-mass black holes as primordial black holes in the inflationary cosmology with running spectral index
T. Kawaguchi, M. Kawasaki*, T. Takayama*, M. Yamaguchi and J. Yokoyama
Mon. Not. Roy. Astron. Soc. **388**, 1426 (2008)
[arXiv:0711.3886 [astro-ph]].
- [118] Cosmological implications of supersymmetric axion models
M. Kawasaki*, K. Nakayama* and M. Senami*
JCAP **0803**, 009 (2008) [arXiv:0711.3083 [hep-ph]].
- [119] Primordial Non-Gaussianity in Multi-Scalar Inflation
S. Yokoyama, T. Suyama* and T. Tanaka
Phys. Rev. D **77**, 083511 (2008)
[arXiv:0711.2920 [astro-ph]].
- [120] Nonthermal dark matter in mirage mediation
M. Nagai* and K. Nakayama*, Phys. Rev. D **76**, 123501 (2007) [arXiv:0709.3918 [hep-ph]].
- [121] Non-Gaussianity in the modulated reheating scenario
T. Suyama* and M. Yamaguchi
Phys. Rev. D **77**, 023505 (2008)
[arXiv:0709.2545 [astro-ph]].
- [122] Stability of metastable vacua in gauge mediated SUSY breaking models with ultra light gravitino
J. Hisano*, M. Nagai*, M. Senami* and S. Sugiyama*
Phys. Lett. B **659**, 361 (2008)
[arXiv:0708.3340 [hep-ph]].
- [123] Affleck-Dine leptogenesis via multiscalar evolution in a supersymmetric seesaw model
M. Senami* and T. Takayama*
JCAP **0711**, 015 (2007) [arXiv:0708.2238 [hep-ph]].
- [124] Solving the cosmic lithium problems with primordial late-decaying particles
D. Cumberbatch, K. Ichikawa, M. Kawasaki*, K. Kohri, J. Silk and G. D. Starkman
Phys. Rev. D **76**, 123005 (2007)
[arXiv:0708.0095 [astro-ph]].
- [125] Revisiting signature of minimal gauge mediation
J. Hisano* and Y. Shimizu
Phys. Lett. B **655**, 269 (2007)
[arXiv:0706.3145 [hep-ph]].
- [126] Primordial Non-Gaussianity in Multi-Scalar Slow-Roll Inflation
S. Yokoyama, T. Suyama* and T. Tanaka
JCAP **0707**, 013 (2007) [arXiv:0705.3178 [astro-ph]].
- [127] Cosmological Constraints on Isocurvature and Tensor Perturbations
M. Kawasaki* and T. Sekiguchi*
Prog. Theor. Phys. **120**, 995 (2008)
[arXiv:0705.2853 [astro-ph]].
- [128] Cosmological Constraints on Neutrino Injection
T. Kanzaki*, M. Kawasaki*, K. Kohri and T. Moroi
Phys. Rev. D **76**, 105017 (2007)
[arXiv:0705.1200 [hep-ph]].
- [129] Relic abundance of dark matter in universal extra dimension models with right-handed neutrinos
S. Matsumoto, J. Sato, M. Senami* and M. Yamanaka
Phys. Rev. D **76**, 043528 (2007)
[arXiv:0705.0934 [hep-ph]].
- [130] Baryon Asymmetry in Heavy Moduli Scenario
M. Kawasaki* and K. Nakayama*
Phys. Rev. D **76**, 043502 (2007)
[arXiv:0705.0079 [hep-ph]].
- [131] Big-Bang Nucleosynthesis with Long-Lived Charged Slepton
M. Kawasaki*, K. Kohri and T. Moroi
Phys. Lett. B **649**, 436 (2007) [hep-ph/0703122].
- [132] Increasing effective number of neutrinos by decaying particles
K. Ichikawa, M. Kawasaki*, K. Nakayama*,

- M. Senami* and F. Takahashi
 JCAP **0705**, 008 (2007) [hep-ph/0703034 [HEP-PH]].
- [133] Graviton emission from a Gauss-Bonnet brane
 K. Konya*
 Phys. Rev. D **75**, 104003 (2007) [hep-th/0701257].
- [134] Baryogenesis via left-right asymmetry generation by Affleck-Dine mechanism in Dirac neutrino model
 M. Senami* and T. Takayama*
 Phys. Rev. D **75**, 105004 (2007) [hep-ph/0701103].
- [135] Affleck-Dine baryogenesis in anomaly-mediated SUSY breaking
 M. Kawasaki* and K. Nakayama*
 JCAP **0702**, 002 (2007) [hep-ph/0611320].
- [136] Constraint on the Effective Number of Neutrino Species from the WMAP and SDSS LRG Power Spectra
 K. Ichikawa, M. Kawasaki* and F. Takahashi
 JCAP **0705**, 007 (2007) [astro-ph/0611784].
- [137] Electric dipole moments in pseudodirac gauginos
 J. Hisano*, M. Nagai*, T. Naganawa* and M. Senami*
 Phys. Lett. B **644**, 256 (2007) [hep-ph/0610383].
- [138] Non-perturbative effect on thermal relic abundance of dark matter
 J. Hisano*, S. Matsumoto, M. Nagai*, O. Saito and M. Senami*
 Phys. Lett. B **646**, 34 (2007)
- [139] Cosmological constraints on gravitino LSP scenario with sneutrino NLSP
 T. Kanzaki*, M. Kawasaki*, K. Kohri and T. Moroi
 Phys. Rev. D **75**, 025011 (2007) [hep-ph/0609246].
- [140] Late-time Affleck-Dine baryogenesis after thermal inflation
 M. Kawasaki* and K. Nakayama*
 Phys. Rev. D **74**, 123508 (2006) [hep-ph/0608335].
- [141] Early reionization by decaying particles in light of three year WMAP data
 S. Kasuya and M. Kawasaki*
 JCAP **0702**, 010 (2007) [astro-ph/0608283].
- [142] Constraining superWIMPy and warm subhalos with future submillilensing
 J. Hisano*, K. T. Inoue and T. Takahashi
 Phys. Lett. B **643**, 141 (2006) [hep-ph/0608126].
- [143] Solving cosmological problem in universal extra dimension models by introducing Dirac neutrino
 S. Matsumoto, J. Sato, M. Senami* and M. Yamanaka
 Phys. Lett. B **647**, 466 (2007) [hep-ph/0607331].
- [144] Inflaton decay through supergravity effects
 M. Endo, M. Kawasaki*, F. Takahashi and T. T. Yanagida
 Phys. Lett. B **642**, 518 (2006) [hep-ph/0607170].
- [145] New two-loop contributions to hadronic EDMs in the MSSM
 J. Hisano*, M. Nagai* and P. Paradisi
 Phys. Lett. B **642**, 510 (2006) [hep-ph/0606322].
- [146] Towards the robustness of the Affleck-Dine baryogenesis
 S. Kasuya and M. Kawasaki*
 Phys. Rev. D **74**, 063507 (2006) [hep-ph/0606123].
- [147] The Gravitino-overproduction problem in inflationary universe
 M. Kawasaki*, F. Takahashi and T. T. Yanagida
 Phys. Rev. D **74**, 043519 (2006) [hep-ph/0605297].
- [148] Relic abundance of dark matter in the minimal universal extra dimension model
 M. Kakizaki, S. Matsumoto and M. Senami*
 Phys. Rev. D **74**, 023504 (2006) [hep-ph/0605280].
- [149] Power Spectrum of the Density Perturbations From Smooth Hybrid New Inflation Model
 M. Kawasaki*, T. Takayama*, M. Yamaguchi

- and J. Yokoyama
 Phys. Rev. D **74**, 043525 (2006) [hep-ph/0605271].
- [150] Implication of Dark Energy Parametrizations on the Determination of the Curvature of the Universe
 K. Ichikawa, M. Kawasaki*, T. Sekiguchi* and T. Takahashi, JCAP **0612**, 005 (2006) [astro-ph/0605481].
- [151] Limit on the Neutrino Mass from the WMAP Three Year Data
 M. Fukugita, K. Ichikawa, M. Kawasaki* and O. Lahav
 Phys. Rev. D **74**, 027302 (2006) [astro-ph/0605362].
- [152] Gauss-Bonnet brane-world cosmology without $Z(2)$ -symmetry
 K. Konya*
 Class. Quant. Grav. **24**, 2761 (2007) [gr-qc/0605119].
- [153] Gravitino overproduction in inflaton decay
 M. Kawasaki*, F. Takahashi and T. T. Yanagida
 Phys. Lett. B **638**, 8 (2006) [hep-ph/0603265].
- [154] Primordial helium abundance: a reanalysis of the izotov-thuan spectroscopic sample
 M. Fukugita and M. Kawasaki*
 Astrophys. J. **646**, 691 (2006) [astro-ph/0603334].
- [155] Universality of strength for Yukawa couplings with extra down-type quark singlets
 K. Higuchi, M. Senami* and K. Yamamoto
 Phys. Lett. B **638**, 492 (2006) [hep-ph/0603219].
- [156] CMB constraints on the simultaneous variation of the fine structure constant and electron mass
 K. Ichikawa, T. Kanzaki* and M. Kawasaki*
 Phys. Rev. D **74**, 023515 (2006) [astro-ph/0602577].
- [157] 511 keV line and diffuse gamma rays from moduli
 S. Kasuya and M. Kawasaki*
 Phys. Rev. D **73**, 063007 (2006) [astro-ph/0602296].
- [158] Investigation of possible dark matter direct detection in electron accelerators
 J. Hisano*, M. Nagai*, M. M. Nojiri and M. Senami*
 Phys. Rev. D **73**, 031701 (2006) [hep-ph/0504068].
- ### Papers in Conference Proceedings
- [159] Gravitational waves from cosmic string - domain wall networks
 T. Hiramatsu, M. Kawasaki*, K. Saikawa*, T. Sekiguchi
 Talk given at the 21st workshop on general relativity and gravitation in Japan, September 26-29, 2011, Sendai, Japan.
- [160] Destructures of ${}^7\text{Be}$ and ${}^7\text{Li}$ in big bang nucleosynthesis through reactions with exotic long-lived sub-strongly interacting massive particles
 M. Kusakabe* and M. Kawasaki*
 Talk given at International Symposium on Origin of Matter and Evolution of Galaxies, 14 - 17 November 2011, Wako, Japan. To be published in the AIP Conference Series.
- [161] Signatures of long-lived exotic strongly interacting massive particles on light element abundances through reactions triggered by the particles
 M. Kusakabe* and M. Kawasaki*
 Talk given at 7th International Workshop on the Dark Side of the Universe, 26 - 30 September 2011, Beijing, China. To be published in the IOP Journal of Physics: Conference Series.
- [162] Effect of exotic long-lived sub-strongly interacting massive particles in big bang nucleosynthesis and a new solution to the Li problem
 M. Kawasaki* and M. Kusakabe*
 Talk given at Hadron Nuclear Physics 2011 (HNP2011) "Quarks in Hadrons, Nuclei, and Hadronic Matter", 21 - 24 February 2011, Pohang, Korea. Published in EPJ Web of Conferences **20**, 04001 (2012).
- [163] SUSY-catalyzed big bang nucleosynthesis as a solution of lithium problems
 M. Kusakabe*, T. Kajino and G. J. Mathews
 Talk given at 24th International Nuclear

- Physics Conference (INPC 2010) 4-9 July 2010. Vancouver, Canada. Published in Phys. Conf. Ser. **312**, 042012 (2011).
- [164] Analytic model for CMB temperature fluctuations from cosmic (super-)strings
D. Yamauchi*, K. Takahashi, Y. Sendouda, C. -M. Yoo and M. Sasaki
Talk given at Yukawa International Symposium (YKIS2010) Cosmology - The Next Generation YKIS2010. 28 Jun - 2 Jul 2010, Kyoto, Japan. Published in Prog. Theor. Phys. Suppl. **190**, 239 (2011).
- [165] Numerical study of Q-ball formation in gravity mediation
T. Hiramatsu, M. Kawasaki* and F. Takahashi
Talk given at Yukawa International Symposium (YKIS2010) Cosmology - The Next Generation YKIS2010. 28 Jun - 2 Jul 2010, Kyoto, Japan. Published in Prog. Theor. Phys. Suppl. **190**, 229 (2011).
- [166] Big Bang Nucleosynthesis with Long-Lived Strongly Interacting Relic Particles
M. Kusakabe*, T. Kajino, T. Yoshida and G. J. Mathews
Talk given at International Astronomical Union (IAU) Symposium 268: Light elements in the Universe 09-13 Nov 2009. Geneva, Switzerland. Published in arXiv:1001.1413 [astro-ph.CO].
- [167] Curvatons in warped throats
T. Kobayashi* and S. Mukohyama
Talk given at INVISIBLE UNIVERSE INTERNATIONAL CONFERENCE: Toward a new cosmological paradigm 29 Jun - 3 Jul 2009, Paris, France. Published in AIP Conf. Proc. **1241**, 620 (2010).
- [168] Solving the Li problem by long lived stau in a stau-neutralino coannihilation scenario
M. Yamanaka*, T. Jittoh, K. Kohri, M. Koike, J. Sato and T. Shimomura
Talk given at EPS-HEP HEP2009 European Physical Society EPS. 16-22 Jul 2009. Cracow, Poland. Published in PoS EPS - **HEP2009**, 115 (2009).
- [169] Gravitational wave background as a probe of reheating temperature of the universe
K. Nakayama*, S. Saito, Y. Suwa and J. Yokoyama
Talk given at 16th International Conference on Supersymmetry and the Unification of Fundamental Interactions (SUSY08) , 16-21 Jun 2008, Seoul, Korea. Published in AIP Conf. Proc. **1078**, 515 (2009).
- [170] Signatures of dark matter annihilation in the light of PAMELA/ATIC anomaly
K. Nakayama*
Talk given at 7th International Heidelberg Conference on Dark Matter in Astro and Particle Physics (DARK 2009) 18-24 Jan 2009, Christchurch, New Zealand. Published in arXiv:0903.4735 [hep-ph].
- [171] Inflationary cosmology of axion models in supergravity
K. Nakayama*
Talk given at Accelerators in the Universe: Interplay between High Energy Physics and Cosmophysics 12-14 Mar 2008, Tsukuba, Japan. Published in AIP Conf. Proc. **1040**, 61 (2008).
- [172] Supersymmetry and cosmology: Inflation, gravitino and axion
M. Kawasaki*
Talk given at International Workshop on Grand Unified Theories: Current Status and Future Prospects GUT GUT07. 17-19 Dec 2007, Katsatsu, Shiga, Japan. Published in AIP Conf. Proc. **1015**, 226 (2008).
- [173] Non-Gaussianity, spectral index and tensor modes in mixed inflaton and curvaton models
K. Ichikawa, T. Suyama*, T. Takahashi and M. Yamaguchi
Talk given at Accelerators in the Universe: Interplay between High Energy Physics and Cosmophysics 12-14 Mar 2008, Tsukuba, Japan. Published in AIP Conf. Proc. **1040**, 116 (2008).
- [174] Universal extra dimension models with right-handed neutrinos
S. Matsumoto, J. Sato, M. Senami* and M. Yamanaka
Talk given at UAE - CERN Workshop on High Energy Physics and Applications UAE-CERN United Arab Emirates. 26-28 Nov 2007, Al Ain, Abu Dhabi, United Arab Emirates. Pub-

- lished in AIP Conf. Proc. **1006**, 122 (2008) [arXiv:0810.0700 [hep-ph]].
- [175] The Neutrino masses and the change of allowed parameter region in universal extra dimension models
S. Matsumoto, J. Sato, M. Senami* and M. Yamanaka
Talk given at 10th International Conference on Topics in Astroparticle and Underground Physics (TAUP 2007) 11-15 Sep 2007, Sendai, Japan. Published in J. Phys. Conf. Ser. **120**, 042007 (2008) [arXiv:0711.2600 [hep-ph]].
- [176] Introducing neutrino mass into universal extra dimension models and solving cosmological problem
S. Matsumoto, J. Sato, M. Yamanaka and M. Senami*
Talk given at International Workshop on Neutrino Masses and Mixings: Toward Unified Understanding of Quark and Lepton Mass Matrices 17-19 Dec 2006, Shizuoka, Japan. Published in Int. J. Mod. Phys. E **16**, 1571 (2007).
- [177] Baryogenesis via left-right asymmetry generated by Affleck-Dine mechanism in Dirac neutrino model
M. Senami* and T. Takayama*
Talk given at International Workshop on Neutrino Masses and Mixings: Toward Unified Understanding of Quark and Lepton Mass Matrices 17-19 Dec 2006, Shizuoka, Japan. Published in Int. J. Mod. Phys. E **16**, 1513 (2007).
- [178] Increasing the effective number of neutrinos with decaying particles
K. Ichikawa, M. Kawasaki*, K. Nakayama*, M. Senami* and F. Takahashi
Talk given at 13th International Symposium on Particles, Strings and Cosmology (PAS-COS 07) 2-7 Jul 2007, London, England Published in AIP Conf. Proc. **957**, 413 (2007).
- [179] Features in the primordial power spectrum: A running spectral index and formation of primordial black holes
M. Kawasaki*, T. Takayama*, M. Yamaguchi and J. Yokoyama
Talk given at International Symposium on Cosmology and Particle Astrophysics (CosPA 2006) COSPA06. 15-17 Nov 2006, Taipei, Taiwan, China. Published in Mod. Phys. Lett. A **22**, 1911 (2007).
- [180] Exact wave propagation in a spacetime with a cosmic string
T. Suyama*, T. Tanaka and R. Takahashi
Talk given at 29th Spanish Relativity Meeting (ERE 2006): Einstein's Legacy: From the Theoretical Paradise to Astrophysical Observation ERE2006 XXIX. 4-8 Sep 2006, Palma de Mallorca, Spain. Published in J. Phys. Conf. Ser. **66**, 012033 (2007).
- [181] The Gravitino-overproduction problem in inflaton decay
M. Kawasaki*, F. Takahashi and T. T. Yanagida
Talk given at SUSY06: 14th International Conference on Supersymmetry and the Unification of Fundamental Interactions SUSY 06 2006. 12-17 Jun 2006, Irvine, California. Published in AIP Conf. Proc. **903**, 677 (2007) [hep-ph/0611166].
- Papers under referee
- [182] CMB power spectra induced by primordial cross-bispectra between metric perturbations and vector fields,
M. Shiraishi, S. Saga and S. Yokoyama*,
arXiv:1209.3384 [astro-ph.CO].
- [183] Femto-lensing due to a Cosmic String,
C. -M. Yoo, R. Saito, Y. Sendouda, K. Takahashi and D. Yamauchi*,
arXiv:1209.0903 [astro-ph.CO].
- [184] Production of ${}^9\text{Be}$ through alpha-fusion reaction of metal-poor cosmic ray and stellar flare,
M. Kusakabe* and M. Kawasaki*,
arXiv:1208.4210 [astro-ph.CO].
- [185] Gravitational waves from smooth hybrid new inflation,
M. Kawasaki*, K. Saikawa* and N. Takeda*,
arXiv:1208.4160 [astro-ph.CO].
- [186] Non-Gaussian bubbles in the sky,
K. Sugimura, D. Yamauchi* and M. Sasaki,
arXiv:1208.3937 [astro-ph.CO].
- [187] Remarks on Hubble Induced Mass from Fermion Kinetic Term,
M. Kawasaki* and T. Takesako*,
arXiv:1208.1323 [hep-ph].

- [188] Full bispectra from primordial scalar and tensor perturbations in the most general single-field inflation model,
X. Gao, T. Kobayashi, M. Shiraishi, M. Yamaguchi, J. Yokoyama and S. Yokoyama*,
arXiv:1207.0588 [astro-ph.CO].
- [189] Pure Gravity Mediation of Supersymmetry Breaking at the LHC,
B. Bhattacharjee, B. Feldstein, M. Ibe*, S. Matsumoto and T. T. Yanagida,
arXiv:1207.5453 [hep-ph].
- [190] Axion cosmology with long-lived domain walls,
T. Hiramatsu, M. Kawasaki*, K. Saikawa* and T. Sekiguchi,
arXiv:1207.3166 [hep-ph].
- [191] Primordial black hole formation from an axion-like curvaton model,
M. Kawasaki*, N. Kitajima* and T. T. Yanagida,
arXiv:1207.2550 [hep-ph].
- [192] Weak lensing generated by vector perturbations and detectability of cosmic strings
D. Yamauchi*, T. Namikawa and A. Taruya
arXiv:1205.2139 [astro-ph.CO].
- [193] Updated constraint on a primordial magnetic field during big bang nucleosynthesis and a formulation of field effects
M. Kawasaki* and M. Kusakabe*
arXiv:1204.6164 [astro-ph.CO].
- [194] A 125 GeV Higgs Boson Mass and Gravitino Dark Matter in R-invariant Direct Gauge Mediation
M. Ibe* and R. Sato
arXiv:1204.3499 [hep-ph].
- [195] Void bias from primordial non-Gaussianities,
T. Sekiguchi and S. Yokoyama*,
arXiv:1204.2726 [astro-ph.CO].
- [196] Solution to Big-Bang Nucleosynthesis in Hybrid Axion Dark Matter Model
M. Kusakabe*, A. B. Balantekin, T. Kajino and Y. Pehlivan
arXiv:1202.5603 [astro-ph.CO].
- [197] Axino dark matter and baryon number asymmetry from Q-ball decay in gauge mediation
S. Kasuya, E. Kawakami* and M. Kawasaki*
arXiv:1202.4067 [hep-ph].
- [198] Revisiting the cosmological coherent oscillation
M. Kawasaki*, N. Kitajima* and K. Nakayama
arXiv:1112.2818 [hep-ph].
- [199] Non-Anomalous Discrete R-symmetry Decreases Three Generations
J. L. Evans, M. Ibe*, J. Kehayias and T. T. Yanagida
arXiv:1111.2481 [hep-ph].
- [200] Probing Extra Matter in Gauge Mediation Through the Lightest Higgs Boson Mass
J. L. Evans, M. Ibe* and T. T. Yanagida
arXiv:1108.3437 [hep-ph].

FACILITIES

KAMIOKA OBSERVATORY

Introduction

There are three operating bodies for the underground site in Kamioka: 1) Kamioka Observatory, Institute for Cosmic Ray Research (ICRR), the University of Tokyo; 2) Kamioka Satellite, Kavli Institute for the Physics and Mathematics of the Universe (Kavli IPMU), the University of Tokyo; 3) and Tohoku University Research Center for Neutrino Science.

They are cooperating each other in many aspects. They work together for safety issues and some of the maintenance costs for the underground environments in common area are shared. But they are independent and operating different facilities and have separate budgets.

Kamioka Observatory is located at 1000m underground (2,700m w.e) of the Kamioka Mine, Gifu prefecture, about 200 km west of Tokyo. Kamioka Observatory was established in 1995, initially to house and operate the Super-Kamiokande (SK) detector which is a 50,000 tons imaging water Cherenkov detector, mainly to measure neutrinos from the sun, atmosphere and supernova, and to look for proton decay and so on. Kamioka Observatory has expanded its role and now it operates XMASS: the direct dark matter search experiment. Kamioka Observatory also accepts experiments to use underground spaces by external research institutions based on the proposals: CANDLES is a double beta decay experiment using ^{48}Ca led by Osaka University and NewAGE is a dark matter experiment led by Kobe University to detect directions of recoil nucleus. There are also experiments to measure precise value of the vertical gravity by a superconductive gravity meter and to measure the earth's horizontal displacement to the level of 10^{-14} by a laser displacement meter.

Brief History and Major Achievements

In 1991, the construction budget for Super-Kamiokande was approved and the 5 year construction project had started. Super-Kamiokande is a 50,000 ton water Cherenkov detector, and the inner 32,000 tons of water are optically separated from the outer-layer, anti-counters, of 2m thickness on

an average. The fiducial volume which is used for the physics analysis is 22,500 tons. One year after the construction had started, the US group joined and they bore a responsibility to construct and operate anti-counters. The Super-Kamiokande detector was built to resolve the remaining problems from Kamiokande, namely the solar neutrino problems and the atmospheric neutrino anomaly. Detection of neutrino bursts from supernovae and proton decay were also very interesting subjects

In 1995, the Kamioka Observatory was officially founded to operate Super-Kamiokande Detector. But about one year before that, in 1994, the computer building was constructed and the computer system was installed.

In 1996, the detector construction was completed and started to take data on 1st of April. Two years later, in 1998, Super-Kamiokande found the up-down asymmetry of the μ -like events in the zenith angle distribution of the atmospheric neutrinos, which provided a clear evidence for neutrino oscillation independent of the flux calculation.

In 1999, the first long baseline neutrino oscillation experiment of the earth scale, K2K, had started, injecting man-made neutrinos produced at KEK PS to Super-Kamiokande, 250 km away from the neutrino source. The experiment was completed in 2004 observing 112 μ -like events whereas 156 such events were expected without oscillation. This confirmed the neutrino oscillation observed in atmospheric neutrinos.

In June 2001, Super-Kamiokande published the 1256 days of data for solar neutrino observations. On the same day, SNO announced their first result on charged current interactions. They have concluded 3.6σ effect by comparing the SK electron scattering data and the SNO charged current data that there are non-electron type neutrinos in the solar neutrinos detected on the earth. This was the first evidence for solar neutrino oscillation.

In 2009, the new long baseline oscillation experiment called T2K was started to look for as yet undetermined mixing angle of θ_{13} . The intense neutrino beam from JPARC, about 50 times higher than that of K2K, was directed to Super-Kamiokande detector 295 km away. In 2011, T2K has shown the

first evidence for non-zero θ_{13} : T2K observed 6 electron-like events with an expected backgrounds of 1.5 ± 0.8 events.

Operation

In 2004, all the Japanese national universities became corporate and the funding system also changed. There have been no more automatic renewals of the operational budget since then. We now need to submit our budget request every year to the university and the university scores the projects. Based on the the score, final allocation is decided by the government. It is then not clear how our budget will continue.

Nevertheless, the budget request to expand the underground laboratory was approved in 2005 and by using the part of the increased budget, we were able to hire scientific and technical staffs although they had fixed terms of the appointment.

In Kamioka Observatory we have two technical staffs who work for the daily maintenance of the underground laboratory. The experiments and related equipments are basically operated by the scientists from each collaboration. Nevertheless it may be necessary to increase the technical support for the experiments. We have set up the 'Safety Section' to oversee the safety issues in underground and therefore we have hired one technical staff, recently. After the incorporation of the national university, the safety issues become very important subject for us.

The number of full-time scientific staff of Kamioka Observatory is 21 (2 professors, 5 associate professors and 14 research associates) and there are three staffs in administration office. Two visiting scientist positions (one professor and one associate professor) can be appointed every year for one year term. These scientific personnels are conducting researches using Super-Kamiokande and have responsibilities to operate the Super-Kamiokande detector and to keep it in good shape, but also they have responsibilities on the matters related to the facilities of the underground laboratory and on the supports for about 5000 man \times day visiting scientists per year, especially for those taking Super-Kamiokande shifts and analyzing the data. The safety issues are one of the important subjects.

Procedure of approving experiments in Kamioka Observatory

Once every year, ICRR receives experimental proposals not only for underground experiments but also for all the relevant experiments to ICRR. And the program assessment committee including some members from outside of ICRR decides if the proposal to be approved or not. This judgement is mostly done based on the scientific point of view. Following this approval, the Kamioka steering committee will discuss and decide if this approved proposal will fit to the underground laboratories. Basically, the Observatory provides the space and facility like electricity, water and so on and the user will bring all the necessary equipments. Practically before any decision is made, the experimental collaboration would negotiate with the Observatory if their experiment would fit in the underground or to judge if the experiment needs a new cavity or not.

After the approval, observatory will keep following their design in a point of view for safety. For example if one uses liquid scintillator, one needs to get permission to use liquid scintillator from local fire department and there are many rules and regulations to follow. Then Observatory sometimes asks the experimental group to change a design by taking into account those regulations.

Facilities

Underground Facilities

The entrance of the underground facilities is located at the distance about 10 minutes drive from the ground office buildings. We have a horizontal access and about a few minutes drive of 1.7 km drift would bring you to the area where undergrounds facilities are located. The Kamioka mine is no more operating and therefore we can access to the facilities 24 hours a day by just driving a car. The map of the facility area is shown in Fig. 1.

Super-Kamiokande and KamLAND (Tohoku University) are shown in circle. CLIO and Laser strain meter are placed at the L-shape laboratory and the length of each arm is 100 m. Labs A to E are under the supervision by Kamioka Observatory and Labs 1 and 2 are the Kavli IPMU laboratories. Lab.A is a back yard of Super-Kamiokande, where we have the electron LINAC for the calibration for Super-K and one Germanium detector. Lab. B is a L-shape laboratory; the length of each arm is 20 m. NewAGE is operating at the end of one arm

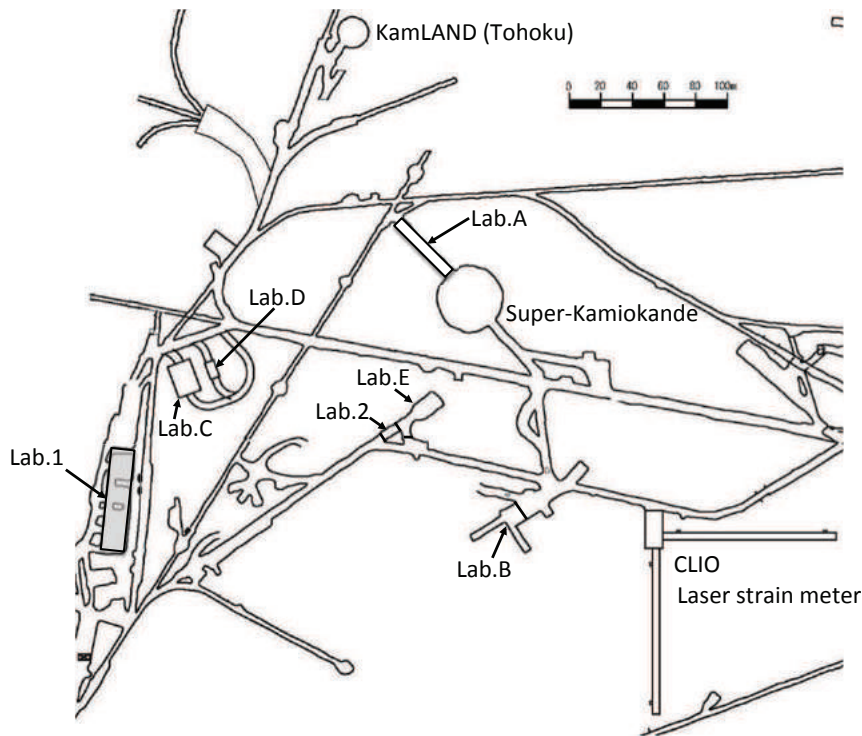


Fig. 1. Layout of Kamioka Observatory.

and the other arm is used by the Super-Conductive Gravity meter. The crossing area is used for various test experiments and preparations. Lab. C (15 m wide and 20 m long) is a hall for XMASS and Lab.D houses CANDLES, the double beta decay experiment using ^{48}Ca . Lab.E is hosting 200 ton EGADS water tank, which has been built for testing the feasibility of the GADZOOKS project for Super-Kamiokande. Lab.1 has various devices to detect radio-active contaminations, impurities and so on. Among them are two high purity Germanium detectors, Gas analyzer, Particle counters, Scanning Electron Microscope and so on. Lab.2 is used for computer clusters. All the laboratories are within 400 m distances.

Environmental Backgrounds

The deep underground provides the low radioactive and low seismic noise environment and gives good opportunities to perform physics experiments requiring such experimental conditions.

At the depth of 2,700 m water equivalence, the cosmic ray muon flux, about 250 muons/m²/day, is $\sim 1/100,000$ of the surface flux.

The environmental gamma ray backgrounds from the wall depend upon locations and energy. It ranges from 0.1~0.2 /MeV/cm²/sec at around

1 MeV and 0.01~0.02 /MeV/cm²/sec at around 2 MeV.

The thermal and non-thermal neutron fluxes in Kamioka Observatory are measured to be

$$\begin{aligned}\phi_n^{thermal} &= 8.3 \pm 0.6 \times 10^{-6} \text{ cm}^{-2} \text{ s}^{-1} \quad \text{and} \\ \phi_n^{non-thermal} &= 1.2 \pm 0.1 \times 10^{-5} \text{ cm}^{-2} \text{ s}^{-1},\end{aligned}$$

respectively. In order to reduce those environmental γ and neutron backgrounds, water shields are most effective and commonly used in Kamioka. There are 2 to 3 m water layers surrounding the inner volume of Super-Kamiokande which would effectively reduce those backgrounds. The 800 tons water tank for the XMASS experiment provides 10^{-7} reduction for neutrons.

The Rn concentration of the mine air varies a few Bq/m³ to ~ 1000 Bq/m³ depending on the season of the year. We intake the air from outside of the mine which is passed through the Charcoal filter to reduce Rn contamination. The so called Rn-free air is circulated in the experimental area. We can provide two grades of the Rn-free air. The standard one is contaminated by 30 mBq/m³ of Rn, and the super-Rn-free air after being passed through the cold charcoal is 3mBq/m³. The amount of flow available is 20 m³/hour and 10 m³/hour, respec-

tively. The U/Th and K contamination in the rocks in the mine are ~ 1.0 ppm for U, ~ 3.2 ppm for Th and 1.6% for K at a typical location.

To study and establish low background environment, we have ICP-MASS spectrometer, GAS MASS spectrometer, and low background Ge detectors in the underground laboratory. Those are available for the users of the underground observatory.

An electron LINAC of which the energy ranges 5 MeV to 15 MeV is set up near the Super-Kamiokande detector for the purpose of the low energy calibration. The energy of the LINAC covers exactly the energy range of the detectable solar neutrinos in Super-K. The DT neutron generator can also be used to produce ^{16}N in the water as a calibration source. Other radio-active calibration sources are available in the underground laboratory.

The seismic noise in the mine is small if you enter in the mine more than 100 m deeper from the mine entrance: the noise level becomes more than 10 times lower than the outside

Ground Facilities

The office building for Kamioka Observatory (ICRR) and Kamioka Satellite (Kavli IPMU) are built close each other and actually connected by passage. Kamioka Observatory operates dormitory where we have 18 single rooms and 1 twin room and 1 Japanese style tatami room. Three meals are served at the dormitory, but need reservation. Kamioka Observatory operates computer system, electronics workshop and chemical workshop in the office building. The computer system consists of 1440 cores with 3.46 GHz and the memory size is 2 GB/core. Disk space available is 2 PB and the access speed is greater than 2.5 GB/s in total. We also have a tape backup system with 1.5 PB. The system is mostly used for the Super-Kamiokande experiment. All the data from Super-K are stored in this system and accessed also from abroad.

Present Scientific Programs

Super-Kamiokande

The studies are continuing on atmospheric, solar and supernova neutrinos and a search for proton decay lasts. In the three flavor analysis for the atmospheric neutrinos, by using the recently measured θ_{13} as an input, we can extensively study mass hierarchy, octant of θ_{23} and even CPV. Those researches

are still in an infancy, but quite interesting results are expected. The role of atmospheric neutrinos are still very important and will continue to be interesting.

The unresolved problem of solar neutrino is an as yet unobserved upturn. In the low energy region the upturn in the spectrum which connects the high energy matter oscillation region (about 0.35 suppression) to the low energy vacuum oscillation region (about 0.6 suppression) must be seen. If there is no upturn seen, then there may be an effect from unknown physics like an existence of sterile neutrinos for example. In order to see the effect, Super-Kamiokande has made tremendous efforts to reduce the energy threshold. We are currently taking data with 3.0 keV trigger threshold and the analysis threshold is 3.5 keV. Eventually we are able to analyze the data at 3.0 keV.

We are preparing for the next Supernova. The electronics and data acquisition system are being upgraded in order to avoid a stall of the data acquisition system for the very high rate bursts from nearby supernovae. We expect 400,000 neutrino events if Betelgeuse will explode and 200,000 events happen within first 0.5 seconds. The Supernova Early Warning System is also ready to send the alarm around the world.

We are continuously looking for protons to decay. The sensitivity close to 10^{34} years for $e\pi^0$ mode and a few $\times 10^{33}$ years for $\bar{\nu}K$ mode may be possible in 10 more years' operation.

The Super-Kamiokande Collaboration consists of 12 Japanese institutions and 9 Institutions from abroad. And total about 120 collaborators are studying and among them about half comes from US institutions. The collaboration runs the experiment and therefore 5 scientists on an average stay on site of Kamioka Observatory throughout the year.

Occasionally SK collaboration has been expanded for a particular scientific subject by adding outside experts, for example to study the cosmic muon flux modulation. Sidereal daily variation of 10 TeV galactic cosmic ray intensity was observed by mostly Shinshu University and some of the Super-Kamiokande Collaboration.

For SK, T2K, XMASS-I, detailed reports are given in the chapters of the Neutrino and Astroparticle Division.

T2K

In 2011, T2K saw the first evidence of non-zero θ_{13} . In 2012, total number of e-like events became 10 while the estimated backgrounds were 2.73 ± 0.37 events giving the 3.2σ significance against zero θ_{13} . The three reactor experiments, Daya Bay, Reno, Double Chooz, have confirmed the non-zero θ_{13} with higher statistical significance in 2012. T2K will continue to take data and study on θ_{13} . But T2K will also approach to the question of the mass hierarchy and octant of θ_{23} which may require a kind of global analysis including the results from other experiments.

XMASS-I

XMASS is a multi-purpose liquid Xenon detector and the final aim is to build a 10 ton fiducial mass detector to study dark matter, pp and ${}^7\text{Be}$ solar neutrinos and neutrino-less double beta decay of ${}^{136}\text{Xe}$. The phase I XMASS has a total mass of 835 kg Xenon and 100kg fiducial volume. XMASS-I has completed the construction in November, 2010. The liquid Xenon was filled and the commissioning run started in January, 2011. By using the whole volume of 835 kg, we have set competitive limits on low mass dark matter, annual modulation, super-WIMPs, dark matter axions and solar axions. We have found two un-expected background sources. One of them comes from the upper part of the ${}^{238}\text{U}$ decay chain contaminated in the Al-seal used between the quartz windows and the metal bodies of the 632 PMTs. The other one comes from the surface ${}^{210}\text{Pb}$ contaminations. Those backgrounds are responsible for $E > 5$ keV. We are developing software to reduce backgrounds in the fiducial. Although we cannot remove Al from the PMT, we change the configuration of the detector by placing the cover on top of the Al-seal to reduce the backgrounds from α 's and β 's. This refurbishment process has started in July, 2012 and will finish in March, 2013. After understanding the background behavior, we will start to build XMASS1.5 which has the fiducial mass of 1 ton comparable to the next generation detectors like XENON1t.

CANDLES (PI: T. Kishimoto, Osaka University)

CANDLES III is now located at Lab.D and taking test data. CANDLES III consists of 96 CaF_2 crystals, total 305 kg, where they have 300g of ${}^{48}\text{Ca}$ which is immersed in liquid scintillator and

is viewed by photomultiplier tubes. For the experiment ${}^{48}\text{Ca}$ enrichment is crucial and various R&D efforts for the enrichment are going on.

NewAGE (PI: K. Miuchi, Kobe University)

NewAGE is a gas chamber to measure the directional information of recoil nucleus from the dark matter interaction. It is in the R&D stage and led by a group of Kobe University. They use a low pressure gas chamber to detect short recoil tracks. Goal is to build an array of chambers each containing 1m^3 of CF_4 at 0.05 bar. Currently a feasibility study is being made by using a chamber of 30 cm cubic containing CF_4 at 0.2 bar with micro TPC for 3D tracking device and μPIC for 2D imaging device.

CLIO

The 100 m laser interferometer (CLIO), the first cryogenic interferometer as a prototype of the future KAGRA gravitational wave telescope, has been operated (see the chapter of the Gravitational Wave Group for detailed report).

Gravity and Geophysics

In parallel to the 100m vacuum pipe of CLIO, there are another interferometer built early in 2005, of which the mirror was fixed to the ground. This interferometer measures the displacement of the ground to a level of 10^{-14} for the study of the earth dynamics by Disaster Prevention Research Institute, Kyoto University and other institutions.

The super-conductive gravity detector has also been set in the underground laboratory. Study of the proper oscillation of the earth is conducted by National Astronomical Observatory and other institutions.

Future Programs

Hyper-Kamiokande

Hyper-Kamiokande is a 0.99 Megaton water Cherenkov detector. The fiducial mass is 0.56 Mt which is viewed by 99,000 pieces of 50 cm diameter PMTs which provide 20% photo-cathode coverage. The characteristic of the Hyper-Kamiokande is that the technologies are well understood and scalable. The neutrino event reconstruction is well established and the quality of the reconstruction is very high. Hyper-Kamiokande could make a measurement of CPV in neutrino oscillation and could

determine mass hierarchy with a combination of a high intensity neutrino beam. Atmospheric neutrinos by themselves can study neutrino oscillation in high precision. It has a highest sensitivity for proton decay and the grand unification may be tested. Neutrino bursts from supernovae are expected and other astrophysical neutrinos may be detected. The international collaboration will be formed soon aiming to start experiment in 2023.

XMASS

The advantage of the single phase detector like XMASS is a scalability. The mass of the detector can be increased from 1 ton to 10 tons and beyond. Target fiducial mass of the original XMASS proposal is 10 tons. For a single phase detector, the better event reconstruction is achieved for a bigger detector due to the more contrast of the event patterns and timing.

The very low energy data in the whole volume can be analyzed without event reconstruction. The lowest energy threshold we had achieved was 0.3 keV for XMASS-I. XMASS also have a capability to detect e/γ events, and therefore is sensitive to low mass DM, Axion Like Particles and Solar Axions. The current experimental situation is that the region where a 100kg detector can explore is more or less excluded by the XENON100 results, and therefore the next stage experiments need to have a sensitivity equivalent to a 1 ton detector has. XMASS1.5 has a fiducial mass of 1 ton, but we aim to build a detector as large as possible. The design of XMASS1.5 needs to consider its extension to 10 ton detector. We need to make many of the detector parts to be common for 10 ton detector. By the minimum modification we can make XMASS1.5 to 10 ton detector.

GADZOOKS

GADZOOKS (Gd project using Super-Kamiokande) adds new value on the on-going experiment, Super-Kamiokande. The aim is to detect neutrinos from past supernovae, namely supernova relic neutrinos (SRN), which carries the history of heavy element synthesis since the beginning of the Universe. Total and an average neutrino energy emitted in the form of Supernova can also be determined.

Currently the experimental sensitivity is only factor of 3 larger than the expected SRN signal. In

order to detect SRN, we need to enhance the detection of the $\bar{\nu}_e$ signal in the process $\bar{\nu}_e + p \rightarrow e^+ + n$. We add Gd in the SK tank to identify neutrons positively. Gd absorbs a neutron producing delayed gammas. By dissolving 0.2% by mass of a gadolinium compound (e.g., 100 tons of $Gd_2(SO_4)_3$ into 50,000 tons of ultra-pure Super-K water) would make the neutron capture efficiency of 90%. The expected SRN signal for 10 year of SK data after the Gd loaded, assuming the detection efficiency of 67% (90% for capture efficiency and 74% selection efficiency), then 33 SRN events will be detected in between 10 and 30 MeV above backgrounds and it makes more than 4σ level signal. Feasibility tests by 200 tons of water tank system (EGADS) is going on: transparency measurement, circulation and recovery test, data taking with Gd loaded water and so on. These tests will be finished by middle of 2013. Then the real installation will be scheduled.

Future Organization

There are three operating bodies for the underground site in Kamioka and the situation is rather complicated. It is better to form a kind of unified organization which makes the underground laboratories and underground experiments much visible and makes our budget situation to be improved. For those reasons, we are preparing a consortium of all the three organizations as core members but to include other institutions that are conducting experiments at Kamioka as collaborating members. Eventually we aim to request budget through the consortium, but this is not clear yet.

AKENO OBSERVATORY

Introduction

The Observatory is in Akeno of Hokuto-city situated 20 km northwest of Kofu and 130 km west of metropolitan Tokyo. The location is at the longitude of 138.5°E and the latitude of 35.8°N . The altitude is ~ 900 m above sea level. It was established in 1977 as a research center for air shower studies in the very high energy region, and it has been administered by the ICRR as a facility of joint-university-use.

Akeno Air Shower Experiments

The Akeno Air Shower Experiment started in 1979 with an array covering 1 km^2 area (the 1 km^2 array, see Fig.1). The array was enlarged to 20 km^2 in 1984 and was gradually expanded to Akeno Giant Air Shower Array (AGASA) of approximately 100 km^2 area by 1990. The AGASA was built to



Fig. 1. Aerial View of Akeno Observatory and 1 km^2 Array Area

detect Ultra-High Energy Cosmic Rays (UHECRs) in the energy range of 10^{20} eV,

One of the distinctive features of Akeno experiments is that the measurements were made over five decades of energies well covering 10^{15} eV - 10^{20} eV by using both the surface detector for electromagnetic component, (Fig.2) and the shielded detector for muon component (Fig.3).

The wide energy coverage was accomplished by the arrays of scintillation detectors of various inter-detector spacings from 3 m to 1 km and with different triggering conditions. This feature of Akeno

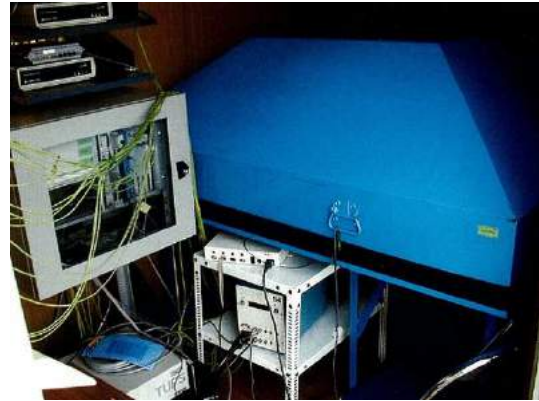


Fig. 2. One of the AGASA surface detectors and its optical fiber data acquisition system.

air shower measurement is well demonstrated in Fig.4, in which the spectra from Akeno 1 km^2 for $10^{14.5}$ eV - $10^{18.8}$ eV [1, 7] and AGASA for $10^{18.5}$ eV - $10^{20.3}$ eV [17] are plotted.

To analyze the data from the arrays of different inter-detector spacings, we employed similar algorithms except the way to estimate the primary energy: the total number of electrons, N_e , is used for the 1 km^2 array, while the local density at 600 m from the shower core, $S(600)$, is used for AGASA. We attribute a shift of $\sim 10\%$ in energy around $10^{18.5}$ eV seen in Fig.4 between the 1 km^2 array and the AGASA to this difference.

The parameter N_e^{max} at the maximum of shower development is considered as one of the good primary energy estimators which does not depend critically on the interaction model or primary composition. The observed N_e in the 1 km^2 array was converted to N_e^{max} using the longitudinal shower development curves determined with constant intensity cut method of integral N_e spectra measured at Mt. Chacaltaya and at Akeno[1]. The flux around the “knee” is compatible with all-particle spectra measured by Tibet AS γ group¹ and by KASKADE group². A change in the index of the power-law energy spectrum, the “second knee” around $10^{17.8}$ eV, was established by the Akeno air shower experiments[7].

*1 Amenomori et al., the Tibet AS γ collaboration, *Astrophys. J.* **678**, 1165 (2008).

*2 T. Antoni et al., the KASKADE collaboration, *Astropart. Physics.* **24**, 1 (2005).



Fig. 3. One of the muon detector housings with concrete shielding.

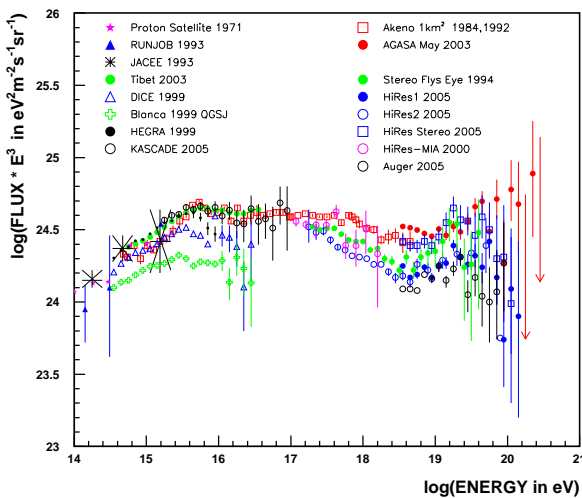


Fig. 4. Akeno energy spectrum measurements for 10^{15} eV - 10^{20} eV.

AGASA

The AGASA was composed of 111 surface detectors, each with plastic scintillator of 2.2 m^2 area and 5 cm thickness [6]. The counters were deployed with $\sim 1 \text{ km}$ spacing covering the ground area of about 100 km^2 in the suburban area of Akeno, outside of the observatory campus. All counters were connected with optical fibers for the coincidence timing measurement and digital data transport to the observatory. The AGASA served as the largest air shower array in the world since its commissioning in 1990 until it stopped data taking in January 2004, when the construction of the succeeding experiment, Telescope Array (TA), started in Utah. It was dismantled in 2007 together with other Akeno air shower arrays.

An exposure of $5.8 \times 10^{16} \text{ m}^2 \text{ s sr}$ above 10^{19} eV was accumulated by AGASA in 13 years of op-

eration. Extensive air showers with zenith angles smaller than 45° and with core locations inside the array area were used for the analysis. The conversion formula from $S(600)$ to the primary energy E_0 [eV] is,

$$E_0 = 2.0 \times 10^{17} \times S(600)^{1.0} \quad (1)$$

which is derived from simulations[5, 13]. The resolution of energy determination is about 25% at 10^{20} eV, which is estimated by analyzing the simulated showers. The overall systematic error in determining the energy scale of the primary cosmic ray was estimated to be 18%[17] by the same simulation. The dominant source of the error was considered to arise from the unknown composition of the primary and the unknown cross section of the hadronic interaction at extremely high energy. The AGASA reported an extension of the energy spectrum beyond the predicted Greisen-Zatsepin-Kuzmin (GZK) cutoff in 1998[13], and a total of eleven UHECR events were observed above 10^{20} eV by 2003[17].

Spectrum of UHECRs

Since the AGASA measurement in 1998, High Resolution Fly's Eye (HiRes)³, Pierre Auger Observatory (PAO)⁴, and Telescope Array (TA)⁵ measured the energy spectra of UHECRs with higher statistics.

The HiRes observed the UHECR using the fluorescence telescope. The PAO and TA measure the spectrum using the surface array consisting of either water tanks (PAO) or plastic scintillators (TA), but the energy scale of the array is determined by the fluorescence telescope using a subset of events observed by the fluorescence telescope and surface array at the same time. The adoption of the energy scale by the fluorescence telescopes is based on its small dependence on the result of air shower simulation.

The energy spectra above 10^{18} eV by AGASA and other experiments are compiled and compared by the working group represented by all UHECR experiments in the UHECR-2012 symposium held at CERN⁶. The result is plotted in Fig.5 with the

^{*3} R.U. Abbasi et al., the HiRes collaboration, Phys. Rev. Lett. **100**, 101101 (2008).

^{*4} J. Abraham et al., the Pierre Auger collaboration, Phys. Lett. **B685**, 239 (2010).

^{*5} T. Abu-Zayyad et al., the Telescope Array collaboration, arXiv:1205.5067v1 (2012).

^{*6} <http://indico.cern.ch/conferenceDisplay.py?confId=152124>

energy scale of each experiment adjusted to a reference energy, which is set halfway between the PAO and TA/HiRes. Following factors were applied for

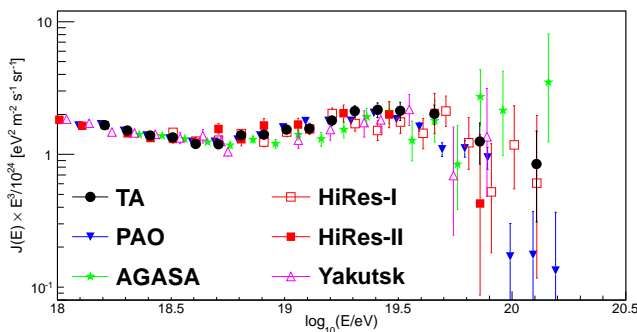


Fig. 5. Recent compilation of UHECR energy spectra. The energy scale of each experiment is adjusted as described in the text.

the energy scale; $\times 1.10$ for PAO, $\times 0.91$ for TA and HiRes, $\times 0.65$ for AGASA and $\times 0.56$ for Yakutsk.

As seen in Fig.5, the overall agreement between experiments is good, and a “dip” structure was seen around $10^{18.7}$ eV by all experiments. The HiRes, PAO and TA confirmed a strong flux suppression above approximately $10^{19.7}$ eV. Although the AGASA spectrum does not demonstrate the cut-off structure, the number of events above 10^{20} eV became only two after the energy rescaling, making the claim of the extended spectrum beyond the GZK cutoff energy [13] statistically insignificant. The estimate of systematic uncertainty of the energy measurement is approximately 20% for all the experiments, and rescalings for the TA/HiRes and PAO are within this limit. Rescaling of the surface array energy, $\times 0.65$ for AGASA and $\times 0.56$ for Yakutsk, indicates that there exist larger systematic uncertainties than originally estimated by running the air shower simulation. This difference of energy scale obtained by the surface array and by the fluorescence telescope remains as a fundamental question in the understanding of the air shower phenomena.

Anisotropy of UHECRs

Several tests for global anisotropy were carried out for AGASA events with energies above 4×10^{19} eV and zenith angles less than 45° . No signature of large scale anisotropy was observed in the arrival direction. The data sample of a total of 47 events, however, contained one triplet and three doublets clustered within 2.5° angular separation [12, 14].

The probability for producing these clusters from uniformly distributed cosmic rays was evaluated to be less than 1%. Later measurements by HiRes and TA in the northern hemisphere also demonstrated no large scale anisotropy. The number of small-angle clusters by HiRes and TA was however at the level of random coincidence^{7, 8}, and no significant auto-correlation as seen by the AGASA was observed.

The arrival direction distribution measured by AGASA in the energy region of 10^{18} eV – $10^{18.4}$ eV showed deviations from the isotropy [15]. A circle of 20° radius was chosen to evaluate the anisotropy of the flux, and an excess toward the galactic center and a deficit toward the anti-galactic center were observed. Statistical significance was higher than 4σ without considering a search penalty factor into account. The measurement was repeated with significantly higher statistics by the Pierre Auger Observatory in the southern hemisphere, and no excess in the galactic center was observed⁹.

Scientific Activities in 2006 - 2011

The study of UHECRs by AGASA in Akeno was succeeded by the Telescope Array (TA) experiment in Utah, USA since 2008. During 2006-2011 after the cessation of AGASA, the Akeno observatory has been used for small scale cosmic ray experiments, astrophysical observations and as a test and maintenance facility of TA by the ICRR and university researchers.

Research and development for the Telescope Array observation in Utah by the TA collaboration: All the fluorescence imaging cameras and a part of the surface detectors of TA were assembled in the Akeno observatory by the TA collaboration team. The detectors were tested in Akeno and shipped to the Utah observation site for the installation. All the unit mirrors of the TA fluorescence telescope were tested in Akeno and the atmospheric monitoring lidar of TA using YAG laser was developed in Akeno.

Observation by the multi-color imager for transients, survey and monstrous explosions (MIT-SuME) by N. Kawai (Tokyo Institute of Tech-

^{*7} R.U.Abbasi et al., the HiRes collaboration, *Astrophys. J.* **610**, L73 (2004)

^{*8} T.Abu-Zayyad et al., the TA collaboration, arXiv:1205.5984

^{*9} P. Abreu et al. the Pierre Auger collaboration, *Astropart. Phys.* **34** 627 (2011)

nology) et al.: One of the three MITSuME robotic telescopes was installed in the Akeno observatory in 2003 on the roof of the unused concrete muon house. The telescope has an aperture of 50 cm, an FOV of $28' \times 28'$ and is equipped with a tri-color CCD camera capable of $g'RcIC$ -bands photometry. It is operated remotely from the Tokyo Tech using dedicated ADSL connections. Upon receiving a GRB alert from Swift or Fermi satellite, it quickly directs the telescope ($9^\circ/s$ maneuverability) toward the GRB direction, and makes a prompt observation of the GRB and its afterglow. Since its commissioning in 2004, the MITSuME telescope in Akeno has been making more than ~ 10 GRB follow-up observations every year, and detected more than 10 GRB afterglows¹⁰. It has been also joining the multi-wavelength campaign for observing AGNs and other transient objects.

Observation of galactic cosmic rays by large area muon telescope by S. Shibata (Chubu University), Y. Hayashi (Osaka City University) et al.: Four layers of proportional counter telescopes, each with 25 m^2 area, were installed in three muon houses in Akeno (Fig.3) and have been continuously measuring the cosmic ray muons since 2003. The mode energy of the primary cosmic rays is approximately 25 GeV corresponding to 2m thick concrete ceiling of the muon house and the latitude of Akeno observatory. The measurement in Akeno is combined with a simultaneous measurement in Ooty, India, and the modulation effects of galactic cosmic rays by the solar activity such as the Forbush decrease and its precursor have been continuously monitored¹¹. These measurements in Akeno and Ooty are intended to contribute to the world space weather monitoring and forecast.

Research and development for a small atmospheric Cherenkov telescope in Akeno observatory by T. Yoshikoshi, M. Ohishi (ICRR), K.Nishijima (Tokai University) et al.: A small alt-azimuth telescope is being setup in Akeno for prototype tests with atmospheric Cherenkov observations of gamma rays¹². Refurbishing of the telescope control system, the unit mirror and optics was

made in 2010 and 2011. A test of a prototype camera using silicon photomultiplier is planned in 2012.

List of Publications

AGASA publications before year 2006

- [1] M. Nagano et al., "Energy spectrum of primary cosmic rays between $10^{14.5}$ and 10^{18} eV", J. Phys. **G10**, 1295 (1984).
- [2] M. Teshima et al., "Expanded array for giant air shower observation at Akeno", Nucl. Instr. Meth. **A247**, 399 (1986).
- [3] M. Teshima et al., "Properties of 10^9 - 10^{10} GeV extensive air showers at core distances between 100 and 3000 m", J. Phys. **G12**, 1097 (1986).
- [4] Y. Matsubara et al., "Photoproduced muons in EAS and the search for gamma-ray initiated showers beyond 10^{16} eV", J. Phys. **G14**, 385 (1988).
- [5] H.Y. Dai et al., "On the energy estimation of ultra-high-energy cosmic rays observed with the surface detector array", J. Phys. **G14**, 793 (1988).
- [6] N. Chiba et al., "Akeno Giant Air Shower Array (AGASA) covering 100 km^2 area", Nucl. Instr. Meth. **A311**, 338 (1992).
- [7] M. Nagano et al., "Energy spectrum of primary cosmic rays above $10^{17.0}$ eV determined from extensive air shower experiments at Akeno", J. Phys. **G18**, 423 (1992).
- [8] S. Yoshida et al., "Lateral distribution of charged particles in giant air showers above 1 EeV observed by AGASA", J. Phys. **G20**, 651 (1994).
- [9] N. Hayashida et al., "Observation of a Very Energetic Cosmic Ray Well Beyond the Predicted 2.7K Cutoff in the Primary Energy Spectrum", Phys. Rev. Lett. **73**, 3491 (1994).
- [10] S.Yoshida et al., "The cosmic ray energy spectrum above 3×10^{18} eV measured by the Akeno Giant Air Shower Array", Astropart. Phys. **3**, 105 (1995).

*¹⁰ The observations are reported in GCN Circulars.

*¹¹ T. Nonaka et al., "Simultaneous Detection of the Loss-Cone Anisotropy with Ooty and Akeno Muon Telescopes", Proc. of the 29th ICRC, **1**, 363-366 (2005).

*¹² T. Yoshikoshi et al., "R & D Studies for Very High Energy Gamma-Ray Astrophysics at Energies Greater than 10 TeV", Proc. of the 32nd ICRC, Beijing, **9**, 226-229 (2011).

- [11] N. Hayashida et al., “Muons (≥ 1 GeV) in large extensive air showers of energies between $10^{16.5}$ eV and $10^{19.5}$ eV observed at Akeno”, J. Phys. **G21**, 1101 (1995).
- [12] N. Hayashida et al., “Possible Clustering of the Most Energetic Cosmic Rays within a Limited Space Angle Observed by the Akeno Giant Air Shower Array”, Phys. Rev. Lett. **77**, 1000 (1996).
- [13] M. Takeda et al., “Extension of the Cosmic-Ray Energy Spectrum beyond the Predicted Greisen-Zatsepin-Kuz'min Cutoff”, Phys. Rev. Lett. **81**, 1163 (1998).
- [14] M. Takeda et al., “Small-scale anisotropy of cosmic rays above 10^{19} eV observed with the Akeno Giant Air Shower Array”, Astrophys. J. **522**, 225 (1999).
- [15] N. Hayashida et al., “The anisotropy of cosmic ray arrival directions around 10^{18} eV”, Astropart. Phys. **10**, 303 (1999).
- [16] K. Shinozaki et al., “Upper limit on gamma-ray flux above 10^{19} eV estimated by the Akeno giant air shower experiment”, Astrophys. J. **571**, L117 (2002).
- [17] M. Takeda et al., “Energy determination in the Akeno Giant Air Shower Array experiment”, Astropart. Phys. **19**, 447 (2003).

NORIKURA OBSERVATORY

Introduction

Norikura Observatory (36.10°N and 137.55°E) was founded in 1953 and attached to ICRR in 1976. It is located at 2770 m above sea level, and is the highest altitude manned laboratory in Japan (Fig. 1). Experimental facilities of the laboratory are made available to all the qualified scientists in the field of cosmic ray research and associated subjects. The AC electric power is generated by the dynamo and supplied throughout the observatory. The observatory can be accessed easily by car and public bus in summer (July-September). The 50th anniversary of Norikura Observatory was celebrated in 2003.



Fig. 1. Norikura Observatory

Norikura Observatory gave manned operation to the observations by the qualified scientists all the year until the year 2003. However, the feasibility of the automatic operation of Norikura Observatory during winter period has been tested since winter 2004 in order to study the possibilities to reduce maintenance and labor costs without causing serious inconveniences for the researches. A long-distance (~40km) wireless LAN system (11M bps) was set up in 2003. Two new easy-to-handle and easy-to-maintain dynamos of 115 KVA each, as shown in Fig. 2 were installed in 2004 as well. The unmanned operation of Norikura Observatory has been mostly successful in winter, during which the battery backed-up solar panels and/or wind power generators kept supplying the electricity to the wire-

less LAN and on-going cosmic-ray experiments.



Fig. 2. A dynamo of 115KV.

Present major scientific interests of the laboratory is focused on the modulation of high energy cosmic rays in the interplanetary space associated with the solar activity and the generation of energetic particles by the solar flares, both of which require long-term observation. This research has been carried out by the group of user universities, where ICRR provides them with laboratory facility. A part of the facility has been open for the environmental study at high altitude such as aerosol-related mechanism in the atmosphere, observation of total ozone and UV solar radiation, for botanical study in the high-altitude environment, etc..

Cosmic Ray Physics

Space weather observation [represented by Kazuoki Munakata, Shinshu University]

Space weather observation is actively made by a 25 m² muon hodoscope at Norikura Observatory ¹

*1 K. Munakata, S. Yasue, C. Kato, J. Kota, M. Tokumaru, M. Kojima, A. A. Darwish, T. Kuwabara and J. W. Bieber, "On the cross-field diffusion of galactic cosmic rays into the magnetic flux rope of a CME", *Advances in Geosciences*, 2, 115-124, eds. W. H. Ip and M. Duldig (World Scientific Publishing Co., USA), (2006).

The anisotropy observed with the global muon detector network (GMDN) provides us with a unique information of the spatial gradient of the GCR density which reflects the large-scale magnetic structure in the heliosphere. The solar cycle variation of the gradient gives an important information on the GCR transport in the heliosphere, while the short-term variation of the gradient enables us to deduce the large-scale geometry of the magnetic flux rope and the interplanetary coronal mass ejection (ICME). Real-time monitoring of the precursory anisotropy which has often been observed at the Earth preceding the arrival of the ICME accompanied by a strong shock may provide us with useful tools for forecasting the space weather with a long lead time. By using a self-supporting power system utilizing the solar panels and batteries, we keep a 25 m² muon hodoscope running at the Norikura Observatory as an impor-

tant component detector of the GMDN. The total power consumption of this detector has been suppressed as low as 36 Watt by replacing all amplifier boards with those using CMOS ICs and by introducing a new recording system using the FPGA. This new system, in which the observation has been automatically carried out by a PC connected with the Internet, also enabled us to monitor the data on the real-time basis for the space weather study.

Solar neutron observation [represented by Yutaka Matsubara, Nagoya University]

Observation of solar neutron has been conducted at the Norikura Observatory since 1990. Neutron is used to clarify the acceleration mechanism of high energy particles in association with solar flares, because the neutron is not reflected by the interplanetary magnetic field. The 64m² solar neutron telescope was constructed in 1996, which is one of 7 solar neutron telescopes deployed at different longitudes to make up a network of 24 hour observation of solar neutrons^{10 11 12 13 14 15 16 17 18 19 20 21 22}. The Norikura 64m² solar neutron telescope has been operated by solar batteries and wind power generators since 2004.

- *² T. Kuwabara, J. W. Bieber, J. Clem, P. Evenson, R. Pyle, K. Munakata, S. Yasue, C. Kato, S. Akahane, M. Koyama, Z. Fujii, M. L. Duldig, J. E. Humble, M. R. Silva, N. B. Trivedi, W. D. Gonzalez and N. J. Schuch, "Real-time cosmic ray monitoring system for space weather", *Space Weather*, 4, S08001-1 10, (2006).
- *³ M. R. Da Silva, A. Dal Lago, E. Echer, A. de Lucas, W. D. Gonzalez, N. J. Schuch, K. Munakata, L. E. A. Vieira, and F. L. Guarnieri, "Muon and neutron observations in connection with the corotating interaction regions", *Adv. Space Res.*, 40, pp348-352, (2007).
- *⁴ Y. Okazaki, A. Fushishita, T. Narumi, C. Kato, S. Yasue, T. Kuwabara, J. W. Bieber, P. Evenson, M. R. Da Silva, A. Dal Lago, N. J. Schuch, Z. Fujii, M. L. Duldig, J. E. Humble, I. Sabbah, J. Kta and K. Munakata, "Drift effects and the cosmic ray density gradient in a solar rotation period: First observation with the Global Muon Detector Network (GMDN)", *Astrophys. J.*, 681, 693-707, (2008).
- *⁵ T. Kuwabara, J. W. Bieber, P. Evenson, K. Munakata, S. Yasue, C. Kato, A. Fushishita, M. Tokumaru, M. L. Duldig, J. E. Humble, M. R. Silva, A. Dal Lago, and N. J. Schuch, "Determination of ICME Geometry and Orientation from Ground Based Observations of Galactic Cosmic Rays", *J. Geophys. Res.*, 114, A05109-1 10, doi:10.1029/2008JA013717, (2009).
- *⁶ A. Fushishita, T. Kuwabara, C. Kato, S. Yasue, J. W. Bieber, P. Evenson, M. R. Da Silva, A. Dal Lago, N. J. Schuch, M. Tokumaru, M. L. Duldig, J. E. Humble, I. Sabbah, H. K. Al Jassar, M. M. Sharma, and K. Munakata, "Precursors of the Forbush Decrease on 2006 December 14 observed with the Global Muon Detector Network (GMDN)", *Astrophys. J.*, 715, 1239-1247, (2010).
- *⁷ A. Fushishita, Y. Okazaki, T. Narumi, C. Kato, S. Yasue, T. Kuwabara, J. W. Bieber, P. Evenson, M. R. Da Silva, A. Dal Lago, N. J. Schuch, M. Tokumaru, M. L. Duldig, J. E. Humble, I. Sabbah, J. Kta, and K. Munakata, "Drift effects and the average features of cosmic ray density gradient in CIRs during successive two solar minimum periods", *Advances in Geosciences*, eds. W. H. Ip and M. Duldig (World Scientific Publishing Co., USA), 21, 199-210, (2010).
- *⁸ M. Tokumaru, M. Kojima, K. Fujiki, K. Munakata, T. Kuwabara and K. Marubashi, "Relation between loop-shaped interplanetary disturbances and the magnetic flux rope", *Advances in Geosciences*, eds. W. H. Ip and M. Duldig (World Scientific Publishing Co., USA), 21, 21-32, (2010).
- *⁹ M. Rockenbach, A. Dal Lago, W. D. Gonzalez, K. Munakata, C. Kato, T. Kuwabara, J. W. Bieber, N. J. Schuch, M. L. Duldig, J. E. Humble, H. K. Al Jassar, M. M. Sharma, and I. Sabbah, "Geomagnetic Storm's Precursors Observed from 2001 to 2007 with the Global Muon Detector Network (GMDN)", *Geophys. Res. Lett.*, 38, L16108-1 4, doi:10.1029/2011GL048556, (2011).

- *¹⁰ "Solar neutron events of October–November 2003", Watanabe, K. *et al.*, *Astrophys. J.*, **636**, 1135–1144, 2006.
- *¹¹ "Solar neutron events in association with large solar flares in November 2003", Watanabe, K. *et al.*, *Adv. Space Res.*, **38**, 425–430, 2006.
- *¹² "Long-lived solar neutron emission in comparison with electron-produced radiation in the 2005 September 7 solar flare", Sako, T. *et al.*, *Astrophys. J.*, **651**, L69–L72, 2006.
- *¹³ "Highly significant detection of solar neutrons on 2005 September 7", Watanabe, K. *et al.*, *Adv. Space Res.*, **39**, 1462–1466, 2007.
- *¹⁴ "A solar neutron telescope in Tibet and its capability examined by the 1998 November 28th event", Muraki, Y. *et al.*, *Astroparticle Phys.*, **28**, 119–131, 2007.
- *¹⁵ "Simultaneous detection of high-energy solar neutrons and protons at Chacaltaya observatory on April 15, 2001", Muraki, Y. *et al.*, in Proc. 30th Int. Cosmic Ray Conf, Merida, **1**, 25–28, 2007.
- *¹⁶ "Search for solar neutrons associated with series of X-class flares during the declining period of solar cycle 23", Matsubara, Y. *et al.*, in Proc. 30th Int. Cosmic Ray Conf, Merida, **1**, 29–32, 2007.
- *¹⁷ "Ion acceleration and neutral emission mechanisms for 2005 September 7 flare", Watanabe, K. *et al.*, in Proc. 30th Int. Cosmic Ray Conf, Merida, **1**, 45–48, 2007.
- *¹⁸ "Energy spectrum for the solar neutron event of September 7 2005, derived from the SNT at Sierra Negra", Gonzalez, L. X. *et al.*, in Proc. 30th Int. Cosmic Ray Conf, Merida, **1**, 57–60, 2007.
- *¹⁹ "Status of the world-wide network of solar neutron telescopes in solar cycle 24", Matsubara, Y. *et al.*, in Proc. 31st Int. Cosmic Ray Conf, Lodz, **1**, On Conference home page, 2009.
- *²⁰ "Detection of high-energy solar neutrons and protons by ground level detectors on April 15, 2001", Muraki, Y. *et al.*, *Astropart. Phys.*, **29**, 229–242, 2008.
- *²¹ "Solar neutron events as a tool to study particle acceleration at the Sun", Valdes-Galicia, J. F. *et al.*, *Adv. Space Res.*, **43**, 565–572, 2009.
- *²² "Physics of ion acceleration in the solar flare on 2005 September 7 determines γ -ray and neutron production", Watanabe, K. *et al.*, *Adv. Space Res.*, **44**, 789–793, 2009.

This collaborative work has started since fiscal 2007 succeeding to the previous project titled ‘Observation of solar neutrons by using a new method’. Although solar cycle 24 has started since 2008, the solar activity has continued to be inactive, and no new solar neutron event has been detected by the network since 2006. The last solar neutron event was on September 7, 2005. This event is unique because it indicates ions were accelerated or trapped at the acceleration region longer than electrons. The summary of 11 solar neutron events detected until 2005 shows that it may not be probable that a very efficient acceleration such as the shock acceleration works for ions at solar flares. This is given by deriving the energy spectrum of neutrons at the solar surface for each solar neutron event with a power law. Power law indices obtained span from 3 to 7. The energy spectrum of the original ions is softer than that of neutron. Therefore an efficient acceleration has not been detected by the observation of solar neutrons so far. This work continues in solar cycle 24 to accumulate more events to obtain definite results related with particle acceleration at the solar surface.

New neutron telescope [represented by Yasushi Muraki, Konan University]

Another effort aiming at observation of highest-energy solar cosmic rays started at the Norikura Observatory. The Sun is an accelerator of protons and electrons in the universe. In association with large solar flares, protons and electrons are accelerated into high energies. It is known that protons are accelerated over 50 GeV in the largest solar flares²³. These high energy particles produce the Ground Level Enhancement(GLE). In order to understand the acceleration mechanism of protons, we have prepared several solar neutron telescopes at the high altitude laboratories in the world. They are located at Gornergrat (3,135m), Mt. Aragats in Armenia (3,200m), Tibet (4,200m), Mauna-Kea in Hawaii (4,200m), Mt. Chacaltaya in Bolivia (5,250m), and at Mt. Sierra Negra in Mexico (4,900m). We have constructed a solar neutron telescopes at Norikura Observatory (2,770m) in 1990 and operated it until 2004²⁴. However due to the

lack of power supply during the winter time since 2005, the first solar neutron telescope (36 m²) has not been operated. From 2008 to 2009, we have decided to make a new solar neutron telescope to utilize the large amount of the plastic scintillator (0.5m³), as shown in Fig. 3, left at the observatory.



Fig. 3. 0.5-m² plastic scintillation counter for a new neutron telescope.

The new solar neutron telescope with use of the recycled plastic scintillator consists of main target where neutrons are converted into protons and of the anti-counters surrounding the target. The signals of neutrons converted into protons are observed by using one photomultiplier from bottom side to reduce the electric power. Furthermore a lead plate with the thickness of 1cm is located over the target and the lead plate is sandwiched by two layers of the plastic scintillator to identify gamma-rays from neutrons. The new solar neutron telescope has a function to reject charged particles with an efficiency of 90%. Therefore the new solar neutron telescope has capability of 1/3 of the 64m² large solar neutron telescope located at the same place. We are waiting large solar flares over our detectors.

Particle production and acceleration mechanism in thunder clouds [represented by Harufumi Tsuchiya, Riken]

High-energy radiations from thunderstorms have been observed by flight measurement, high-mountain observations and ground-based measurement. There are two types of those radiations as-

*²³ “ Observation of solar neutrons associated with the large flare on 1991 June 4”, Muraki, Y. *et al.*, *ApJ*, **400**, L75-L78, 1992.

*²⁴ “ Detection of high-energy solar neutrons and protons by ground level detectors on April 15, 2001”, Muraki, Y. *et al.*, *Astropart. Phys.*, **29**,

sociated with thunderstorms. One is short-duration radiations with duration of 1 ms or less. The other is long-duration emissions lasting for a few seconds to a few minutes, or a few tens of minutes on rare occasions. It is believed that both emissions originate from electrons accelerated in strong electric fields formed in lightning and thunder clouds. However, compared with the former, the latter has remained less understood due to lack of a large sample of observations.

To investigate production mechanism of long-duration emissions and the relevant electron acceleration, we installed at Norikura Cosmic-ray Observatory a radiation detection system and environmental sensors to measure light and electric fields during 2008–2010. The radiation system consists of a spherical NaI scintillator and a thin plastic scintillator that is placed just above the NaI counter. During the period, the system detected one long-duration bursts as well as five short-duration events.

Figure 4 shows the long-duration event observed during thunderstorms on 2008 September 20²⁵. The event lasted for 90 sec. Figure 4(Bottom) represents an observed photon spectrum extending from 10 keV to 10 MeV. This indicates that electrons can be accelerated to at least 10 MeV in a quasi-stable thundercloud electric field. In addition, we compared the observed spectrum with model ones, and concluded that a gamma-ray source is located 60 m–130 m (at 90% confidence level) apart from our detector. Given these results, the observed emission was found to consist of not only gamma rays but also electrons. This was the first simultaneous observation of gamma rays and electrons in long-duration bursts

Study of air fluorescence [represented by Naoto Sakaki, Aoyamagakuin University]

Observation of night sky background is carried out at Mt.Norikura for basic study of ultra high energy cosmic-ray physics.

The JEM-EUSO mission is going on in order to study ultra high energy cosmic rays (UHECRs), especially above 10^{20} eV. A 2.5m telescope with 60° FoV will be attached to the International Space Station in 2017 and detect fluorescence in near UV band from extensive air showers induced by UHE-

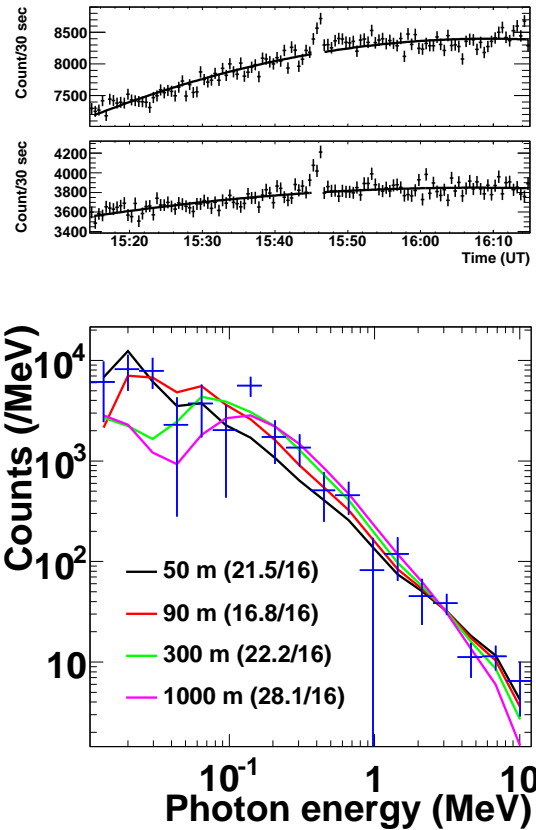


Fig. 4. (Top) Count rates per 30 sec observed by the >10 keV NaI scintillator and (Middle) by the > 100 keV plastic one. (Bottom) The photon spectrum observed by the NaI scintillator.

CRs. Observation of UHECRs from a satellite orbit has not been done yet, so that the knowledge of background light intensity is important to realize the observation. We have measured it from a balloon altitude, but the opportunity is limited. We started the background measurement at Mt.Norikura.

Two 1 inch multi-anode photomultipliers (MAPMTs) developed for EUSO was used with UV filters. The center wavelengths of the filters were 337, 350, 358, 370, 380, 391, 400nm with 10nm band width. In addition BG3 filter was used to detect light in wider range from 330nm to 430nm. The MAPMTs were collimated to 7° FoV. The data was taken with the photon counting method.

We have observed several nights for three years. The intensity at zenith was almost constant at 600-800 photons/ns sr m² for BG3 filter. The spectral intensity was about 1.5-2 times larger than those measured at La Palma and Namibia. The estimated portion of star light and zodiacal light was $\sim 30\%$ and artificial light and night glow at upper atmosphere

*²⁵ “ Observation of an energetic radiation burst from mountain-top thunder clouds”, H. Tsuchiya *et al.*, Phys. Rev. Lett. **102**, 255003 (2009), Citation Index:13.

may be the main components at Mt. Norikura. Night sky background measured at Mt. Norikura is shown in Fig. 5.

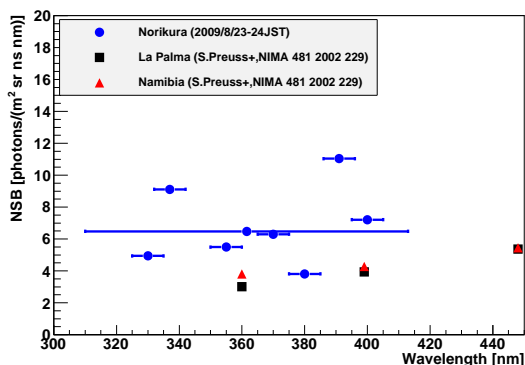


Fig. 5. Spectrum of night sky background measured at Mt. Norikura compared with those at La Palma and Namibia.

Environmental Study

Atmospheric aerosol particles and water soluble gases [represented by Takashi Shibata, Nagoya University]

One of the interesting topics is atmospheric environment especially relating with atmospheric aerosol particles and water soluble gases. The cosmic ray observatory at Mt. Norikura provides us very unique opportunity for the observations of atmosphere at free-tropospheric conditions with its high altitude, AC power supply at the site, accommodation facility, and easy accessibility. From year 2000 to 2007, we conducted continuous monitoring (mostly mid-May to mid-October) of meteorological parameters, number-size distribution of aerosols, aerosol chemical composition, ozone and radon concentrations, and column amount of aerosols from sky radiometer and ceilometers. We also collected rain, fog, water-condensed aerosol samples. These samples combined with other observed parameters were used in publications^{26 27 28} in the following subjects:

*26 “Nucleation mode particles in up-slope valley winds at Mt. Norikura, Japan: implications for the vertical extent of new particle formation events in the lower troposphere”, Nishita, C., K. Osada, K. Matsunaga, Y. Iwasaka, *J. Geophys. Res.*, **113**, D06202, doi:10.1029/2007JD009302, 2008.

*27 “Temporal variation of water-soluble ions of free tropospheric aerosol particles over central Japan”, Osada, K., Kido, M., Nishita, C., Matsunaga, K., Iwasaka, Y., Nagatani, M., Nakada, H., *Tellus*, **59B**, 742-754, 2007.

*28 “Number-size distributions of free tropospheric aerosol particles at Mt. Norikura, Japan: effects of precipitation and air-mass transportation

- (1) Polluted air pumping effects over central Japanese Alps in summer
- (2) Seasonal variation of aerosol chemistry in free troposphere
- (3) Vertical profiles of aerosols and clouds near the top of the atmospheric boundary layer.

Ceilometer (lidar with small output energy) was installed in summer 2002, and was operated in 6 summer seasons. The aerosol and cloud profiles near the top of the atmospheric boundary layer have been observed. Some events of Asian dust were detected.

Observations of total ozone and UV solar radiation with Brewer spectrophotometer [represented by Mahito Ito, Japan Meteorological Agency]

Observations of total ozone and UV solar radiation with Brewer spectrophotometer on the Norikura mountains are made^{29 30 31}.

Aerological Observatory started this research as a joint project with the ICRR. Purpose of this study is based on the concept of developing Regional Brewer Calibration Centre in Asia and study of total ozone, total sulfur oxide and global/diffuse UV included solar radiation on the high mountains. Observation results by using Brewer spectrophotometers and other instruments for the observation period of three summer seasons of recent three years between 2009 to 2011 are summarized as follows;

- (1) Daily means of ds (direct-sun-observation) O₃ (total ozone) at Norikura for the observation periods were approx. 280 to 290 milli-atm-cm (i.e., total integrated amount of ozone above the observation site being 2.8mm to 2.9 mm at 1 atm) and were running on the lower values of approx. -3 to -6% compared to the value at Tsukuba (36.06 N, 140.13 E, 39 m a.s.l.) at almost same latitude. Day-to-

pathways”, Nishita, C., K. Osada, K. Matsunaga, Y. Iwasaka, *J. Geophys. Res.*, **112**, doi:10.1029/2006JD007969, 2007.

*29 “Observations of total ozone and UV solar radiation with Brewer spectrophotometers on the Norikura mountains in 2009.”, Ito, M., M. Takano, H. Oguri, M. Takita, H. Shimodaira and H. Ishitsuka, *Jour. of the Aerological Observatory*, **69**, 41-54 2011.

*30 “Observations of total ozone and UV solar radiation with Brewer spectrophotometers on the Norikura mountains, Northern Japanese Alps, from 2009.”, Ito, M., S. Shimizu, Y. Noto, T. Shimamura, M. Takano, M. Takita, H. Shimodaira and H. Ishitsuka, *The 13th WMO Biennial Brewer Workshop, Beijing, China in 2011*, 2011.

*31 “Total ozone and UV solar radiation with Brewer spectrophotometers at Norikura of Northern Japanese Alps, in recent three years.”, Ito, M., S. Shimizu, Y. Noto, T. Shimamura, M. Takita, H. Shimodaira and H. Ishitsuka, *Jour. of the Aerological Observatory*, **70**, in contribution.

day variations at Norikura were also small against Tsukuba. On the other hand, daily mean of $ds\ SO_2$ (total sulfur oxide) values were not recognized at Norikura.

(2) Absolute calibration of Brewers for $ds\ O_3$ and $ds\ SO_2$ observations could be carried out at Norikura in the clear day within the zenith-angle range from 7.928 (maximum) to 1.028 (minimum) in unit of air mass at Norikura, where one air mass unit is defined to be the distance traversed in the atmosphere by solar light perpendicular to the ground. O_3 and SO_2 Extra-Terrestrial Coefficients (=ETC), i.e., instrumental coefficients of Brewers could be produced as about 10 samples. As an example of the calibration in 2011, the average of O_3 ETC of Brewers was identical within 1% to the currently used coefficient.

(3) In comparison to the data acquired at Tsukuba, the average of daily total GL_{UV} (global UV = all-sky UV integrated above the horizon) at Norikura measured in the wavelength range CIE (corresponding to the Erythema UV region defined by a committee "Commission Internationale de L'Éclairage") for the observation periods indicated the intensities of approx. +23 % in 2009 to -6 % in 2011. The low intensity in 2011 was due to the bad weather on the Norikura Mountain. In the case of clear days, the GL_{UV} at Norikura indicated high intensities of approx. +35 to +52 % against the values at Tsukuba. On the other hand, the GL_{UV} increased in the short wavelength range at Norikura against the average at Tsukuba. The altitudinal increasing rate of GL_{UV} in the clear day indicated the calculated amounts of approx. +13 to +18 % per 1,000 m.

This joint project had been clarifying the low total O_3 , high UV in clear day, low turbidity and etc. at Norikura against the value at Tsukuba. Those environmental conditions are useful for the intercomparison and the absolute calibrations with Brewers. The continuous observations with Brewers and other instrument are very important for the clarification of the seasonal variation and the coefficient trends.

Effect of snow cover on pine shrub *Pinus pumila* in the alpine region [represented by Emiko Maruta, Toho University]

High mountainous habit is one of the most severe habits for plant life and sometimes dwarf

shrubs cannot survive. In the alpine regions of Japan, the dwarf shrub *Pinus pumila* (Japanese name : Haimatsu) forms communities together with small alpine plants, whereas dwarf shrubs occur only in the transition zone between the alpine region and the subalpine forest in Europe and North America. This characteristic of alpine vegetation is considered to be owing to winter heavy snow in the alpine regions of Japan. The purpose of this study is to elucidate how snow cover protects Haimatsu from winter environmental stresses in the alpine region of Mt. Norikura^{32 33}.

*32 "Needle browning and death in *Pinus pumila* in the alpine region of central Japan were not related to mechanical damage of cuticle and cuticle thickness.", Nakamoto A., Ikeda T., Maruta E., Can. J. For. Res. 42, 167-178 (2012).

*33 "Needle traits of an evergreen, coniferous shrub growing at wind-exposed and protected sites in a mountain region: does *Pinus pumila* produce needles with greater mass per area under wind-stress conditions?", Nagano S., Nakano T., Hikosaka K and Maruta E., Plant Biology 11(Suppl.1), 94-100, (2009).

RESEARCH CENTER FOR COSMIC NEUTRINOS

Research Center for Cosmic Neutrinos was established in 1999 to promote research of cosmic neutrinos. The members of this center belong to the Neutrino and Astroparticle Division and the research activities of the members are described in the section of the Neutrino and Astroparticle Division. In this section, the activities of this center other than those described in that section are described.

The Research Center for Cosmic Neutrinos, together with the members of the computer committee in ICRR, is in charge of the computer system and the related network system for the inter-university research programs of ICRR. The system has been renewed in Jan. 2008. The system consists of 1120 CPU's for large scale computing together with several server computers for the system control and networking. The system had ~ 500 TB disk space when it was upgraded in Jan. 2008. Then the system was upgraded further to a 1250 TB disk system in July 2010. The system is running and maintained well with the overall running efficiency (system run time/calendar time) of better than 95% (as of year 2010). Due to the Tohoku Earthquake and the subsequent shortage of the electricity in the Tokyo area in 2011, the system was operated with a reduced number of CPU's until Oct. 2011. In addition, a backup power system was installed into the main part of the computer system, also in 2011. At present, this center is leading the plan for the computer upgrade scheduled in Jan. 2014.

Since spring 2000, Research Center for Cosmic Neutrinos, together with the external members, has been organizing domestic neutrino workshops in order to stimulate research in neutrinos. These workshops have been held as one of the ICRR inter-university research programs. The date and the main topic(s) for each workshop between 2006 and 2012 are summarized in Table 1.

In addition, we, together with colleagues in Korea, have organized topical international workshops. The title of the workshops were "2nd International Workshop on a Far Detector in Korea for the J-PARC neutrino Beam" and "3rd International Workshop on a Far Detector in Korea for the J-PARC neutrino Beam". The earlier one was held at Seoul National University on July 13-14, 2006,

Table 1. Summary of the domestic neutrino workshops that have been organized by this center between 2006 and 2012.

	Date	Main topic(s)
1	Jul. 6, 2006	WMAP 3 year results and new data presented at Neutrino 2006
2	Feb. 20, 2007	Studies of non-standard physics with neutrinos
3	Nov. 2, 2007	New neutrino oscillation data and the neutrino mixings
4	Jun. 27, 2008	Status of the neutrino studies
5	Feb. 9, 2010	θ_{13}
6	Mar. 9, 2011	High energy astrophysical neutrinos
7	Mar. 29, 2012	θ_{13}

and the later one at the Hongo-campus of the University of Tokyo, on Sep. 30 and Oct. 1, 2007. (The first workshop was also organized by this Center in 2004.) About 60 and 40 scientists participated in these workshops, respectively.

Another international workshop that we had deeply involved was the "Workshop on Next Generation Nucleon Decay and Neutrino Detectors 2007", which was held in Hamamatsu on Oct. 2-5, 2007.

Since the establishment of this center, this center has carried out public lectures once every year in Kashiwa, typically in the afternoon of a Saturday in spring. In 2009, it was decided to carry out public lectures twice a year jointly with Institute for the Physics and Mathematics of the Universe (IPMU, since 2012 the name is changed to Kavli Institute for the Physics and Mathematics of the Universe). This center is still taking a major role in organizing the spring part of the joint public lectures. Each time, 2 lecturers give a lecture on the topic of his/her scientific research, and typically 200 public audiences come to listen to the lectures. Table 2 summarizes the date, the place and the lecturers in each public lecture.

This center has been acting as the body for accepting the ICRR inter university programs related to the underground laboratory for low-level radioisotope measurement in the Kashiwa campus

Table 2. Summary of the neutrino public lectures between 2006 and 2012. Since 2009, the lectures are co-hosted by ICRR and IPMU. Only public lectures organized by this center are listed after 2009.

	Date	Lecturers
1	April 22, 2006	Kunio Inoue (Tohoku) Takaaki Kajita (ICRR)
2	April 7, 2007	Toshitaka Kajino (NAOJ) Takaaki Kajita (ICRR)
3	April 12, 2008	Tsuyoshi Nakaya (Kyoto) Naoshi Sugiyama (Nagoya)
4	April 18, 2009	Naoki Yoshida (IPMU) Kazuaki Kuroda (ICRR)
5	April 17, 2010	Masato Takita (ICRR) Shigeki Sugimoto (IPMU)
6	April, 2011	Canceled due to the Tohoku Earthquake
7	April 14, 2012	Masahiro Teshima (ICRR) Hiroshi Karoji (IPMU)

and researches that are carried out using the ICRR computer system. The underground laboratory is equipped with 4 Ge detectors mainly for the measurements of cosmic radioactive isotopes. The scientific activities related to this laboratory is described separately.

LOW-LEVEL RADIOISOTOPE MEASUREMENT FACILITY

Low-level radioisotope measurement facility was built at Kashiwa campus in 2000 with the relocation of ICRR from Tanashi campus in Tokyo. Historically, the facilities originated in Nokogiri-yama laboratory set up under Mt. Nokogiri-yama approximately 40 years ago, and the initial objectives were low-level counting to investigate cosmogenic nuclides in extraterrestrial materials such as cosmic dust falling down to the earth surface and/or the ocean. The new laboratory at Kashiwa is located in a basement 23 m from the surface. The floor space is approximately 47 m² and all of the walls are painted by "MINEGUARD" which is a special paint to block radon gas from the reinforced concrete.

In this laboratory, four High-Purity Germanium (HPGe) detectors are installed to measure natural radioactivity of various kinds of samples by gamma ray spectroscopy. All of HPGe detectors are well type with U-style cryostats. Each HPGe detector except Det. No. 3 in Table 1 is surrounded by an ultra low-background shield with 15 cm thick low background lead. The specifications of these detectors are shown in Table 1. The data acquisition for the HPGe detector are computer controlled, and the identification of the radioisotopes is automated. In addition, environmental data of the laboratory such as temperature, humidity, atmospheric pressure, radon density, weights of liquid nitrogen vessel for cooling HPGe detectors, are monitored and logged by the network data logging system as shown in Fig.1. Oxygen-density-meter is continuously monitored by a TV camera, and is displayed at the entrance level floor. Before entering the underground laboratory, we are obliged to check if (1) Ventilator is working, and (2) Oxygen density is not

lower than 20.9%. These monitor data can be seen at <http://157.82.231.248/xfer/disk>.

This facility has been utilized for low-level counting of the cosmogenic (Thema 1,2) and environmental (Thema 1-3) radioisotopes in a variety of samples such as micrometeoroids sampled in Antarctica, aerosols in air, dry and/or wet fallout materials in precipitation and so on.

Thema 1: Detection of time variations for cosmogenic ⁷Be by Yoshihisa Sakurai (Yamagata Univ.) et al.: Temporal variation of ⁷Be concentrations in atmosphere has been measured for 8 years from 2000 at Yamagata ¹. The yearly profile of the ⁷Be concentration indicates the variation in galactic cosmic rays owing to solar modulation. The yearly ⁷Be concentration was mainly varied by the solar modulation of the ⁷Be production rates. The daily ⁷Be concentrations have two significant periodic components of 19 days and 36 days. The 36 day component implies a relationship between the solar rotation and the vertical air mass transportation under quiet solar activity.

Daily variation of cosmogenic nuclide ⁷Be concentration has been measured since September 2009 at Mt. Chacaltaya with the altitude of 5200 m to observe 27 day periodic variation relating to solar rotation ². The seasonal variation of the ⁷Be concentrations are clearly shown with a minimum in January of the summer and a maximum in July of the winter. The ratios of the minimum to the maximum are 31%. The daily profiles are different between the ⁷Be and ²¹⁰Pb concentrations. The wavelet analysis showed the ⁷Be concentrations indicate a 27 day periodicity during the summer season in Southern hemisphere.

Thema 2: Determination of ²⁶Al radioactivity in Antarctic meteorite samples by Takaaki Fukuoka (Rissho Univ.) et al.: Micromete-

Table 1. Specifications of HPGe detectors.

Det. No.	Well Dia.(mm)	Vol.(cc)	Manu. Year
1	10	190	1997
2	16	170	1997
3	16	116	1986
4	16	160	2005

*1 H. Sakurai et al., "Daily Variation of Cosmogenic Nuclide Be⁷ Concentrations in High Altitude Atmosphere at Mt. Chacaltaya at the solar minimum", Proc. of the 32nd Int. Cosmic Ray Conf. (2011).

*2 S. Kikuchi, H. Sakurai et al., "Temporal Variation of Be⁷ concentrations in atmosphere for 8 y from 2000 at Yamagata, Japan; solar influence on the Be⁷ time series", J. Environmental Radioactivity, **100**, 515 (2009).

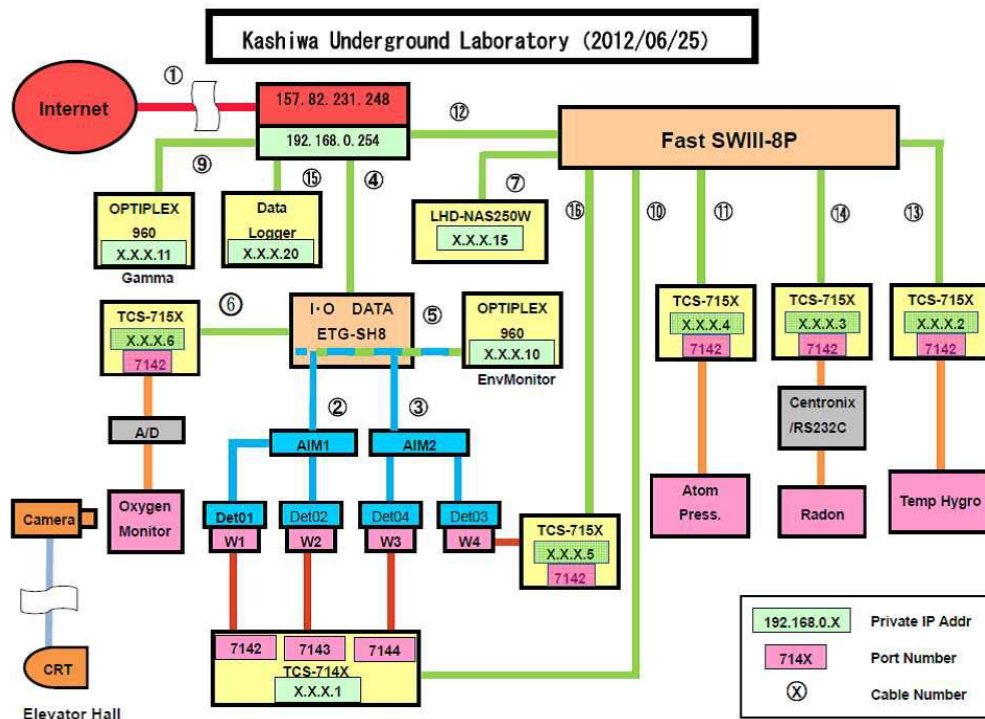


Fig. 1. Data acquisition and monitoring of Kashiwa Underground Laboratory

orites in Antarctic ice were detected by Ir with instrumental neutron activation analysis³. The accretion rate of micrometeorites was estimated from Ir concentration in snow around Dome Fuji Station and ice shards obtained during ice core drilling at Dome Fuji Station, Antarctica. The accretion rates were estimated for 120k years ago, 5k years ago and at present, as $(3.2 \pm 0.9) \times 10^2$ ton/year/earth, $(8.6 \pm 0.18) \times 10^3$ ton/year/earth and $(1.3 \pm 0.10) \times 10^3$ ton/year/earth, respectively. These estimates were comparable to those of previous studies, however the rate of 120 k year ago was approximately an order of magnitude lower than the others.

Thema 3: Evaluation of the erupted radioactivities into the environment by Hideo Ohashi (Tokyo Univ. of Marine Sci. and Tech. et al.: The TEPCO Fukushima Dai-ichi nuclear power plant explosions occurred in March, 2011 triggered

*3 A. Miura, Y. Saito, Y. Tazawa, H. Fukuoka, T. Noguchi, H. Motoyama, "Micrometeorites in Antarctic ice detected by Ir: estimation of 120k year old accretion rate", *J. Radioanal. Nucl. Chem.* **291**, 213 (2012).
 H. Kusuno, M. Kobayashi, T. Fukuoka and H. Kojima, "Determination of ²⁶Al contents for Antarctic meteorites using extremely low background γ -ray counting system of ICRR, university of Tokyo", *Meteoritics & Planetary Science*, **41**, A103 (2006).
 H. Kusuno, M. Kobayashi, T. Fukuoka and H. Kojima, "Determination of ²⁶Al contents in Antarctic meteorites using extremely low background γ -ray counting system of ICRR, University of Tokyo, for dating of terrestrial age.", *Antarctic Meteorites*, **30**, 48 (2006).

by the Great East Japan Earthquake. As radioactive materials have been scattered around the environment, we have started the radioactivity measurement.

To estimate the accretion amount of ¹³⁴Cs and ¹³⁷Cs, swimming pool water have been sampled three times, 29, 30 April, 27 July and 9 November from five elementary school and one junior high-school and one abolished elementary school in Kawamata-machi, Fukushima, located 30 to 50 km away in the 305 degrees azimuth angle from the power plant. Yamakiya Junior High-school is located in the scheduled evacuation zone. Swimming pools of the five elementary schools are unwatered and cleaned in early July. Time series variation of ¹³⁴Cs and ¹³⁷Cs concentration data is quite controversial.

We measured activity size distributions of ¹³⁴Cs and ¹³⁷Cs in aerosols collected 47 days after the accident at Tsukuba, and determined the activity median aerodynamic diameters of those nuclides. From the analysis of other aerosol components, sulfate was the potential transport medium for these nuclides, and re-suspended soil particles were not the major airborne radioactive substances at the time of measurement. This explains the relatively similar activity sizes of radio-cesium measured at

various sites during the Chernobyl accident ⁴.

*⁴ N. Kaneyasu, H. Ohashi, F. Suzuki, T. Okuda, F. Ikemori, "Sulfate Aerosol as a Potential Transport Medium of Radiocesium from the Fukushima Nuclear Accident", *Environmental Science and Technology*, **46**, 5720 (2012)

GRAVITATIONAL WAVE PROJECT OFFICE

Gravitational wave project office was established at the beginning of the financial year of 2011 to assist the construction of KAGRA¹ gravitational wave telescope. The organization of this office is illustrated in Fig. 1. Main office is set in Kashiwa campus and its Kamioka branch is in Kamioka. It is an internal organization placed in Astrophysics and Gravity Division of ICRR.

KAGRA project is hosted by ICRR, which means the funding comes through University of Tokyo and all procurements are made through ICRR. However, the number of researchers working for KAGRA construction belonging to other organizations is larger than the staffs belonging to ICRR. Therefore, three collaboration members of KEK are recruited as guest researchers at the ICRR and two research staffs are temporarily moved to ICRR from NAOJ. Besides these staffs, there are many other collaboration members who belong to other organizations.

- coordination of collaboration meetings
- technical supports for the KAGRA construction
- support for education of graduate students
- bridging collaboration members and ICRR administration office
- others

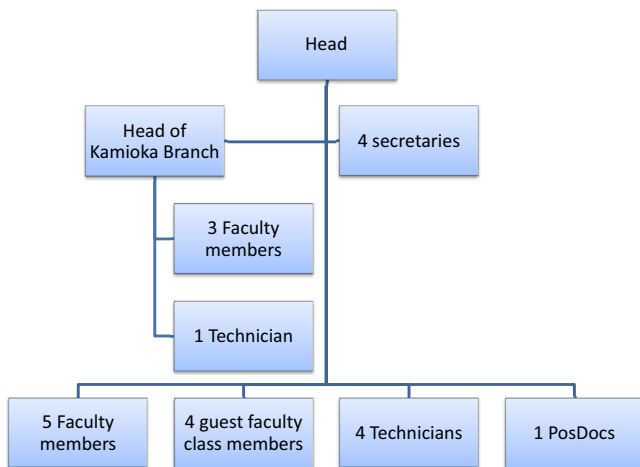


Fig. 1. Organization of the Gravitational Wave Project Office

The role of this office is to support execution of KAGRA project by ICRR staffs with these collaboration members. Main works are:

- finance planning
- management of collaboration
- support for the execution of KAGRA budget

*¹ nicknamed in January, 2012 by public contribution for LCGT

APPENDIX

A.1: ORGANIZATION

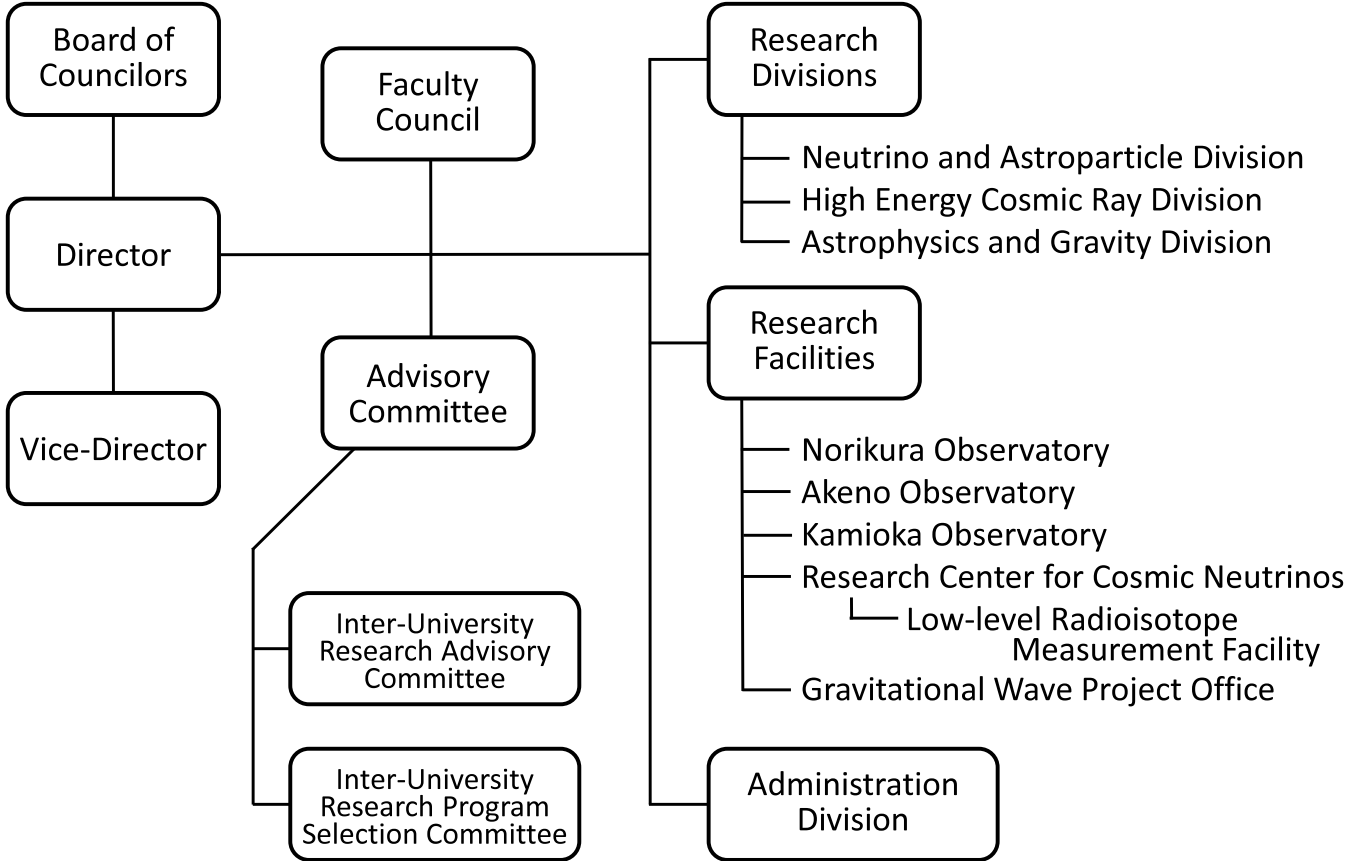


Fig. A.1-1 Organization of the Institute for Cosmic Ray Research as of April 2012.

A.2: ICRR STAFFS (2012)

The number of tenured researchers (Professors, Associate Professors, and Research Associates) in ICRR was essentially unchanged; it is 37 in both 2006 and 2012. This is due to the balance between newly allocated posts by the University of Tokyo, and the un-filled posts (after retirement or departure of the staff) under a general rule in the University of Tokyo, which is based on a law to restrict the total number of employees in the governmental agency.

The University of Tokyo established a post re-

allocation system to assign new posts to departments and institutes. Under this system, each department or institute submits a post re-allocation proposal to the University of Tokyo. Then the posts might be re-allocated to them after the evaluation of the proposal.

The Table below summarizes staffs of ICRR in 2012. In FY2012, ICRR accepted three visiting professors and two visiting associate professors, which are not shown in this table.

Table A.2-1 Numbers of ICRR staffs as of April 2012.

Professors	Associate Professors	Research Associates	Technical Staffs	Project Associate Professors ¹	Project Research Associates ¹	Post-Doctoral Fellows	Total
9	14	14	8	1	14	14 + 3 ²	77

*¹ Project Associate Professors and Project Research Associates have fixed terms.

*² 3 JSPS Post-Doctoral Fellows studying in ICRR.

A.3: BUDGET (FY2007–2011)

After the restructuring of national universities in 2004, the same level of government revenue funding as of FY2004 has been maintained for each fiscal year with a limited amount of yearly cut due to the government's general saving policy (Table A.3-1). Funding for specific research projects, design-

ated as "Promotion of Science" in Table A.3-1, changes depending on the project status. An increase of the total annual budget after FY 2010 is due to the start of KAGRA construction. Other sources of research fund are listed in Table A.3-2.

Table A.3-1 Revenue and research grant for Promotion of Sciences (in thousand yen).

	2007	2008	2009	2010	2011
Personnel Expenses	624,000	632,000	590,000	576,000	653,000
Supplies and Facilities	1,253,000	1,121,000	1,292,000	1,048,000	1,400,000
Sub-Total	1,877,000	1,753,000	1,882,000	1,624,000	2,053,000
Promotion of Science	252,000	235,420	349,000	2,509,000	4,406,000
Grand Total	2,129,000	1,988,420	2,231,000	4,133,000	6,459,000

Table A.3-2 Other research funds (in thousand yen).

	2007	2008	2009	2010	2011
Trust Fund	21,730	77,180	77,408	38,000	29,239
Private Scholarship	10,930	3,000	12,000	760	0
Others	0	1,000	1,000	1,000	500
Total	32,660	81,180	90,408	39,760	29,739

B.1: AGREEMENTS OF INTERNATIONAL ACADEMIC COOPERATION

Table B.1-1 Agreements of academic cooperation with the ICRR, or the University of Tokyo, and overseas universities and research organizations.

Country	University/Institute	Year of Agreement
China	Institute of High Energy Physics, Chinese Academy of Sciences	1995
USA	College of Science, University of Utah	1995
USA	School of Physical Science, University of California, Irvine	1995
USA	Graduate School of Arts and Sciences, Boston University	1995
Australia	University of Adelaide	1995 ¹
Russia	Institute for Nuclear Research, Russian Academy of Science	2001
Australia	Faculty of Life and Physical Sciences, University of Western Australia	2007
Korea	College of Natural Science, Seoul National University	2009
USA	CIT LIGO Laboratory, California Institute of Technology	2009
USA	Department of Physics and Astronomy, University of Hawaii at Hilo	2010
Italy	European Gravitational Observatory/ Virgo Collaboration	2011
China	Shanghai United Center for Astrophysics, Shanghai Normal University	2011
UK	Institute for Gravitational Research, University of Glasgow	2011
Taiwan	College of Science, National Tsing Hua University	2011
China	SICCAS-GCL Research & Development Center, Shanghai Institute of Ceramics, Chinese Academy of Sciences	2012
USA	College of Science, Louisiana State University	2012
Italy	University of Sannio at Benevento Department of Engineering	2012
China	National Astronomical Observatories, Chinese Academy of Sciences	2012

*¹ The agreement between ICRR and the Department of Physics and Mathematical Physics was originally signed in 1995 and later upgraded to the agreement between the universities in 2001.

B.2: INTERNATIONAL MEETINGS

Table B.2-1 List of international meetings hosted or co-hosted by ICRR.

Date	Place	Symposium/Workshop Title	Participants
Feb. 22–24, 2006	Kashiwa	International Workshop on Energy Budget in the High Energy Universe	126
Jul. 13–14, 2006	Seoul	2nd International Workshop on a Far Detector in Korea for the J-PARC Neutrino Beam	61
Feb. 23–25, 2007	Hawaii	Twenty Years after SN1987A	102
Sep. 30–Oct. 1, 2007	Tokyo	3rd International Workshop on a Far Detector in Korea for the J-PARC Neutrino Beam	44
Oct. 2–5, 2007	Hamamatsu	Workshop on Next Generation Nucleon Decay and Neutrino Detector 2007 (NNN07)	98
Aug. 25, 2008	Kashiwa	Inauguration Ceremony and Symposium of Telescope Array	108
May 27–29, 2009	Hayama	World-Wide Network for Gravitational Wave Observation (58th Fujihara Seminar)	84
May 16–21, 2010	Kyoto	Gravitational Wave Advanced Detector Workshop (GWADW2010)	107
Dec. 10–12, 2010	Nagoya	Recent Progress of Ultra-High Energy Cosmic Ray Observation (UHECR2010)	114
Dec. 13–16, 2010	Toyama	Workshop on Next Generation Nucleon Decay and Neutrino Detector 2010 (NNN10)	96
Jun. 3–9, 2012	Kyoto	XXV International Conference on Neutrino Physics and Astrophysics (Neutrino 2012)	612

B.3: INTER-UNIVERSITY COLLABORATIVE RESEARCHES

As one of the “Joint Usage/Research Centers” in Japan, ICRR has been supporting inter-university collaborative researches. Annually ICRR issues calls for applications of collaborative researches. The following tables summarize the annual numbers of the applications after selection.

Table B.3-1 Annual numbers of applications for collaborative research programs.

Facilities	2006	2007	2008	2009	2010	2011	Subtotal
Kamioka Observatory	33	36	39	35	40	40	223
Akeno Observatory	7	4	4	3	7	6	31
Norikura Observatory	5	7	10	9	8	6	45
Low-Level Radioisotope Measurement Facility	6	6	6	6	6	6	36
Cryogenic Laser Interferometer in Kashiwa ¹	4	4	3	0	1	1	13
Laboratorial Facility in Kashiwa	7	5	3	5	7	17	44
Computer Facility in Kashiwa	6	7	11	9	10	9	52
Conference Facility in Kashiwa	6	7	6	8	6	4	37
Emulsion Facility in Kashiwa ²	2	3	3	3	1	1	13
Overseas Facilities ³	16	12	14	15	12	14	82
Annual Sums	92	91	99	93	98	104	576

*1 The first laser interferometer using cryogenic mirrors developed in Kashiwa.

*2 The emulsion facility had been open to all the scientists who had wanted to carry out joint research programs. Recent shrinking demands for these facilities, however, let ICRR suspend annual calls for relating applications from 2012.

*3 The Tibet AS γ Observatory, Observatory for Highest Energy Cosmic Rays in Utah, Chacaltaya Observatory of Cosmic Physics, and International Astrophysical Observatory in Australia. The observatory in Australia was closed in 2011. Applications for domestic activities corresponding to these overseas works are included here.

B.4: EDUCATIONAL ACTIVITIES

One of the important functions of ICRR is to educate graduate students directly at ICRR as a part of the Graduate School of Science, the University of Tokyo, and indirectly at graduate schools of domestic/foreign universities through collaborative research programs.

Table B.4-1 Annual numbers of accepted master/doctor theses.

	2006	2007	2008	2009	2010	2011	Subtotal
Master theses at ICRR	13	3	13	6	12	5	52
Master theses at domestic universities	20	23	19	14	16	19	111
Total numbers of master theses in Japan ¹	33	26	32	20	28	24	163
Doctor theses at ICRR	1	7	5	9	3	2	27
Doctor theses at domestic universities	2	1	2	2	3	9	19
Doctor theses at foreign universities	4	3	4	4	8	19	42
Total numbers of doctor theses	7	11	11	15	14	30	88

*¹ Since the numbers of master theses are not available for all the collaborating foreign universities, only the domestic numbers are tabulated.

B.5: PUBLIC RELATIONS

Overview

The ICRR employs two scientific staffs dedicated for public relations: one in Kashiwa since 2006 and another in Kamioka since 2008. They form Public Relations Committee together with ICRR researchers to look after following outreach and public relations activities of the institute:

1. ICRR web site
2. Reports and annuals
3. Guided tour
4. Scientific display
5. Public lectures and lessons

ICRR web site

Web site renewal

The ICRR main web site was renewed in 2008 using the content management system (CMS). We adopted the Movable Type (MT) of Six Apart Ltd., which enabled us to update the web site easily from the terminals connecting to the ICRR network. It turned out to be very useful for the rapid communication of important information during the Great East Japan Earthquake time as we were able to update the web site using the MT system when the FTP server did not work.

Access Analysis

According to the access analysis of the web page started in 2010, an average number of the access is 250 per day on weekdays. The maximum was 542 accesses on July 25, 2011, the next day of the live broadcast from Kamioka on the gravitational wave project. The viewer of the live broadcast was nearly 30 thousands, far much larger than the accesses to the web page the next day. We are considering to make a search engine optimization and introduce interactive contents in the ICRR web page.

Reports and Annuals

The ICRR has three periodicals; annual report, institute handbook, and “ICRR News”. The annual

report is a record of scientific activities of the institute. It addresses the experts in science and is written in English. The institute handbook addresses the general public, and is written in both Japanese and English. It contains an introductory description of research projects and observatories, a brief history, organization and statistical facts of the institute. The contents are updated each year. The “ICRR News” is a flash report of 10-20 pages in Japanese on the recent scientific activities of the institute. It is issued quarterly and is distributed to the science community in Japan. The Public Relation Committee and scientific staffs are in charge of editing these periodicals. All the periodicals are also available on the web page.

Guided Tour

The number of people visiting the ICRR in Kashiwa and Kamioka Observatory every year is a few thousands. A variety of visitors exists from general public to experts in science: they are school students, neighbors of the institute, officials from the ministry and municipal government, teachers and researchers and many others. They are guided by the science staffs and ICRR researchers.

Scientific display

For the outreach, we organized scientific displays in the museums of science, high schools and universities, and art galleries. The contents are video pictures of introducing ICRR experiments, samples of detector hardware and equipment, and poster of explanations. Displays in the museum of science attracted many people, but they are the interested people in science and the outreach impact was considered not very large. We then organized displays in art galleries and universities. This attempt was successful and each display attracted a few hundred persons. We continue such approaches as well for the effective outreach to the general public.

Public lectures and lessons

The institute has been making public lectures each year in April in Kashiwa-city on the subject of neutrinos, cosmic rays and the cosmology. It attracts around 200 audiences and is very popular among Kashiwa citizens and students, giving good feeling to support our academic activities (see section of RCCN for details). Since 2009, public lectures are co-hosted with the neighboring institute Kavli IPMU and we give public lectures twice a year. We have been also requested to give lessons at high schools, and delivered scientific lectures on cosmic ray physics, particle physics, cosmology and other subjects. We believe these activities contribute for raising next generation scientists and for promoting people's widespread support on science.

C: REPORT FROM THE FUTURE PLANNING COMMITTEE (2007)

Date: August 31, November 26, 2007

Committee members:

J. Arafune (Chairperson), S. Yoshida, K. Inoue, T. Terasawa, N. Mio, M. Teshima, M. Kawasaki, M. Nakahata, and M. Mori (Secretary)

Observers:

Y. Suzuki (Director of ICRR), F. Kajino (Executive chairperson of CRC)

1. General Remarks

It has been a great success for ICRR to participate in the Kamiokande project with collaborators and take the initiative in Super-Kamiokande project, that makes ICRR the worldwide leading organization in the neutrino physics/astronomy. However, ICRR should take a further leadership in these research areas. For this purpose, it will be indispensable, and also a severe challenge, to find new attractive themes and to prepare a suitable organization/research system for their execution.

The committee had a symposium to discuss how to optimize the management among several future plans with which ICRR is currently concerned. It was specifically investigated whether these plans can meet such expectations, as well as how the status of organizing the system for their execution is at present.

Considerable opinions were exchanged in the symposium: Each plan exhibits a wide variety of its promising attractiveness and potential of feasibility, though many of them have not been well examined yet. At present, the research groups are too diverged in order to principally investigate the projects, which should be focused on in a scale suitable for the ICRR capability. Under the circumstance that the experimental project becomes large-scale and internationalized, the group rearrangement in a proper scale will assure a principal contribution to the research community. On the other hand, since flexible experiments or R&D led by a small group is invaluable as an investment for the future, integration of the group is not the only

inevitable way in the ICRR organization. In the next section, the present status is described for each plan proposed in the symposium, including issues to be further examined. Each proposal is classified into “Proposal Program” and “R&D program”; the former is feasible and the latter needs R&D.

2. Comments on individual projects

2-1. IceCube++ with AURA

IceCube can attain the sensitivity enough to detect the GZK neutrino after its completion. The committee accepts the significance of the proposed Outrigger, which increases the effective volume in the energy range of GZK neutrino without a radio observation. The committee further requires its quantitative evaluation. Radio wave detection (IceRay) is effective only in the highest energy range. Uncertainty still remains in the detection method, the problem of LPM effect for instance.

This proposal is categorized into “Proposal Program”, but some R&D is still necessary. Because no ICRR members join this project, it is difficult to recommend it as a research project of ICRR at present. However, it is also worth continuing investigation as one of the possible future missions in the division of highest-energy cosmic rays, and being judged again for the mission recommendation.

2-2. Development of GeV gamma ray detector with high-energy resolution

The idea is interesting in that the lightweight gamma ray observatory utilizes a superconducting magnet. However, reexamination of the instrumental design, so as to increase the sensitivity ten times more, for example, should be made, since GLAST will be launched soon (one possible idea, for instance, is to increase in size as well as to save weight even if the bremsstrahlung observation is resigned). It is also insufficient to examine the system of total design including freezer and coolant, and to estimate the manpower responsible for the experiment.

This proposal is categorized into “R&D Program”, but it is unacceptable to recommend as a program that requests the budget by designating ICRR as a host institute.

2-3. Megatons-class water Cherenkov detector development

Proton decay, if discovered, will be of great significance to physics. However, there is still uncertainty in theoretical predictions of the proton lifetime. Therefore a proton-decay experiment should be designed for rich sensitivity to a range of physics topics even if it is only possible to obtain a lower limit on the lifetime of the proton.

With regard to neutrino observation, if the mixing angle θ_{13} is shown to be relatively large, it becomes reasonable to construct a megaton-size detector. However, the photosensitive surface area of the detector is directly linked to the cost of the detector and needs to be optimized for the physics of interest. A larger surface area is necessary to observe lower energy phenomena, such as 6 MeV γ expected in the neutral current interactions of supernova neutrinos and the proton decays into νK^+ . On the other hand, there are other physics targets which do not require a large photosensitive area. Therefore, in the case of a restricted budget, priorities should be taken into account among possible physics targets. The addition of Gd to tag neutrons produced in neutral current events is a potential option if reduction of radioisotopes without loss of transmissivity is demonstrated.

This proposal should be preferentially promoted under the category of an “R&D program”. If low-cost manufacturing of optical sensors becomes feasible, the physical scope of the experiment could be expanded. It is necessary to ensure sufficient manpower by employing more project researchers, for example.

2-4. International collaboration by using large-scale Cherenkov telescope arrays for the gamma ray astronomy

Development of the gamma ray astronomy in the southern sky is the initial achievement of the CANGAROO group. However, the international situation is changing day by day. It is important to be pointed out promptly how to realize the experiment that Japan can demonstrate its research ability by

achieving valuable results under international collaboration.

Though this proposal seems categorized into “R&D Program”, further reexamination is necessary. The proposal suggests that after reorganization and expansion, the group takes charge of the subsystem of CTA, which is the international collaboration for the future plans of ground gamma-ray observatories. In such a situation, then, it should clearly be presented how to manage CANGAROO facilities, what part to be assigned, how to demonstrate the significance and leadership of Japan’s team to obtain results, and how to proceed the R&D such as the development of a prototype.

2-5. Liquid Xenon experiment of astroparticle (XMASS experiment)

The R&D efforts for XMASS to date is highly appreciated. Therefore, the committee judged this proposal appropriate to be accepted as one of the ICRR projects. The committee expects steady progress of the Phase-1 experiment which explores the existence of dark matter. The committee also realizes the importance of investigating 0ν double beta decay and solar neutrino, which will be the targets in Phase-2.

Phase-2 should be preferentially promoted under the category of “R&D program”, simultaneously with Phase-1. Thorough care should be taken on the safety control.

2-6. Next plan for Tibet AS γ experiment (Tibet AS+MD+YAC): Research in gamma-ray astronomy in 100 TeV range (10-1000TeV) and the chemical composition of primary cosmic ray in the knee-energy range

It is significant to figure out the chemical composition of cosmic rays in the “knee” energy range if its measurement is surely possible. This is because of its importance in the problem of the source/acceleration/propagation of cosmic rays. However, the committee suggests that the part of the plan depends on the Monte-Carlo calculation which should be further elaborated.

As for a gamma-ray observation project, there will undoubtedly be a severe international competition among MAGIC/HESS, or the future CTA (3km square). But this project has an advantage over them, in that it enables to search the whole sky in the northern hemisphere as well as the extended

gamma-ray sources. The other advantage is its early feasibility due to the moderate amount of the necessary budget. It is anticipated that there are only a few gamma-ray sources in the northern sky and that these sources provide statistically-limited energy spectral data in 100 TeV range. However, as early as the research starts, the cost effectiveness in the expected result is acceptable in comparison with those in the international collaboration with other bigger projects.

As “Proposal Program”, the committee expects it to be proceeded in a short period of time by acquiring a grant such as KAKENHI, in addition to supporting the China’s effort of securing the budget of their own at the same time.

2-7. Research in the highest energy cosmic rays

The committee is looking forward to the first data detected by the complete Telescope Array in the northern hemisphere, which is statistically superior to those by AGASA or HiRes. Though the proposal of inter-calibration by setting up the same water tank as at Auger (or setting up the ground detector of TA at Auger) is interesting, the committee did not show a clear view on it. Shower detection by radio observations should further be examined on the issues such as the possibilities of self-triggering, widening the lateral distribution, and so on.

Operation of the TA equipment, which has been just built, should be supported as “Proposal Program”. In the TALE project, it is expected to early secure the budget in the US side. However, there are still many unsatisfactory points in other proposals under the “R&D Program” category, such as radio observations, which need more examination. The committee requires the necessity of these reexaminations as well as a consideration of solid plans in the future, including the possibility of participating in the North Auger.

2-8. Synthetic research in gravitation waves

While it is definitely significant if the first direct detection of gravitational waves is realized, the budgetary request for LCGT project is disappointingly delayed due to the incomplete financial framework for big projects after privatization of national universities. If the budget for Advanced LIGO is approved, only one or two years remain to be eligible to compete for the first discovery. On the other hand, the detection of gravitational waves

becomes highly reliable when they are simultaneously observed in the international observatory network. Therefore, it is of great importance to construct LCGT in time for the cooperative observations, even if it can not detect gravitational waves at first.

The committee expects early budgeting under the category of “Proposal Program”, and also anticipates highly internationalized collaboration.

2-9. Clarification of the past/present/future in the cosmic and terrestrial environment by the high-precision analysis of cosmogenic nuclide

The committee understands the importance of accelerator mass spectrometry because of its usefulness in a wide variety of research areas, covering from natural sciences to humanities. However, it is difficult at present to request a budget for this “Proposal Program” to ICRR, and to construct the accelerator as the ICRR facility. In constructing the accelerator, consultation with other research institutes will also be necessary. The committee further requires considering another possibility of collaboration with the experimental group. For instance, in the case of applying a symposium as a joint research of ICRR, the support from ICRR is desired.

2-10. Ashra project

The basic idea of the Ashra equipment is interesting. Its wide-angle and high resolution properties, if implemented efficiently to realize the conceptual design, look promising. The committee gave some questions about the detail of the development consequence in the component technologies. The proposer’s reply to them, however, could not convince the committee that the problems are resolved. The initial plan, the detection of gamma-rays and high-energy cosmic neutrinos, also needs more manpower of researchers to this project and a verification by simulations which substantiates the sensitivity. The committee did not accept this proposal at this stage as the mission of ICRR.

3. Proposal about the directionality of the research as a core mission of ICRR in future

Proposal of gravitational waves needs a big budget. Therefore, in order to carry it out early, the pursuits of diverse and flexible possibilities including a reorganization of the institutional structure are desired. At present, besides the ongoing projects,

this gravitational wave observation is the only future plan that is sufficiently elaborated. The committee looks forward to its realization, which is also far from easy. That is why ICRR must exert strenuous efforts for the future.

How to promote the future observations of ultra high-energy cosmic rays should be judged from the international research trend as well as from the experimental achievements of Telescope Array, whose construction will be completed soon.

For the study of the chemical compositions of cosmic rays in Tibet, the early realizations of new observations and refined simulations are desired.

The committee further looks forward to the R&D studies of XMASS and megatons-class water Cherenkov detector, both of which should be supported by ICRR as the host institution.

Proposals of the cosmic gamma-ray observation mainly constitute (i) the CANGAROO group's participation in CTA, (ii) the observations by the ground telescope array together with water Cherenkov light detection in Tibet, (iii) the Ashra first stage plan using its unique observation equipment, and (iv) the experiment with a superconducting magnet. The proposal (i) is the largest one with a lot of issues to be resolved. The proposal (ii), being not parallel to the worldwide mainstream for the Cherenkov telescope, is a unique and moderate-scale feasible plan if the budget is available. The proposal (iii) could not convince the committee whether it can give the proposed performance. The committee concluded that the proposal (iv) still needs more examination.

IceCube++ with Aura was proposed for the research of high-energy cosmic neutrino. This proposal needs to examine the collaborating system as well as the results of R&D research.

Because the number of projects ICRR can support is limited, it is desired to consolidate those projects that share the common physical purposes. Especially, there are a lot of ICRR experimentalists who are interested in the gamma-ray research. Accordingly, continuous examination of the gamma-ray area may be necessary by making a proposal content more attractive to these researchers and by considering the possibility of international collaboration via the group reorganization.

The future plan of ICRR is not only limited to the projects proposed at present. It is also necessary to raise the ambitious projects which are beyond the

present research categories. For instance, the research possibility of the early cosmic hydrogen history by 21cm radio observations with the redshift $z = 10 \sim 100$ is being examined by some people within ICRR, but not proposed officially at present. The committee encourages in-depth examination of the relationship between the physical significance of this observation and particle physics, the rough estimate of its cost, the possibility of training talents to develop new technologies, and so on.

The future plan of ICRR will certainly be a big experimental project under the international collaboration. In such a situation, Japan's groups should elaborate the research plan showing their deep contribution and principal demonstration.